ANALYSIS OF THE NUCLEAR ROLE OF RPB5

BINDING PROTEIN (URI/RMP) IN PROSTATE CELLS

PAOLO MITA

A dissertation submitted in partial fulfillment of the requirements for the degree of

DOCTOR OF PHILOSOPHY

DEPARTMENT OF BASIC MEDICAL SCIENCE

NEW YORK UNIVERSITY

SEPTEMBER, 2012

_____

SUSAN K. LOGAN, PH.D.

DEDICATION

For my mother who taught me the beauty of learning,

and for my father and my sister who are always there for me.

ACKNOWLEDGEMENTS

I would like to thank with all my heart my mentor, Dr. Susan Logan, for her invaluable support and help in any problem or difficult situation I encountered during these years at NYU. She has been an inspiration not only as a scientist, but also as a person. With her unconditional support she pushed me to explore new ideas, and grow as a scientist and a man. She always nurtured my scientific curiosity, and for that I will be forever grateful. I also would like to thank Dr. Logan for her incredible way to gently instill new scientific ideas in my mind; so gently that I initially always thought they were mine. And finally for her unshakeable trust in me and my scientific skills that always pushed me to do my best and more.

I also thank the other members of Dr. Logan's lab, Susan Ha, Rachel Ruoff, Eugine Lee and Eric Schafler, who have been not only my colleagues, but also my friends, and who made the time in the lab enjoyable even during periods of frustration. I also thank Dr. Garabedian and the members of his lab who were always ready and happy to help me with invaluable advice and stimulating discussions.

I would also like to thank my committee members, Dr. Hannah Klein, Dr. Brian Dynlacht and Dr. Gregory David for their invaluable help in discerning the best path to follow in the intricate maze of my research. They taught me to answer a scientific question choosing a straight line instead of long and convoluted deductions.

I want to thank also my sister and my father who always supported me, making me feel their love even on the other side of the ocean. And finally I would like to thank Kenneth Linsley who has been my life outside the lab for all these years. Thanks to him and his love I did not forget that life existed even far from the bench.

ABSTRACT

Unconventional prefoldin RPB5 Interactor (URI) was identified as a protein that binds the RPB5 subunit of polymerases and functions as a transcriptional repressor (Dorjsuren N., MCB, 1998). Although URI interacts with RNA polymerases, our microarray analysis of genes affected by depletion of URI did not show a general effect on transcription and only 5% of the genes were affected. We also showed that URI binds and regulates the stability of Art-27, an epithelial-specific androgen receptor (AR) cofactor. URI, in complex with Art-27, represses androgen receptor mediated transcription and plays a critical role in anti-androgen action (Mita P., MCB, 2011). Although several proteins have been identified as URI interactors the mechanism by which URI represses transcription is unknown. To gain functional insight into the mechanism of URI repression we performed a mass spectrometry analysis of proteins interacting with URI in the nucleus of prostate cells. This analysis confirmed the previously reported interaction of URI with the three RNA polymerases, TFIIF, the Paf-1 complex and the R2TP/prefoldin-like complex. The analysis also identified novel interactors including the transcriptional repressor KAP1/TRIM28 and the phosphatase PP2A. We show that URI binds PP2A phosphatase and thereby regulates KAP1 phosphorylation. Depletion of URI induced KAP1 hyper-phosphorylation and de-repression of KAP1 regulated genes. These data are interesting in light of the recently discovered role of KAP1 in retroelement repression.

Moreover, our mass spectrometry analysis showed a correlation between the URI phosphorylation state, polII CTD phosphorylation, and the recruitment of proteins involved in active polII transcription supporting the idea that URI phosphorylation could function as a metabolically activated "switch" that controls polII elongation on specific genes. We also show that URI is involved in the DNA damage response in mammalian cells and that the URI/Art-27 complex plays a role in prostate cell differentiation and luminal-epithelial cell specification.

Collectively, the data presented in this thesis demonstrate that URI, together with its "partner" Art-27, is part of a novel transcriptional repressor complex that plays a role in a wide range of cellular processes including cell differentiation, DNA damage and tumorigenesis.

TABLE OF CONTENTS

LIST OF FIGURES

CHAPTER 4:

CHAPTER 5:

XIII

CONCLUSION AND FUTURE DIRECTIONS

XIV

LIST OF TABLES

LIST OF APPENDICES

INTRODUCTION

I. PROSTATE CANCER

Excluding skin cancer, prostate cancer is the most common diagnosed cancer in men in the USA comprising about 29% of the estimated cases in 2012 [2]. Despite this high incidence, prostate cancer is accountable for only 9% of the estimated cancer deaths in men compared to the 29% death rate caused by lung cancer. Nevertheless prostate cancer is the second leading cause of cancer death after lung cancer; 1 out of 6 men will be diagnosed with prostate cancer in 2012 [2]. This apparent discrepancy between diagnosed cases and prostate cancer deaths can be explained by the high (nearly 100%) probability of complete remission from the disease in the first stages of its progression (about 90% of the diagnosed cases) (prostate cancer foundation 2012 data; http://www.pcf.org). In fact prostate cancer is a disease characterized by well-defined stages. Most diagnosed cases are organ-confined and clinically localized tumors that are relatively indolent. The availability of a highly accessible blood test for prostate cancer diagnosis facilitated the increase of the cases identified in these first and less aggressive stages. The standard test used today for prostate cancer diagnosis is the measurement of PSA protein (prostate-specific antigen) in the blood. PSA is a serine protease normally secreted by the prostate but measurable in the blood upon disruption of the normal prostate architecture because of the development of a tumor [3]. The use of PSA screening for the diagnosis of prostate cancer has been controversial since its introduction in the early 1990s. The controversy today is caused by the fact that the widespread use of PSA testing led to a vast increase in over-treatment of indolent prostate cancers that could likely be managed with "watchful waiting" [4]. This clinical challenge is posed by the lack of markers that distinguish indolent from aggressive tumors in prostate cancer patients diagnosed with low grade prostate cancer. However, the use of PSA measurement is still very useful in monitoring disease progression. If patients present elevated blood PSA concentration they will

2

undergo biopsy to determine the stage of the disease graded by Gleason scoring from 1 to 5 based on histopathological analysis [5]. Organ confined tumors with a low Gleason score will be treated with radiation therapy or brachytherapy while tumors with a Gleason score higher than 3 will undergo surgical excision (radical prostatectomy). More advanced cancers are characterized by metastatic tumors for which these regimens are usually followed or substituted with androgen deprivation therapy. At this stage patients are treated with anti-androgens like bicalutimide that inhibit androgen receptor function and/or luteinizing hormone-releasing hormone (LHRH) agonists that block the production of testosterone by the testis (chemical castration). Unfortunately, after initial regression most of the tumors treated with hormonal or anti-androgen therapy will recur as castration resistant prostate cancer (CRPC), able to grow in the absence or at very low concentration of hormone. CRPC is still untreatable today because of the high resistance of these tumors to standard chemotherapeutic treatment [6]. The lack of available treatment for CRPC is a major clinical challenge in prostate cancer therapy and it underscores the need to better understand the pathways involved in the development of this fatal stage of the disease.

Prostate cancer develops into different stages that are quite different at least at the molecular level (fig. A). Prostate intraepithelial neoplasia (PIN) is today accepted as the precursor stage for prostate cancer [7]. In this first stage, epithelial cells start to lose their monolayer organization and the prostate glands become more convoluted and multistratified. The adenocarcinoma stage arises mostly from the luminal epithelial cells of the prostate (more than 95% of the cases [3]), inducing progressive loss of the basal cell population. As discussed above most of these tumors are latent and will never progress. The latent prostate adenocarcinoma can however become aggressive cancer, characterized by disruption of the prostate boundaries and invasion of the tumor into the surrounding tissues. Metastatic prostate cancer is the most aggressive stage of the disease that, if resistant to castration, will

lead to death. Several molecular changes have been associated with the development of the different stages of prostate cancer such as inactivation of the PTEN phosphatase, MYC over-expression and TMPRSS2:ETS fusion (fig. A).
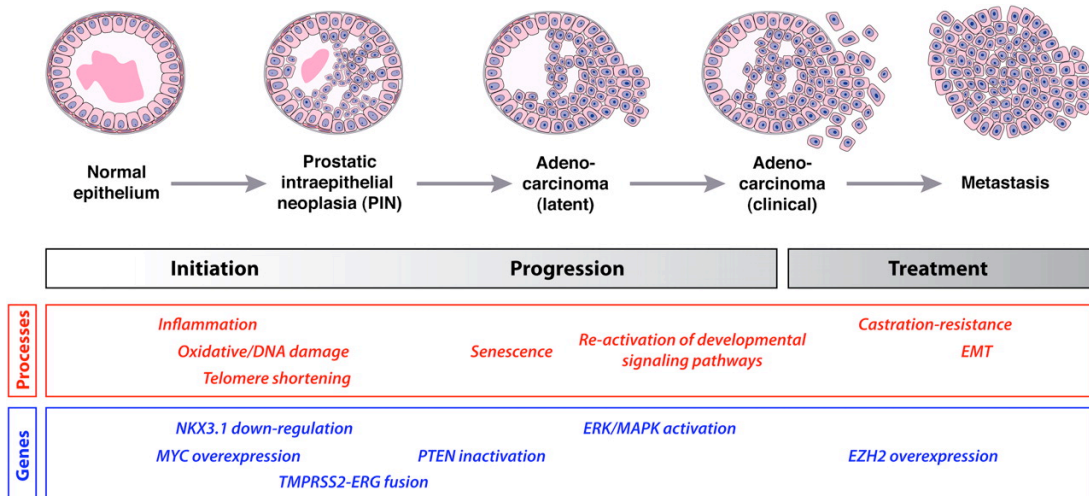
Figure A. Schematic of the development of prostate cancer. On the bottom the main molecular changes that characterize the different stages of the disease are reported [3].

In particular the fusion of the promoter of the androgen responsive gene TMPRSS2 to the coding region of several members of the ETS family of transcription factors (ERG, ETV1 and ETV4), is found in most prostate cancers and it recently revolutionized the idea of chromosomal translocation in solid tumors [8] [9].This chromosomal translocation fuses the promoter of TMPRSS2, containing strong AREs, to the 3' coding region of ETS transcription factors that, after fusion, become regulated by the androgen receptor. The most common TMPRSS2:ETS translocation is the TMPRSS2:ERG found in 40-70% of prostate cancers compared to the other TMPRSS2:ETS translocations found in less than 1% of cancers [10]. TMPRSS2 and ERG are separated by just 3Mb on chromosome 21 and it has been suggested that the androgen receptor mediates chromosomal proximity of the TMPRSS2 and

ERG loci to increase formation of the TMPRSS2:ERG fusion in LNCaP prostate cell lines and primary prostate tumor cells [11]. In particular the fusion was highly increased upon double strand break induced by ionizing radiations (IR) [12]. Moreover Lin and colleagues showed that derepression of LINE1 elements and specifically of the LINE1 ORF2, containing endonuclease activity, highly increases the formation of the TMPRSS2:ETS translocations (TMPRSS2:ERG and TMPRSS2:ETV1) induced by hormone treatment [11, 13]. Interestingly they noticed that repression of the PIWIL1 protein induced increased expression of LINE1 ORF2. PIWI proteins have been shown to repress repetitive elements like the LINE1 transposons in germ cells [14] and more recently in somatic cells [15]. Moreover LINE1 ORF2 endonuclease activity has been reported to be elevated in prostate cancer. LINE1 ORF2 was recruited on the site of chromosome fusion and, through its endonuclease activity, it highly increased the formation of the androgen/DNA damage dependent TMPRSS2:ETS translocation [13]. Other key enzymes were shown to work in concert with AR and LINE1 ORF2 to induce the TMPRSS2:ETS translocations. Among them the activation induced cytidine deaminease (AID), the growth arrest and DNA-damage inducible protein GADD45α and the ATP-dependent DNA helicase II/DNA repair protein XRCC5/Ku80 [13]. These intriguing observations led to the hypothesis that the TMPRSS2:ETS translocations are induced by the concurrent action of AR-mediated transcription and genotoxic stress that induce the over-expression of enzymes like GADD45 and LINE1 ORF2, mediating fusion of the two chromatin domains (TMPRSS2 untraslated region and ETS coding regions) brought into proximity by AR (fig. B).

Figure B. Proposed mechanism for TMPRSS2:ETS fusion formation [13]. DNA damage response induced proteins mediate the fusion of the two chromosomal loci brought in close proximity by AR.
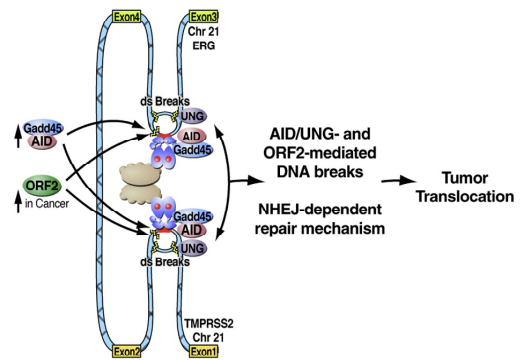
Several studies have been conducted to evaluate the importance of TMPRSS2:ETS translocation in the development of prostate cancer. TMPRSS2:ETS translocations were found in low grade PIN in about 50% of the analyzed cases suggesting that these translocations can occur as an early event. Also TMPRSS2:ERG transgenic mice have a higher incidence of PIN but not cancer and the incidence of PIN was increased with age [16]. Therefore, the formation of TMPRSS2:ERG translocation is not sufficient to induce prostate cancer but could be a coadjuvant event leading towards carcinogenesis. It is quite established, though, that higher expression of ETS transcription factors, caused by the fusion, drives the development of primary cancers. Also, knock down of ETS gene expression slows down cancer growth suggesting an important role of TMPRSS2:ETS translocation in the development of the disease [17]. Moreover, studies of the spatial pattern of ERG alteration showed a complex progression of chromosomal alteration: first, formation of the TMPRSS2:ERG translocation, then loss of the sequence between TMPRSS2 and ERG and finally duplication of the ERG fusion gene [17]. However, the role of ETS expression in the development of metastatic prostate cancer is still debated. TMPRSS2:ERG frequency in metastases is generally lower than in corresponding primary tumors [17]. It is also important to notice that, although the majority of the ETS fusion "partners" are androgen regulated genes,

6

like TMPRSS2, the ETS fused proteins can be expressed in an androgen independent-fashion [18]. This observation may explain the presence of a cohort of patients that does not respond to androgen withdrawal therapy. A mechanism of development of castration resistant prostate cancer proposes the direct binding of ETS1 (and supposedly of other ETS transcription factors) to AR. This binding can trigger androgen independent activation of AR mediated transcription, inducing recruitment of AR on the DNA in the absence of androgens. In line with this hypothesis, over-expression of ETS1 induces AR nuclear accumulation and androgen independent transcription of AR regulated genes [19]. Because of the accepted correlation between ETS fusions and prostate cancer, therapeutic approaches targeting pathways associated with ERG over-expression or molecules upstream of ERG (MAPKs) have been proposed [17].

As mentioned above, most prostate cancers arise from the luminal epithelial cells. Less than 2% of the tumors can, however, develop from neuroendocrine (NE) prostate cells [20] or acquire a NE-like status. The prostate is comprised of four cell types [21] (fig. C):

- basal cells with lower or negligible AR expression. They surround the prostate gland and are organized as a monolayer supporting the epithelial cells. During prostate cancer development the basal layer is lost.

- Luminal epithelial cells from which most prostate cancers arise. They are terminally differentiated, secretory columnar cells that face the lumen of the gland.

- Neuroendocrine cells. This type of cell grows independently of androgen availability and they are scattered throughout the prostate epithelium.

- Stromal cells that surround the prostate gland.

Figure C. Organization of the different types of prostate cells in a prostate gland [3]
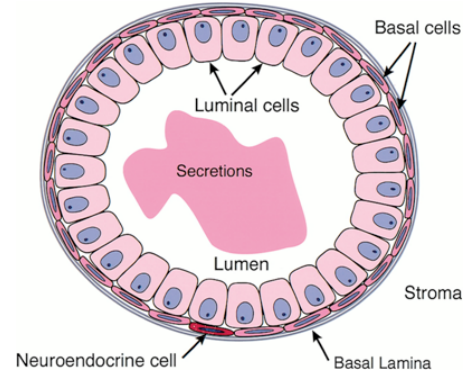
It is belived that because neuroendocrine cells are castration-resistant, regions of neuroendocrine differentiation are more commonly observed following recurrence after prostatectomy and androgen deprivation therapy [22]. Also, increased expression of neuroendocrine markers correlates with tumor progression, poor prognosis, and the androgen-independent state. An alternative explanation for the increased neuroendocrine cell population in prostate cancer could be a possible transdifferentiation of prostate cancer cells originated from epithelial cells. In this context some prostate cells are able to become "NE-like cells" that acquire the NE phenotype and express NE markers [23]. This idea introduces the two main hypotheses on prostate cancer development:

1) adaptation hypothesis: advanced/castration resistant prostate cancers develop after an accumulation of pro-tumorigenic aberrations that allow the formation of a highly aggressive and heterogeneous population of cells ultimately able to acquire an androgen independent phenotype.

2) Clonal selection hypothesis: advanced/castration resistant prostate cancers arise from a "prostate cancer stem cell" already present during the first stages of prostate cancer and are able to survive in the absence of hormone. This hormone refractory

feature of the prostate stem cells will allow them to survive the anti-androgen therapy and castration. The androgen independent cancer stem cells will then repopulate the prostate and give rise to a CRPC.

Despite the fact that primary prostate tumors contain multiple independent histological foci of cancer that are often genetically distinct [24], it has been shown that multiple metastases in the same patient are clonally related, therefore demonstrating the monoclonal origin of metastatic prostate cancer [25]. These and other observations seem to favor the clonal selection hypothesis although no convincing data support and favor one hypothesis over the other.

Regardless of the origin of advanced prostate cancer it is interesting to notice that, even in the context of CRPC, androgen receptor (AR) activation and AR signaling is found sustained in the majority of prostate cancers, suggesting a key role for AR in normal prostate as well as in prostate cancer [26]. A better understanding of the molecular mechanisms that regulate AR function and AR-mediated transcription is essential for the development of new preventative and curative strategies against all stages of prostate cancer.

II. ANDROGEN RECEPTOR (AR)

The androgen receptor is a member of the nuclear receptor super-family and more specifically it is part of the steroid hormone receptor family. AR is a transcription factor activated by the binding of androgens like testosterone (T) or the more potent 5α-dihydrotestosterone (DHT). The androgen receptor protein is characterized by several domains essential for its activity [27, 28]:

- the N- terminal domain that includes the activation function 1 (AF1) that acts independently of androgens

- the DNA binding domain (DBD) comprised of two Zn-finger domains

- the hinge region

- the C-terminal domain that includes the ligand binding domain (LBD) and an androgen dependent activation function 2 (AF2). The AF2 is important for the recruitment of cofactors containing an LXXLL motif [29]. These proteins assist and regulate AR-mediated transcription [30, 31].

A N/C terminus interaction was also shown to be essential for full AR transcriptional activity although the mechanism is still unclear [32].

Once bound to DHT the androgen receptor undergoes conformational changes that cause the dissociation of heat shock proteins (hsps) bound to AR in the cytoplasm [33, 34]. AR unbound to hsps such as hsp90 and hsp70, is able to dimerize and translocate into the nucleus where AR can bind the DNA on specific sites called androgen response elements (AREs). The consensus ARE sequence consists of two palindromic half sites spaced by three base pairs (AGAACAnnnTGTTCT). However, DNA-binding sites in natural gene promoters and enhancers may deviate considerably from the consensus sequence [35]. The binding of AR to the AREs is possible if chromatin is in an open and permissive state. Indeed it has been shown that the AR binding pattern on DNA is dictated by other proteins called pioneer factors that "prepare" the DNA for AR binding through chromatin remodeling and histone mark modification [36]. Among these pioneer factors, FoxA1 has been shown to be important for AR binding [37] especially to AREs that diverge from the canonical ARE sequence and therefore have a lower binding affinity for AR [38]. It has been suggested [37, 39] that changes in FoxAl expression could explain a misregulated and newly acquired AR transcriptional landscape. In particular a class of M-phase associated cell cycle genes was reported to be targeted by AR

binding particularly in CRPC cells compared to androgen sensitive cells [37]. This intriguing view of AR transcription misregulation could, at least in part, explain a molecular change in AR function between normal and prostate cancer cells. In normal prostate epithelium, AR acts as a transcription factor that regulates differentiation and inhibits proliferation. In fact, probasin-Cre mediated conditional deletion of AR, leads to increased proliferation and decreased expression of differentiation markers in normal prostate cells [40]. On the contrary, in prostate cancer, AR supports survival and proliferation of luminal cells, promotes metastasis and suppresses proliferation of basal cells [41]. This evidence suggests that AR undergoes a molecular "switch" during prostate cancer progression that makes AR essential for prostate cell proliferation. In line with the idea that, in prostate cancer cells, AR acquires new functions involved in cell proliferation, AR was shown to act as a licensing factor for DNA replication in prostate cancer cells but not in normal cells [42-44]. In these studies AR was shown to regulate the expression and protein stability of cdc6, a protein that initiates DNA replication. Consequently, in prostate cancer cells, AR protein needs to be regulated throughout the cell cycle and completely degraded during mitosis. Indeed, stabilization of mitotic androgen receptor protein causes inhibition of cancer cell proliferation [44].

Another explanation for the "gain-of-function" of AR in cancer cells comes from the observation that castration induces regression of prostate cancer through induction of apoptosis. *In vitro*, on the other hand, androgen dependent prostate cell lines simply stop growing in the absence of hormone and they do not undergo apoptosis [45]. This simple obsevation suggests that the pro-apoptotic signal triggered by hormone deprivation is induced by the stroma that surrounds the prostate glands in vivo. This hypothesis was validated by tissue recombination experiments showing that androgen is not able to induce proliferation of prostate epithelial cells in mice depleted of AR from the stroma [46]. Moreover, it was also shown that prostate cancer cells are able to bypass the need of the paracrine signals coming

11

from the stroma, thus inducing a different autocrine mechanism that stimulates androgen-dependent growth. Several molecules have been proposed to be important for the epithelial-mesenchymal interaction in prostate. The pathways that mediate this interaction during prostate organogenesis comprise the Wnt/β-catenin, the FGF (fibroblast growth factor) and the Hedgehog pathways [47-49]. These data underscore a complex scenario in which the androgen receptor has distinct roles and responds in cell context specific manner. Misregulation of the AR complex signaling in the context of other cellular events, such as the "switching" from a paracrine to an autocrine regulation, would confer acquired functionality to AR in a specific cell type.

In addition to changes in mesenchymal/epithelial interaction and altered recruitment of AR on DNA as a result of misexpressed pioneer factors, several other processes, that induce AR signaling misregulation in prostate cancer, have been shown [3, 26, 50]:

- increased activation of the androgen receptor by increased de-novo synthesis of testosterone and DHT in tumor tissues [51]

- amplification and increase in AR expression[52]

- gain of function mutations of AR that confer response to other steroid hormones, greater sensitivity to androgens or increased protein stability [53, 54]

- expression of short isoforms of AR encoding constitutively active AR [55-57]

- ligand-independent activation of AR by alternative pathways such as the MAPK, HER1/2 or NFKB (outlaw pathways) [58] [59]

- misregulated expression or function of AR cofactors [31, 60]

Cofactor recruitment is a crucial regulatory step in nuclear receptor activation. Upon ligand binding the nuclear receptors, including AR, undergo a conformational change that creates a hydrophobic groove at the top of the ligand binding pocket, enabling the docking of leucine-

rich, LxxLL motif-containing cofactors [61]. The nuclear receptor cofactors control conformation, nuclear-cytoplasmic localization, movement, DNA recognition, chromatin remodeling, and binding or release of the basal transcription factors [62]. The nuclear receptor cofactors can be classified as co-activatiors or corepressors. The co-activators positively regulate the nuclear-receptor mediated transcription recruiting the RNA polymerase II (polII) complex or chromatin remodeling proteins that make the DNA more transcriptionally active. The co-repressors, on the contrary, are proteins that inhibit nuclear receptor function through several mechanisms including the recruitment of proteins or complexes that render chromatin more compacted and less accessible to polII transcriptional machinery. More than 200 proteins have been shown to affect the transcription of the nuclear hormone receptor, acting as corepressors or coactivators [60]. Although AR has high sequence homology with the LBDs of other nuclear receptors and folds in a similar manner, AR appears to interact with coactivators in a unique fashion. The AR-LBD interacts poorly with the p160 class of LxxLL-containing cofactors used by other members of this receptor superfamily. It was shown that AR possesses an LxxLL-like, phenylalanine-rich FxxLF motif within its N-terminus (NTD), able to tightly bind the 'coactivator' pocket in the LBD and creating a N/C interaction characteristic of the androgen receptor [35, 63]. Also crystallographic analysis showed that AR possesses multiple surfaces for coactivator recruitment suggesting that the AR engages different classes of cofactors under different circumstances [60].

The transcriptional output of the ligand activated androgen receptor is the result of the combination of AR transactivation and transrepression signals. This fine-tuning of AR response is conferred by the binding and release of cofactors that orchestrate a complex network of signal response. It is not surprising that the aberrant expression or function of cofactors can lead to disease and tumorogenic development [62]. Though the majority of the androgen receptor coregulators are coactivators an increasing interest has been given to

corepressors [64]. Several mechanisms can be used by corepressors to interfere with androgen receptor transcription [31]:

- Inhibition of AR nuclear translocation and DNA binding. Examples of this class of corepressors are ARA67/PAT1, which promotes AR retention in the cytoplasm, calreticulin, that inhibits AR binding to the DNA and the p21-activated kinase 6 (PAK6)

- Recruitment of histone deacetylases (HDACs). Examples of this class of corepressors are HDAC1 itself, TGIF that binds the sin3A complex and HDAC1 and ARR19 (androgen receptor corepressor 19KDa) that recruit HDAC4.

- Interference with coactivators binding to AR. An example of this class of corepressors is cyclin D1 that inhibits P/CAF binding to AR.

- Interference with AR N/C interaction. Examples of this class of corepressors are Filamin A and hRad9.

- Recruitment of other corepressors. Examples of this class of corepressors are RACKI and PATZ proteins.

- Targeting the basal transcriptional machinery. Several members of the mediator complex that bridge polII machinery to the transcription factors, have been shown to interact with AR and affect its transcriptional function [65, 66]. For example the mediator protein 1 (MED1) has been shown to act as an AR cofactor through its LXXLL site and also through a non-canonical binding motif [66]. In particular, phosphorylation of MED1 on threonine 1032 was demonstrated to be essential for the recruitment of other mediators and for the initiation of transcription mediated by nuclear hormone receptors including ER and AR [67] [65]. Moreover MED1 was shown to be essential for AR looping from the enhancer regions to the promoter [68] of several androgen regulated genes. Indeed, it is now well accepted that most of the AR binding sites on the DNA are enhancer regions [69] that loop back to the promoter

of androgen regulated genes to recruit polymerase II transcriptional machinery. AR looping from the enhancer to the promoter of the PSA genes was elegantly demonstrated by Dr. Brown's laboratory [65, 70]. Also the elongation factor P-TEFb, that mediates the phosphorylation of polII C terminal domain (CTD), has been shown to bind the androgen receptor through its kinase subunit [71]. Interference with the interaction of AR with these regulators of polymerase II function would likely inhibit AR mediated transcription. The elongation factor ELL and the component of the negative elongation factor (NELF) that increases RNA polymerase II pausing, have been shown to regulate the transcription mediated by other nuclear receptors [72, 73].

Key co-repressors are the nuclear receptor corepressor 1 (NCoR1) and the silencing mediator for retinoic acid and thyroid hormone receptors (SMRT/NCOR2) that function as scaffolding to recruit other cofactors [64]. NCoR proteins belong to several of the classes of corepressors described above. They recruit HDAC proteins [74], they can compete with the binding of coactivators, recruit other corepressors, interfere with the N/C interaction of AR homodimer and affect polII recruitment [74].

The functional mechanism by which corepressors, like NCoR, can suppress AR or transcription of other nuclear receptors, is still under investigation. Recent studies analyzed the genome-wide recruitment of different corepressors along with histone marks and revealed a complicated interplay between coactivators and corepressors. The two main mechanisms proposed for corepressor action are the following [74]:

- Classic model of recruitment by transcription factors: according to this hypothesis the corepressors are recruited to inactive nuclear receptors and the switch from binding corepressors to coactivators triggers the activation of gene transcription. Examples of this class of corepressors are nuclear receptor-interacting protein 1 (RIP140/NRIP1), prohibitin 2 (PHB2), and the transcription intermediary factor 1a (TIF1a/TRIM24).

15

These corepressors are canonical repressors containing an LXXLL domain and are recruited in a ligand-dependent manner.

- Cyclical model: this model takes into consideration the recent discoveries that, at least for some genes, active transcription requires the cyclical recruitment of corepressors, such as HDACs, and coactivators. Interestingly, HDACs are more abundant on active genes than on repressed genes [75]. It has been suggested that deacetylation may reset the chromatin structure for subsequent rounds of transcription. These findings seem to indicate that some genes are in a paused state, ready to be transcribed, but not yet active [74]. Stimuli that trigger histone acetylation will then recruit RNA polII and initiate productive transcription. In the case of NCoR1 and NCoR2, TBL1 and TBLR1 have been shown to act as "nuclear corepressor exchange factors" (NCoEx) that mediate the ubiquitination-dependent release of corepressors that induce transcription activation [76]. Interestingly TBL1 and TBLR1 proteins are core components of the NCoR complexes suggesting that these repression complexes are already primed to release upon their recruitment. The events that induce the switch from repression to de-repression are still not well understood for many repression complexes.

The evidence supporting the existence of both of these two mechanisms suggest a complex scenario designed to tightly regulate transcription mediated by nuclear receptors.

Finally, many proteins bind to AR, and act as AR corepressors, but their precise mechanism of action has not yet been elucidated. Examples of these corepressors are the sex-determining region Y (SRY) transcription factor, HBO1 protein and the EbpI protein, a member of the Erb/HER2 family of receptors [31]. Also, the androgen receptor trapped clone 27 (Art-27) [77] is an androgen receptor corepressor interacting with the N-terminus of AR for

which no functional mechanism has been described. This thesis work is part of an effort to understand the mechanism of repression of the Art-27 complex also comprising URI.

III.   ANDROGEN RECEPTOR TRAPPED CLONE 27 (ART-27)

Art-27, also known as SKP2-associated protein 1 (STAP1) and encoded by a gene called ubiquitously-expressed transcript (UXT), is an androgen receptor cofactor that was isolated from an androgen-stimulated LNCaP cell library, in a two-hybrid screen designed to identify proteins that interact with the N-terminal activation domain of the androgen receptor [77]. The primary sequence of ART-27 is conserved throughout evolution from worms to humans and its predicted protein structure shows structural homology to the prefoldin-α family of chaperones [78]. Art-27 was shown to bind the AR N-terminus as well as other transcription factors such as glucocorticoid receptor (GR), estrogen receptor (ER), sp1 and the TBP associated factor $TAF_{II}130$. Art-27 is specifically expressed in the epithelial/luminal cells and not in the stroma of prostate and breast glands and its expression is regulated during development. In particular, in prostate, Art-27 is expressed upon differentiation of the glands after budding from the urogenital sinus as shown by Art-27 staining of 15 and 21-week old human fetal prostate. The specific expression of Art-27 upon differentiation of prostate cells was also confirmed in castrated versus control rats [79]. *In vivo*, the Art-27 specific expression pattern correlates with activation of cAMP-response element binding protein (CREB), a transcription factor that is recruited to the ART-27 promoter and is required for epidermal growth factor (EGF)-induced expression of ART-27 [80]. E2F transcription factors were also shown to bind the promoter of Art-27 and suppress its transcription through binding to members of the retinoblastoma (Rb) protein family (specifically the pocket protein family members p107 and p130) [81].

17

Art-27 was shown to inhibit AR-mediated transcription. Overexpression of Art-27 in HEK-293 cells expressing AR and a luciferase reporter under the control of multiple AREs induces decreased luciferase expression [82]. Also, knock down of Art-27 in LNCaP prostate cell lines by siRNA induced increased expression of canonical androgen regulated genes like PSA, NKX3.1 and FKBP5. Depletion of Art-27 also impairs the response of prostate cells to bicalutamide, a known anti-androgen clinically used against prostate cancer. Knock down of Art-27 induced loss of bicalutimide-mediated repression of several androgen regulated genes such as PSA, KLK4, NKX3.1, TNFRSF10B and others. In the absence of Art-27, bicalutamide switches from being an AR antagonist to a partial agonist able to induce the expression of androgen regulated genes. Also, in line with evidence demonstrating the role of Art-27 as an androgen receptor corepressor, overexpression of Art-27 in the androgen sensitive LNCaP cell line, induced inhibition of growth [79].

Interestingly, Art-27 expression was shown to be decreased in prostate cancer compared to normal tissues [79] and loss of nuclear Art-27 correlated with the development of prostate cancer into castration resistant prostate cancer (CRPC) [78]. Moreover Art-27 corepressor function and Art-27 binding to AR was impaired in cells expressing mutations of AR found in prostate cancer (AR P340L and AR E2K) [83]. This data suggests that, in prostate, Art-27 acts as a tumor suppressor.

Velocity gradient sedimentation of Hela cell nuclear extracts showed that Art-27 cosediments at a high molecular weight (over 240 KDa) suggesting that Art-27 is part of one or more large multiprotein complexes [77]. Several mass spectrometry and immunoprecipitation experiments performed in non-prostate cells identified several interactors of Art-27. The search for proteins interacting with the S-phase kinase-associated protein 2 (SKP2) indentified Art-27 as an interactor [84]. In HeLa cells Art-27 was also found to bind the two single-stranded DNA-stimulated ATPase and ATP-dependent DNA helicases

TIP48/RUVB1 and TIP49/RUVB2, the RNA polymerase subunit RPB5/POLR2E, prefoldin2 (PFDN2) and prefolin4 (PFDN4) components of the prefoldin chaperone complex and the RPB5 interacting protein RMP/URI [84]. More recent work identifies Art-27 as a RNA polymerase II interacting protein and more specifically as a protein interacting with the polII core subunit RPB1/POLR2A, containing the C-terminal domain (CTD) phosphorylated on serine2 and serine5 by the kinase complex p-TEFb [85, 86]. Interestingly Art-27, together with URI, RPB5 and other proteins, was identified as part of a R2TP/prefoldin-like complex important for the assembly of RNA polymerase II in the cytoplasm of eukaryotic cells [87]. Art-27 was also shown to be an essential part of the NF-kB complex that regulates NF-kB transcriptional activity [88]. In addition, Art-27 has been shown to be important for the virus-induced activation of NF-κB and IFN regulatory factor 3 regulating the translocation of TRAF3 and TNFR-associated death domain protein in the mithocondria [89]. Other roles of Art-27 comprise binding to the transcription repressor EVI1 [90] and Amyotrophic Lateral Sclerosis 2 (Als2) protein [91], induction of mitochondrial aggregation and binding to the centrosome to regulate centrosome function [92].

For the purpose of this work the nuclear role of Art-27, in particular as an AR corepressor, will be specifically considered.

IV.   UNCONVENTIONAL PREFOLDIN RPB5 INTERACTOR (URI)

The Unconventional prefoldin RPB5 Interacting proten (URI), also known as RPB5-Mediating Protein (RMP) is encoded by the C19orf2 gene [93] and it was identified by Far Western as a RPB5 interacting protein [94]. RPB5 is a shared subunit of the three RNA polymerases, it is essential for polII transcription with overlapping functions to the RPB1 CTD domain [95] and it

is considered important for mediating RNA polymerase interaction with factors that affect transcription [96]. RPB5 was shown to directly interact with Hepatitis B Virus X protein (HBx) and with the basal transcription factor IIB. URI was also shown to interact with TFIIF subunit RAP30 [97, 98] [94] and to interfere with the binding of HBx to RPB5 [94]. In line with the idea that URI is part of a complex that regulates RNA polymerase transcription, URI was also shown to bind parafibronin, a component of the Paf-1 complex involved in promoting polymerase II CTD phosphorylation and histone modification during elongation [99]. Also URI was found to be part of a R2TP/prefoldin-like complex that assembles the RNA polymerase II complex in the cytoplasm [87] [100] [85]. This complex comprises 11 subunits: URI, Art-27, RPB5, prefoldin 2 (PFDN2), prefoldin 6 (PFDN6), the DNA helicases TIP49 and TIP48 previously shown to bind Art-27 and URI, WD repeat domain 92 (WDR92), p53 and DNA damage-regulated protein 1 (PDRG1), PIH1 domain containing 1 (Pih1D1) and RNA polymerase II associated protein 3 (RPAP3/Spaghetti). Interestingly, 5 of these proteins (URI, Art-27, PFDN2, PFDN6 and PDRG1) are prefoldin or prefoldin-like proteins. Bioinformatic analysis of URI structure (Phyre version 2.0, [101]) revealed that URI has an N-terminus α-prefoldin structure similar to Art-27, and a large and complex C-terminus where several phosphorylation sites cluster together [102] and to which several proteins have been shown to interact (Fig. D). Two different splicing variants for URI, URI α and URI β, have been identified, but their characterization, and specific expression or role is still not known.
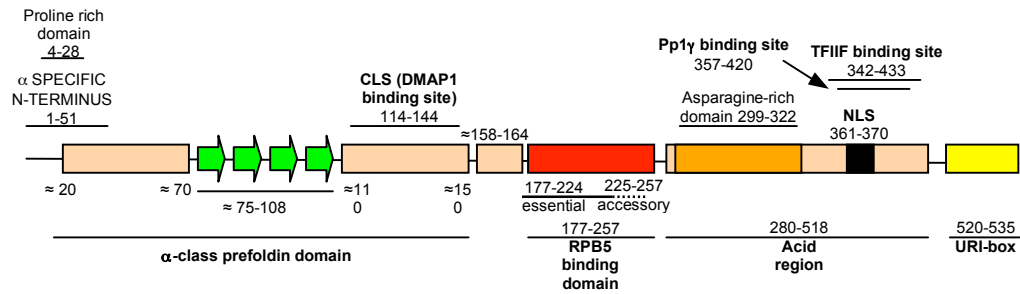
Figure D. Schematic of URI protein domains. The numbers indicate the amino acid number from 1 (N-terminus) to 535 (C-terminus).

URI was shown to be a transcriptional repressor by chloramphenicol acetyltransferase (CAT) assays in which a GAL4-CAT reporter (5 tandem repeats of GAL4 binding sites upstream of the CAT gene) and a GAL4-VP16, a chimeric activator with the GAL4 DNA-binding domain fused to VP16 activation domain, were transfected in HepG2 cells. Concurrent transfection of full length URI induced inhibition of VP16 transcription activation. URI overexpression also inhibited transcription induced by HBx and NFkB [94, 97]. The authors also suggested that, despite the fact that URI inhibits several transcriptional activators, the URI-mediated repression is not a general process because, for example, p53 transcription seemed to be unaltered by URI [94, 97]. Although URI was shown to bind RNA polymerases and several proteins involved in transcription, very limited work has been done to characterize the transcriptional and nuclear function of URI.

More recent reports from the W. Krek laboratory identified URI as a critical node in the mToR pathway. In particular, URI was shown to be essential for the response of Saccharomyces cerevisiae to nutrient starvation conditions [84]. In fact URI can be phosphorylated downstream of the mToR pathway by the p70S6 kinase (S6K1) upon various stimuli such as IGF1 and insulin. This mToR-dependent phosphorylation of URI was inhibited by rapamycin, a specific inhibitor of mToR complex 1 and an indirect inhibitor of mToR

complex 2 [103]. In HeLa cells URI was demonstrated to bind and inhibit PP1γ phosphatase in the mitochondria. Phosphorylation of URI by S6K1 kinase on serine 372 induces release of PP1γ from URI binding. Un-bound PP1γ phosphatase becomes active and it is able to dephosphorylate several substrates involved in apoptosis including BAD1 which, in its dephosphorylated form, can trigger programmed cell death. Furthermore, active PP1γ can dephosphorylate p70S6K and URI in a feedback loop [104, 105]. Known PP1 interacting proteins include the Aurora kinases (A, B and Ipl1), Bcl proteins (Bcl-2, Bcl-XL, Bcl-w), NCoR, Rb protein, p53 and CREB. The dephosphorylated form of CREB has been demonstrated to be more stable and is not targeted for degradation [106]. The binding of URI to a PP1 phosphatase was not surprising because of the presence of two known motifs that mediate binding to PP1 phosphatase [107, 108] in the URI primary amino acid sequence. URI contains a degenerate RVXF domain (a.a. 522-526) in the URI box domain, at the protein C terminus, and also a KGILK similar sequence in the URI acidic region (a.a. 407-411). These motifs are found in several PP1 interacting proteins and their presence within the URI sequence strengthens the finding that URI is able to bind PP1 phosphatases.

Based on the mitochondrial function of URI and in contrast with its nuclear function as a transcriptional repressor, URI should act as an oncogene. Indeed, in the mithocondria, URI is able to control the pro-survival signal downstream of the mToR pathway through the regulation of the PP1γ phosphatase. Increased expression of URI was shown to induce sustained activation of the mToR pathways even in conditions of nutrient deprivation. The oncogenic role of URI was recently demonstrated in ovarian cancer [109, 110] and hepatocellular carcinoma [111]. In these tumor cells URI promotes proliferation and survival through a PP1γ and p70S6 kinase-dependent mechanism. Also, in ovarian cancer, URI-amplification correlates with rapamycin and cisplatin resistance [109]. Moreover C19orf2 is one of 8 genes shown to be altered in cytarabine (ara-C)-resistant leukemic cell lines

22

compared to parental cells. Ara-C interferes with DNA synthesis, inhibits DNA and RNA polymerase transcription and is the main drug used for the treatment of acute myeloid leukemia [112].

Interestingly URI depletion was also associated with DNA instability in C. elegans [113] and in Drosophila [114]. In C. elegans URI deletion induced sterility, G2/M arrest and HUS-1 and p53 dependent apoptosis in the germ cells [113]. In Drosophila URI was shown to bind PP1α phosphatase and transcribing RNA polymerase and to be highly expressed in embryos, pupae and adult gonads. Intriguingly in the Drosophila testis, URI is expressed in the apical region where the stem cells and the less differentiated spermatogonia reside. Also, as in C. elegans, URI deletion induced partial sterility and cell death in the germline caused by DNA instability [114]. These data seem to suggest a role for URI in DNA damage and DNA integrity particularly in germline cells.

A screen to identify proteins that interact with the jumonji domain of the yeast zinc finger protein Gis1 revealed that Bud27 (the yeast counterpart of URI [115]) is part of a multimeric complex important in transcription, sumoylation and DNA repair [1] (fig. E). The Gis1 protein was demonstrated to be important for restricting caloric growth as part of the ToR/sch9/rim15/gis1 pathway. Interestingly the JMJ (jumonji) proteins have a demethylating activity in mammalian cells, similar to their bacterial homologues. The JMJ protein JHDM2A was also shown to function as an AR coactivator [116-118]. Gis1 is a DNA damage responsive repressor of PHR1 (photoreactivation lyase 1), a gene that encodes a DNA repair enzyme. Bud27/URI was demonstrated, by yeast two hybrid experiments, to directly interact with the Gis1 protein as well as with Pig2 (a putative PP1 subunit), and two proteins of unknown function, Zrg8 and Gds1 (fig. E). In addition URI interacts with Sgs1 protein, a homologue of the human RECQ involved in homologous recombination in response to stalled replication forks and double strand breaks. Bud27/URI binds directly or indirectly to 11 other

proteins found to be part of the Gis1 complex in yeast (Bud27/URI binds to all but 3 of the 19 proteins of this complex). Among the binding partners of particular interest are Sir4, involved in transcription silencing, Mft1, involved in transcription elongation and Taf8, a TFIID subunit. The three proteins belonging to the Gis1 complex that do not interact with Bud-27/URI are involved in sumoylation suggesting that Bud-27/URI may be not involved in this function.
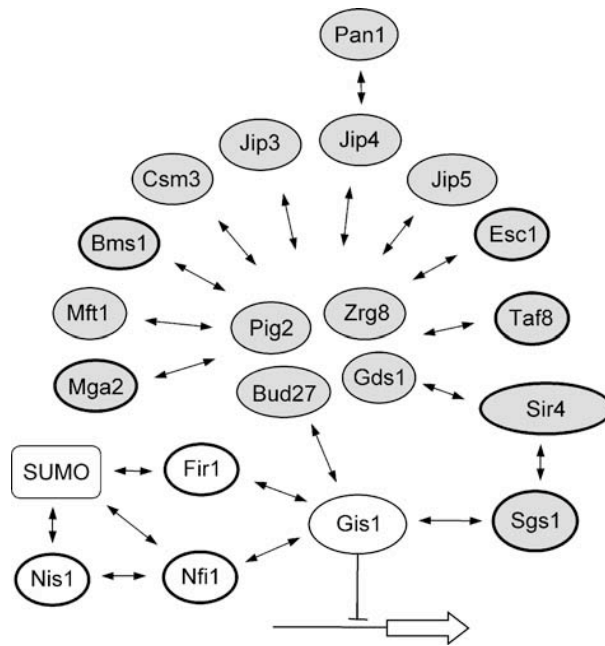
Figure E. Proteins that interact with the Bud27 bait are shown in grey. Proteins that are known to be sumoylated or interact with SUMO have bold outlines. [1].

Interestingly, a screen performed in yeast to identify proteins involved in the Ty1 retrotransposon movement showed that deletion of URI induced high Ty1 mobility, second to spt5 deletion [119]. This data could be functionally linked to the GIS1 complex described above and to the observed role of URI in DNA stability in C. elegans and Drosophila. Finally yeast URI (Uri1p) was shown to promote translation initiation [120].

In its entirety, this body of data indicates that URI is a multifunctional protein with distinct roles in the different cellular compartments (mitochondria, cytoplasm, nucleus).

Moreover the studies performed in yeast underscore a complex and still unknown role of URI in RNA polymerase transcription, DNA stability and chromatin structure.

V.   KRAB ASSOCIATED PROTEIN 1 (KAP1)

The KRAB (Krüeppel-associated box)-associated protein 1 (KAP1), also known as KRIP1 (KRAB-A-interacting protein 1), TIF1β (transcription intermediary factor 1β) or TRIM28 (tripartite motif-containing protein 28) was identified in 1996 as a KRAB-domain interacting protein [121-123]. The Krueppel-associated box (KRAB) is a domain composed of about 50-75 amino acids that is found at the N-terminus region of the Krueppel-type C2H2 zinc finger proteins (ZFPs) [124, 125]. The Krueppel-type C2H2 ZFPs represent about one third of eukaryotic Zinc finger proteins and, as a result, these proteins make up the largest family of transcription regulators in mammals with about 290 members.

KAP1/TRIM28/TIF1β is highly related to three other TRIM proteins, TIF1α, TIF1γ and TIF1δ. All the TIF proteins, including KAP1, contain a TRIM domain at the N-terminus, a central TIF1 signature sequence (TSS) and a C-terminal homodomain (PHD)/ bromodomain [126]. The TRIM domain is composed of an RBCC domain that comprises a Ring-(really interesting new gene) finger domain, two B-box zinc fingers and a coil-coil domain. Although the three TIF proteins have high homology there is little overlap among their functions [127]. TIF1α, for example, was shown to be a coactivator for nuclear hormone receptors [128, 129] and, unlike KAP1/TIF1β it binds very weakly to the KRAB domain, while TIF1γ has a role in hematopoiesis and transforming growth factor (TGF) signaling [130]. In line with their different functions the TIF1 proteins also have a different expression pattern; KAP1/TIF1β is

ubiquitously expressed, TIF1δ is restricted to testis in particular stages of spermatid development and TIF1α is mainly expressed in the central and peripheral nervous systems early in development [126].

The N-terminal RBCC domain of KAP1 is responsible and sufficient for the interaction with the KRAB-ZFPs [127]. Biochemical evidence suggests that KAP1 binds the KRAB domain as a homo-trimer to promote folding and encapsulation of the KRAB domain into a protease-resistant core [131]. The central region of KAP1, between the RBCC and PHD/bromo domain, has a pentameric sequence (PxVxL) that interacts with the chromoshadow domain of the HP1 proteins. The interaction with HP1 was shown to be essential for the KAP1 transcriptional repression function [132]. The C-terminal domain of KAP1, comprising the PHD and bromodomain, is responsible for the binding to chromatin modifying enzymes, specifically Mi2α/CHD3, a member of the NuRD/HDAC histone deacetylases complex and SETDB1, a methyl-transferase that methylates histone H3 on lysine 9 (H3K9). The recruitment of these chromatin remodeling factors by KAP1 induces formation of facultative heterochromatin and maintains the transcriptional repressive state within heterochromatin regions [124]. It is thought that of the two chromatin modifications (histone acetylation and H3K9 trimethylation) acetylation may play a minor role in KAP-1 mediated repression because inhibitors of histone deacetylases (HDACs) only partially relieve KAP1 mediated repression [133].

All these data clearly suggest that KAP1 is a scaffold protein with a modular structure that allows interaction of KAP1 with DNA binding proteins through its N-terminus, and induces recruitment of a repression complex comprising of HDACs and histone methyltransferases through its C-terminus (fig. F).

The ability of KAP1 to repress transcription through the maintenance and formation of a transcriptionally non-permissive chromatin state, has been functionally linked to an important

role in development [134] and germ cell differentiation [135]. KAP1 knock out mice are embryonically lethal and die after implantation and before gastrulation [134]. Interestingly, embryos from these mice have reduced ectoderm cell number, morphological alterations of the endoderm and absence of mesoderm formation. The crucial role of KAP1 in mesoderm formation was also demonstrated in vitro using embryonal carcinoma F9 cell lines which are able to differentiate into mesoderm-like cells upon retinoic acid treatment [132]. In line with a crucial role in early development, KAP1 is highly expressed in the embryo as early as embryonic day E4.5. More recent studies show that KAP1-HP1 interaction is essential for post-gastrulation development, but not to promote the role of KAP1 during spermatogenesis [136]. Also KAP1 has been shown to affect chromatin and DNA methylation of imprinting control genes during early embryogenesis through the binding to ZFP57 [137]. In mice KAP1 is also indispensable for the convergent extension and morphogenesis of extra-embryonic tissues through the action of the ZFP568, another KRAB-ZFP [138]. During spermatogenesis KAP1 is expressed in Sertoli cells and round spermatids in which it is associated with heterochromatin structures and meiotic chromosomes. KAP1 is not expressed in spermatogonia. Mice lacking KAP1 specifically in the germ cells present testicular degeneration due to shedding of immature germ cells and disappearance of stem spermatogonia [135]. Interestingly KAP1 interaction with HP1 is not necessary for Sertoli cell function during spermatogenesis suggesting that KAP1 interaction to HP1 is not essential for all KAP1 functions [136]. KAP1 was also shown to interact with MAGE I transcription factors, a class of proteins normally expressed only in developing germ cells, the trophoblast and placenta. These proteins are re-expressed during cancer and they correlate with tumor aggressiveness [139]. It has also been shown that sex-determining region Y (SRY) utilizes KAP1 to induce transcription repression. SRY was shown to bind the protein KRAB-O, a KRAB containing protein derived from an alternative splicing of the ZFP784/208 that does not

27

contain zinc finger motifs. KRAB-O, therefore, can bridge SRY transcription factor to KAP1 and to the repression complex [140]. SRY is thought to be a transcriptional repressor that suppresses ovarian differentiation and activates testicular differentiation [141]. This function is probably mediated through the regulation of Sox9 by SRY [142].

Because of these data demonstrating an essential role of KAP1 in embryogenesis and differentiation, it is not surprising that recent work showed that the SETDB1/KAP1 complex has an important role in maintenance of embryonic stem cell (ESC) pluripotency [143-145]. Interestingly, in mouse embryonic stem cells, KAP1 was demonstrated to bind the transcription factors Oct3/4 and components of the SWF/SNF complex such as BrgI, SmarcD1 and BAF155 [143]. Notably KAP1 had already been previously shown to bind SWF/SNF proteins, forming a complex also comprising the nuclear hormone co-repressor NCoR1 [146].

Despite the great knowledge of the KAP1 complex and the KAP1 interacting proteins, and the extensive data connecting KAP1 to differentiation and embryonic development, the precise mechanism that mediates KAP1 function is still debated. Few target genes regulated by KAP1 have been described, although ChIP-seq or ChIP-chip experiments revealed more than 7000 binding sites for KAP1 on the entire genome [126]. The strongest KAP-1 binding sites are in the 3'-coding exons of ZNF genes. Mutation of the KAP1 RBCC domain induced loss of KAP1 recruitment on these genes suggesting that ZFPs target KAP1 to these DNA regions. This evidence suggests, therefore, that the ZFPs can autoregulate their own expression [147]. The sites of KAP1 binding on the 3' exons of ZFPs, however, are just a few of the sites to which KAP1 binds. Other binding sites are in intragenic regions or near the gene transcription start site (TSS). Interestingly deletion of the RBCC domain did not affect KAP1 binding to these TSS proximal regions suggesting a novel mechanism of recruitment for KAP1, independent of ZFPs. Mutation analysis shows that the central region of KAP1 is important for the recruitment to promoter targets [148]. Unexpectedly, alligment of gene

28

expression data from KAP1 depleted cells compared to control cells, and the ChIP-seq recruitment of KAP1 revealed very few genes whose expression is affected by KAP1 depletion and on which KAP1 is recruited on the promoter or coding region. This result led the authors to conclude that KAP1 may play a role distinct from transcription regulation at the majority of DNA binding sites [148]. A possible explanation comes from the demonstration that KAP1 is able to mediate long-range transcriptional repression through heterochromatin spreading. This result suggests that recruitment of KAP1 to a specific DNA region could affect the expression of genes positioned several tens of kilobases away from the site of KAP1 binding [149]. These puzzling results and unexpected questions are under investigation.

The activity of KAP1 is regulated by post-trancriptional modifications. The C-terminus of KAP1 that recruits the repression complex (SETDB1, HDACs) was shown to be SUMOylated on several lysines (K554, K575, K676, K750, K779, K804)[150, 151]. The PHD domain of KAP1 has E3 ligase activity and is able to sumoylate the adjacent bromodomain. Sumoylation of KAP1 creates the correct interface for the recruitment of the repression complex and also stimulates the histone methyltransferase activity of SETDB1 bound to KAP1 [152]. Interestingly, KAP1 was also shown to be phosphorylated on serine 824 and serine 473 downstream of the DNA damage pathway [153]. Serine 824 was shown to be phosphorylated by the ataxia telangiectasia mutated (ATM) kinase [154, 155] while serine 473 is phosphorylated by the cell-cycle checkpoint kinase chk1 [156]. Serine 473 is located near the HP1-interacting motif PXVXL and therefore its phosphorylation was critical for KAP1 interaction with HP1 and KAP1 mediated gene silencing [157]. Phosphorylation on serine 824 has been shown to interfere with sumoylation and therefore inhibits the recruitment of the repression complex. In fact, phosphorylation of KAP1 ser824 induced de-repression of known KAP1 regulated genes involved in apoptosis and cell cycle arrest (namely p21$^{\text{WAF1/CIP1}}$, GADD45α, BAX, NOXA and PUMA) [153, 158]. Interestingly the group of Dr. D.K. Ann

demonstrated that PP1 phosphatase α and β can regulate KAP1 serine 824 phosphorylation [158]. In particular PP1α was shown to constitutively bind KAP1 while PP1β binding is induced by DNA damage caused by doxorubicin. It has also been shown by chromatin immunoprecipitation experiments that the PP1-KAP1 interaction occurs on the chromatin.

It is clear that KAP1 has a role in the DNA damage response. As mentioned above, upon ATM activation KAP1 is phosphorylated and genes usually repressed by the KAP1 complex can be expressed. These genes are involved in cell cycle arrest and apoptosis. Also, upon DNA damage, KAP1 is rapidly recruited on DNA damage foci where it colocalizes with several DNA damage response proteins [154]. In particular, colocalization of phosphorylated KAP1 with the p53-binding protein 1 (53BP1) was shown to be essential for the repair of double strand breaks (DBS) located in heterochromatic domains [159]. It has been proposed that recruitment and phosphorylation of KAP1 on the DNA damage loci induces chromatin relaxation through the dissociation of KAP1 from the CHD3 helicase that is part of the Mi2α complex [160]. It is possible that KAP1 recruitment and phosphorylation promotes chromatin decondensation required for the access of DNA repair proteins, and subsequent KAP1 dephosphorylation and resumoylation can induce recondensation after repair [126].

KAP1 has been also shown to regulate apoptosis in a transcriptionally independent manner. Interaction of KAP1 with the E3 ubiquitin ligase MDM2 was demonstrated to inhibit p53 acetylation stimulating the interaction with HDAC1 and inducing p53 ubiquitination and degradation [161, 162]. Moreover KAP1 can independently promote p53 ubiquitination through its E3 ubiquitin ligase activity of the PHD domain [161]. Also, KAP1 binds MAGE proteins that can regulate KAP1-mediated transcriptional gene repression [139] and can also enhance the KAP1-MDM2-p53 complex resulting in suppression of p53 and tumor cell proliferation [163].
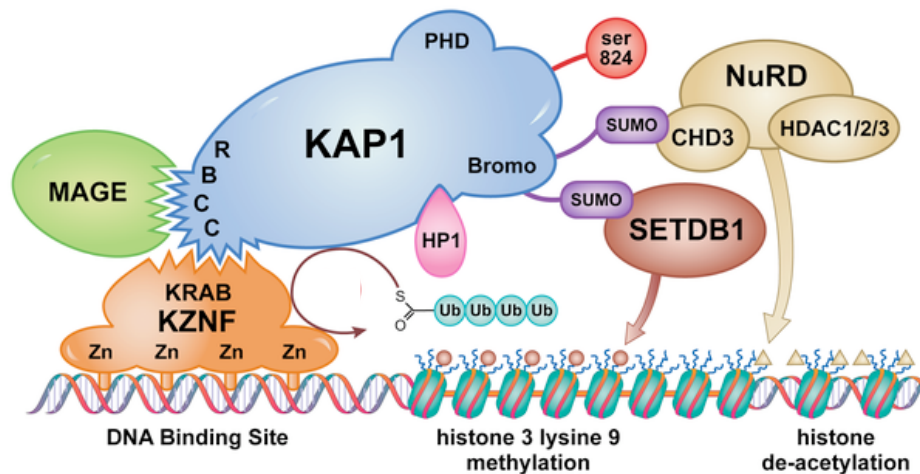
Figure F. Schematic of recruitment of the KAP1 complex on DNA. KRAB-ZFPs can bind DNA and recruit KAP1 through the KRAB domain that binds the RBCC region on the N-terminus of KAP1. SETDB1 and the histone deacetylase complexes NuRD and CHD3/MI2α can be recruited in a sumoylation dependent manner to KAP1. Phosphorylation on serine 824 represses sumoylation and therefore regulates recruitment of SETDB1 and HDAC complexes. KAP1 also binds HP1, which interacts with H3K9me3 and stabilizes KAP1 interaction with the heterochromatic domain of the DNA. KAP1 also binds MAGE proteins [139].

KAP1 was recently shown to control endogenous retrovirus repression in embryonic stem cells but not in embryonic fibroblasts (as described in the introduction section VI) [164] [126]. Given this finding it was not surprising that the histone methyl transferase SETDB1, recruited on the DNA by KAP1, was also involved in suppression of retroelements in embryonic stem cells [145, 165]. Interestingly, KAP1 was involved not only in the reactivation of endogenous retroviruses but it was also shown to inhibit integration of HIV-1 and other viruses [166-168].

Finally KAP1 is thought to suppress recombination. KAP1 recruitment on the 3'-end of highly homologous ZFPs that contain many repetitive domains in their 3'-end, was suggested to mediate heterochromatinization of these regions to prevent recombination-mediated deletion [126, 169].

The fact that KAP1 is involved in the control of apoptosis and cell cycle arrest upon DNA damage, and that it controls endogenous retrovirus repression and virus insertion as well as the fact that it can suppress recombination led to the idea of KAP1 as the "guardian of the genome". Also the fact that depletion of KAP1 has a very limited effect on gene expression despite the many DNA sites to which KAP1 is recruited, makes KAP1 an enigmatic protein for which the mechanism of action is still under investigation and subject to debate [126].

VI.   TRANSPOSONS

Transposable elements (TE) or transposons are DNA sequences that have the capablility to "move" within the genome of a cell. Transposons are thought to be remnants of germline infections by exogenous retroviruses during the course of evolution [170]. Remarkably, about 44% of the human genome is comprised of transposable elements but just a small portion of these transposons are still active today [171]. The transposable elements can be divided into DNA or RNA families of transposons. DNA elements, which make up ~3% of the human genome, are able to "jump" within the genome with a "cut-and-paste" process. The DNA elements can, indeed, excise themselves from the genome and move and reinsert into a new DNA site. The DNA transposons in the human genome are not mobile anymore although they were active during early primate evolution, until ~37 million years ago [172]. The RNA transposons, also called retrotransposons or retroelements, duplicate through RNA

intermediates using a "copy-and-paste" process. Retroelements can be classified in long terminal repeat (LTR) and non-LTR elements depending on the presence or absence of flanking highly repeated domains. Human LTR elements account for about 8% of the genome and their activity is quite limited [172]. The most studied LTR elements are the human endogenous retroviruses (hERV) and among those, hERV-K elements have been reported to still maintain some activity [173]. In contrast to humans, rodents retain a high level of LTR-element activity [174]. The vast majority of human TEs result from non-LTR retrotransposons that can be classified in long interspersed element-1 (LINE-1 or L1) (constituting about 17% of the human genome), short interspersed elements (SINE) represented by Alu elements (with more than 1 million copies in the human genome) and the most recently characterized SVA elements (with about 3000 copies in the human genome) [175]. The non-LTR retroelements are the only class of TEs that was unequivocally shown to be still active in the human genome and to be the cause of genetic disorders [172]. L1 elements are the most "successful" retroelements in the human genome. L1 canonical full length is about 6kb in length and is characterized by a 5' untranslated region (UTR) with an internal RNA polII promoter, two open reading frames, ORF1 and ORF2, encoding RNA binding proteins (ORF1), endonuclease and reverse-transcriptase (ORF2), and a 3' UTR containing a polyadenylation signal of variable length [172]. L1 is the only autonomous TE of the human genome. Alu and SVA elements indeed need to "borrow" the retrotransposition machinery encoded by the L1 elements and, therefore, they are sometimes referred to as "parasite's parasite" [172].

Because the uncontrolled movement of transposons can have a deleterious effect on the genome, cells developed several mechanisms for the repression of these repetitive elements. It has been shown that transposon expression can be inhibited by [176]:

- DNA methylation (proposed to have evolved primarily for the repression of retroelements)

- histone modification

- RNA interference (RNAi) mechanisms.

DNA methylation of cytosine at CpG dinucleotides is a well-established mechanism for gene repression in mammals and plants but is absent in Drosophila and C. Elegans. Two DNA methylase enzymes are mainly involved in the methylation of CpG islands:

DNMT3, that mediates *de-novo* DNA methylation, and DNMT1, which is responsible for the maintenance of methylation. DNMT1, indeed, has preference for hemi-methylated DNA and is essential for the re-establishment of DNA methylation during DNA replication [176]. How these DNA methyltransferases recognize the specific DNA domains that need to be methylated is still debated. Measurement of retroelement reactivation in mice lacking DNMT3 (isoform a and/or isoform b) showed a mild reactivation of retroelements compared to the 50-100 fold increase in expression of retroelements (specifically IAP elements) observed in DNMT1 knock out embryos [145, 177].

Endogenous retroviruses, the predominant and remaining active class of retroelements, are also repressed by histone methylation. Genome wide maps of histone and DNA methylation showed that the two modifications are intricately linked, positively correlate with H3K9 and K27 methylation, and negatively correlate with H3K4 methylation. Histone methyltransferase and DNMT deletion experiments revealed that, during development, DNA methylation is dispensable and the key mechanism for ERV silencing is histone H3K9 trimethylation, while, in differentiated cells, DNA methylation is essential and H3K9me3 is not necessary for ERV silencing [176]. More specifically, recent studies identified SETDB1 (ESET/KMT1E) as a key methyltransferase that mediates repression of retroelements through tri-methylation of H3K9 in embryonic stem cells [145, 165]. As mentioned above the recruitment of SETDB1 on the DNA is mediated by KAP1 interaction with KRAB-ZFPs and indeed KAP1 has also been shown to be essential for the control of retroelements in

embryonic stem cells [164]. Interestingly the emergence of endogenous retroviruses (ERVs) during evolution coincides with the rise of the KRAB-ZFP family, perhaps suggesting that this class of DNA binding proteins evolved in an attempt to fight ERV expression. In line with this idea it is also possible that RNA interference mechanisms are more specific in mediating the repression of evolutionarily more ancient LTR and non-LTR retrotransposons [176].

A third way through which retroelements are repressed is the RNAi machinery. Small RNA silencing of repetitive elements has been well established in plants and Drosophila. In particular the PIWI-interacting RNA (piRNA) pathway was shown to be responsible for retroelement repression in Drosophila. In germ cells, PIWI (P-element induced wimpy testis in Drosophila), Aubergine and Ago3 proteins are able to bind piRNAs, 24-30 nucleotide sequences transcribed from repeat-rich clusters and generated by a Dicer-independent process. piRNA-PIWI/Aubergine/Ago3 complexes can recognize transcribed retrolements and mediate their degradation and cleavage [178]. Also, Piwi proteins bound to piRNA can directly repress the transcription of transposones binding the 3' end of the retroelements [179]. PIWI hortologues have been identified in mouse and named MIWI, MILI and MIWI2 [180, 181].

The repression of transposons is particularly important during early development when "waves" of demethylation and chromatin re-setting take place to ensure pluripotency of the zygote. The repression of retroelements is also an essential and tightly regulated mechanism in embyonic stem cells [145] and germ cells [176]. Indeed knock down of key components of the machinery (SETDB1, PIWI proteins, KAP1, DNMT1 and others) that repress retroelements, induces embryonic lethality and sterility. Also these proteins are predominantly expressed in embryos, ovary, testes and thymus underscoring their importance in development and germline differentiation [176]. Until recently, it was assumed that, in somatic cells, mobile elements were irrevocably repressed in heterochromatin domains and, because DNA demethylation and reactivation of chromatin happen primarly in embryonic cells

and the germline, the mobile elements were thought to be completely inactive in somatic cells. However, methylation can be regulated, especially during differentiation processes. Also, the fidelity of DNA methylation is not perfectly reproduced after each cell division, allowing a window of opportunity for retrotransposition to happen [182]. More recent reports demonstrate active retroviruses in somatic cells such as neuronal, Sertoli and vascular endothelial cells [175, 183-187]. Also the majority of human cancers, including prostate cancer and cell lines derived from cancer, have, in general, higher endogenous expression of the full length L1 and Alu retroelements [173, 175].

There is evidence suggesting that transposons are the cause for mammalian evolution and several reports suggest that mobile elements are at the origin of genes involved in placenta formation [188]. For instance the syncytin proteins, responsible for the formation of the syncytiotrophoblast in the placenta, are derived from envelope proteins of endogenous retroelements [176]. Also, genes important in the V(D)J recombination during lymphocyte development (recombination-activating genes RAG1 and RAG2), originate from ancient mobile elements [188]. But the presence of mobile elements in our genome can also have destructive effects. Reactivation of ERVs in mice was shown to cause diabetes, kinked tail and limb malformation [176].

The potential for insertion of mobile elements into both coding and regulatory regions of the genome led scientists to hypothesize an association of retroelement reactivation with disease. In particular retroelements have been associated with cancer for decades and, despite the fact that many hypotheses and functional models of transposons' role in cancer have been proposed, few cancer types and diseases have been directly linked to mobile elements [175, 189, 190]. This could be explained via an overinterpretation of the role of mobile elements in cancer, or by the technical difficulties in detecting insertion of transposons and in identifying chromatin rearrangement caused by mobile elements. For example,

recombinations caused by Alu elements take place in the vicinity of the retroelement sequence, making it impossible to determine whether the Alu sequences located close to the break point contributed to the particular genomic rearrangement [189]. However, several mechanisms by which transposable elements can participate in human cancer have been proposed:

- INSERTION MUTAGENESIS: the genome wide, relatively random spread of TEs can induce insertions within genes with important biological functions [189]. Examples of human cancers caused by Alu or L1 elements are the disruption of BRCA, MYC [191] and APC genes in breast and colon cancer [192, 193]. It has been also shown that retrotransposition of TEs is highly increased and supported by cells with defective DNA damage repair or apoptosis pathways [175]. Because these aberrations are common features of cancer cells it is likely that TE movement has a much higher impact in tumor cells compared to normal cells.

- RECOMBINATION: even if TEs do not insert in chromatin regions with key genes involved in tumor repression they could still induce detrimental effects through recombination. Because of their inclusion of highly repetitive sequences, TEs can serve as a source for non-allelic homologous recombination (NAHR) that leads to duplication or deletion of sequences between the participating elements. This mechanism is likely limited to Alu retroelements and not likely relevant to LINE1 retroelements probably because of the longer distance between adjacent L1 inserts compared to the average distance between Alu elements. An example of Alu dependent recombination linked to breast cancer is the mutation of the BRCA1 gene, which has a very high density of Alu elements (41.5% of the gene) [194]. Recombination events that lead to cancer have been observed not only in the germline, as for BRCA1, but also in somatic cells, as for MYB and MLL1

recombination in AML (acute myeloid leukemia) and T-ALL (T-cell acute lymphoblastic leukemia) [175]. Instability of Alu elements was also shown to be 10,000 times higher in p53 null compared to wild type background [195].

- DNA DOUBLE STRAND BREAK: as mentioned above in section I, the endonuclease encoded by the ORF2 of LINE1 was shown to cause DNA double strand breaks involved in TMPRSS2:ETS translocation in prostate cancer [13]. Very little is known about the role of TE, induced double strand breaks in human diseases but it is possible that mobile elements can contribute to the DNA lesions that lead to chromosomal instability in cancer.

- CHANGES IN CANCER TRANSCRIPTOME: a more subtle effect of retroelement insertion is caused by their interference with the transcription of nearby genes. The fact that TEs contain promoters, RNA polymerase binding sites, polyadenylation signals and splice donor or acceptor sites, means they can cause misregulation in the expression or in the splicing of nearby genes [175]. LINE1, Alu and SVA elements have been all reported to be able to affect the transcription of genes close to their site of insertion. Also, the presence of repetitive sequences in opposite orientations within the TEs can induce the formation of double stranded RNA, consequently modified by RNA editing enzymes and potentially leading to an effect on transcription of the nearby genes.

Moreover, mobile elements have been shown to induce apoptosis, senescence and cell cycle arrest in cancer cells when the balance between the activity of mobile elements and the ability of the host genome to tolerate mutagenesis, is perturbed [189]. This observation implies that the harmful activation of TEs is more likely to cause diseases in a mutated p53 and DNA damage repair background. Also recent studies show that p53 can activate LINE 1 elements,

probably to amplify the p53-mediated DNA damage response to retroelements expression [196]. Many external stimuli that cause DNA damage and cell cycle arrest such as puromycin, cycloheximide, etoposide, cisplatin and UV have been shown to induce reactivation of Alu elements [175]. All these data suggest that the reactivation of retroelements upon radiotherapy or chemotherapy could possibly increase chromatin instability and contribute to the evolution of therapy resistant cancers.

In particular, retroelement reactivation caused by hypomethylation of their promoter sequences has been suggested to have a role in prostate cancer [173]. One possible link between retroelements and prostate cancer came from the observation that LINE1 ORF2 endonuclease is important for the formation of the TMPRSS2:ETS translocation, as mentioned before [13]. Also, AR intragenic rearrangement, found in a subset of tumors and causing the expression of a constitutively active form of AR, was proposed to originate from L1 reactivation because of the presence of L1 elements in the break/fusion points of these rearrangements within the AR gene [55, 56]. Interestingly, treatment of prostate cancer cell lines with a reverse transcriptase inhibitor (Abacavir), successfully used in the treatment of HIV infection, induces inhibition of growth, migration and invasion. This inhibition was specific for prostate cells (PC3 and LNCaP) and not observed for the non-transformed human fibroblast cell line WI-38 [197]. Also, two human endogenous retroviruses (HERK17 and HERV-K_22q11.23), the promoters of which can be fused with the coding region of ETS transcription factors (similar to the TMRPSS2 promoter/ERG fusion), were shown to be upregulated in a subset of prostate cancers and also to be directly regulated by the androgen receptor [173].

Overall, mounting data supports the idea that what was once considered "junk" DNA containing repetitive elements, has an important role in crucial biological processes like development, differentiation and cancer. Especially in the area of TE activation in somatic

cells, further exploration is necessary to gain a more definitive view on the role and importance of these intriguing genetic elements in cellular biology and human pathology.

CHAPTER 1:

REGULATION OF ANDROGEN MEDIATED TRANSCRIPTION

BY RPB5 BINDING PROTEIN (RMP/URI)

Work described in this chapter was previously published in *Molecular and Cellular Biology* as the article "Regulation of Androgen Receptor-Mediated Transcription by RPB5 Binding Protein URI/RMP" [82].

1.1 URI represses AR-mediated gene transcription

It has been reported that URI is a transcriptional repressor [94], and while URI mRNA is altered in prostatic intraepithelial neoplasia (PIN) and advanced prostate cancer [198], the role of URI in AR-mediated transcription is unknown. Therefore, to examine the putative role of URI in AR-mediated transcription, luciferase reporter gene assays were conducted using HEK293 cells transfected with FLAG-URI along with AR and an androgen-responsive ARR3-luciferase reporter. Cells were treated with or without the synthetic androgen R1881 for 24 hours before luciferase measurement. The results show that expression of URI resulted in decreased AR-mediated transcription both in the absence or presence of R1881 (fig. 1a).
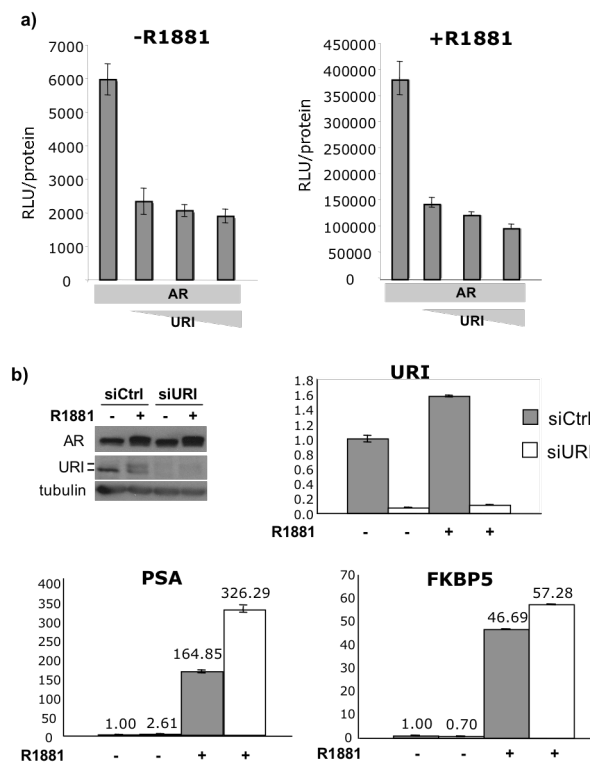
Figure 1. URI represses androgen receptor-mediated transcription

a) HEK-293 cells were transfected with the indicated plasmids together with AR and an ARR3-luciferase reporter construct. 24 hours post-transfection, cells were treated with (right panel) or without (left panel) 10nM R1881 for 24 hours. The experiment was conducted in triplicate and the error is represented by the standard deviation. b) URI was depleted in LNCaP cells using siRNA against URI (siURI) or siRNA control (siCtrl) as described in the materials and methods. After knockdown, cells were treated for 24 hours with or without 10nM R1881. URI (thick marks indicate the two bands of URI protein) and AR proteins were analyzed by Western blotting and tubulin was used as

loading control. The relative mRNA levels of URI, PSA and FKBP5 were quantified by Q-PCR using specific primers. Values were normalized to RPL19 mRNA.

To examine the impact of URI on endogenous gene transcription, the expression of two well-characterized androgen-regulated genes, PSA and FKBP5, were evaluated in the presence or absence of URI protein. LNCaP cells were transfected with a control siRNA or a siRNA against URI and then treated with or without R1881. Measurement of PSA and FKBP5 mRNA via quantitative-PCR analysis (Q-PCR) showed that knockdown of URI induced an increase in PSA and FKBP5 mRNA transcription without affecting AR protein levels (fig. 1b). These data indicate that URI acts as an AR repressor.

1.2 URI is required for bicalutamide repression of AR-mediated transcription

To determine if URI has a role in gene repression mediated by AR antagonists, we investigated whether the loss of URI affected AR antagonist (bicalutamide, BIC) repression of the AR target genes PSA and FKBP5. LNCaP cells were depleted of URI under conditions of hormone starvation (10% charcoal-stripped FBS) and then treated with or without bicalutamide in complete media supplemented with 10% FBS. FBS contains adequate endogenous steroids to activate AR, thus obviating the need to add exogenous androgens. Cells treated with media supplemented with 10% charcoal-stripped FBS (CFBS) after knockdown were used as a baseline for AR-mediated transcription analysis. The mRNA was isolated and the expression of PSA and FKBP5 was measured by Q-PCR. As expected, bicalutamide treatment reduced androgen-mediated transcription of PSA and FKBP5 by 39.3% and 64.1% respectively (fig. 2a and b). Bicalutamide-mediated repression was alleviated in the presence of URI siRNA, as repression of PSA was reduced from 39.3% to 12.7% (fig. 2a) and FKBP5 repression was reduced from 64.1% to 25.5% (fig. 2b). This result

indicates that URI, like Art-27 [78] is important in bicalutamide-mediated transcriptional repression of androgen-regulated genes.
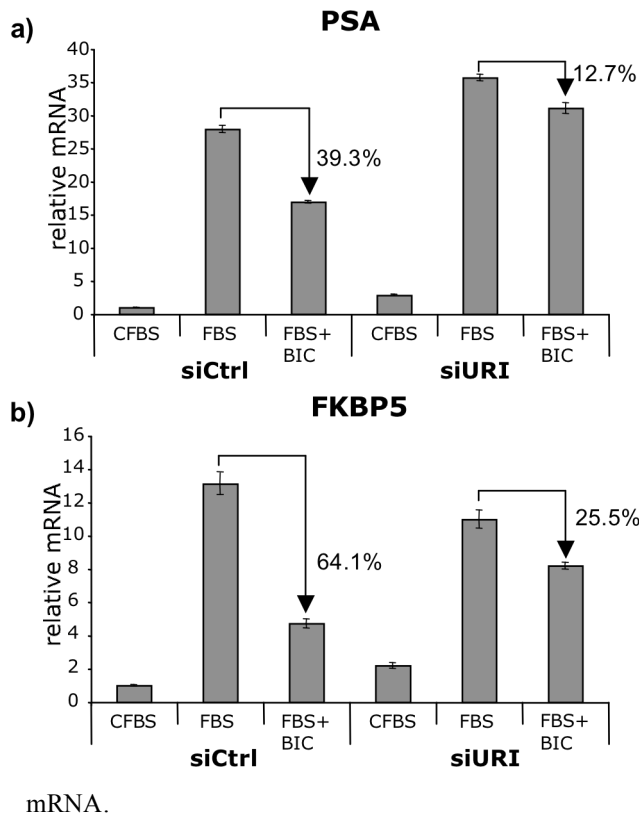
Figure 2. URI affects bicalutimide response

a-b) LNCaP cells were treated with siRNA control or siRNA against URI as described in the materials and methods. After knockdown performed in 10% charcoal-stripped FBS (CFBS), cells were treated for an additional 24 hours with media containing 10% CFBS, 10% FBS or 10% FBS plus bicalutamide (10mM). mRNA was then isolated and the relative levels of PSA (a) and FKBP5 (b) mRNA were measured and normalized to RPL19 mRNA.

1.3 URI inhibits LNCaP anchorage-independent growth

We next analyzed the growth of LNCaP cells either stably over-expressing URI or depleted of URI by stable shRNA targeting (fig. 3a). These experiments did not reveal any differences in cell proliferation between control cells or cells with altered expression of URI when grown in monolayer. We speculated that URI might impact anchorage-independent growth and therefore performed experiments to assess the ability of cells over-expressing URI to grow in

soft agar. Both control LNCaP cells harboring an empty vector and LNCaP-URI cells were cultured for 10 to 15 days in soft agar. Colony number and area were then measured. While over-expression of URI did not change the number of colonies (fig. 3c), the colonies formed by the LNCaP-URI cells were smaller (p<0.0001) than the colonies formed by control LNCaP cells (fig. 3d). This suggests that URI over-expression diminishes the ability to grow in anchorage-independent conditions as measured by colony formation in agar but does not directly affect cell growth.

To determine if URI also affects bicalutamide repression of prostate cancer cell growth, soft agar colony assays were performed in the presence or absence of BIC. As expected, bicalutamide strongly inhibited individual colony growth in control LNCaP cells (LNCaP-vector (fig. 3e) and LNCaP-shNS (fig. 3f) ± BIC). Over-expression of URI further inhibited cell growth in soft agar in the presence of BIC (fig. 3e, 0.078±0.003 versus 0.039±0.007). Moreover, knockdown of URI in LNCaP-shURI cells grown in the presence of BIC alleviated bicalutamide repression (fig. 3f, 0.07±0.005 versus 0.1±0.011). These findings further indicate an important role for URI in bicalutamide action.

Altogether, these results suggest that URI acts like a putative tumor suppressor to repress AR-mediated gene transcription and inhibit anchorage-independent growth. URI probably does not have a direct role in cell cycle regulation because its over-expression or depletion does not affect the growth of adherent LNCaP cells. However, the changes induced by URI over-expression or depletion confer a disadvantage or advantage respectively for the anchorage-independent growth of prostate cancer cells.
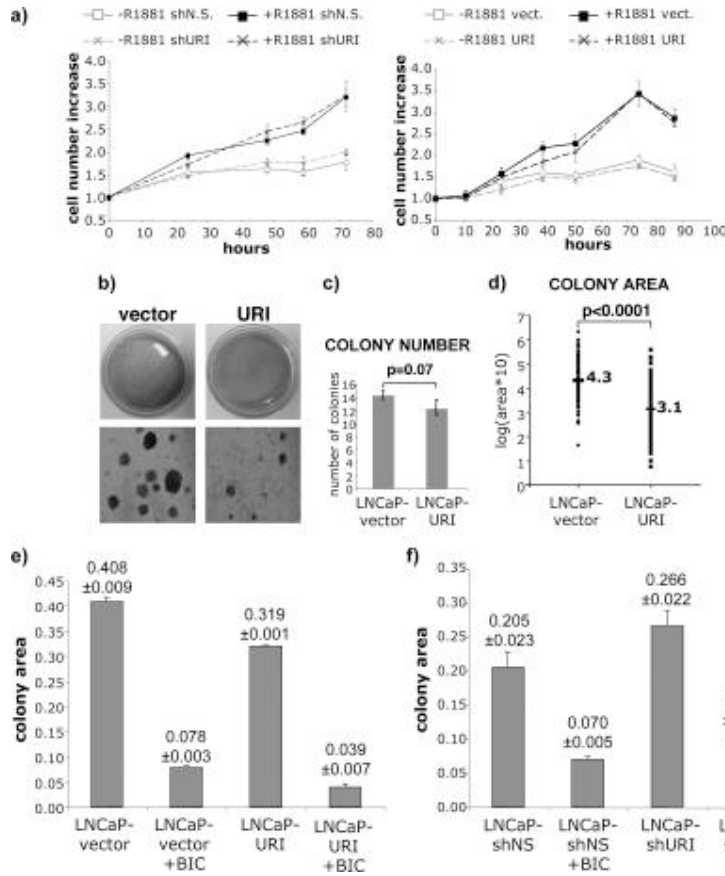
Figure 3. URI inhibits LNCaP anchorage-independent growth

a) Shows growth curves of LNCaP cells depleted of URI (left panel) or overexpressing URI (right panel). LNCaP stable cell lines were cultured in hormone starved media (-R1881) or in the presence of 0.1nM R1881 (+R1881). Cell number was measured by neutral red uptake. Each time point was normalized for the initial number of cells at time zero. b) LNCaP cells stably over-expressing an empty vector (LNCaP-vector) or URI (LNCaP-URI) were grown in soft agar for 15 days as described in the materials and methods. Representative colonies are shown. c) The number of colonies in 10 random fields was counted. d) The area of 200 colonies for each condition was measured. Area is reported in logarithmic scale and the geometrical mean is also indicated. Statistical analysis was performed using the Wilcoxon test for colony area and the Student's t-test for colony number. e-f) LNCaP-vector and LNCaP-URI or LNCaP stably expressing a control shRNA (LNCaP-shNS) or an shRNA against URI (LNCaP-shURI) were grown in the presence or absence of bicalutamide (10mM) for 15 days in soft agar. The area of 200 colonies from each treatment was measured. All differences between colony areas were statistically

significant (p<0.0001). The results shown are representative of three independent experiments done in triplicate.

1.4 URI is phosphorylated in response to androgen downstream of mToR

URI was previously shown to be phosphorylated in response to several stimuli downstream of the mTOR pathway [84, 104]. Furthermore, in prostate cells, the mToR pathway is activated by androgen treatment following AR transcriptional activation [199]. To determine if URI expression or modification is affected by androgen treatment, we treated the prostate cancer cell line LNCaP with increasing concentrations of the synthetic hormone R1881 for 24 hours. Western-blot analysis indicates that URI appears as a single band in the absence of hormone. Following hormone treatment, a URI band with slower electrophoretic mobility appears and URI can be visualized by Western blotting as a double band. Moreover, expression of the upper band of URI is increased in a hormone-dependent manner (fig. 4a), suggesting that URI is modified in response to a pathway activated downstream of AR.

Given our interest in URI's role in the nucleus, we evaluated whether hormone-dependent phosphorylated URI was present in the nucleus versus the cytoplasm of LNCaP cells. Nuclear/cytoplasmic fractionation was performed in LNCaP cells treated with 10 nM R1881 for 24 hours. The results indicate that the phosphorylated form of URI is present in both cellular compartments (fig. 4c). λ-phosphatase assays using LNCaP cell lysates treated for 24 hours with 10nM R1881 confirmed that the hormone-dependent upper band of URI was due to phosphorylation (fig. 4b).
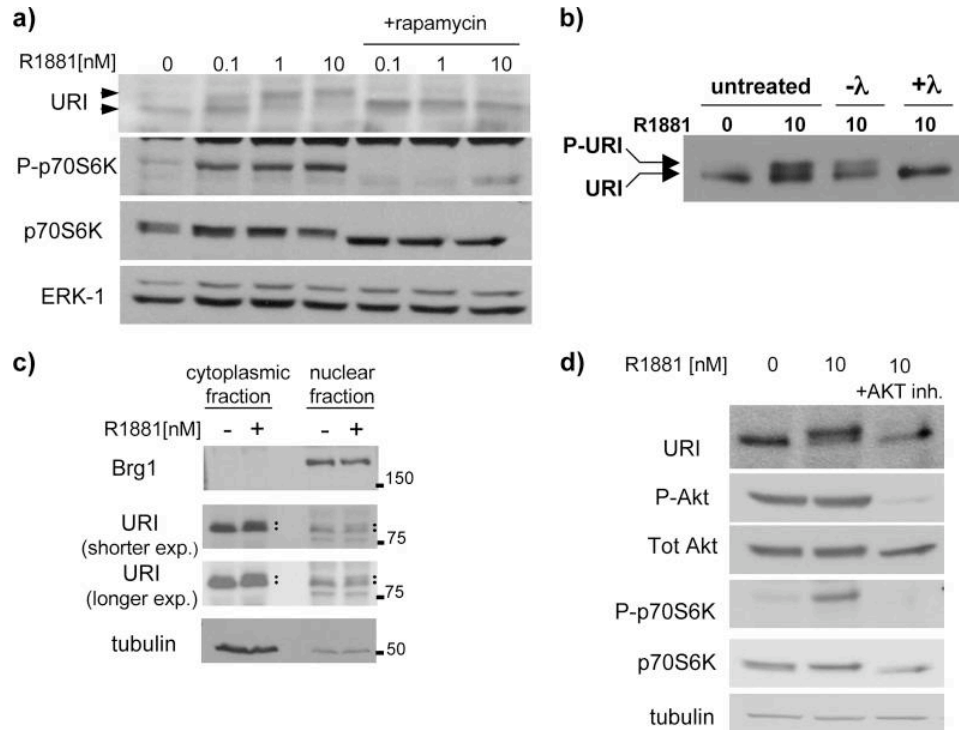
Figure 4. Hormone treatment results in URI phosphorylation downstream of mToR

a) LNCaP cells were starved in 10% charcoal-stripped FBS (CFBS) overnight and then treated for 24 hours with ethanol (0nM) or increasing concentrations of R1881 in the presence or absence of rapamycin (100nM). Whole cell lysates were analyzed by Western blotting for the indicated proteins. ERK-1 protein was used as loading control. The arrows indicate the two bands of URI. b) lambda phosphatase assay. LNCaP cells were treated as in a) and cell lysates were treated without (-λ) or with (+λ) λ-phosphatase. c) Nuclear and cytoplasmic fractions were prepared from LNCaP cells treated with 0nM or 10nM R1881 for 24 hours. Brg1 and tubulin were used as nuclear and cytoplasmic markers, respectively. Dots on the URI blots indicate the two bands of URI. d) LNCaP cells were cultured as in a) in the presence or absence of 20μM Akt inhibitor VIII.

It has been reported that in the mitochondria, URI is phosphorylated by p70S6 kinase downstream of mToR [104]. To determine if androgen-mediated URI phosphorylation is mToR-dependent, LNCaP cells were treated with increasing concentrations of R1881 in the presence or absence of rapamycin, a known mToR inhibitor. In the presence of rapamycin, the hormone-dependent upper band was completely inhibited, suggesting mToR-dependent phosphorylation of URI. mToR-dependent phosphorylation of p70S6K on threonine 389 is shown to confirm inhibition/activation of the mToR pathway (fig. 4a).

Previous studies link mToR with Akt activation in prostate cancer [200, 201], and it is well established that in a high percentage of prostate cancers PTEN phosphatase is mutated or deleted. In these tumors, aberrant PTEN expression results in Akt hyper-activation. Therefore, to determine if hormone-dependent URI phosphorylation is affected by Akt inhibition, we treated LNCaP cells (that have constitutively active Akt because of a mutated PTEN) with 0 or 10nM R1881 for 24 hours in the presence or absence of Akt inhibitor VIII. URI phosphorylation was completely inhibited in the presence of Akt inhibitor (fig. 4d), and phosphorylation of p70S6K was also greatly diminished.

The observation that URI protein is phosphorylated on multiple sites downstream of the mToR pathway suggests that URI phosphorylation could integrate extracellular and metabolic stimuli with androgen receptor transcriptional regulation.

1.5 URI binds Art-27 in prostate cells

URI was identified as an Art-27 binding partner in an immunoprecipation and mass spectrometry experiment conducted in HeLa cells [84]. Art-27 is a well-established AR co-repressor whose nuclear expression correlates with decreased prostate cancer recurrence [78]. To determine if the effect of URI on AR-dependent transcription was mediated by Art-27, we initially asked if URI and Art-27 were in complex in prostate cells. Immunoprecipitation

experiments were performed using whole cell lysates from the prostate cancer cell lines LNCaP, LAPC4 (data not shown) and PC3. In all cell lines analyzed, URI co-immunoprecipitates with Art-27 and vice versa (fig. 5a and b). Co-immunoprecipitation experiments from cytoplasmic and nuclear fractions were also performed, verifying that URI interacts with Art-27 in both cellular compartments (data not shown). URI also immunoprecipitates with Art-27 in PC3 cell lines that do not express AR protein, indicating that the URI-Art-27 interaction can be AR-independent (fig. 5b). Although Art-27 interaction with AR was previously observed [77], we were not able to co-immunoprecipitate AR with URI (fig. 5a, right panel). These results may indicate either that there is an Art-27/AR complex that does not include URI, or more likely that our URI antibody cannot recognize URI in complex. Alternatively, the URI-Art-27-AR complex may be in low abundance, transient, or not preserved under the cell lysis conditions and immunoprecipitation.

To verify that URI and Art-27 were expressed in the same cells in vivo and therefore potentially part of a protein complex in human prostate cells, we analyzed the expression of URI, Art-27 and AR in consecutive sections of human prostate tissues, using a polyclonal antibody that specifically recognizes URI protein as indicated by a diminished signal in cells depleted of URI by shRNA shown by Western blot (fig. 5c). In vivo staining showed that URI, Art-27 and AR were expressed in prostate epithelial cells (fig. 5d) with only negligible URI and Art-27 expression in the stroma, as previously reported [79]. These observations indicate that AR, URI and the AR cofactor, Art-27, are co-localized in prostate epithelial cells.
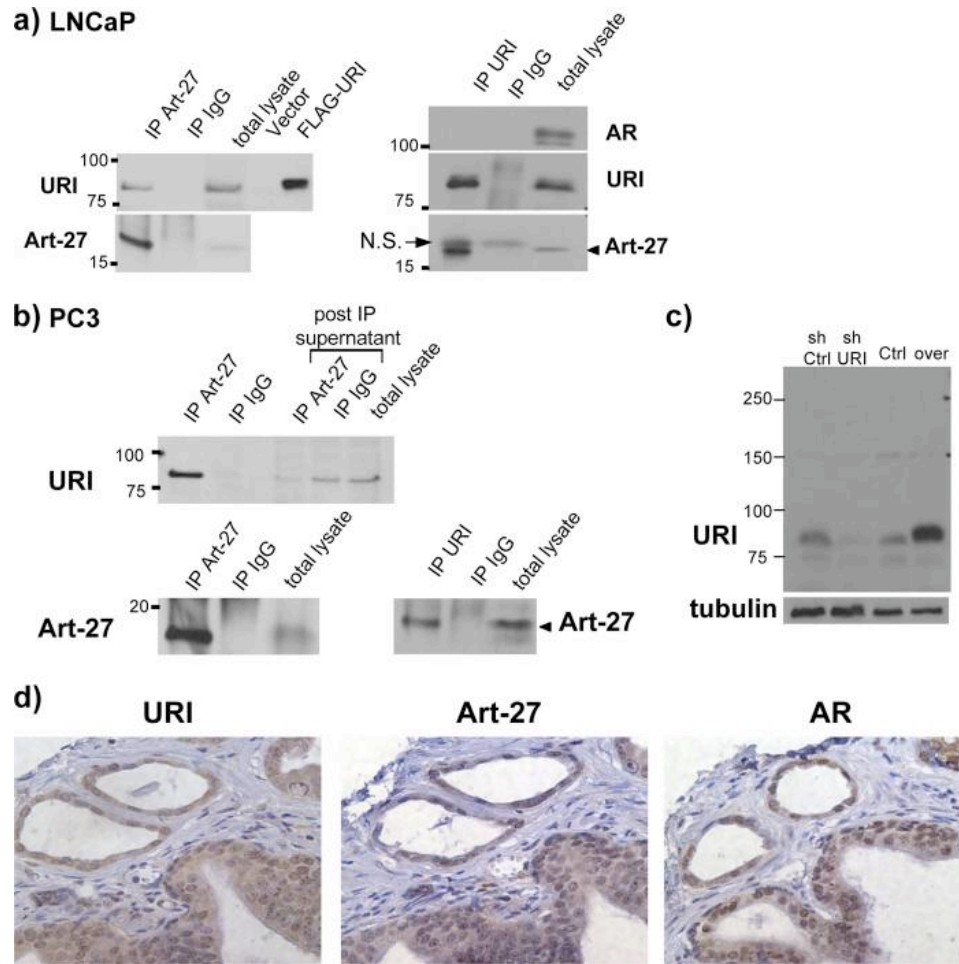
Figure 5. URI interacts with Art-27 in prostate cells

a) LNCaP or b) PC3 cells were cultured in complete media. Whole cell lysates were incubated with antibody against Art-27, URI or control antibody against normal-rabbit IgG (Art-27 IP) or normal mouse IgG (URI IP). Immuno-complexes were precipitated and analyzed by SDS-PAGE and membranes were probed with the indicated antibodies. The arrow indicates a non-specific (N.S.) band and the arrowheads Art-27 protein c) Validation of the polyclonal anti-URI antibody used for the tissue staining. The panel shows Western blot analysis of lysates from cells expressing an shRNA control (shNS) or an shRNA against URI (shURI), an empty vector (Ctrl) or FLAG-URI (over). d) Consecutive sections of human prostate tissues were immuno-stained with URI, Art-27 or AR antibodies to show the

51

co-localization of the three proteins in epithelial prostate cells. Positive immunoreactivity appears brown, and cells that are not stained appear blue due to hematoxylin.

1.6 URI affects Art-27 protein stability

The fact that Art-27 and URI co-immunoprecipitate from prostate cell protein extracts (fig. 5) suggests that they are in complex in vivo. To determine if loss of one component of the complex affects the other, protein levels of URI or Art-27 were selectively diminished in LNCaP cells using transient transfection of siRNA pools directed against one of the two proteins. A non-specific siRNA was used as a control. The results indicate that specific depletion of Art-27 protein correlated with loss of URI protein and depletion of URI protein correlated with loss of Art-27 (fig. 6a and b). Interestingly, we observed that the band of un-modified URI (lower band) is preferentially decreased (fig. 6a) upon Art-27 depletion. This suggests that the phosphorylated form of URI might be part of a more stable complex. Moreover, Q-PCR analysis revealed that Art-27 degradation upon URI depletion is due to a post-transcriptional event because Art-27 mRNA was not affected by URI depletion (fig. 6d). Consistent with these results, stable over-expression of URI in either HEK293 (fig. 6c) or LNCaP cells (fig. 6f) resulted in stabilization of Art-27 protein without affecting Art-27 mRNA (fig. 6e).

To understand the effect of modulation of URI protein on Art-27 protein levels we treated cells with cycloheximide to block protein translation. LNCaP stable cell lines over-expressing URI (LNCaP-URI, with LNCaP-vect as a control) or depleted of URI (LNCaP-shURI, with LNCaP-shNS as a control) were used (fig. 6i). Cells were lysed at the indicated time points and Art-27 protein level was analyzed by Western blotting (fig. 6f-h). As in the previous experiments, the amount of Art-27 protein was increased in URI over-expressing LNCaP cells and decreased in URI knockdown cells (compare fig. 6f to fig. 6g with the same time of exposure). In control

cells (shNS and LNCaP-vect.), the half-life of Art-27 is longer than 8 hours and we were not able to detect any protein loss after 8 hours of CHX treatment. However, upon URI loss, Art-27 protein has a half-life of about 6.5 hours (fig. 6h). The same analysis was performed for AR. In both control cells and LNCaP cells over-expressing or lacking URI, AR had a half-life of about 6 hours (data not shown), suggesting that URI has no effect on AR protein stability. Therefore, changing the stoichiometry of either URI or Art-27 protein results in altered levels of the other, and supports the hypothesis that URI and Art-27 are in complex.
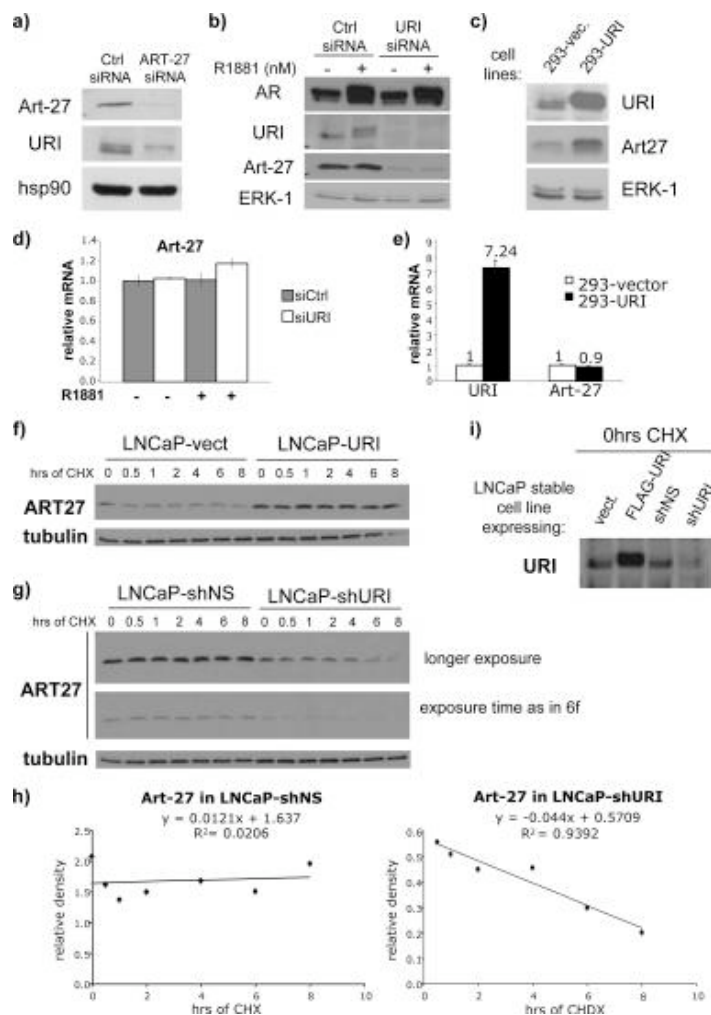
Figure 6. URI and Art-27 affect each other's stability

a) Art-27 was depleted from LNCaP cells grown in media supplemented with 10% FBS as described in the materials and methods, using either control (Ctrl) siRNA or siRNA against Art-27. Indicated proteins were analyzed by Western blotting. Hsp90 protein was used as a loading control. b) LNCaP cells were depleted of URI using siRNA against URI (URI siRNA). Cells were then treated with 0 or 10 nM R1881 for 24 hours. AR, URI and Art-27 protein levels were analyzed by Western blotting. c) 293 cells stably over-expressing an empty vector (293-vec.) or a FLAG-URI (293-URI) construct were lysed and Art-27 and URI protein levels analyzed by Western blotting. ERK-1 protein was used as a loading control. d) LNCaP cells were treated as described in panel b. e) 293 cells stable cell lines were treated as described in panel c. mRNA was isolated and URI and Art-27 mRNA was quantified by Q-PCR. All values were normalized to RPL19 mRNA.f-g) LNCaP cells stably over-expressing an empty vector (LNCaP-vect) or URI (LNCaP-URI), shRNA control (LNCaP-shNS) or shRNA against URI (LNCaP-shURI) were treated for the indicated times with 25μM cycloheximide (CHX). Cells were lysed and an equal amount of protein from each sample was loaded on a polyacrylamide gel. Tubulin, used as loading control, and Art-27 proteins were analyzed by Western blotting. h) Densitometry analysis of Art-27 bands was graphed for LNCaP-shNS and LNCaP-shURI cells. i) URI protein level at the beginning of the experiment (0hrs CHX) was also analyzed by Western blotting to verify the over-expression or depletion of URI.

1.7 Diminution of URI protein levels results in decreased Art-27 and increased AR on the NKX3.1 gene

Overall, our studies suggest that URI and Art-27 act in concert to regulate gene transcription. Since previous ChIP analyses indicated that Art-27 is recruited to the NKX3.1 gene [78], we tested whether Art-27 and URI functionally interact at NKX3.1 regulatory sites. ChIP analysis was performed in LNCaP cells stably expressing a non-silencing shRNA (LNCaP-shNS) or an

shRNA against URI (LNCaP-shURI). NKX3.1 was specifically examined because we observed a highly reproducible recruitment of Art-27 on a region close to the transcription start site (TSS). The results show that decreasing URI protein levels results in a decrease of Art-27 occupancy on the NKX3.1 gene, consistent with the idea that loss of URI depletes the pool of Art-27 directly involved in transcription regulation (fig. 7a).

Since NKX3.1 is an AR-regulated gene, we also determined if URI knockdown affected AR recruitment on the known AREs in the 3' untranslated region (UTR) of NKX3.1 [202]. Interestingly, upon URI knockdown, we observed an increase of AR recruitment at both AREI and AREII in the UTR of NKX3.1, suggesting a direct role of URI in AR transcription regulation (fig. 7b). Further, enhanced AR recruitment likely explains the increase in NKX3.1 mRNA observed in response to URI knockdown (fig. 7c).
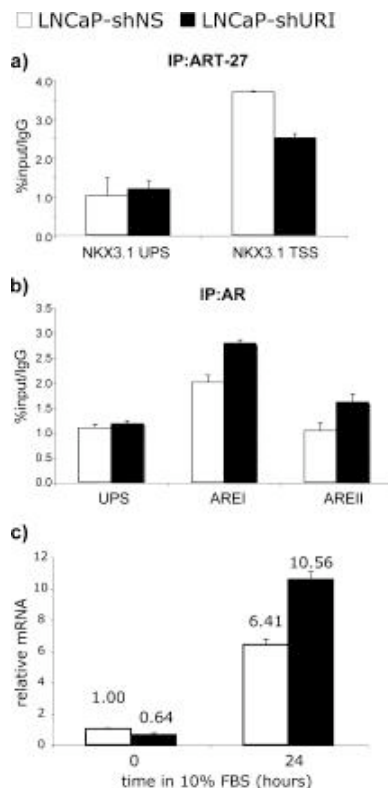
Figure 7. URI loss decreases Art-27 and increases AR recruitment on chromatin

ChIP was performed as described in the materials and methods. a) Art-27 recruitment on a control NKX3.1 up-stream region (UPS) and on a region of NKX3.1 close to the transcription start site (NKX3.1 TSS). b) AR recruitment on NKX3.1 UPS and AREI and AREII in the 3' untranslated region of NKX3.1. The results are expressed as percent of input normalized for IgG recruitment. c) Q-PCR analysis of NKX3.1 transcript after serum starvation for 18 hours (0 hours) and 24 hours of 10% FBS treatment (cells were treated with doxycycline 1μg/ml for 48hrs to induce shRNA expression).

1.8 URI and Art-27 have similar effects on AR mediated gene transcription

To understand the broader role of URI in AR-mediated gene transcription, we performed genome-wide expression profiling to identify genes affected by decreased levels of URI protein using DNA microarray technology. The mRNA was isolated from LNCaP cells depleted of URI and treated in the same way as in the previously published analysis of genes affected by Art-27 knockdown [78]. LNCaP cells were treated with control siRNA or siRNA against URI, with or without 10nM R1881 for 24 hours. mRNA was isolated and hybridized to the Affymetrix Chip HG_U133.2. Each knockdown was performed in duplicate. Androgen-dependent genes obtained from the Art-27 knockdown and URI knockdown experiments were compared (fig. 8a). Most genes responded in the same way to hormone treatment in the control cells, indicating good reproducibility between the two sets of experiments. In line with our finding that URI and Art-27 proteins are tightly dependent on one another, we observed a substantial overlap of androgen-dependent genes in cells depleted of Art-27 and cells depleted of URI. Interestingly, when comparing overlapping probes, 30 and 49 probes were up- or down-regulated respectively by hormone only upon URI or Art-27 depletion, suggesting that these genes become hormone-dependent in the absence of Art-27 or URI. Additionally, 83 and 28 probes were up- or down-regulated respectively by hormone only in control cells, suggesting that Art-27 and URI are essential for the hormone responsiveness of these genes. Principle component analysis shows that both URI and Art-27 knockdown have a similar effect on gene expression; samples depleted of URI or Art-27 and treated with hormone cluster together compared to their respective control (fig. 8b).
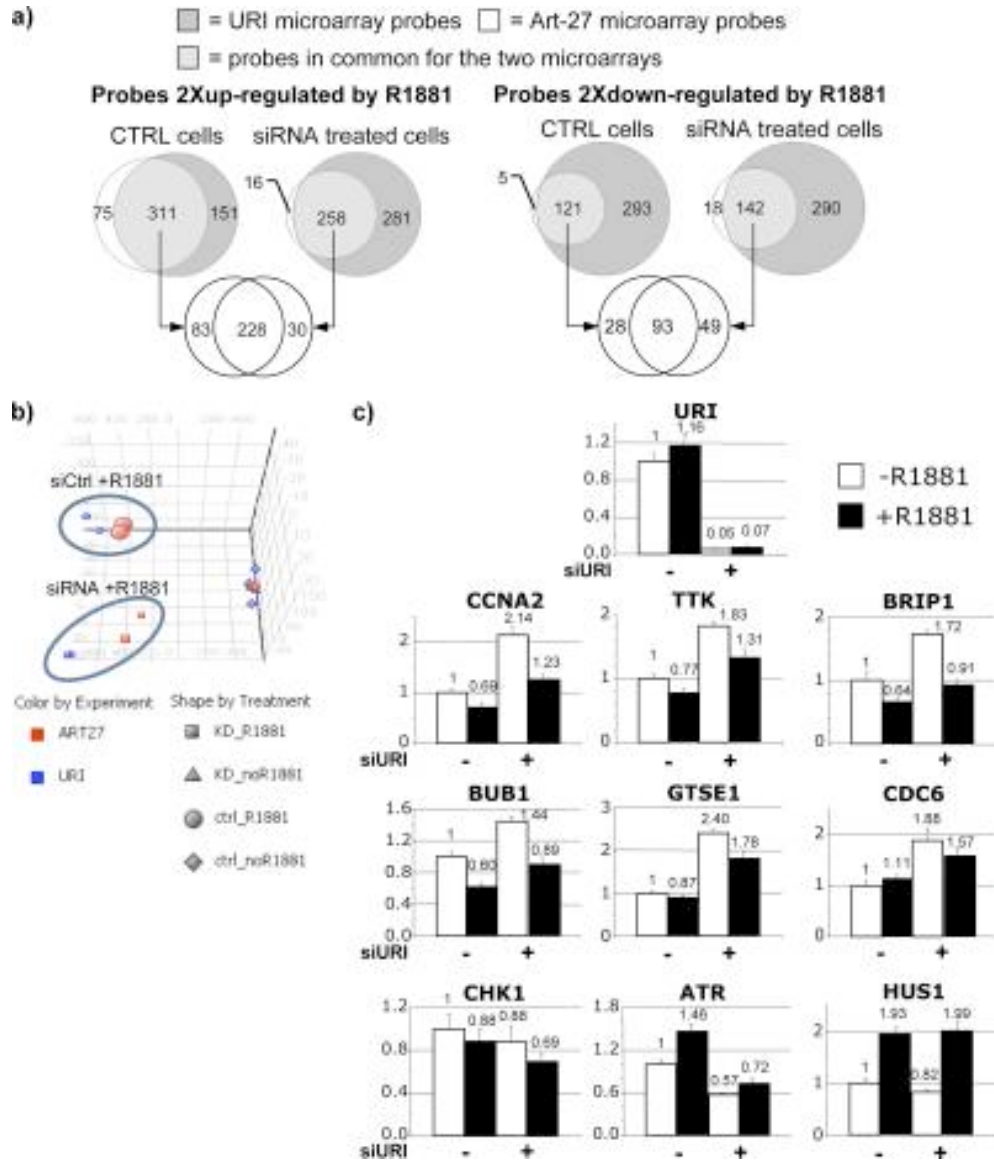
Figure 8. URI loss affects AR transcription similarly to Art-27 loss

LNCaP cells were depleted of URI or Art-27 and analyzed as described in the materials and methods. a) The Venn diagrams show the number of probes up- or down-regulated after R1881 treatment in the two microarrays for Art-27 and URI knockdown. Overlapping areas in light grey are proportional to the number of probes in common between the two microarrays. b) The three principal components with the

greatest variance for the gene expression profiles of the Art-27 and URI microarrays were plotted in a three-dimensional space using PCA analysis. c) LNCaP cells were treated with siURI or siCtrl (- siURI) as described in the materials and methods. Q-PCR analysis of the expression of a subset of genes previously (18) shown to be affected by Art-27 knock-down (the relative mRNA amount is reported for each bar).

We previously demonstrated that Art-27 depletion has an effect on a subset of genes involved in DNA damage response and cell proliferation (namely CCNA2, TTK, BRIP1, GTSE1, CDC6, BUB1, CHK1, ATR and HUS1) [78]. We therefore measured the expression of these genes upon URI depletion (fig. 8c). Q-PCR analysis showed that URI knockdown affects the expression of most of these genes in a similar manner as Art-27 knockdown, again suggesting that URI and Art-27 not only physically but also functionally interact. Interestingly, the DNA damage-related genes CHK1 and HUS1 did not change upon URI knockdown, while ATR expression was inhibited by URI depletion. The transcription of these DNA damage-related genes, in contrast, was shown to be up-regulated upon Art-27 knockdown (18), possibly suggesting URI- and Art-27-specific functions (fig. 8c). Collectively, these results show a strong interdependence between Art-27 and URI and suggest that Art-27 and URI act in concert to regulate gene transcription.

1.9 Gene expression analysis of URI depleted prostate cells

To identify androgen dependent genes that are transcriptionally regulated by URI, we performed a genome-wide microarray analysis of LNCaP cells depleted of URI in the presence or absence of androgen. We compared the genes up- or down-regulated by R1881 treatment in LNCaP control cells (treated with control siRNA) with the genes up- or down-

regulated by R1881 in LNCaP cells lacking URI (treated with a siRNA against URI). We analyzed the gene expression of the following samples:

1) LNCaP cells transfected with siCtrl (siRNA control) and treated for 24hrs with 0nM hormone (R1881)

2) LNCaP cells transfected with siCtrl and treated for 24hrs with 10nM R1881

3) LNCaP cells transfected with siURI (siRNA targeting URI) and treated for 24hrs with 0nM R1881

4) LNCaP cells transfected with siURI (siRNA targeting URI) and treated for 24hrs with 10nM R1881.

To identify the genes regulated by AR we calculated the fold induction comparing cells treated with R1881 and cells hormone starved for the respective siRNA treatments (siCtrl and siURI). We therefore divided the URI affected genes into the following 4 groups of genes:

1)   genes up-regulated by R1881 only in the presence of URI (URI=activator)

2)   genes up-regulated by R1881 only in the absence of URI (URI=repressor)

3)   genes down-regulated by R1881 only in the presence of URI (URI=repressor)

4)   genes down-regulated by R1881 only in the absence of URI (URI=activator)

Genes for which the expression of which was up- or down- regulated by R1881 at least 2 fold were considered androgen dependent. Because of this artificial cut-off many genes highly affected by URI were not identified as URI-regulated simply because in both the absence or presence of URI they had a R1881 fold change bigger than 2. To try to solve this problem, for each gene we calculated the "fold of the fold" as the ratio between the R1881 dependent fold in control cells over the R1881 dependent fold in URI depleted cells. We considered URI regulated genes those that have a "fold of the fold" bigger than 1.2. After this analysis many genes considered regulated by URI were discarded because their R1881 dependent fold was too close to the cut off of 2. An example of these genes was the nuclear factor I/B (NFIB) that

had a fold increase of 2.0067 upon R1881 treatment in control cells and a fold increase of 1.9436 in URI depleted cells. The gene was initially identified as upregulated by hormone only in control cells (with fold bigger than 2) but not in URI depleted cells (with fold barely lower than 2). The "fold of the fold" for this gene was 1.032 (=2.0067/1.9436) and therefore it was discarded. Moreover, genes that were not identified as URI regulated simply considering the R1881 dependent fold induction were reconsidered upon calculation of the "fold of the fold". An example of these genes was the male germ cell-associated kinase (MAK) that had a fold increase of 18.75 upon R1881 treatment in control cells and a fold increase of 9.33 in URI depleted cells. Because both of the folds were bigger than 2, this gene was not considered to be affected by URI even if the logarithmic fold of induction in control cells was twice of the logarithmic fold of induction in URI depleted cells. The "fold of the fold" of this gene was 2 (18.75/9.33) and therefore it was reconsidered as a URI regulated gene. The lists of the identified genes are reported in supplemental tables S1-8. Several genes of interest were validated by Q-PCR. We isolated mRNA from LNCaP cells treated in the same way cells were treated for the microarray analysis. URI depletion had an effect on androgen induced genes like IGFBP3, IGF1, MBD2 or MAK as well as on androgen repressed genes such as TNFR10D or IL1RN. These effects are not due to a general effect of URI depletion on transcription because genes like IL2RA were not affected. Interestingly, only 5% of the genes showed a change in transcription upon URI depletion, suggesting a gene specific role of URI in transcription regulation. GO analysis did not show clustering of the URI regulated genes in any relevant functional class. However, when we analyzed non-overlapping probe sets that differed between siCtrl and siURI treated cells according to whether they were previously identified to be up-regulated or down-regulated in cancers (oncogene database), a pattern emerged. Genes characterized previously as increased in cancer (colored in shades of red in figure 9; [1] and [4]) are up-regulated upon hormone stimulation only in the presence of URI or

down-regulated upon hormone stimulation only when URI was depleted, suggesting that URI is important for expression of oncogene-like genes. Consistent with this pattern, genes found to be decreased in cancer (colored in shades of green in figure 9; [2] and [3]) are up-regulated upon hormone stimulation only in the absence of URI and down-regulated only when URI was present in the cell, suggesting that URI represses the transcription of tumor-suppressor like genes (figure 9).
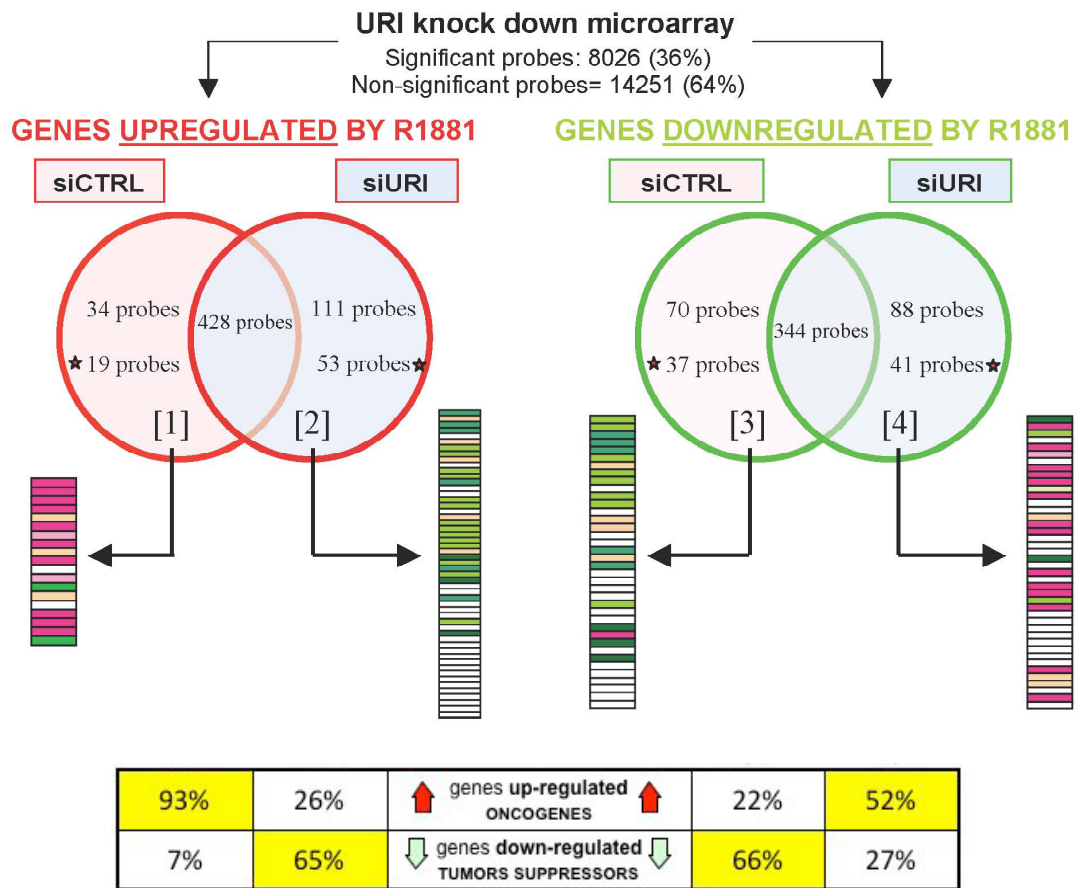
Figure 9. Schematic of URI knock down microarray analysis. The stars indicate significant probes that were differentially regulated by URI knock down. The heat-maps shown below the Venn diagrams indicate genes within each group that are increased (red or pink) or decreased (dark or light green) in cancer. The darker the color, the stronger the link to cancer. White boxes indicate that there is no

61

evidence supporting the regulation of the gene in cancer. The bottom box shows the percentage of URI regulated genes found up or down regulated in cancer compared to the total number of URI regulated genes for each group. Genes repressed by URI are decreased in cancers and the genes activated by URI are increased in cancers.

Overall this result indicates that genes highly regulated in cancers are extremely sensitive to the presence or absence of URI protein. We hypothesize that URI directly represses the transcription of some genes (genes negatively regulated by URI) and indirectly activates the transcription of other genes, probably through the regulation of other transcription factors. As mentioned before, the genes directly repressed by URI are found to be decreased in cancers and the genes indirectly activated by URI are found to be increased in cancers. This is in line with the idea that the URI up-regulation in PIN detected by Tomlins and colleagues [198] may represent an initiating event in prostate cancer that results in enhanced expression of growth promoting genes and inhibition of growth suppressing genes.

We also performed CONFAC analysis (http://morenolab.whitehead.emory.edu/cgi-bin/confac.pl?id=1529) to identify the transcription factor (TF) binding sites enriched in each of the aforementioned 4 groups of genes (1. genes up-regulated by R1881 only in the presence of URI (URI=activator), 2. genes up-regulated by R1881 only in the absence of URI (URI=repressor), 3. genes down-regulated by R1881 only in the presence of URI (URI=repressor), 4. genes down-regulated by R1881 only in the absence of URI (URI=activator)). Interestingly, this analysis revealed a TF enrichment only in list 1 and 4 and no statistically significant enrichment in lists 2 and 3. This result is in line with the idea of URI being a repressor of AR mediated transcription because the genes of lists 1 and 4 are genes activated by URI and lists 2 and 3 contain genes repressed by URI. Therefore URI seems to

function directly as a repressor while it has activation functions through the regulation of specific TFs for the genes of group 2 and 3. The most enriched TFs were:

KLF4, E2F1, OCT1, NKX2.5, MYOD, HES1, FOXO4, CREB, GATAs, SOX4, TCF4 and POU1F1.

Overall these data suggest that URI is a transcriptional repressor of hormone regulated genes. Also, misregulation of URI induces aberrant expression of genes found up- or down- regulated in prostate cancer, suggesting a pivotal role for URI in tumor formation/progression.

1.10 The URI/Art-27 protein complex binds chromatin independently of AR

The results presented above indicate that URI may affect AR transcription through the stabilization of the AR co-repressor Art-27. We also showed that loss of URI impacts AR recruitment to a target gene. One possible explanation for the increased AR recruitment on DNA in cells depleted of URI is that an URI-containing complex binds and possibly modifies chromatin. To determine if URI binds chromatin we isolated the cytoplasmic- and nuclear-soluble fraction (S2 and S3 respectively) from the nuclear- insoluble fraction (P3) of LNCaP cells grown in complete media [203]. The P3 fraction, which contains DNA and proteins tightly bound to chromatin, was then treated with micrococcal nuclease (MNase) for the indicated times to release chromatin-bound proteins into the soluble fraction. Western blot analysis showed that URI and Art-27 are bound to chromatin and, after treatment with MNase, URI and Art-27 pass from the insoluble to the soluble fraction (fig. 10a). Tubulin was used as control to ensure the complete absence of the cytoplasmic fraction in the P3 fraction. Histone H3 was found to be present in the soluble P3 fraction before MNase treatment (0 minutes of MNase treatment) and increased with subsequent nuclease treatment. As expected, AR as well as

RPB5 and RPB1 (the largest subunit of RNA polymerase II) are also bound to chromatin from

LNCaP cells cultured in complete media.
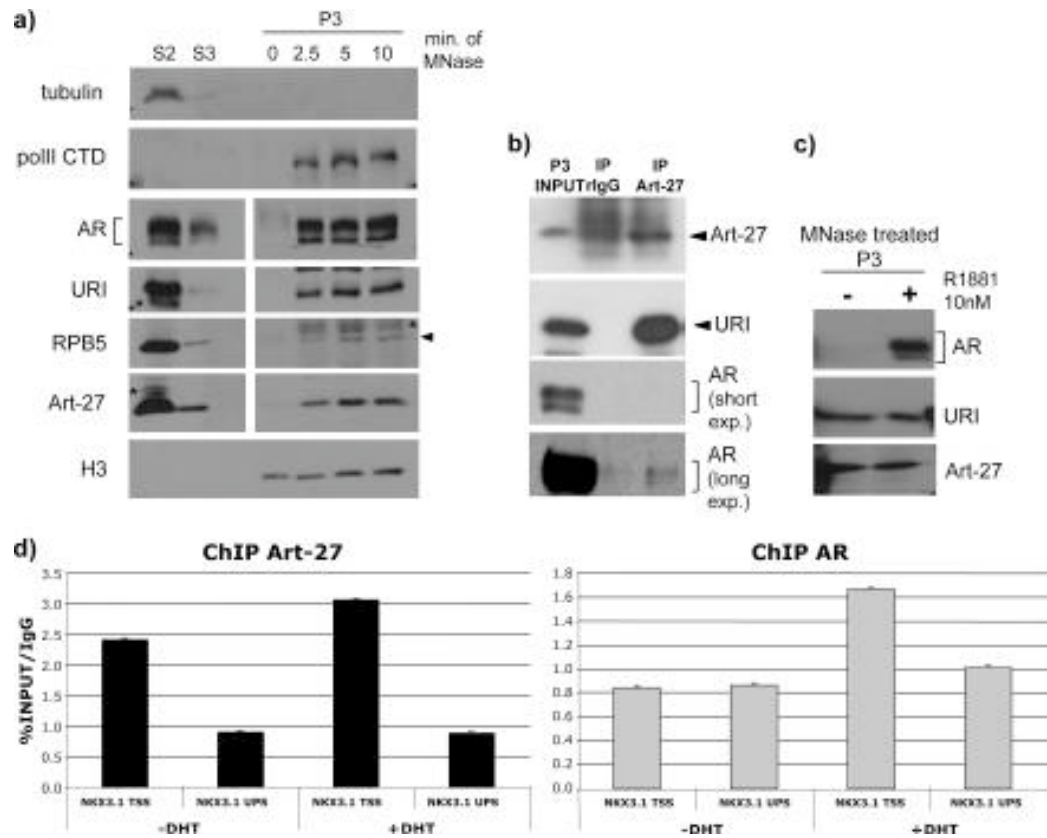
Figure 10. URI and Art-27 bind to chromatin in an androgen-independent manner

a) Western blotting of fraction P3 treated with micrococcal nuclease (MNase) for the indicated times. The cytoplasmic-soluble fraction (S2), nuclear-soluble fraction (S3) and nuclear-insoluble fraction (P3) were isolated from LNCaP cells growing in complete media. b) Fraction P3 treated with MNase (P3 INPUT) was used to immunoprecipitate Art-27 with specific rabbit antibodies against Art-27 or control rabbit antibodies (rIgG). A longer exposure of the AR blot (AR (long exposure)) is presented to show the small fraction of AR immuno-precipitated with Art-27. c) LNCaP cells were hormone starved for 24 hours and then treated for an additional day with or without R1881 (10nM). AR, URI and Art-27 proteins from the P3 fractions treated with MNase were analyzed by Western blotting. b) ChIP of Art-

27 (left panel) and AR (right panel) after 3 days of hormone starvation followed by 4 hours of treatment with or without DHT 10nM. All the results are expressed as percent of input normalized for IgG recruitment. d) ChIP of Art-27 (left panel) and AR (right panel) after 3 days of hormone starvation followed by 4 hours of treatment with or without DHT 10nM. All the results are expressed as percent of input normalized for IgG recruitment.

To determine if the chromatin-bound URI is in complex with Art-27, the P3 fraction was isolated from LNCaP cells and treated with MNase. Art-27 was then immunoprecipitated from the MNase-treated P3 fraction. Western blot analysis revealed that URI co-immunoprecipitates with Art-27 (fig. 10b) from the MNase treated nuclear fraction, suggesting that URI binds to Art-27 on chromatin. We also found that a small fraction of AR binds Art-27 on chromatin as expected from the previously observed interaction of Art-27 with AR, and in line with the established role of Art-27 as an AR co-repressor.

The experiments described above examine the interaction of URI, Art-27 and AR under normal non-synchronized growth conditions. To understand the behavior of these proteins in response to hormone treatment, the same biochemical fractionation scheme was performed using hormone-starved LNCaP cells or cells treated for 24 hours with the synthetic androgen R1881 (10nM). As expected, AR was completely absent in the chromatin fraction of hormone-starved cells but was bound to the DNA in LNCaP cells treated with R1881. Surprisingly, URI and Art-27 were bound to chromatin both in the presence and absence of hormone (fig. 10c), suggesting that a fraction of URI and Art-27, probably in complex with one another, bind chromatin independently of the AR.

To confirm that Art-27 and URI are already on the chromatin before AR recruitment, specifically on the NKX3.1 gene, we performed ChIP assays in the presence or absence of hormone (fig. 10d). Consistent with the fact that URI and Art-27 bind chromatin in an

androgen-independent manner, analysis of AR and Art-27 at the Nkx3.1 transcription start site (TSS) shows that, while AR is recruited in response to DHT, Art-27 is present at the TSS in the presence and absence of hormone. Altogether, our results suggest that the Art-27/URI complex is present at sites of AR binding within the Nkx3.1 gene prior to the recruitment of AR.

These results, together with the previously reported binding of URI and Art-27 to the helicases TIP49 and TIP48 and RNA pol II [84, 85], supports the hypothesis that Art-27 and URI bind DNA prior to the recruitment of AR, perhaps modifying chromatin structure.

1.11 Art-27 recruitment on the NKX3.1 gene

To gain a better understanding of the role of Art-27/URI complex in gene transcription we investigated recruitment of Art-27 along the entire NKX3.1 gene using ChIP assay. We immuno-precipitated AR, Art-27 and RNA polymerase II. Because we were not able to ChIP URI with multiple antibodies from a variety of sources, we hypothesize that URI is likely buried within a big multiprotein complex wherein the antibody epitopes are masked. However our data suggest that URI is recruited on the DNA together with Art-27 (fig. 11b) and therefore recruitment of one protein is likely to reflect recruitment of the other. In line with this idea Art-27 has two peaks of recruitment on the NKX3.1 gene (fig. 11a), a major peak on the TSS and a second smaller peak on the known AREI enhancer region in the 3'UTR of NKX3.1. Finding Art-27 at the TSS is predicted based on interaction with URI, a known interactor with the RPB5 subunit of polymerase. In addition the presence of Art-27 at the AREI supports our previous finding indicating that Art-27 interacts with AR [77]. As expected, AR is strongly recruited on the 3'UTR AREI region and polII is present on the body of the gene with a stronger peak of recruitment on the TSS of NKX3.1. Collectively these results show that Art-27, probably in complex with URI, is recruited on NKX3.1 TSS and ARE.
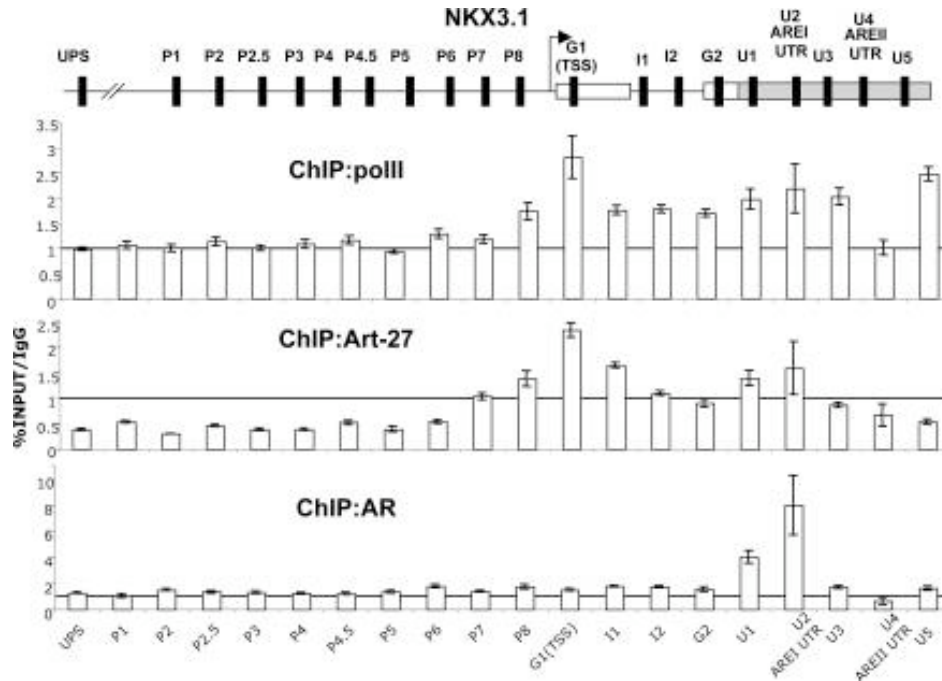
Figure 11. Art-27 is recruited on the TSS and 3'UTR AREI of NKX3.1

ChIP was performed as described in the materials and methods. In the upper panel a scheme of NKX3.1 gene is shown. The regions amplified by Q-PCR after ChIP are represented by the black boxes. The white boxes show the 2 exones and the gray box represents the 3'UTR region of NKX3.1. A control NKX3.1 up-stream region (UPS) was used as control. In the three lower panels polII, Art-27 and AR recruitment on the whole NKX3.1 gene and promoter is shown. A line at 1 shows the control value obtained performing ChIP using IgG control antibody.

1.12 Art-27 is part of the URI transcriptional-repression complex

We showed that Art-27 is recruited on the DNA and it is found at the ARE and TSS of the androgen regulated NKX3.1 gene (fig. 11). Because we also showed a tight interaction between Art-27 and URI in the cytoplasm, in the nucleus (fig. 5) and in the nuclear fraction of prostate cells (fig. 10), it is likely that Art-27 and URI are recruited together on the NKX3.1

gene. To directly show that URI and Art-27 are part of a novel transcriptional repression complex we fused the DNA binding domain of Gal4 (G4dbd) to the C-terminus of URI protein (URI-G4). A stable 293T-TetON (293T-REX from Invitrogen) cell line expressing a luciferase reporter gene controlled by a TK (thymidine kinase) promoter downstream of five G4 binding sites was used to generate stable cell lines overexpressing URI-G4dbd (fig. 12). The 293-TREX-luciferase cell line was previously extensively used by the Reinberg laboratory to demonstrate the transcriptional effect of several proteins fused to the G4dbd [204, 205].
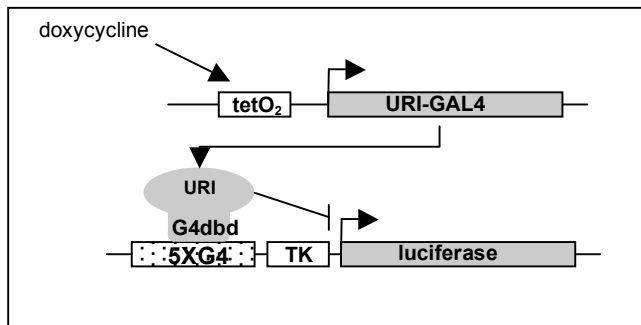
Figure 12. Schematic of the 293T-REX-luciferase-URIG4dbd system.

The repression of luciferase by URIG4dbd was measured in luciferase experiments in which URIG4dbd was transiently expressed. The expression of URI was controlled by either increasing the amount of URIG4 DNA transfected in 293T-REX cells (fig. 13b) or increasing the concentration of doxycycline (fig. 13a). In both conditions increased URIG4dbd expression induced a decrease in luciferase expression (quantified as luciferase repression) confirming the role of URI as a transcriptional repressor (fig. 13).
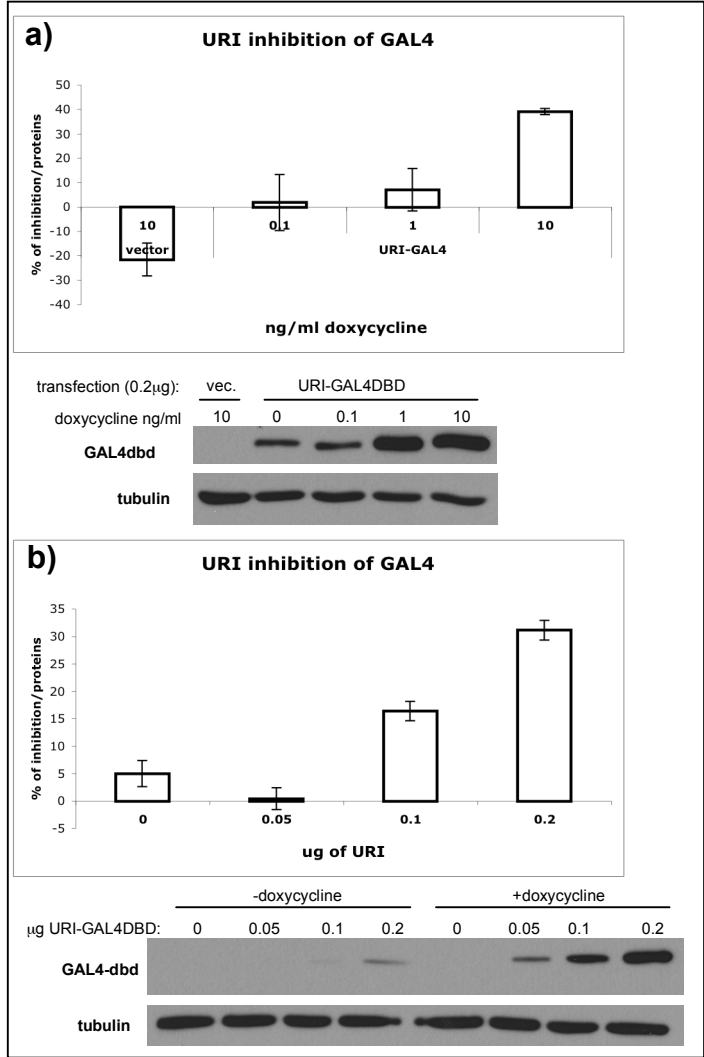
Figure 13. URI is a transcriptional repressor. 293TREX-luciferase cells were transfected with 0.2μg of URI-G4 (a) or with an increased amount of URI-G4 DNA (b). An empty vector was transfected as control and after 24 hrs from transfection cells were treated with increasing concentrations of doxycycline (a) or with 1μg/ml of doxycycline (b). Luciferase was measured and reported as percentage of repression normalized for total proteins quantified by Bradford assay. The expression of URI-G4 and tubulin (loading control) was also analyzed by Western blotting.

293T-REX-luciferase cell clones stably overexpressing URIG4dbd were generated and screened for URIG4dbd expression and luciferase repression. As expected, the expression of URI was directly correlated to the repression of luciferase as shown in figure 14.
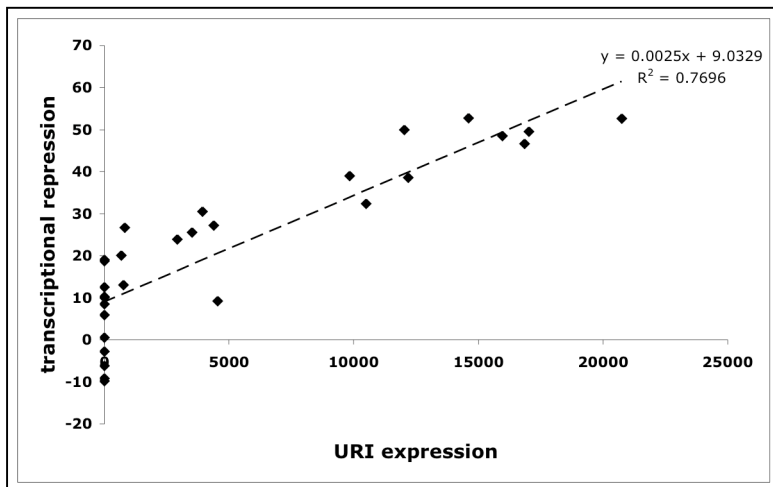
Figure 14. URI expression directly correlates with luciferase transcriptional repression in 293T-REX-luciferase-URIG4dbd cells. The expression of URIG4dbd protein was quantified for 29 different clones by Western blotting. The percent of luciferase repression (100*(luciferase fluorescence units in the presence of doxycycline/ luciferase fluorescence units in the absence of doxycycline)) is reported on the Y axis.

Control cells simply overexpressing the G4dbd were also generated (293T-REX-luciferase-G4 cells). This 293T-REX-luciferase-G4 system was also used in chromatin immunoprecipitation (ChIP) experiments using a G4dbd specific antibody (Millipore) or an Art-27 antibody to analyze URIG4dbd and Art-27 recruitment on the luciferase gene. Repression of luciferase expression was determined by Q-PCR measurement of luciferase mRNA and URIG4dbd protein was analyzed by Western blotting using a G4dbd antibody (SIGMA) or a URI specific antibody. As expected luciferase transcription was inhibited by URIG4dbd expression induced by doxycycline treatment (fig. 15 a and b). ChIP assay showed that G4dbd was recruited to the G4 binding site upstream of the luciferase gene in control 293T-REX-G4 cells, (fig. 15c upper left panel) but this recruitment does not affect luciferase transcription (fig. 15b). URI-G4dbd is also recruited on the G4 binding site upon doxycycline treatment, (fig. 15c upper

70

right panel) mediating repression of luciferase expression. ChIP of endogenous Art-27 confirmed that Art27 is recruited with URI to the G4 DNA binding domain demonstrating that Art-27 is part of the URI repression complex (fig. 15c lower panel).
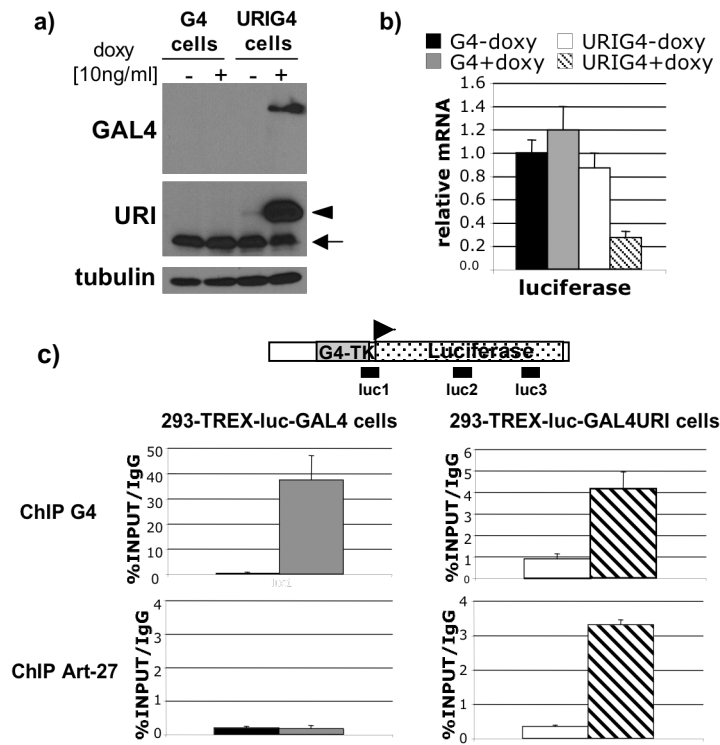
Figure 15. Art-27 is part of the URI transcriptional-repression complex. 293T-REX-luciferase-G4 control cells and 293T-REX-luciferase-URIG4 cells were treated with or without doxycycline (10ng/ml) for 24 hours. After incubation, proteins, mRNA and chromatin were isolated to analyze a) URIG4 expression by Western blotting, b) luciferase expression by Q-PCR and c) URIG4 and endogenous Art-27 recruitment on the luciferase gene promoter by ChIP. Only the regions amplified by Q-PCR using luc1 primers are reported in b) and c).

No recruitment of URIG4dbd and Art-27 on the body (luc2 primers) or 3' end (luc3 primers) of the luciferase gene was detected as expected because of the tethering of URI to the G4 binding domain upstream of the TK promoter.

1.13 Discussion

In this study we identify URI, a RPB5 interacting protein, as a new protein involved in controlling androgen receptor transcription. We demonstrate that URI is part of a complex containing the previously identified AR co-repressor Art-27. URI and Art-27 are characterized by domains that share high homology with the alpha subunits of prefoldin. Prefoldin is a heterohexameric chaperone that is known to be involved in the presentation of unfolded target proteins to the cytosolic chaperonins [206]. Despite this structural homology, we did not observe chaperone activity for Art-27 and URI. We ruled out the possibility that URI is itself a target protein for facilitated folding by c-cpn/CCT/TRiC using an in vitro binding assay of URI to CCT as previously described by Vainberg and colleagues [206] (data not shown). This observation suggests that URI and Art-27 play a different role than that canonically ascribed to prefoldin. Furthermore, URI and Art-27 do not affect AR stability and/or localization (data not shown). Importantly, URI and Art-27 strongly affect the stability of one another, strengthening the idea that these two proteins interact in vivo in prostate cells.

URI was identified as a protein that binds RPB5, a subunit shared by all three RNA polymerases. This fact, together with the observations presented above, suggests that URI may act as a mediator to connect the transcriptional machinery to AR, possibly through Art-27. URI and Art-27 interact through the four beta strands of their prefoldin domains [84] while Art-27 binds the androgen receptor through the two flanking alpha helices (Markus and Garabedian, unpublished results), supporting this hypothesis. Although we were not able to co-immunoprecipitate URI with AR (fig.5a), Art-27 co-immunoprecipitates with AR [77]. The

72

interaction between AR and URI could be difficult to detect due to the transient nature of the interaction, the inability of the URI antibody to recognize URI in complex with other proteins, or the instability of the complex under the conditions of the immunoprecipitation. Alternatively, there may be a pool of Art-27 protein bound to the androgen receptor but not to URI. While the precise mechanism is unclear, changes in URI mRNA [198] during prostate cancer progression could represent altered regulation of the AR transcriptional landscape in prostate cancer.

While URI mRNA is decreased in late stage prostate cancer [198], loss of nuclear Art-27 correlated with more aggressive disease [78]. Protein expression of URI in late-stage prostate cancer has yet to be examined, but considering the interdependent expression of Art-27 and URI it would not be surprising if the decrease in URI in advanced cancers correlated with loss of nuclear Art-27 and with higher tumorigenic potential. In line with this idea, we showed that URI loss affects the response of LNCaP cells to bicalutamide, a known androgen receptor antagonist (fig.2), and that URI over-expression decreases LNCaP anchorage-independent growth (fig.3). Therefore, an analysis of URI protein levels and regulation during prostate cancer progression could give a functional explanation for Art-27 protein loss during the later stages of prostate cancer, giving new insights on the development of castration-resistant prostate cancers.

Previous reports [85, 87, 100] identified an R2TP/prefoldin-like complex comprised of URI and Art-27, which is responsible for the cytoplasmic assembly of RNA polymerase II. In a mass spectrometry analysis of URI interactors performed by our lab using LNCaP cell lysates (chapter 2), we also observed the interaction of URI with the R2TP/prefoldin-like complex. Interestingly, the R2TP/prefoldin-like complex shares several subunits with the R2TP complex comprised of the chaperone proteins p23 and heat shock proteins hsp90. The p23/hsp90 complex (R2TP complex) regulates the estrogen receptor (ER), and in particular the small

chaperone p23 was reported to affect ER binding to chromatin [207]. Moreover, a comparison of URI and p23 expression levels in the cohort of prostate tumors analyzed by Sawyer and colleagues [208] show a very high correlation between p23 and URI (odds ratio/correlation= 23.2, 95% confidence), suggesting a possible functional correlation between p23 and URI in prostate cells. Our focus, however, was on the role of URI as a transcription regulator. Consistent with the idea that URI is also present in the nucleus, our mass spectrometry analysis of URI nuclear interactors identified several nuclear proteins such as RPB1 phosphorylated at ser2/ser5, MLL1, various components of the mediator complex, elongation factors and TAFs (TATA box binding proteins) that suggest a direct role of URI and Art-27 in transcription. Moreover, the demonstrated binding of URI to the general transcription factor TFIIF and to the Paf-1 complex [97, 99] strengthens the idea that nuclear URI plays an important function in transcription regulation independent of its cytoplasmic role as a chaperone for Pol II complex assembly.

Co-stabilization of URI and Art-27 makes it very difficult to discern independent functions for the two proteins. Our microarray analysis of mRNA expression in LNCaP cells depleted of URI or Art-27 demonstrates substantial overlap in gene profiles due to the loss of one or the other protein. Our results indicate that URI stabilizes Art-27 protein in the cytoplasm and nucleus of prostate cells and that URI loss decreases the Art-27 bound to DNA. On the NKX3.1 gene, knockdown of URI resulted in a decrease of Art-27 protein recruitment. Decreasing the repressive effects of Art-27 on AR-mediated transcription upon URI knockdown could explain the transcriptional up-regulation of androgen-regulated genes like PSA, FKBP5 and NKX3.1. Interestingly, knockdown of URI also results in increased recruitment of AR on NKX3.1 AREs. This result cannot be explained through an effect of URI on Art-27 co-repressor activity and/or stability. However, the mechanisms by which Art-27 is able to repress AR transcription are still unknown. Our results (fig.9 and 11) suggest that URI

and Art-27 could be involved in chromatin remodeling and chromatin structure, ensuring accurate recruitment of the androgen receptor to the AREs of androgen regulated genes. This hypothesis is supported by the finding that a fraction of URI and Art-27 is bound to the chromatin in an androgen-independent manner, (fig.9) and by previous reports indicating that URI interacts with chromatin remodeling proteins like the helicases TIP49 and TIP48 [84]. Our ChIP analysis of Art-27, AR and polII recruitment across the entire NKX3.1 gene (fig. 11) demonstrates a recruitment of Art-27, probably in complex with URI, on the TSS and on the AREI enhancer region in the 3' UTR of NKX3.1. These data are consistent with the reported binding of Art-27 to AR [77] and with the binding of URI to RNA polymerase II [94, 98, 114]. Also Art-27 is recruited with a URI-G4dbd fusion protein to a G4 binding domain, mediating repression of transcription of the downstream luciferase gene in 293T-REX-luciferase cells (figure 16). This result supports the idea that URI, together with Art-27, is part of a novel transcriptional repression complex. The data presented here also suggests that an Art-27-URI containing complex binds chromatin in an androgen independent manner and loss of this complex may affect chromatin structure, which in turn could be responsible for aberrant AR recruitment and transcription.

CHAPTER 2:

MASS SPECTROMETRY ANALYSIS OF NUCLEAR URI

INTERACTORS IN PROSTATE CELLS

2.1 MASS SPECTROMETRY ANALYSIS OF NUCLEAR URI INTERACTORS IN LNCaP PROSTATE CELLS.

URI/C19orf2 has been characterized as a transcriptional repressor [94] but little is known about the mechanisms by which URI can inhibit gene transcription. We previously showed that URI, in complex with Art-27, functions as a repressor of the androgen receptor in prostate cells [82]. To better understand URI mediated transcriptional repression we performed mass spectrometry analysis to identify proteins that interact with URI in the nucleus of prostate cells. We focused our study on nuclear proteins to investigate the largely unexplored role of URI in transcription regulation. Control LNCaP cells, stably over-expressing an empty vector (LNCaP-vect.) or LNCaP cells constitutively expressing a FLAG tagged URI (LNCaP-URI), were used for this analysis. The number of peptides retrieved for each co-immunoprecipitated protein was compared between control cells and URI over-expressing cells (Table 1). We identified a protein as a URI interactor if it immunoprecipitated from URI over-expressing cells, but not from control cells in both replicate experiments performed. By these criteria, we identified 36 proteins that interact with URI in the nucleus of prostate cells. As expected, we found 10 subunits of RNA polymerase I, II or III (Table 1, asterisks) including RPB5/POLR2E, the previously identified URI interactor. We also confirmed URI interaction with Art-27, together with 3 other prefoldin proteins and PDRG1, a prefoldin like protein. In addition, we identified all the components of the R2TP/prefoldin-like complex (Table 1, arrowheads) proposed to be important for the assembly of the RNA polymerase II complex (Table 1, arrowheads). The two helicases RUVBL1 and RUVBL2, components of the R2TP/prefoldin-like complex, were also identified although we noted a low number of peptides also present in one of the two vector controls. Among the novel URI interactors we focused on the KAP1/TRIM28 protein, because of its well characterized role in gene repression, and on the PP2A phosphatase, because of the role of URI in regulation of PP1γ phosphatase in the

mitochondria [94] (Table 1, gray lines) (chapter 3). Interestingly, in at least one replicate experiment, peptides from the PP1α and PP1β phosphatases that interact with KAP1 [158] were also identified, as well as peptides from the regulatory subunit A of PP2A (although peptides from the latter were also present in the control immunoprecipitation).

Accession	URI-flag(1)	vector(1)	URI-flag(2)	Vector(2)	description	
IPI00477619	70	0	55	0	C19orf2 RPB5-mediating protein isoform a	◄
IPI00002408	37	0	27	0	RPAP3 Isoform 1 of RNA polymerase II-associated protein 3	◄
IPI00024163	32	0	26	0	POLR3A DNA-directed RNA polymerase III subunit RPC1	*
IPI00291093	23	0	18	0	POLR2E DNA-directed RNA polymerases I, II, and III subunit RPABC1	*
IPI00465211	22	0	18	0	WDR92 HZGJ	◄
IPI00021405	22	0	7	0	LMNA Isoform A of Lamin-A/C	
IPI00005657	19	0	15	0	PFDN6 Prefoldin subunit 6	◄
IPI00006052	17	0	13	0	PFDN2 Prefoldin subunit 2	◄
IPI00550995	15	0	13	0	PIH1D1 PIH1 domain-containing protein 1	◄
IPI00027887	14	0	13	0	PDRG1 p53 and DNA damage-regulated protein 1	◄
IPI00220045	13	0	3	0	POLR3E Isoform 1 of DNA-directed RNA polymerase III subunit RPC5	*
IPI00170862	12	0	3	0	UXT ubiquitously-expressed transcript isoform 1	◄
IPI00301346	10	0	13	0	POLR3B DNA-directed RNA polymerase III subunit RPC2	*
IPI00031960	9	0	9	0	POLR1A DNA-directed RNA polymerase I subunit RPA1	*
IPI00005179	8	0	9	0	POLR1C Isoform 1 of DNA-directed RNA polymerases I and III subunit RPAC1	*
IPI00910997	6	0	4	0	cDNA FLJ57486	
IPI00026952	6	0	4	0	PKP3 Plakophilin-3	
IPI00215978	6	0	3	0	POLR3D DNA-directed RNA polymerase III subunit RPC4	*
IPI00216318	6	0	2	0	YWHAB Isoform Long of 14-3-3 protein beta/alpha	
IPI00003309	5	0	4	0	POLR2H DNA-directed RNA polymerases I, II, and III subunit RPABC3	*
IPI00856080	4	0	4	0	GPN3 Isoform 2 of GPN-loop GTPase 3	
IPI00010157	4	0	2	0	MAT2A S-adenosylmethionine synthetase isoform type-2	
IPI00477279	4	0	2	0	RPL12P2 similar to ribosomal protein L12	
IPI00430770	3	0	5	0	SUPT6H Isoform 2 of Transcription elongation factor SPT6	
IPI00554788	3	0	5	0	KRT18 Keratin, type I cytoskeletal 18	
IPI00796337	3	0	3	0	PCBP2 poly(rC) binding protein 2 isoform a	
IPI00006379	3	0	3	0	NOP58 Nucleolar protein 5	
IPI00429689	3	0	2	0	PPP2CB Serine/threonine-protein phosphatase 2A catalytic subunit beta isoform	
IPI00438229	2	0	8	0	TRIM28 Isoform 1 of Transcription intermediary factor 1-beta	
IPI00031627	2	0	5	0	POLR2A DNA-directed RNA polymerase II subunit RPB1	*
IPI00031661	2	0	4	0	NOC4L Nucleolar complex protein 4 homolog	
IPI00410067	2	0	3	0	ZC3HAV1 Isoform 1 of Zinc finger CCCH-type antiviral protein 1	
IPI00009659	2	0	3	0	RPRD1B Regulation of nuclear pre-mRNA domain-containing protein 1B	
IPI00032439	2	0	2	0	POLR1D Isoform 1 of DNA-directed RNA polymerases I and III subunit RPAC2	*
IPI00032406	2	0	2	0	DNAJA2 DnaJ homolog subfamily A member 2	
IPI00015361	2	0	2	0	PFDN5 Prefoldin subunit 5	
IPI00872177	0	0	4	0	PPP1CB 41 kDa protein	
IPI00550451	3	0	0	0	PPP1CA Serine/threonine-protein phosphatase PP1-alpha catalytic subunit	
IPI00554737	3	2	0	0	PPP2R1A Serine/threonine-protein phosphatase 2A 65 kDa regulatory subunit A alpha isoform	
IPI00021187	18	5	18	0	RUVBL1 Isoform 1 of RuvB-like 1	◄
IPI00009104	18	2	21	0	RUVBL2 RuvB-like 2	◄

Table 1. Mass spec analysis of URI nuclear interactors

Complete list of nuclear URI interactors obtained from immunoprecipitation of FLAG-URI from control cells (vector) and URI overexpressing cells (URI-flag). The analysis was repeated twice and the

number of peptides retrieved in the two analyses are reported together with the international protein index (Accession) and the description for each protein. Interesting proteins that were also retrieved in control samples are reported in two lower tables. Arrowheads show the components of the R2TP/prefoldin-like complex and asterisks show RNA polymerase subunits. The interaction of URI to the proteins in the grey rows is explored in chapter 3.

Of note, we did not identify DMAP1 (DNA methyltransferase 1 associated protein 1) as a URI interacting protein. It has been shown in HLE cells (human hepatoma cell line) that DMAP1 binds URI and dictates its nuclear translocation, possibly masking a cytoplasmic localization sequence in the second α-helix of the URI prefoldin-like domain [209]. We performed several experiments to explore the possible binding of URI to DMAP1 protein but we were not able to observe binding between the two proteins. Immunoprecipitation of URI from cells overexpressing DMAP1 and URI did not show binding of URI to DMAP1, and immunoprecipitating DMAP1 did not induce URI co-immunoprecipitation (data not shown). Also immunofluorescence experiments using LNCaP cells overexpressing a HA-tagged DMAP1 and a flag-tagged URI did not show co-localization of the two proteins; DMAP1 is exclusively nuclear while URI is mainly present in the cytoplasm and just a small fraction of URI protein is present in the nucleus (data not shown).

We decided to further validate the interaction of URI with RPB5, the shared subunit of RNA polymerase I, II and III (paragraph 2.2), and the URI interaction with PDRG1 (paragraph 2.3) which, like URI and Art-27, is another prefoldin-like protein. To gain more insight into the nuclear-cytoplasmic translocation of the URI-Art-27 complex, we also explored the binding of URI to the rest of the R2TP/prefoldin-like complex (paragraph 2.4).

2.2   URI INTERACTS WITH RPB5/POLR2E PROTEIN AND REGULATES ITS STABILITY AND TRANSCRIPTION.

URI was initially identified by Far-Western as a RNA polII subunit 5 interacting protein and therefore named RMP (RPB5 mediating protein) [94]. The region of interaction of URI and RPB5 was mapped to a domain encompassing amino acids 177-257 of the currently annotated URI1/URIα sequence. More specifically aa 177-224 were shown to be essential for binding to RPB5, while aa 224-257 have an accessory role for the binding of URI to RPB5 [94]. Moreover RPB5 was shown to be the subunit functioning as the interface between polII and the R2TP/prefoldin-like complex responsible for the cytoplasmic assembly of RNA polymerase II [87].

We decided to validate and better explore the interaction of URI to RPB5 that we also clearly observed in our mass spectrometry analysis. We therefore subcloned a deleted flag-URI (URIΔRPB5) lacking the essential domain of interaction with RPB5 (aa 177-224).
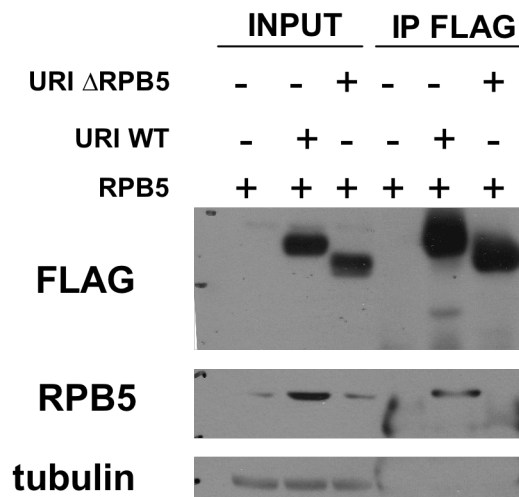
Figure 16. URI interacts with RPB5. 293 cells were transfected with RPB5 and URI wild type (URI WT) or URI deleted of the RPB5 binding domain (URIΔRPB5). After 48 hrs from transfection cells were lysed and part of the lysate used for the immunoprecipitation of URI using FLAG antibodies. The expression and immunoprecipiation of URI and RPB5 was analyzed by Western blotting. Tubulin was used as loading control.

Immunoprecipitation of flag-URI from 293 cells overexpressing flag-URI and wild type RPB5 clearly show binding between the two proteins. As expected flag-URIΔRPB5 does not interact with RPB5 confirming the data previously reported by Dorjsuren and colleagues [94] (fig. 16). Interestingly, overexpression of URI induced increased RPB5 protein while overexpression of URIΔRPB5 did not have any effect on RPB5 expression. This result suggested that URI binding to RPB5 is able to stabilize RPB5 protein in a similar manner to the URI dependent stabilization of Art-27. To confirm that the absence of co-immunoprecipitation of URIΔRPB5 with RPB5 was due to absence of binding between the two proteins and not simply to a lower amount of RPB5 protein in cells overexpressing URIΔRPB5, we performed the same immunoprecipitation experiment reported above in the presence or absence of MG132 inhibitor. MG132 inhibits protein degradation through the proteasome and, therefore, we predicted it would increase the level of RPB5 protein even in cells not overexpressing URI. Indeed we observed that cells treated with MG132 have a similar elevated level of RPB5 protein. In this experiment, as in the one presented in figure 16, RPB5 interacts with URI WT while it does not interact, or it interacts very poorly, with URIΔRPB5 (fig. 17).
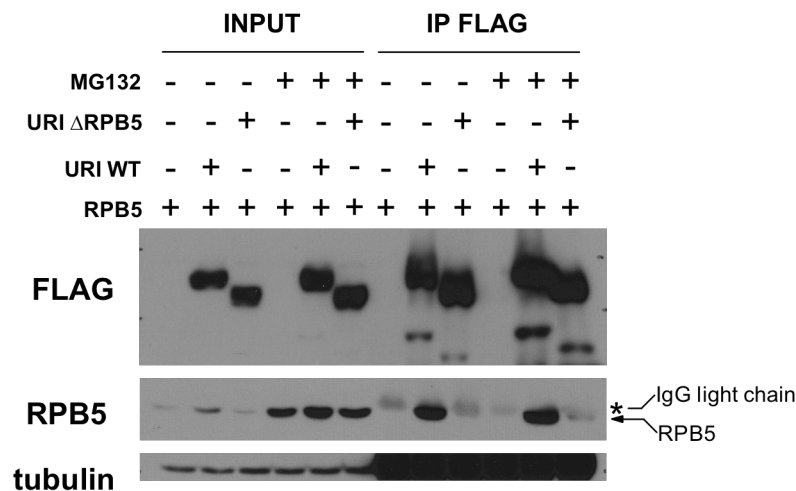
Figure 17. URI binds and stabilizes RPB5 protein. The experiment was performed as in fig.16 but in the presence or absence of 25μM MG132.

To demonstrate that URI and RPB5 interaction is direct we also transcribed/translated URI and RPB5 using an in vitro reticulocyte system. ^{35}S was included in the reaction to label the proteins. A fraction of the in vitro transcribed/translated URI WT or URIΔRPB5 and RPB5 proteins were mixed 1:1 and incubated at 4°C for 4h. After incubation, flag-URI was immunoprecipiated using a flag antibody. The precipitated immunocomplexes were extensively washed and analyzed by SDS-PAGE. Reactions in no antibody or no URI construct were used as negative control. Transcription/translation of URI and RPB5 produced proteins with the anticipated size (≈90KDa for URI and ≈24KDa for RPB5). The URI constructs (both URI WT and URIΔRPB5) also produced smaller products that migrate between the 50KDa and 37KDa markers. RPB5 clearly immunoprecipitates with URI WT and not with URIΔRPB5. Also no bands were detected in the two negative control lanes (fig. 18). These observations confirm that URI and RPB5 bind directly through URI aa 177-224.
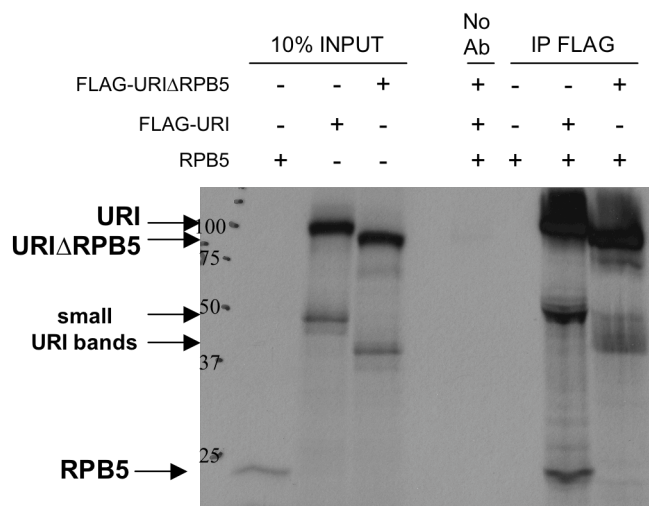
Figure 18. URI and RPB5 directly interact. In vitro transcribed/translated and ^{35}S labelled RPB5, URI WT and URIΔRPB5 proteins were mixed and used to immunoprecipitate URI with a FLAG antibody. Input solutions and immunoprecipitated complexes were analyzed by SDS-PAGE.

We also asked if the increase in RPB5 protein in cells overexpressing URI was due, at least in part, to an increase in RPB5 transcription. mRNA from 293 cells stably overexpressing a control vector or a flag-tagged URI was isolated and URI and RPB5 message quantified by Q-PCR (fig.19).
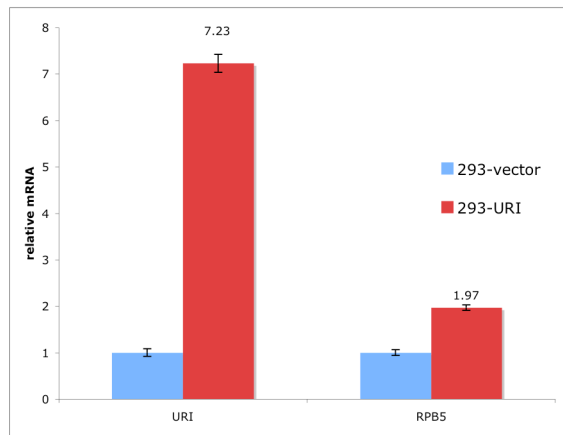
Figure 19. URI increases RPB5 transcription. mRNA was isolated from 293 stable cell lines overexpressing an empty vector (293-vector) or a construct encoding flag-URI (293-URI). URI and RPB5 mRNA were quantified by Q-PCR. The URI and RPB5 mRNA of 293-vector cells were set as 1.

Overexpression of URI induced doubling of RPB5 mRNA suggesting that URI overexpression induced not only a stabilization of RPB5 protein but also an increase in RPB5 transcription. Overall these data suggest a tight relationship between URI and RPB5 protein in prostate cells.

We also performed luciferase experiments to explore the importance of RPB5 binding in the URI mediated transcription repression of AR-mediated transcription. LNCaP stably over-expressing a luciferase reporter downstream of the probasin promoter containing known androgen response elements (AREs) (LB1-LNCaP), were used for these luciferase experiments. An empty vector, a construct encoding wild type URI or a construct encoding URIΔRPB5 were transfected in LB1-LNCaP cells. Afer 24 hours of hormone starvation cells were treated with or without 10nM R1881 for an additional 24 hrs. Cells were then lysed and

luciferase measured and normalized by protein concentration measured by Bradford assay
(fig. 20).
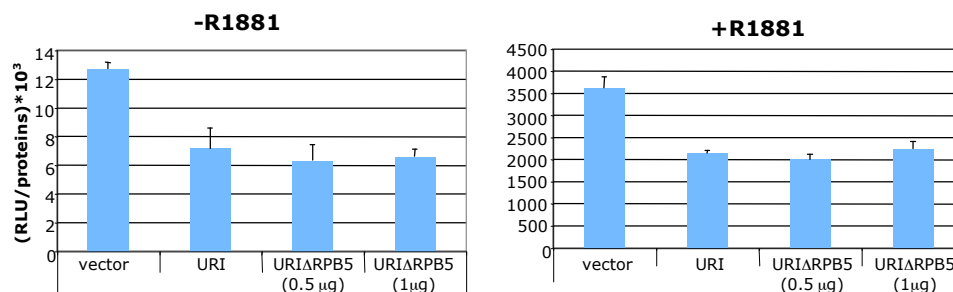
Figure 20. RPB5 binding is not necessary for URI mediated repression of AR mediated transcription. LNCaP-LB1 cells were transfected with an empty vector or a vector encoding URI or URIΔRPB5. 0.5µg or 1µg of URIΔRPB5 construct were transfected. After 24hrs of hormone starvation cells were treated with or without 10nM R1881 for an additional 24hrs. The luciferase units normalized by protein content is reported.

Both URI wild type and URIΔRPB5 reduce AR-mediated transcription of the luciferase reporter either in the absence or presence of R1881. This evidence suggests that URI-mediated repression of AR-dependent transcription is not mediated by the binding of URI to RPB5 protein or probably to the whole RNA polymerase II complex.

2.3   URI BINDS AND STABILIZES PDRG1 PROTEIN.

P53 and DNA damage-regulated gene 1 (PDRG1) is a novel and currently understudied gene that encodes a homonymous protein of approximately 15KDa, characterized by a β-prefoldin like domain [210]. PDRG1 gene was shown to be upregulated by UV radiation and downregulated by p53 protein. Interestingly PDRG1 protein expression was also shown to be upregulated in several cancers (colon, rectum, ovary, lung, stomach, breast and uterus) and

depletion of PDRG1 in colon cancer cell lines was shown to induce a decrease in cell proliferation [211]. PDRG1 is also part of the R2TP/prefoldin like complex which also comprises URI and Art-27 proteins [87]. We were interested in exploring the interaction between URI and PDRG1 for several reasons:

- The hypothesized involvement of PDRG1 in DNA damage, cell cycle and chromatin stability.

- The misregulation of PDRG1 in several cancers.

- The similarity in structure between PDRG1 (β-prefoldin like protein), Art-27 (α-prefoldin like protein) and the N-terminus of URI (α-prefoldin like domain).

- The fact that, according to our mass spectrometry analysis, PDRG1 is a nuclear interactor of URI. PDRG1 has a molecular weight similar to Art-27 that we showed binds strongly and directly to URI. However, compared to Art-27, PDRG1 has an even more abundant number of peptides retrieved in our two immunoprecipitation/mass spectrometry experiments, suggesting a strong interaction between URI and PDRG1.

For these reasons we decided to validate the interaction of URI with PDRG1 by co-immunoprecipitation experiments in prostate cells. LNCaP cells stably expressing an empty vector or a construct encoding flag-URI were used to assay PDRG1 interaction with endogenous and over-expressed URI as well as with endogenous Art-27 (fig. 21). Lysates from LNCaP-vector and LNCaP-URI cells were used to immunoprecipitate endogenous URI with a monoclonal anti-URI antibody, overexpressed URI with a flag antibody (SIGMA) and Art-27 with a polyclonal anti-Art-27 antibody. As expected, endogenous or overexpressed URI efficiently pulled down endogenous Art-27. Interestingly the amount of Art-27 protein coimmunoprecipitated with URI or flag-URI is the same as the amount of Art-27 protein immunoprecipitated using anti-Art-27 antibody, suggesting a 1:1 stoichiometry for the URI-Art-27 complex(es). It also supports our hypothesis that Art-27 and URI are tipically bound to each

other in prostate cells. We observed the same behavior for PDRG1 protein which co-immunoprecipitates with overexpressed flag-URI, endogenous URI or with Art-27.
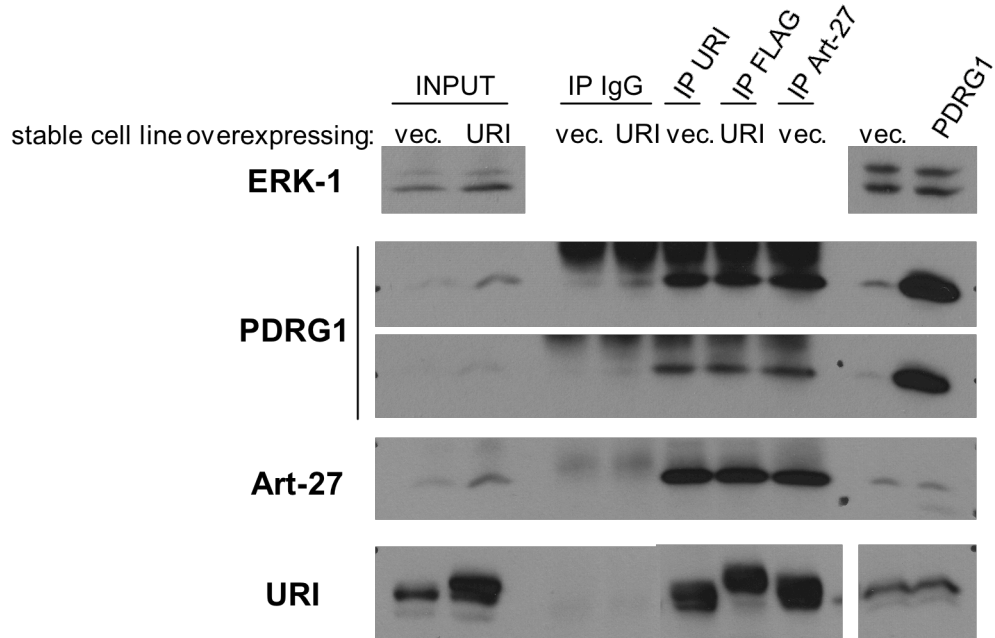
Figure 21. URI and Art-27 interact with PDRG1 in LNCaP prostate cells. LNCaP-vector cells and LNCaP-URI stable cell lines were used to immunoprecipitate URI, flag-URI and Art-27. The immunocomplexes were analyzed by Western blotting using the indicated antibodies. ERK1 is used as loading control. LNCaP cells transiently overexpressing an empty vector or a construct encoding PDRG1 were also analyzed for the expression of PDRG1, URI and Art-27.

Interestingly, we noticed that overexpression of URI induced increased PDRG1 protein in a similar manner to the stabilization of Art-27 protein that we previously reported. Overexpression of PDRG1 in LNCaP cells, on the other hand, does not seem to affect the endogenous Art-27 or URI proteins (fig. 21, last 2 lanes). To explore the effect of URI on

PDRG1 protein, lysates obtained from LNCaP cells depleted of URI by siRNA treatment were analyzed for PDRG1 and URI protein expression. Cells were also treated with or without 10nM R1881, a synthetic androgen, to assess if PDRG1 protein was affected by androgen treatment. As for Art-27, knock down of URI either in the presence of absence or hormone, induces a decrease of PDRG1 protein (fig. 22).
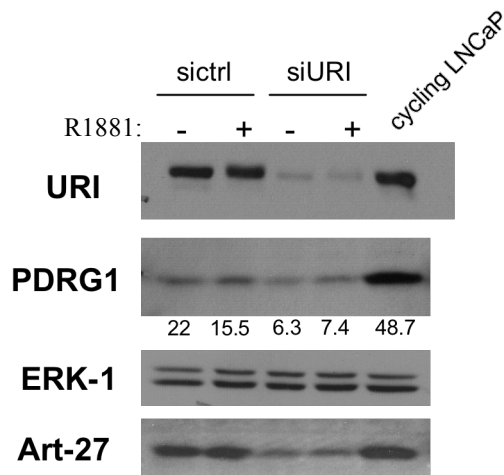
Figure 22. Depletion of URI induces a decrease in PDRG1 protein. LNCaP cells were treated sequentially two times with siRNA control (siCtrl) or siRNA against URI (siURI) for 4 hours. After knock down cells were treated with or without R1881 10nM for 24hrs and then lysed in Triton buffer. Cell lysates were analysed for Art-27, PDRG1 and URI expression by Western blotting. ERK1 protein is used as loading control and LNCaP cell lysates from normally cycling cells cultured in complete media are used for comparison. The numbers reported below the PDRG1 blotting are densitometry analysis of PDRG1 protein bands (ImageJ).

Overall these results indicate that URI and PDRG1 interact with each other in prostate cells. Most likely URI, PDRG1, Art-27 and RPB5 are part of a common multiprotein complex in which URI has a pivotal role because changes in URI expression induce either destabilization of the whole complex or increased expression of different members of the complex. The R2TP/prefoldin like complex has been previously shown to be comprised of URI, Art-27, PDRG1 and RPB5 together with other proteins (namely prefoldin 2 (PFDN2) and prefoldin 6

(PFDN6), the two DNA helicases TIP49 and TIP48, PIH1D1, RPAP3/spaghetti and WDR92).

Our mass spectrometry and immunoprecipiation experiments suggest that URI is an essential protein for the stability of several members of the R2TP/prefoldin like complex. Because this complex was shown to be important in the assembly of the RNA polymerase II complex in the cytoplasm of the cells, URI probably has an important role in this process. Interestingly our mass spectrometry analysis showed that the R2TP/prefoldin-like complex binds to URI in the nucleus of prostate cells suggesting that URI and the prefoldin-like complex is probably moving with RNA pol II from the cytoplasm to the nucleus.

2.4 URI FOLLOWS THE R2TP/PREFOLDIN-LIKE COMPLEX AND RNA POLYMERASE II MOVEMENT FROM THE CYTOPLASM TO THE NUCLEUS.

RNA polymerases (RNA pol) play a fundamental role in the cell. RNA polymerases I and III synthesize non coding RNAs while RNA pol II is responsible for the transcription of mRNAs and capped non coding RNAs. RNA pol I, II and III are composed of 14, 12 and 17 subunits some of which are shared among the three polymerases. Despite the great knowledge about the structure and function of the RNA polymerases little is known about their assembly. RNA polymerase I was shown to be assembled on the gene promoter where the pol I subunits can either assemble or be exchanged in a cell cycle dependent manner [212, 213]. A study that used a combination of quantitative mass spectrometry analysis and fluorescence microscopy demonstrated that, unlike RNA polymerase I, the RNA polymerase II complex is assembled in the cytoplasm by a chaperone-like complex [87]. This complex was named R2TP/prefoldin-like complex because four of its subunits were components of the previously identified R2TP yeast complex (TIP48, TIP49, RPAP3/hSpaghetti, PIH1D1) [214], and additionally five subunits were prefoldin-like proteins (URI, Art-27, PDRG1, PFDN2 and PFDN6). RPB5, the common

subunit of RNA polymerase I, II and III, was shown to be the interface that connects the R2TP/prefoldin like complex to the RNA polymerase complex (fig. 23).
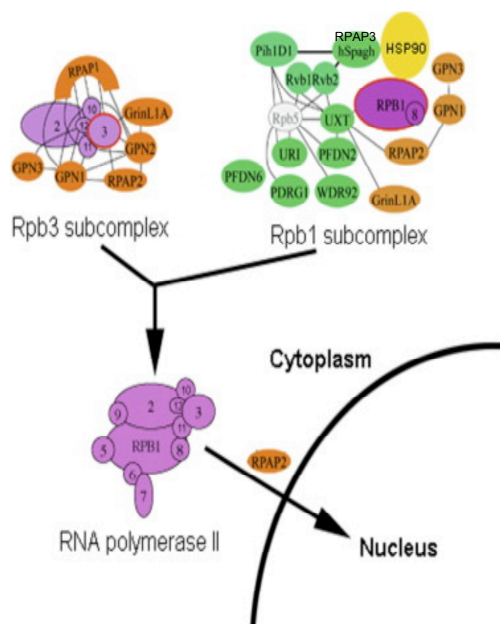
Figure 23. Schematic of RNA pol II assembly. RNA polII is first assembled in the cytoplasm as two subcomplexes containing RPB3 and RPB1, respectively. The RPB1-containing complex is bound to the R2TP/prefoldin-like complex that mediates the assembly of the entire pol II complex before translocation into the nucleus. (Mol Cell. 2010 Sep 24;39(6):912-24).

We also identified all the components of the prefoldin like complex in our mass spectrometry analysis of URI nuclear interactors (table 1). The data presented above also suggest an important role of URI in maintaining the integrity of the entire complex because depletion of URI protein induces disassembly and destabilization of the complex, while over-expression of URI increased expression of several subunits of the complex such as Art-27, PDRG1 and RPB5. To explore the role of URI in the R2TP/prefoldin-like complex we generated a LNCaP stable cell line over-expressing a URI protein fused to EGFP. This cell line was used to visualize URI movement upon treatment with compounds shown to affect the localization of pol II subunits. In particular, we used α-amanitin, which binds the large subunit of human RNA polymerase II (RPB1) and irreversibly stalls it on the DNA [215]. This results in

transcriptional arrest and degradation of RPB1. Upon degradation of RPB1, RNA pol II disassembles and is exported into the cytoplasm through the CRM1/XPO1 exportin [216]. Leptomycin B (LMB) is a specific inhibitor of the CRM1 exportin that induces retention of the pol II subunit into the nucleus even after RPB1 degradation induced by α-amanitin (fig. 24) [216]. Actinomycin D induces RNA pol II stalling on the DNA similar to α-amanitin, but it does not induce RPB1 degradation and disassembly of the RNA pol II complex [215].
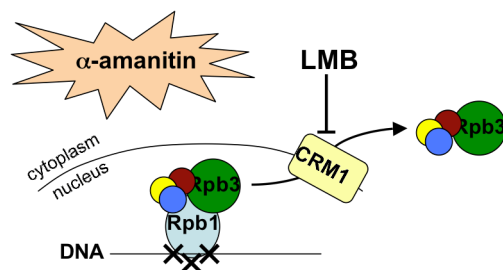
Figure 24. α-amanitin induces RNA pol II stalling and RPB1 degradation. Consequently the other pol II subunits (including RPB3) are exported into the cytoplasm through CRM1. Leptomycin B (LMB) inhibits CRM1, inducing accumulation of RNA pol II subunits in the nucleus upon α-amanitin treatment. Actinomycin D also induces RNA pol II stalling but it does not induce degradation of RPB1 causing the accumulation of pol II subunits in the nucleus even in the absence of LMB.

In LNCaP-URI-EGFP cell lines URI is mainly cytoplasmic (fig. 25, top left panel). Upon treatment with α-amanitin, which induces RNA polII stalling on the DNA, URI became more uniformly distributed between the cytoplasm and the nucleus suggesting that URI binds stalled RNA polymerase II accumulating in the nucleus (fig. 25, top right panel). Treatment of the cells with α-amanitin and leptomycin B (LMB) induced increased nuclear localization and, in some cells (fig. 25, bottom left panel, arrowheads), URI became mainly nuclear. These data suggest that, like the RNA polymerase subunits, URI is pumped out from the nucleus into the cytoplasm through the CRM1 exportin. In cells treated with actinomycin D (fig. 25, bottom right panel) which induces RNA pol II stalling but not pol II disassembly, URI became

predominantly nuclear, suggesting tight binding of URI to RNA polymerase II even under conditions of stalled polymerase and transcriptional arrest.
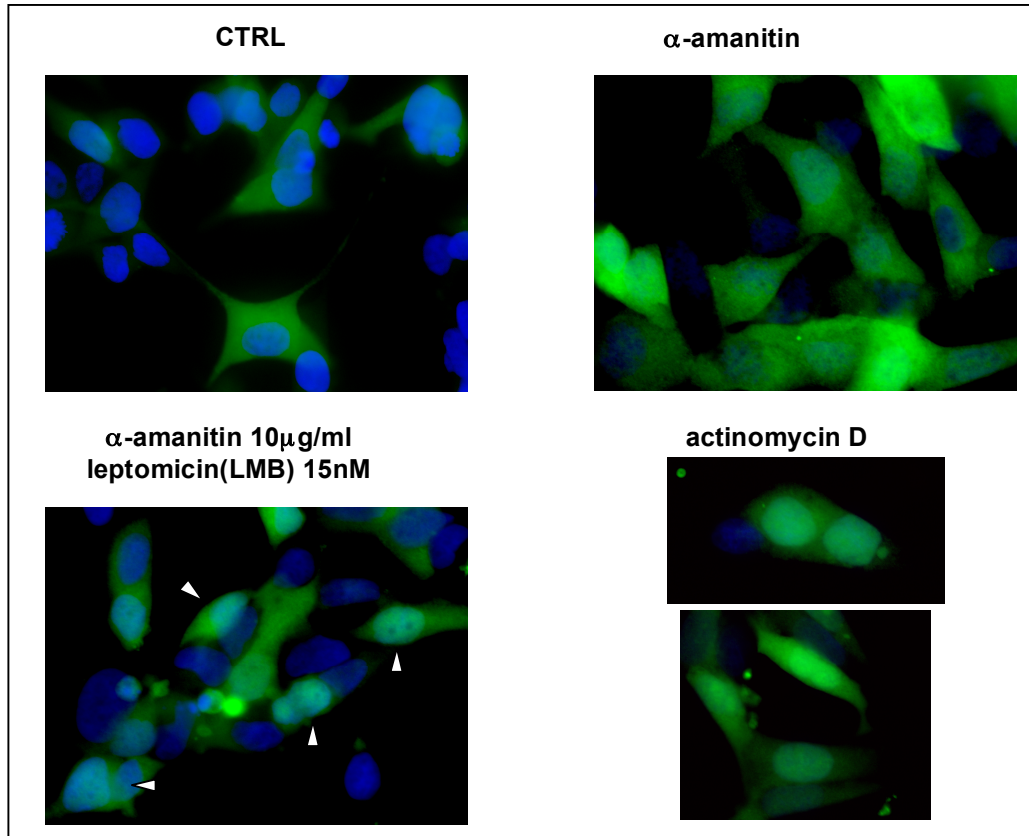
Figure 25. URI and RNA pol II co-localization. LNCaP cells stably overexpressing an URI-EGFP fusion protein were used to visualize URI localization. Cells were treated with α-amanitin, α-amanitin + leptomycin B or with actinomycin D. Cells were counterstained with DAPI (visualized as blue fluorescence).

As expected, Art-27 staining in the same cells and conditions presented in figure 25 showed a very similar localization to URI (not shown).

We identified the whole R2TP/prefoldin-like complex in the nucleus of prostate cells. Therefore, we argue that URI in complex with Art-27 and the rest of the R2TP/prefoldin-like complex subunits assembles the RNA pol II complex in the cytoplasm and then translocates into the nucleus with RNA polymerase II. The data shown in figure 25 (and the data reported in section 2.5 below) support the idea that URI is tightly bound to RNA pol II suggesting that the Art-27/URI complex could be brought to the DNA by pol II. In contrast with this hypothesis, chromatin immunoprecipitation of pol II performed using LNCaP cells treated with or without hormone (data not shown) shows a hormone-dependent recruitment of polII on the transcription start site (TSS) of the hormone regulated NKX3.1 gene. On the other hand, as mentioned in chapter 1 (fig. 10), Art-27, supposedly in complex with URI, is recruited to the DNA in a hormone independent manner, in contrast with the idea that URI and Art-27 may be recruited to the DNA with RNA polymerase II in response to hormone treatment. The interaction of URI with polymerase shown in figure 25 is in apparent contrast with the fact that Art-27 and URI are present on chromatin prior to hormone treatment and the role of the URI/Art-27 containing complex in regulation of polymerase and chromatin need to be explored in more detail. It is also difficult to reconcile the transcriptional repressive effect of the Art-27/URI complex and the role of the two proteins in assembling the RNA polymerase complex. A better understanding of the mechanism of URI/Art-27 transcriptional repression would perhaps clarify these apparent contradictions.

2.5   ANALYSIS OF URI PHOSPORYLATION AND URI-INTERACTING PROTEINS

The phosphorylation and acetylation status of the immunoprecipitated flag-URI and URI nuclear interacting proteins was also analyzed by mass spectrometry. This analysis revealed differences between the two immunoprecipitation experiments we performed for mass spectrometry. In the first experiment URI was phosphorylated on threonine 241 and serine

243. These residues are part of an interesting cluster (^{241}TTSS^{244}) shown to be phosphorylated in HeLa cells upon epidermal growth factor (EGF) stimulation [217], and predicted to be phosphorylated by casein kinase 2 (CK2). Phosphorylation of threonine 241 and serine 243 was also interesting because these amino acids are part of the accessory RPB5 binding domain. Other sites of phosphorylation of URI detected in our mass spectrometry analysis were serine 412 in the URI domain, shown to be important for TFIIF interaction [97], and serines 442 and 449 located between TFIIF interaction domain and the URI box. Interestingly serine 442 was shown to be phosphorylated in the G1 phase of the cell cycle in a proteomic study aimed to identify mitosis-specific phosphorylation sites [102]. All these sites of URI phosphorylation were identified in the first experiment but not replicated in the second experiment, suggesting a difference in the metabolic status of LNCaP cells used for the two experiments.

URI MODIFICATIONS					
experiment 1			**experiment 2**		
aminoacid	domain	type of modification	aminoacid	domain	type of modification
T241	RPB5 accessory binding domain	phosph.	K89	hook of the prefoldin-like domain	acetylation
S243	RPB5 accessory binding domain	phosph.	K466	C terminus	acetylaton
S412	TFIIF binding domain	phosph.			
S449	C terminus	phosph.			
S442	C terminus	phosph.			
K230	RPB5 accessory binding domain	acetylation			

Table 2. URI modification detected by mass spectrometry in the two replicate experiments.

We also identified several sites of acetylation of URI. In the first experiment URI was acetylated on lysine 230, in the RPB5 accessory binding domain, while in the second

experiment URI was acetylated on lysine 89, in the hook of the prefoldin-like domain, and lysine 466, between the TFIIF interaction domain and the URI box. A summary of URI phosphorylation and acetylation sites in the two mass spectrometry analyses is reported in Table 2.

We also decided to investigate if URI post-transcriptional modifications interfere with its interaction with other proteins of interest. In particular we tested if phosphorylation of URI on T241 and S243 interferes with the binding to RPB5 because these two residues reside in the RPB5 accessory binding domain. We also investigated the effect of lysine 89 acetylation on the interaction of URI with Art-27 because amino acid 89 is part of the prefoldin-like domain hook that we (chapter 3) and other groups showed to be essential for URI binding to Art-27. We generated URI $T^{241}A\_S^{243}A$ and URI $K^{89}A$ and expressed these constructs and wild type URI in 293 cells together with RPB5 or a HA tagged Art-27.
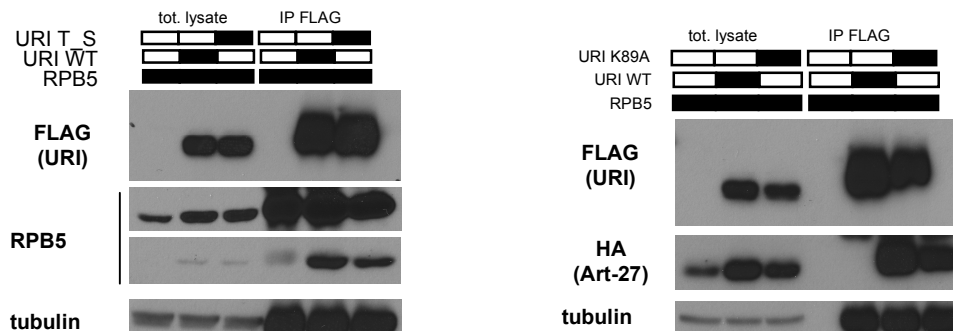
Figure 26. URI phosphorylation on T^{241}, S^{243} and URI acetylation on K^{89} does not interfere with URI interaction with RPB5 and Art-27. 293 cells were transfected with a construct encoding RPB5 or HA-Art-277 and with URI wild type (WT), URI $T^{241}A\_S^{243}A$ (URI T_S) or URI $K^{89}A$. Flag-URI was then immunoprecipitated with FLAG antibodies and HA-Art-27 and RPB5 were analyzed by Western blotting using specific antibodies. Tubulin was used as loading control.

Both the URI mutants interact with RPB5 or Art-27 similarly to wild type URI (fig. 26) indicating that URI $T^{241}S^{243}$ phosphorylation does not interfere with RPB5 interaction and URI K^{89} acetylation does not interfere with Art-27 interaction. However, it is important to note that because the kinase and the cellular signaling that induces phosphorylation or acetylation of URI is not known, we cannot exclude the possibility that basal URI modification at these sites is not enough to observe differences in interaction between overexpressed URI WT and URI mutants with associated proteins. It is possible that unstimulated cells, used for mass spectrometry analysis and for the immunoprecipitation experiments presented in figure 26, have very low URI $T^{241}S^{243}$ phosphorylation and URI K^{89} acetylation that were detected by mass spectrometry due to the high sensitivity of this technique. Further experiments that explore the role of URI phosphorylation and acetylation on these sites will need to be done and will be likely of great biological interest considering the previously demonstrated importance of post-transcriptional modification for URI regulation and function [82, 84, 104].

Together with the phosphorylation and acetylation status of URI we also analyzed the modification of URI interacting proteins that immunoprecipitated from nuclear fractions with URI. This analysis identified Paf1, RTF1, CTR9 and Leo1, components of the Paf1 complex previously identified as an interactor of URI [99]. This evidence suggests that, even if the analysis of modified URI interactor proteins had a lower cut-off for non-specific interactions, the analysis was still reliable and produced previously validated interactors not found in the simple analysis of URI interacting proteins. The comparison of the proteins involved in RNA polymerase II transcription revealed a striking difference between the two replicate experiments (fig. 27). In the first experiment in which URI was found phosphorylated on several sites, few proteins belonging to the RNA pol II elongating complex were found. RPB8, RPB5 and RPB1 were the only pol II subunits immunoprecipitated with URI and interestingly,

these subunits are the components of the subcomplex assembled by the R2TP/prefoldin-like complex prior to assembly of the whole RNA pol II complex (fig. 23). Also, few mediator proteins were immunoprecipitated in this first experiment and MED1, shown to be important for nuclear receptor mediated transcription [218, 219], was only phosphorylated on one site (serine 1449). MED1 hyperphosphorylation has been shown to be essential for the recruitment of other mediator proteins and the assembly of a functional mediator complex [65]. A MED1 phosphorylated on 38 different sites was co-immunoprecipitated with URI in the second experiment suggesting that in this experiment URI was bound to actively transcribing pol II. Supporting this idea, we also found bound to URI the three elongation factors ELL1, 2 and 3, four components of the Paf1 complex, five different TAF proteins, fifteen mediator proteins and several components of RNA polymerase II (RPB5, RPB1, RPB8, RPB2, RPB9, RPB3, RPB7 and RPB11B1). More importantly we also found the main subunit of the RNA pol II, RPB1, phosphorylated on serine 2 and threonine 5 of the C-terminal domain (CTD), which is known to be hyperphosphorylated during active transcription. The binding of URI to all these proteins clearly indicates binding to an actively transcribing polymerase supporting the previously reported evidence that in Drosophila, URI binds RNA pol II engaged in active transcription [114].

URI was found differentially modified in the two experiments that we performed and in these experiments the status of the RNA pol II was also clearly different (RNA pol II was not engaged in transcription in the first experiment and RNA pol II was actively transcribing in the second experiment). It is possible that URI phosphorylation may be an important step that triggers the cascade of events that lead to active transcription by pol II. According to this idea URI would act as an important hub of regulation that "translates" extracellular signaling into particular landscapes of transcription activation.

URI (phosphorylated and unphosphorylated) binds these components of RNApolII (unphosphorylated) in both experiments
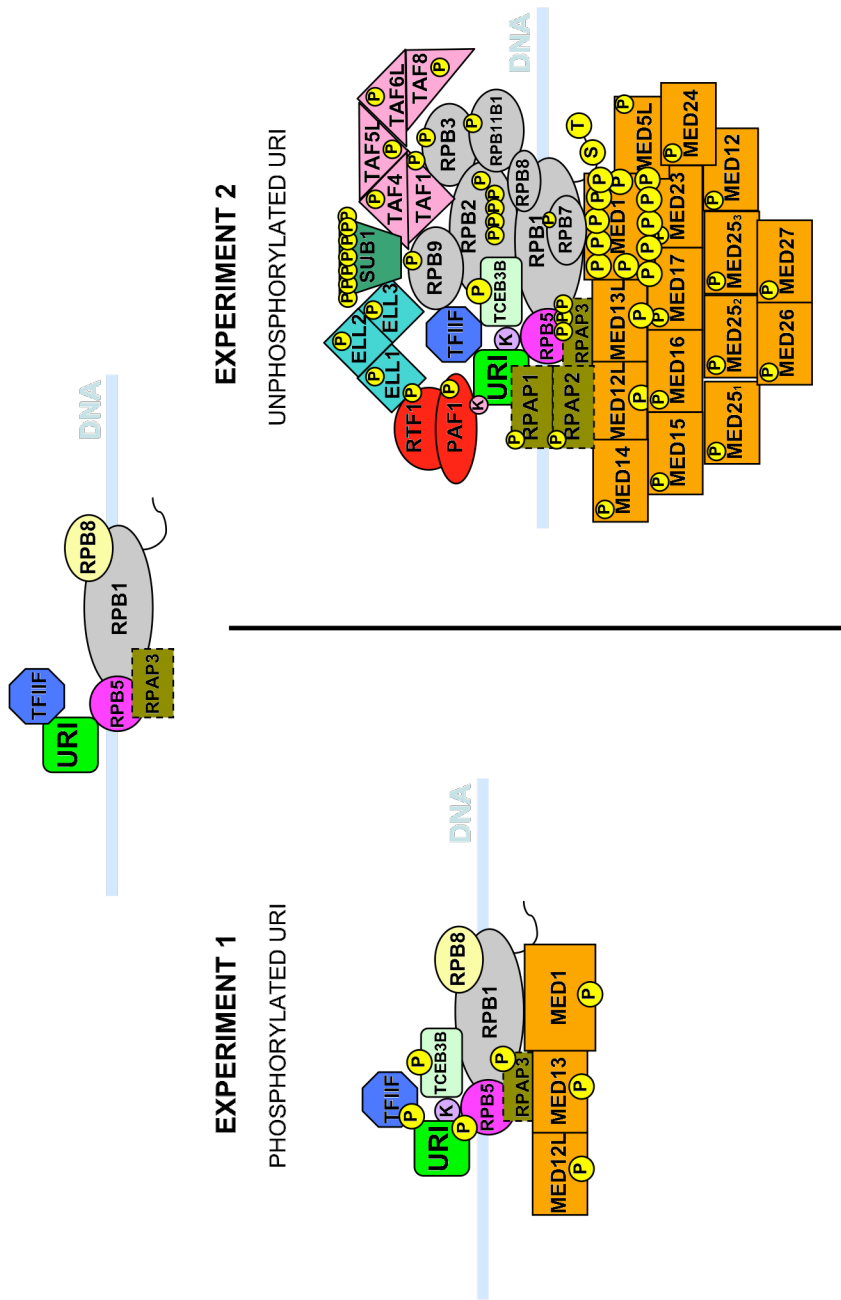
Figure 27. Schematic of the modified proteins involved in RNA pol II transcription found to interact with URI in the two mass spectrometry experiments performed using nuclear extracts of LNCaP prostate cells.

2.6 DISCUSSION

URI was previously shown by several independent reports to be a scaffold protein that coordinates the interaction of proteins involved in transcription such as TFIIF [97], the Paf-1 complex [99] and the RNA polymerase II itself through the binding to the RPB5 subunit [94]. URI was identified as a RNA polymerase interacting protein able to repress transcription and we also show that this repressive function holds true in the context of androgen receptor mediated transcription [82]. Despite the several proteins identified as URI interactors, including the androgen receptor corepressor Art-27, the molecular mechanism by which URI is able to repress transcription is unknown. To shed light into the mechanism of URI transcriptional repression, we performed a mass spectrometry analysis to identify proteins that specifically bind URI in the nucleus of prostate cells. This analysis confirmed the previously published interaction of URI with RPB5 and Art-27 and further characterizes an intriguing chaperone-like complex suggested to mediate the RNA polymerase II complex assembly in the cytoplasm of the cells. This complex was named R2TP/prefoldin-like complex because of the shared subunits with the yeast R2TP complex and the homology of several components with the prefoldin proteins. We showed that URI is a key component of the R2TP/prefoldin-like complex because depletion of URI induces degradation of several components of the complex, including Art-27, PDRG1 and RPB5, suggesting destabilization of the entire complex upon URI loss. Also, URI overexpression induces increased expression and stability of Art-27, PDRG1 and RPB5. Interestingly, experiments that examine URI cytoplasmic/nuclear translocation using a stable cell line expressing a URI-EGFP fusion protein, show that URI (and Art-27) follow the RNA polymerase II components into the nucleus and also that the URI complex can be exported back into the cytoplasm by CRM1 exportin, a mechanism also used by RNA pol II subunits to translocate into the cytoplasm to be recycled for the formation of new pol II complexes. Our data suggest that URI and Art-27 bind pol II as part of the

R2TP/prefoldin-like complex in the cytoplasm and then move into the nucleus with pol II. It is intriguing to hypothesize that the URI/Art-27 complex is recruited onto DNA through binding to pol II but our ChIP experiments do not support this idea. Indeed, in the androgen dependent LNCaP cell line, pol II is recruited on the TSS of the androgen receptor regulated gene NKX3.1, in an androgen-dependent manner. Art-27 recruitment on chromatin, on the other hand, is androgen independent, suggesting an alternative and pol II independent mechanism for the recruitment of the Art-27/URI complex onto DNA. Our mass spectrometry analysis clearly shows that, under unspecified conditions that lead to URI dephosphorylation, URI, probably still bound to Art-27, can bind actively transcribing pol II. If the phosphorylation of URI initiates polymerase II transcription it is intriguing to hypothesize a role of URI in controlling the switch of pol II from transcription initiation to pausing and finally to elongation. Interestingly, the TFIIF and the Paf1 complex, found to interact with URI by previous studies and by our mass spectrometry analysis, are proteins that bind pol II during both initiation and elongation and they are instrumental in the switch from stalled to elongating pol II. The CTD domain of the RPB1 subunit plays a key role in this switch through regulation of its serine 2 and serine 5 phosphorylation. Interestingly, in yeast, the RNA polymerase subunit RPB5, the first identified URI interactor, was proposed to have overlapping functions with RPB1 CTD domain [95].

Overall, the evidence presented in this chapter points towards an important role of the URI/Art-27 complex in RNA polymerase II function. This idea is supported by the work of Dorjsuren and colleagues [94] who identified URI as a RPB5 interacting protein, but the mechanism of URI action is unclear. Our work adds insight to the understanding of URI mediated transcription repression by implicating Art-27 as a new member of this complex.

CHAPTER 3:

URI BINDS KAP1 PROTEIN AFFECTING ITS

PHOSPHORYLATION AND TRANSCRIPTIONAL REPRESSION

FUNCTION

3.1 URI interacts with KAP1 protein in the nucleus of prostate cells

To better understand URI mediated transcriptional repression we performed mass spectrometry analysis to identify proteins that interact with URI in the nucleus of prostate cells as reported in chapter 2. We identified several proteins involved in transcription regulation and also previously reported to interact with URI (Table 1, chapter 2). We identified subunits of RNA polymerase I, II or III (Table 1, asterisks), confirmed URI interaction with Art-27 and identified all the components of the R2TP/prefoldin-like complex (Table 1, arrowheads). Among the novel URI interators we focused on the KAP1/TRIM28 protein, involved in gene repression, and on the PP2A phosphatase, because of the role of URI in regulation of PP1γ phosphatase in the mitochondria [94] (Table 1, gray lines). In at least one replicate experiment, peptides from the PP1α and PP1β phosphatases that interact with KAP1 [158] were also identified, as well as peptides from the regulatory subunit A of PP2A (although peptides from the latter were also present in the control immunoprecipitation).

To validate URI interaction with KAP1 we performed co-immunoprecipitation experiments using HEK293 cells over-expressing KAP1 and an empty vector or FLAG-URI (fig. 28a). Endogenous KAP1 protein also co-immunoprecipitated with URI in LNCaP cell nuclear extracts (fig. 28b). Because KAP1 was shown to be phosphorylated in response to DNA damage [151, 153, 156, 160] and URI is also modified upon a diverse range of treatments [82, 84], we tested if doxorubicin treatment affected the interaction between URI and KAP1. URI was immunoprecipitated from nuclear extracts of LNCaP cells treated with or without doxorubicin for 1 hour. Equal levels of KAP1 protein co-immunoprecipitated with URI in treated and untreated cells (fig. 28c) suggesting that URI interacts with KAP1 independently of DNA damage and KAP1 phosphorylation. Interestingly, PP1α phosphatase was also shown to bind KAP1 in the presence or absence of DNA damage [158].
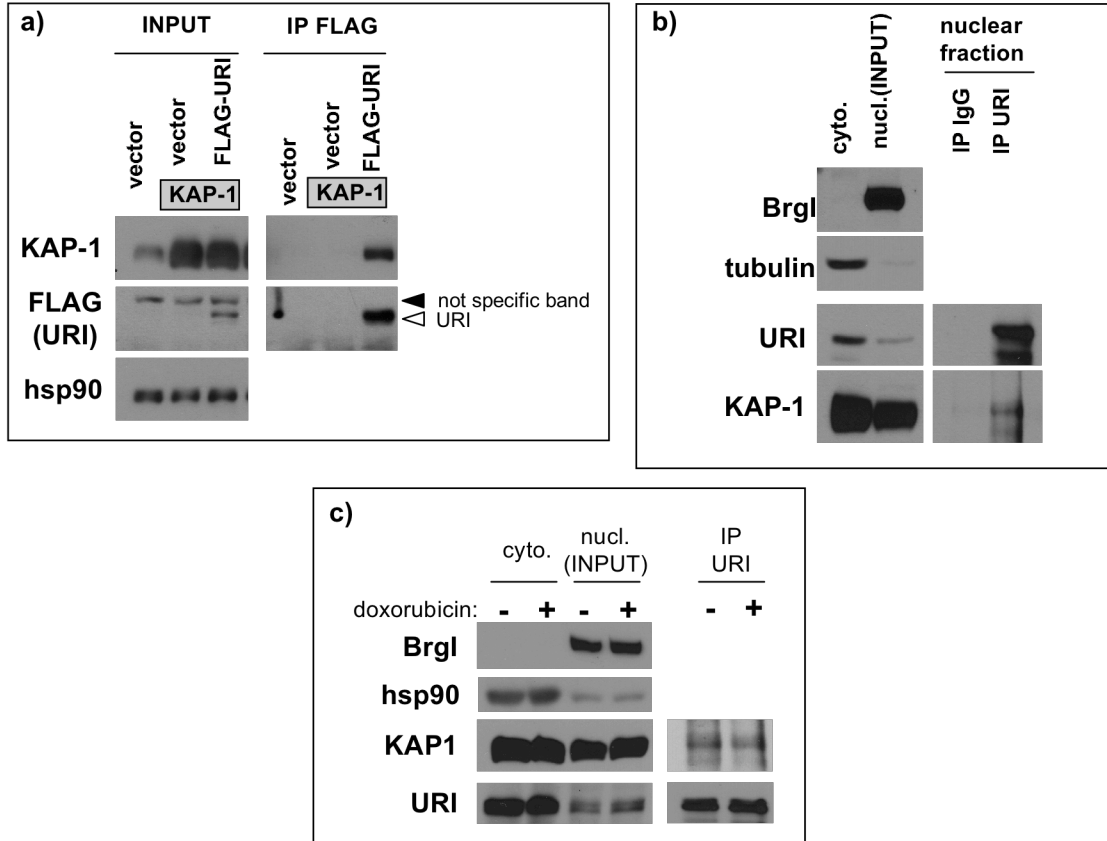
Figure 28. URI interacts with KAP1. a) HEK293 cells have been transfected with an empty vector or a vector encoding KAP1 protein (grey boxes). Cells transfected with KAP1 were also transfected with an empty vector or a FLAG-URI encoding vector. Cell lysates (INPUT) were used to immunoprecipitate URI using a FLAG antibody (IP FLAG). Western blotting analysis was performed using the indicated antibodies. The black arrowhead indicates a non-specific band while the white arrowhead indicates the FLAG-URI band. Hsp90 protein was used as a loading control. b) Cytoplasmic (cyto.) and nuclear (nucl.) fractions were isolated from LNCaP cells. Nuclear fractions were used for the immunoprecipitation of URI. A normal mouse IgG was used as control (IP IgG). BrgI and tubulin were used as nuclear and cytoplasmic markers respectively. c) URI was immunoprecipitated as in b from nuclear extracts of LNCaP cells treated with or without doxorubicin 1μM for 1 hour.

To identify the protein domains responsible for the interaction with KAP1 we generated deletions and truncations of URI (fig. 29a).
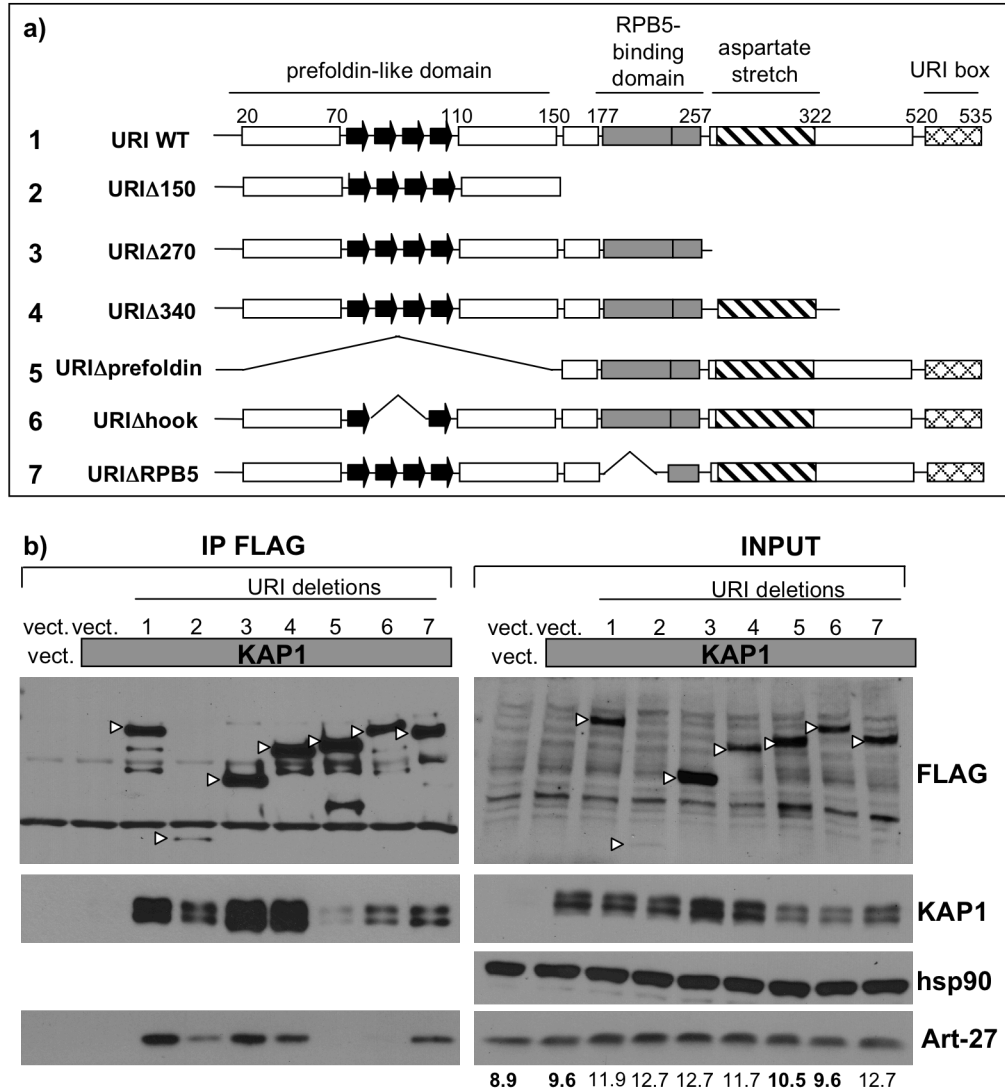
Figure 29. URI binds KAP1 through multiple domains of interaction. a) schematic of the seven URI constructs used to map the domains of interaction between URI and KAP1. The known URI domains are reported and the numbers on top indicate the corresponding amino-acid number. b) An

empty vector (vect.), KAP1 (gray box; 5μg) and the different URI constructs were transfected in HEK293 cells (10μg total DNA transfected into all transfections). 48 hrs after transfection cells were lysed. Part of the lysate was used as INPUT (right panel) and another part (≈1mg of proteins) was used to immunoprecipitate URI using FLAG antibodies. The immunocomplexes were analyzed by Western blot using the indicated antibodies. Numbers on the bottom show the densitometry units for the Art-27 bands in the INPUT. Arrowheads indicate the URI deletions/truncations.

Immunoprecipitation assays showed that all the deleted forms of URI interacted with over-expressed KAP1, suggesting that the URI-KAP1 interaction involves multiple domains of interaction (fig. 29). The N-terminal prefoldin-like domain and, more specifically, the two alpha helices flanking the four beta strands of the URI prefoldin-like structure, seem to be the most important for URI interaction with KAP1. URI deleted of the whole prefoldin-like domain (lane 5) has a very weak interaction with KAP1 compared to URIΔhook mutant (lane 6) suggesting stronger interaction of KAP1 with the two alpha-helices of the URI prefoldin-like domain. These results also suggest that Art-27 binding to URI is not necessary for KAP1/URI interaction. We previously reported [82] that binding of URI to Art-27, stabilizes Art-27 protein and, indeed, URI deletions that do not interact with Art27 (URIΔprefoldin, lane 5 and URIΔhook, lane 6) show Art-27 protein levels comparable to vector-only lanes and do not exhibit increased expression of endogenous Art-27 protein as in the cases where the Art-27 binding site within URI is intact (lanes 1-4 and 7). Altogether these data show that URI binds KAP1 in the nucleus of prostate cells.

3.2 Depletion of URI results in increased KAP1ser824 phosphorylation in the presence of doxorubicin

KAP1 was previously shown to be phosphorylated on serine 824 in response to DNA damage downstream of the ATM kinase [158]. To explore the role of URI in KAP1 phosphorylation, LNCaP cells stably over-expressing an inducible shRNA control (LNCaP-shNS) or a shRNA against URI (LNCaP-shURI) were treated for 30 minutes with 1µM doxorubicin, a strong inducer of the DNA damage response (DDR). Short exposure of LNCaP cells to 1µM doxorubicin induced a negligible increase of nuclear KAP1 phosphorylation but depletion of URI clearly increased nuclear KAP1 phosphorylation upon doxorubicin treatment (fig. 30a). BrgI and tubulin or hsp90 were used as nuclear and cytoplasmic markers respectively. Because URI is a RPB5 interactor protein, the phosphorylation status of the RNA polymerase carboxy-terminal domain (CTD) on serine 2 was also analyzed. PolII CTD serine 2 phosphorylation was not affected by URI depletion indicating that KAP1 is specifically phosphorylated upon URI depletion. Because the LNCaP cell line expresses wild type p53 and because KAP1 was shown to regulate p53 target gene expression in cells with mutant or attenuated p53 function [153], we performed the same experiment shown above using the p53 null prostate cell line PC3. The same effect of URI depletion shown in LNCaP cells was recapitulated in the PC3 cells. In PC3 stable cell lines (PC3-shNS and PC3-shURI) depletion of URI induced an increase in phosphorylated KAP1, upon treatment with doxorubicin 1µM for 30 minutes, similar to the increase induced in LNCaP cells (fig. 30b). It has been previously reported that KAP1 phosphoryation on serine 824 is mediated by ATM kinase [155]. To determine if KAP1 hyper-phosphorylation upon URI depletion was due to a direct role of KAP1 and not to hyper-activation of ATM kinase we analyzed the changes of ATM phosphorylation on serine 1981 in the presence or absence of URI. Treatment of LNCaP cells with doxorubicin clearly induced activation of ATM kinase measured by the increase in the phosphorylation on

serine 1981, a known autophosphorylation site used as a marker for ATM activation [220]. Depletion of URI, on the other hand, did not affect ATM phosphorylation and activity (Fig. 30c). These results indicate that the DDR-dependent phosphorylation of KAP1 downstream of ATM kinase is directly modulated by URI.
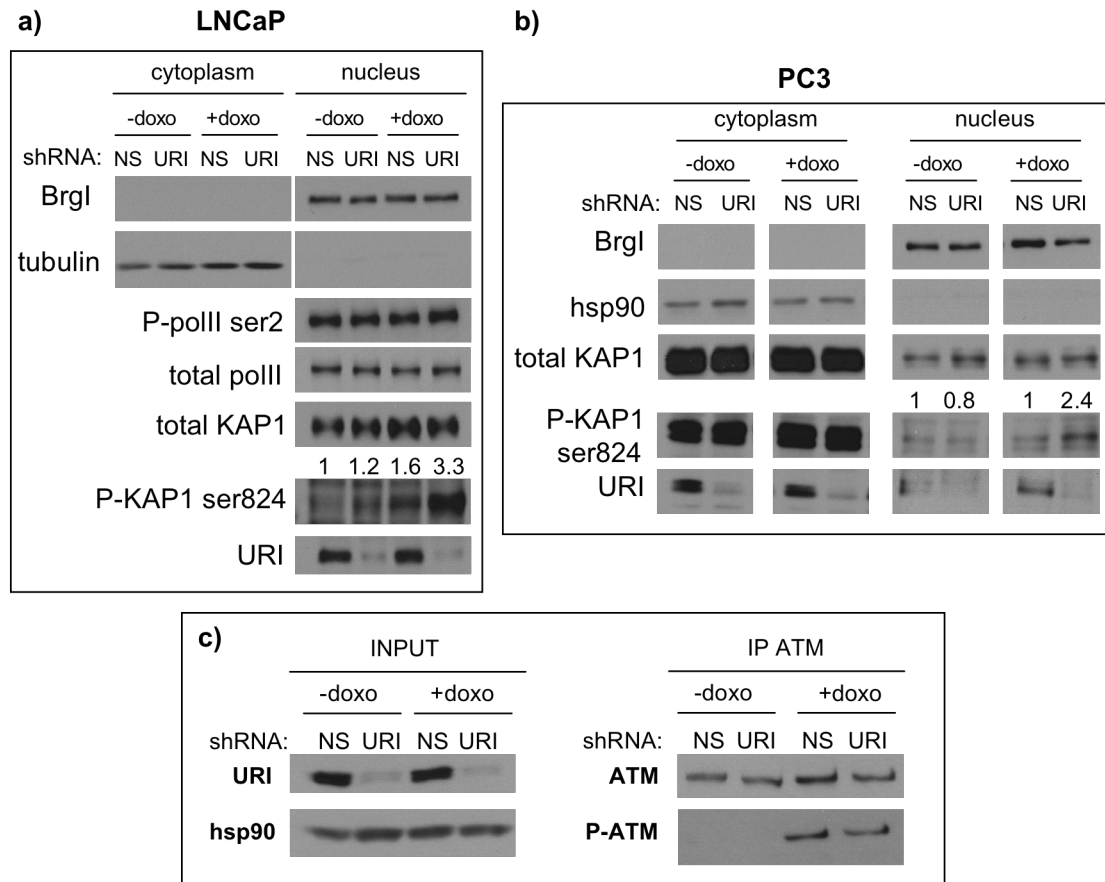
Figure 30. URI depletion induces increased phosphorylation on serine 824 of nuclear KAP1. a) Cytoplasmic and nuclear fractionations were isolated from LNCaP-shNS and LNCaP-shURI cell lines. Cells have been treated with doxocyclin 1μg/ml for 3 days and with or without doxorubicin 1μM for 30 minutes. BrgI and tubulin were used as nuclear and cytoplasmic markers respectively. Numbers on the P-KAP1 ser824 blot indicate the densitometry units of the phospho-KAP1 bands relative to the band of

phospho-KAP1 in control cells set as 1. b) A similar experiment to the one presented in a) was performed using PC3-shNS and PC3-shURI cell lines. BrgI and hsp90 were used as nuclear and cytoplasmic markers and relative densitometry units for the phospho-KAP1 bands are also reported. c) LNCaP-shNS and LNCaP-shURI were treated with or without doxorubicin 1μM for 30 minutes and ATM was immunoprecipiated (IP ATM). Hsp90 was used as a loading control for the INPUT samples.

3.3 Depletion of URI de-represses KAP1 regulated genes in p53 mutated or null prostate cells

KAP1 phosphorylation on serine 824 interferes with its SUMOylation and subsequent recruitment of the repression complex resulting in de-repression of the KAP1 target genes p21, Bax, Noxa and Puma in doxorubicin treated cells [158]. Given that URI depletion results in KAP1 phosphorylation in doxorubicin treated cells (Fig. 30) we hypothesized that cells depleted of URI will also have higher expression of KAP1 target genes. However, since p53 will also be activated upon doxorubicin treatment and p21, Bax, Noxa and PUMA are also p53 target genes, we reasoned that the effect of URI acting via KAP1 would be evident only in a p53 mutant background.

Indeed, LNCaP cells, which express wild type p53, responded very rapidly and more potently to doxorubicin treatment as shown by the strong activation of p21, BAX and NOXA at lower doxorubicin concentrations (1μM versus the 2 μM for PC3 cells) and shorter time points (3 to 12 hours in LNCaP cells versus 12 to 30 or 36 hours for PC3 and LAPC4 cells) (Fig. 31 a-c).
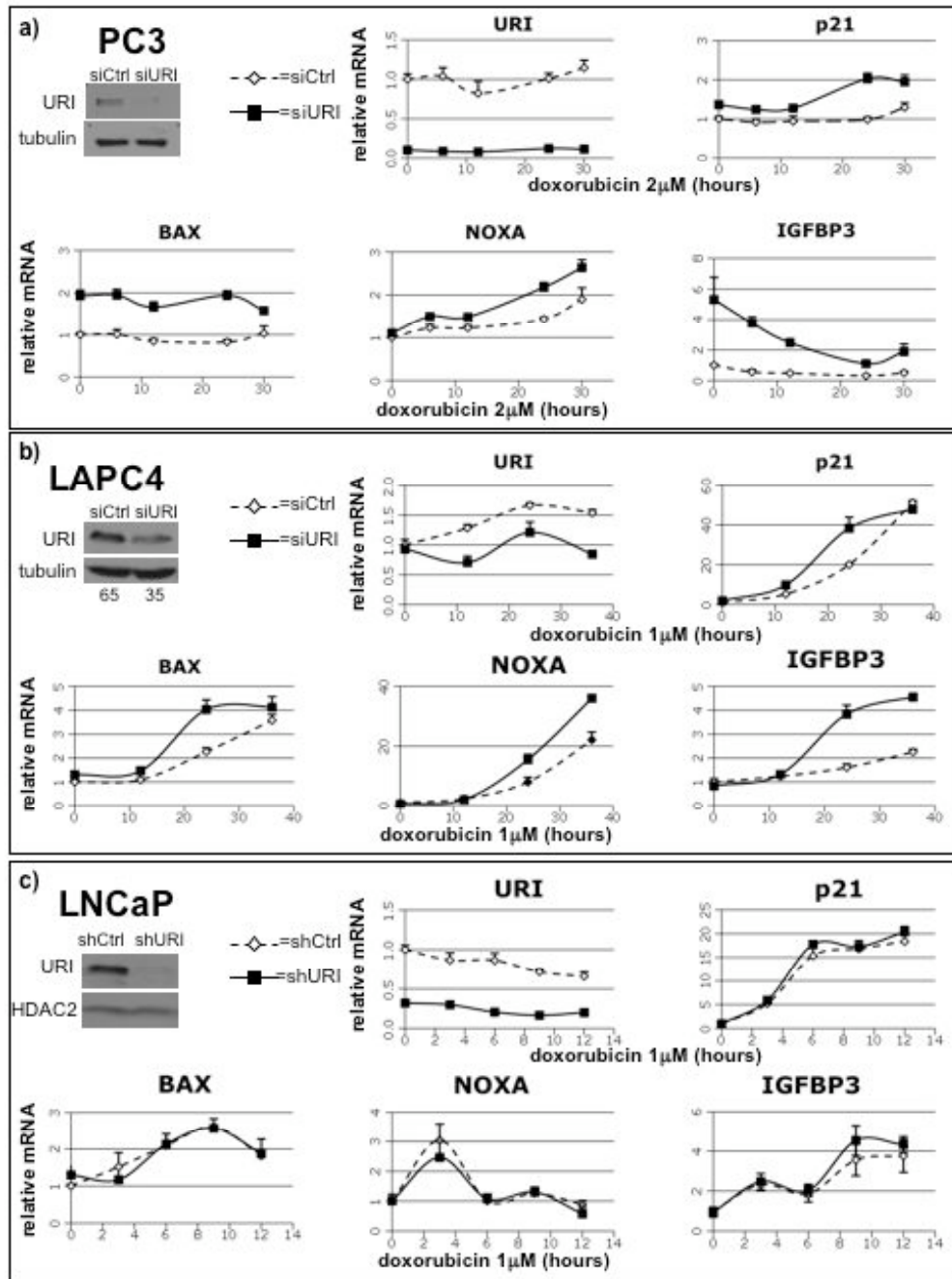
Figure 31. URI depletion induces increased transcription of KAP1 regulated genes in p53 null cells. PC3 a) and LAPC4 b) cells were depleted of URI by siRNA treatment. LNCaP c) cells were depleted of URI by stable overespression of shRNA against URI (shURI). Upon URI depletion cells

were treated with doxorubicin for the indicated times and the mRNA of URI and KAP1 regulated genes (p21, BAX, NOXA and IGFBP3) were measured by Q-PCR. Western blots for URI show effective depletion of URI proteins. The numbers below the LAPC4 blot indicate densitomentry analysis of the URI band. Tubulin and HDAC2 were used as loading controls.

As might be expected in a p53 wild type background, LNCaP cells depleted of URI by stable expression of shRNA against URI (LNCaP-shURI) express BAX, NOXA and p21 in response to doxorubicin similarly to control cells stably overexpressing a non silencing shRNA (LNCaP-shNS). In contrast, doxorubicin treated p53 mutant PC3 and LAPC4 cells depleted of URI by siRNA, showed increased expression of p21, Bax and Noxa (fig. 31a and b) compared to cells transfected with a control siRNA. We also measured the expression of IGFBP3, a gene highly affected by KAP1 depletion and to which KAP1 is recruited as shown by ChIP-sequence analysis [148]. As expected, IGFBP3 expression was also increased upon URI depletion only in p53 mutated cells. IGFBP3 expression was not affected by URI depletion in LNCaP cells as we showed for the other known KAP1 regulated genes (fig. 31c). These results suggest that URI plays a role in the regulation of KAP1 dependent transcription repression probably by modulation of its phosphorylation status.

3.4   URI depletion induces reactivation of mobile elements in a cell specific manner

KAP1 and SETDB1 methyl-transferase, play a key role in the repression of some types of retroelements in embryonic stem cells [145, 164, 165]. In addition, LINE-1 and Alu elements have been shown to be expressed in prostate cell lines including PC3 and LNCaP cells [173]. We therefore hypothesized that URI may play a role in retroelement repression. This idea is also supported by the fact that, a genetic screen to identify genes and functional classes involved in Ty1 element repression in yeast, identified bud27 (homologue of the human URI)

and SPT5, an elongation factor as the top two genes that repress Ty1 mobility [119]. On the basis of these previous findings we decided to measure the expression of LINE-1, Alu and HERV_K elements upon URI deletion in prostate cells. We reasoned that if a KAP1 complex is involved in retroelement repression in prostate cells, then KAP1 hyper-phosphorylation induced by doxorubicin treatment should increase retroelement expression. Moreover, we hypothesized that URI depletion should increase the expression of retroelements in a similar manner to the induction of KAP1 target genes p21, BAX. NOXA and IGFBP3 shown in figure 31. The expression of LINE-1, two Alu elements (AluYa5 and AluYb8) and two HERV_K elements (HERV_K17 and HERVK_22q11.3) was measured by Q-PCR. Two different primers (LINE1_5' and LINE1_3') were used to measure the expression of unspliced LINE1 (5' primer) and total LINE1 (3' primer) as previously described [173]. As predicted doxorubicin treatment induced increased expression of LINE and Alu elements and URI depletion resulted in derepression and even higher expression of these retroelements in the androgen responsive cell line LAPC4 (Fig. 32b). HERV_K elements were not affected or decreased upon doxorubicin treatment but depletion of URI still increased their expression in LAPC4. In LNCaP cells we did not detect an increase in retrotransposon expression upon doxorubicin treatment but observed increased expression of total LINE1 and AluYb8 compared to control cells not depleted of URI (Fig. 32c). In PC3 cells, lacking androgen receptor, the expression of LINE-1 and Alu elements did not increase with doxorubicin treatment and was not affected by URI depletion (Fig. 32a).
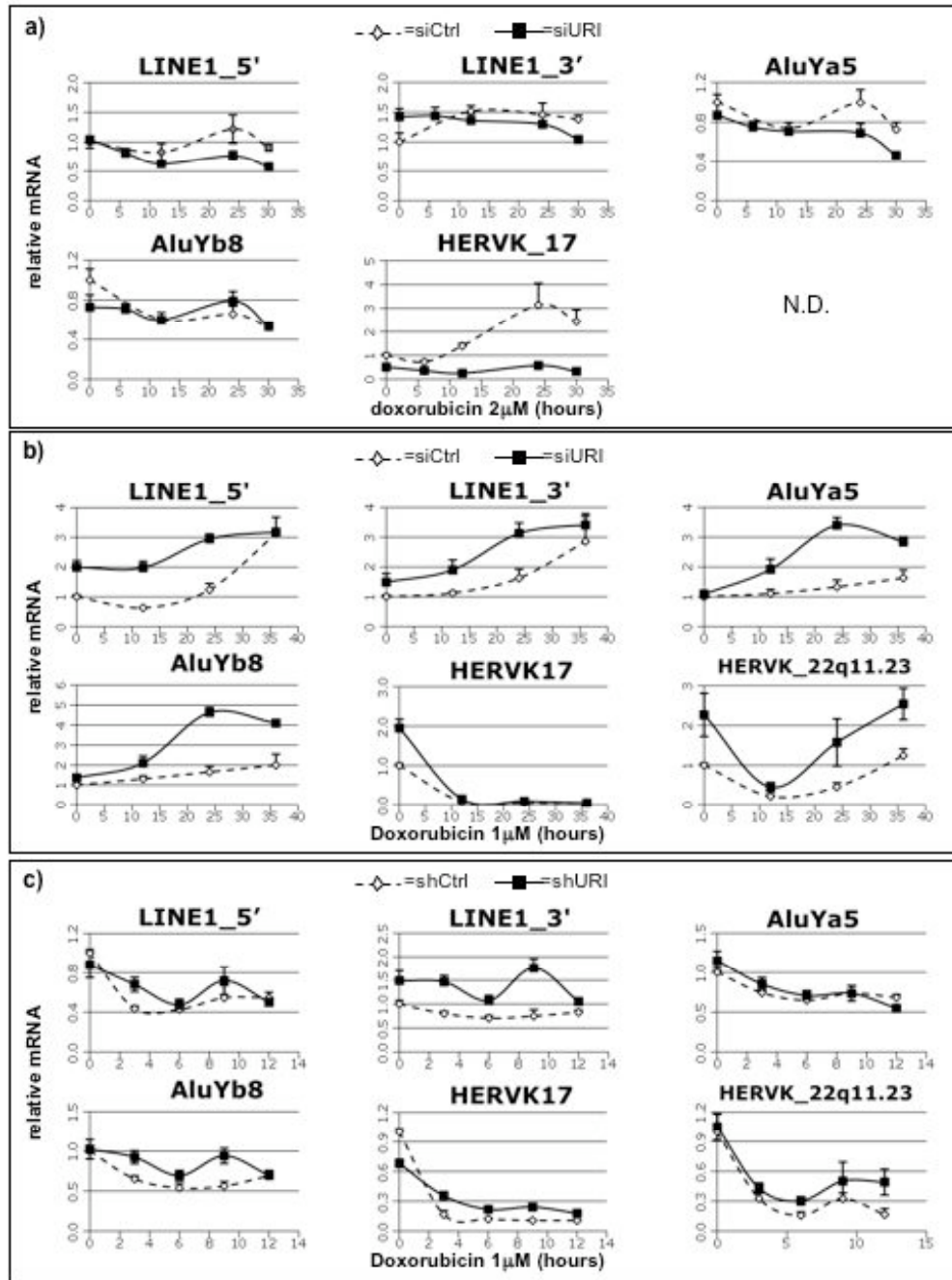
Figure 32. URI depletion induces retrotransposon expression in androgen responsive cell lines.

PC3 a) and LAPC4 b) cells were depleted of URI by siRNA treatment. LNCaP c) cells were depleted of

URI by stable overespression of shRNA against URI (shURI). Upon URI depletion cells were treated

with doxorubicin as in figure 31 and the mRNA of the indicated retroelements were measured by Q-PCR. The expression of HERVK_22q11.23 in PC3 cells was too low to give reliable measurements and was considered non detected (N.D.).

Thus, in p53 mutant AR positive LAPC4 cells, deletion of URI induces KAP1 hyper-phosphorylation (Fig. 30) interfering with KAP1-mediated repression of LINE1, Alu and HERV_K retroelements as well as KAP-1 mediated repression of genes involved in apoptosis and cell cycle arrest (p21, BAX, NOXA). Overall, we observed an effect of URI depletion on the expression of some or all of the analyzed retroelements only in androgen responsive cell lines (LAPC4 and LNCaP), but not in androgen receptor negative PC3 cells, implicating androgen receptor in the expression of these KAP-1 regulated elements in prostate cells. Interestingly, direct involvement of the androgen receptor in retroelement expression in prostate cells has been previously reported [173]. Overall, results presented here indicate that URI depletion affects major biological functions of KAP1 including the repression of retroelements. This finding may also be relevant to the increase of genomic instability resulting from URI deletion in the Drosophila [114] and C. elegans [113] germline.

3.5   URI binds active PP2A phosphatase

Experiments presented above show that URI binds and regulates the phosphorylation of KAP1 protein (figs. 28-30) thus modulating its transcription repression function (fig. 31). Mass spectrometry analysis of nuclear URI interactors revealed that URI binds PP2A phosphatase (Table 1) suggesting that perhaps URI can recruit PP2A to de-phosphorylate KAP1. KAP1 was previously shown to be de-phosphorylated by PP1α and PP1β phosphatases and indirectly affected by PP2A depletion [158]. To validate the IP/mass spec results we

performed co-immunoprecipitations and showed URI and PP2A interaction in LNCaP nuclear extracts either in the presence or absence of DDR (fig 33a).
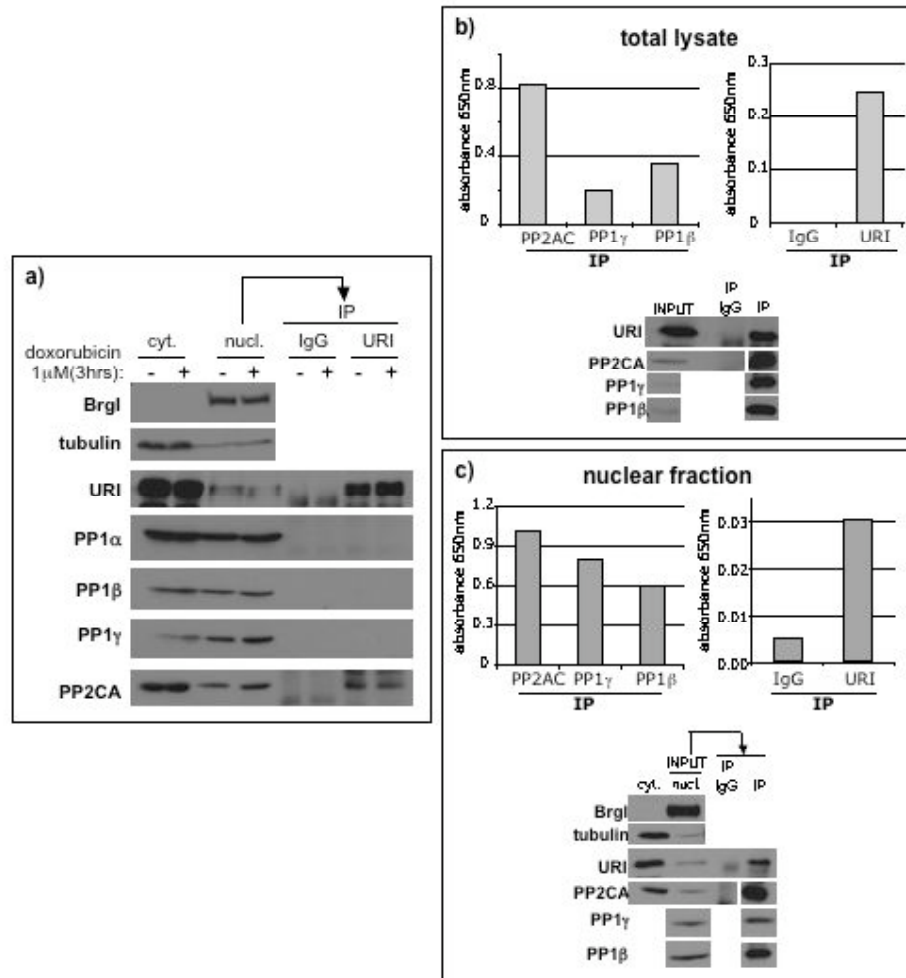
Figure 33. URI binds active PP2A. Nuclear URI was immunoprecipitated using LNCaP nuclear extracts. Normal mouse IgG was used as control. a) The immunoprecipitation was performed after treating LNCaP cells with or without 1μM doxorubicin for 3 hours. The immunocomplexes co-immunoprecipitated with URI were analyzed by Western blot using the indicated antibodies. Tubulin and BrgI were used as nuclear and cytoplasmic markers respectively. b) Proteins immunoprecipitated

with URI antobodies as well as the proteins immunoprecipitated using IgG control or PP2A, PP1γ and PP1β specific antibodies, were tested for their ability to dephosphorylate a phospho-peptide used as substrate in phosphatase assays. The histograms show the absorbance of a malachite solution proportional to free phosphates present in solution after incubation of the phospho-substrate with the indicated immunoprecipiated proteins. The phosphatases assay was performed using total lysate (b, top panels) or nuclear lysate (b, lower panels). Western blotting of the immunoprecipitated proteins is also reported.

We could not detect any binding of URI to PP1α, β or γ in the same immunoprecipitation experiments suggesting that URI specifically binds PP2A phosphatase in the nucleus of prostate cells. Since previous studies showed that URI binds and inactivates PP1γ in the mitochondria [104], we reasoned that URI might also inactivate PP2A in prostate cells. Phosphatase assays were performed measuring the dephosphorylation of a threonine phosphopeptide (K-R-pT-I-R-R, Millipore) used as a substrate for immunoprecipitated PP2A. We performed immunoprecipitations with cytoplasmic or nuclear extracts using URI antibody or normal mouse IgG as a control. The URI immunocomplexes or the IgG immunoprecipitated control proteins were mixed with a solution of phospho-peptide substrate and incubated in phosphatase buffer. The free phosphate released upon dephosphorylation of the substrate by URI-associated phosphatases was quantified using a malachite solution which turns green in the presence of inorganic phosphate and can be measured at 650nm. Phosphatase assays demonstrated that both cytoplasmic and nuclear PP2A co-immunoprecipitated with URI is still active (Fig. 33b and c). As positive controls, we also immunoprecipitated PP2A, PP1α and PP1β and demonstrated some specificity for PP2A in this assay (fig. 33b and 33c). The levels of immunoprecipitated proteins are presented in Figure 33c. These data suggest that, in

contrast to URI-PP1γ binding in the mitochondria, binding of URI to PP2A protein in the nucleus does not inhibit phosphatase activity.

Consistent with an indirect role of PP2A on KAP1 phosphorylation, PP2A de-phosphorylates and inactivates ATM, the kinase that phosphorylates KAP1 serine824 in response to DNA damage (DDR) [221]. However, URI directly binds to KAP1 and we did not observe an increase of ATM phosphorylation upon URI depletion (fig. 30c). Therefore we, hypothesize a direct and ATM-independent role of URI in the regulation of KAP1 phosphorylation.

3.6 KAP1ser824 is a substrate of URI-bound-PP2A phosphatase

KAP1 was shown to be dephosphorylated by PP1α and PP1β in the absence or presence of DNA damage respectively [158]. Results presented above suggest that PP2A in complex with URI might directly dephosphorylate KAP1. To determine if KAP1ser824 can be directly dephosphorylated by PP2A phosphatase we immuno-precipitated phospho-KAP1 from LNCaP cells treated for 1 hour with 5μM doxorubicin. Beads bound to phospho-KAP1 were mixed with beads binding PP2A phosphatase immuno-precipitated from untreated LNCaP cells. Nuclear extracts were used to specifically explore the effect of nuclear PP2A on nuclear phospho-KAP1. Western blot analysis indicated that, as expected, there is robust phosphorylation of KAP1 upon doxorubicin treatment (Fig. 34a, right panel, first lane). Phosphorylation of KAP1 on serine 824 was highly reduced in the presence of immunoprecipitated PP2A but not affected by the presence of immunocomplexes immunoprecipited using a control IgG (fig. 34a). This result suggests that nuclear phosho-KAP1ser824 is a substrate for nuclear PP2A phosphatase. To ensure that the dephosphorylation of nuclear KAP1 was mediated by PP2A phosphatase and not by an associated phosphatase, we also incubated KAP1 immunoprecipitated from the nucleus of

doxorubicin treated LNCaP cells, with 0.5U of purified GST-PP2AC protein (Millipore). Immunoblotting using a specific phospho-KAP1ser824 antibody showed a clear decrease in phosphorylated KAP1 in the presence of GST-PP2AC purified protein (Fig. 34b) suggesting that KAP1 can be a target of PP2A.
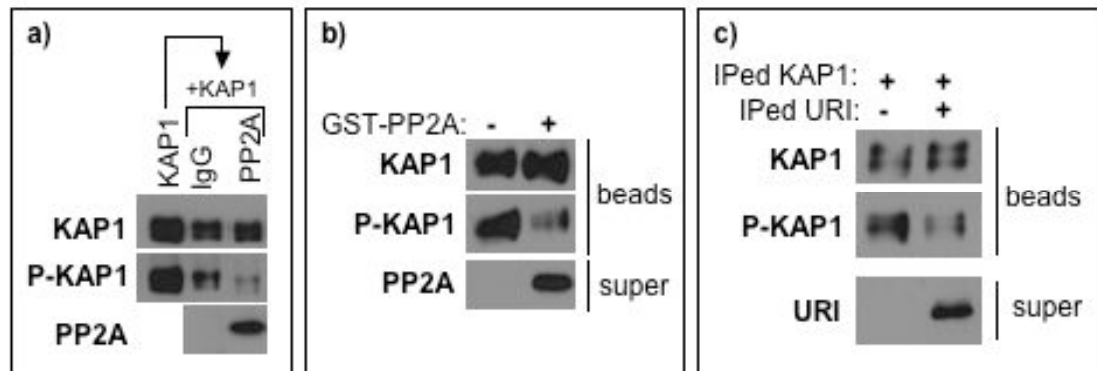
Figure 34. Phospho-KAP1ser824 is dephosphorylated by PP2A. a) KAP1 immunoprecipitated from nuclear extracts of LNCaPcells treated with doxorubicin 5μM for 1 hour (first lane) were mixed with PP2A phosphatase immunoprecipitate from nuclear extract of untreated LNCaP cells. As control, part of the immunoprecipitated KAP1 was mixed with immunocomplexes precipitated using control mouse IgG. After incubation for 20 minutes at 30ºC, the reaction was stopped with Laemmli buffer and proteins blotted with the indicated antibodies. b) KAP1 immunoprecipitated from nuclear extract of LNCaP cells as in a) was incubated with or without purified GST-PP2A followed by the addition of Laemmli buffer to the beads (beads) and verification of the presence of PP2A (super) by Western blotting. Total- and phospho-KAP1 were also quantified by Western blotting. c) KAP1 immunoprecipitated from nuclear extract of LNCaP cells as in a) and b) was mixed with FLAG-URI immunoprecipiated from the nucleus of untreated LNCaP-URI cells. URI was eluted from the beads with a 3XFLAG peptide. KAP1 beads were mixed with buffer or an equal volume of FLAG-URI solution. After incubation, the reaction was stopped by adding Laemmli buffer to the beads (beads) and

the supernatant was collected to confirm the presence of URI (super). URI, total- and phospho-KAP1 were analyzed by Western blotting.

To demonstrate that phospho-KAP1 is dephosphorylated by URI-bound PP2A phosphatase we used a stable LNCaP cell line over-expressing a FLAG-URI (LNCaP-URI). As in the previous experiments we immunoprecipiated phosphorylated KAP1 from the nuclear extracts of LNCaP cells treated with doxorubicin. We also immunoprecipitated FLAG-URI from nuclear extracts of LNCaP-URI cells using FLAG-conjugated beads and a 3XFLAG peptide to elute URI off the beads. Eluted URI was then mixed with beads binding phosphorylated KAP1. Following incubation for 20 minutes at 30°C, the supernatant was then collected (Fig. 34c, super) and the beads resuspended in Laemmli buffer (Fig. 34c, beads). Western blot analysis showed that co-incubation of phospho-KAP1 beads with URI immunocomplexes containing PP2A phosphatase (Fig. 33) induced robust de-phosphorylation of KAP1 demonstrating that URI binds a phosphatase able to dephosphorylate KAP1 (fig. 34c). Altogether these results suggest that URI-bound-PP2A dephosphorylates KAP1 serine 824 in nuclear extracts of prostate cells.

3.7 Inhibition of PP2A pheonocopies the effect of URI depletion to enhance KAP1 S824 phosphorylation

We showed that URI binds KAP1 and that depletion of URI results in hyper-phosphorylation of KAP1, suggesting that URI brings PP2A phosphatase to the KAP1 complex, thus regulating its phosphorylation and function as a transcriptional repressor. To test this hypothesis we made two predictions. 1) Specific inhibition of PP2A with nanomolar concentrations of okadaic acid (OA) in a range that does not inhibit PP1 phosphatases should result in hyperphosphorylation of KAP1 similar to what is observed upon URI depletion; 2) Treatment of URI depleted cells

with OA should have no effect on KAP1 dephosphorylation because although PP2A will be inhibited, it will not interact with URI within the KAP1 complex. To test these hypotheses we used LNCaP-shNS and LNCaP-shURI cells treated with 1µM doxorubicin for 1 hour in the presence or absence of 30nM OA (fig. 35). As expected, nuclear KAP1 phosphorylation was increased in cells depleted of URI (lane 6) compared to control non-silencing cells (lane 5); also KAP1 was hyperphosphorylated in control cells treated with OA (lane 7) comparably to cells depleted of URI and treated with OA (lane 8). While the impact of OA treatment or URI depletion on KAP1 phosphorylation in the cytoplasm was minimal (lanes 1-4), we did observe an increase in the higher mobility URI band shown to be a phosphorylated form of URI [82, 84, 104] suggesting that PP2A mediates dephosphorylation of URI itself. Overall, these results support the hypothesis that in the nucleus URI modulates KAP1ser824 phosphorylation by recruiting PP2A phosphatase to the KAP1 complex.
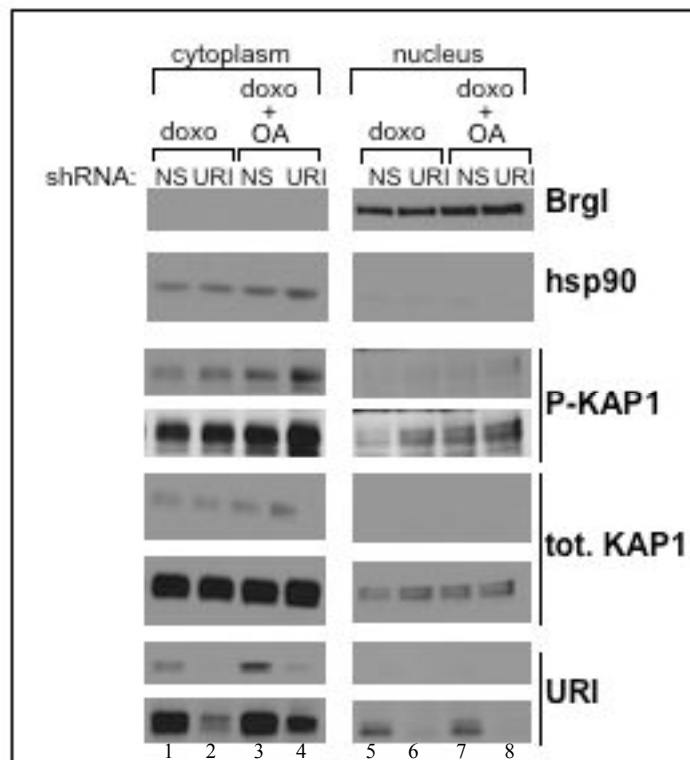
Figure 35. Inhibition of PP2A pheonocopies the effect of URI depletion to enhance KAP1 S824 phosphorylation. LNCaP-shNS and LNCaP-shURI were treated for 1 hour with doxorubicin 1µM (doxo) in the presence or absence of 30nM okadaic acid (OA). The nuclear and cytoplasmic fractions were

isolated and the indicated proteins were analyzed by Western blotting. BrgI and hsp90 were used as nuclear and cytoplasmic markers respectively. Two different exposures are reported to more accurately show differences between treatments in the cytoplasmic (upper panel, shorter exposure) and in the nuclear (lower and longer exposure) fractions.

3.8 KAP1 binding to PP2A is mediated by URI

The data presented above strongly suggest that URI mediates the binding of PP2A phosphatase to KAP1 protein. To test this hypothesis we performed co-immunoprecipitation experiments of KAP1 and PP2AC (PP2A catalytic subunit) in cells treated with control or URI shRNA. KAP1 was immunoprecipitated from nuclear extracts isolated from LNCaP-shNS and LNCaP-shURI cells treated with 1µM doxorubicin for 1 hour. Western blot analysis of the cytoplasmic and nuclear fractions confirmed that URI was depleted in both cytoplasmic and nuclear extracts in LNCaP-shURI cells. Depletion of URI did not affect cellular levels of KAP1 or PP2AC (Fig. 36, left panel). Immunoprecipitation of KAP1 from the nuclear extract of LNCaP-shNS control cells showed binding of KAP1 to PP2A phosphatase. This binding was completely abolished in LNCaP-shURI cells (Fig. 36, right panel) indicating that, in the presence of doxorubicin, PP2A protein recruitment to the KAP1 complex is URI dependent (Fig.36).
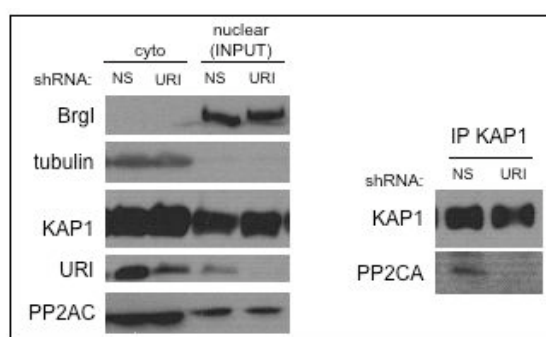
Figure 36. KAP1 binding to PP2A is mediated by URI. Cytoplasmic and nuclear fractions were isolated from LNCaP-shNS and LNCaP-shURI stable cell lines treated with doxycycline and doxorubicin 1µM for 1 hour. Part of the fractions

was used to analyze the expression of the indicated proteins (left panel) and the rest of the nuclear extract was used to immunoprecipitate KAP1. The immunoprecipitated KAP1 and the coimmunoprecipiated PP2A were analyzed by Western blotting.

Based on these results we propose a model according to which, under doxorubicin treatment, URI targets PP2A phosphatase to KAP1 and within this protein complex PP2A modulates the phosphorylation of KAP1 and URI itself (Fig. 37).
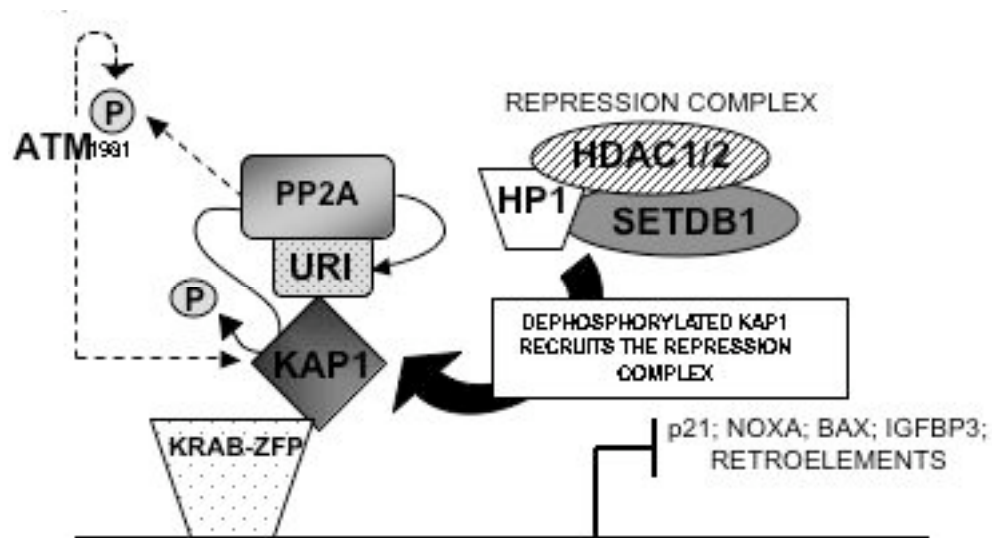
Figure 37. Model of PP2A recruitment on the KAP1 complex through URI protein. Dephosphorylation of KAP1 by PP2A on serine 824 induces recruitment of the repression complex and repression of the KAP1 regulated genes including retrotransposons.

3.9   URI loss induces decreased H3K9me3 on the NKX3.1 promoter and coding region.

KAP1 functions as a scaffolding protein for the recruitment of a complex that mediates transcription repression [126] and long range heterochromatization [149]. It has also been shown that not all genes are sensitive to KAP1 mediated repression and that the genes susceptible to the KAP1 mediated silencing carried high levels of repressive histone marks in the promoter and coding region, but they are located in gene-rich and transcriptionally active domains [222]. KAP1 mediates its transcription repression function mainly through the activity of the histone methyl transferase SETDB1 that mediates H3K9 trimethylation [133]. We previously showed that Art-27, probably in complex with URI, is recruited on the NKX3.1 gene (figure 11, chapter 1). We therefore wanted to analyze the level of H3K9me3 on NKX3.1, a gene up-regulated upon URI loss. We performed ChIP experiments using LNCaP-shNS and LNCaP-shURI cells treated with or without androgen. As expected, in control cells, hormone treatment known to activate NKX3.1 transcription, leads to decreased H3K9me3 in the promoter of the gene and increased H3K9me3 in the coding region (fig. 38b). It is well established that H3K9me3 has a bivalent significance: it is a repression mark if present on the promoter region and an activation mark if present on the coding region of the genes [223]. Upon URI depletion we observed a decrease of the H3K9 mark on the whole NKX3.1 gene, promoter and coding region (fig. 38a). The more pronounced effect was observed in the promoter region where H3K9me3 levels in the absence of hormone were comparable if not lower than the H3K9me3 levels observed in the presence of hormone (fig. 38b). These data support a role of URI in the epigenetic regulation of gene transcription, and more specifically on the deposition of repressive marks such as H3K9me3.
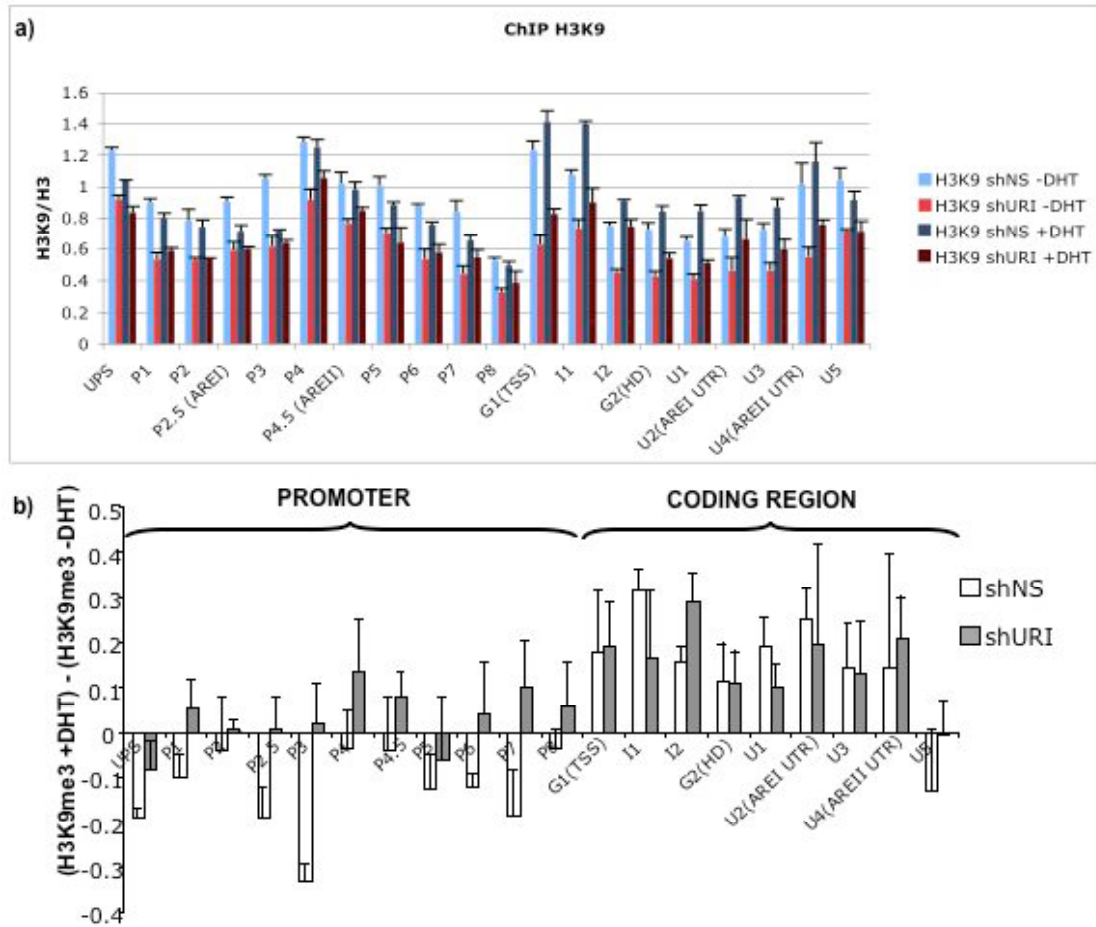
Figure 38. URI loss induces decreased H3K9me3 on the NKX3.1 promoter and coding region.

LNCaP-shNS or LNCaP-shURI were hormone starved for 3 days and then treated for 4 hours with or without 10nM DHT. After treatment, cells were fixed and chromatin was processed for ChIP using H3K9me3 specific antibodies. ChIP results are presented as a) H3K9me3 signal over histone H3 (H3) signal or b) as a difference of the H3K9me3 signal in the presence of hormone minus the H3K9me3 signal in the absence of hormone (positive values mean increased H3K9me3 upon hormone stimulation and negative values mean decreased H3K9me3 upon hormone stimulation).

3.10   DISCUSSION

URI is a transcriptional repressor that interacts with RNA polymerase II through binding to the POLR2E/RPB5 subunit [94]. URI has been shown to repress transcription of reporter constructs controlled by the VP16 transactivator [94], the TK promoter (fig. 13-15, chapter 1) and the androgen receptor response element (ARE) (fig. 1, chapter 1)[82]. Dorjsuren and colleagues also found that URI is able to repress several other transcriptional activators with the exception of p53 (discussion of unpresented data in [94]). Despite the fact that the transcriptional repression function of URI was its first identified function, the mechanism of repression is still unknown. In an attempt to clarify the role of URI in transcription regulation we performed a mass spectrometry analysis of nuclear URI interactors using LNCaP prostate cell lines. This analysis confirmed several previously identified URI interactors such as RPB5, Art-27 and the R2TP/prefoldin-like complex. Among the novel interactors of URI we found KAP1/Trim28/TIF1β, a scaffolding protein recruited on chromatin by members of the KRAB-Zn finger proteins [121, 124]. KAP1 was demonstrated to mediate gene silencing through the recruitment of a repression complex comprising the methyl transferase SETDB1, HDAC1/2 histone deacetylases and HP1 proteins [121]. Interestingly KAP1 repression activity is regulated by phosphorylation and therefore by the activity of several phosphatases involved in the modulation of KAP1 repression [158]. In this chapter we showed interaction of URI with KAP1 in the nucleus of prostate cells. This interaction modulates KAP1 phosphorylation on serine 824, a site that if phosphorylated interferes with KAP1 ubiquitination and consequently with KAP1-mediated repression of genes like p21, BAX, NOXA and IGFBP3. Interestingly these genes encode for proteins involved in apoptosis and cell cycle arrest and they are also tightly controlled by p53. Therefore, as also observed by other laboratories [153], changes in KAP1 activity can be more easily detected in p53 null or p53 impaired backgrounds (PC3 or LAPC4 but not LNCaP cell lines). We showed that URI affects KAP1 phosphorylation and

123

activity through the recruitment of the PP2A phosphatase another novel interactor of URI. We also demonstrate that PP2A is able to directly dephosphorylate KAP1 phospho-serine 824. Therefore, we propose a model whereby URI targets the PP2A phosphatase to the KAP1 complex to modulate ATM dependent phosphorylation of KAP1 upon DNA damage. Several reports demonstrated a role of KAP1 and KAP1 phosphorylation in DNA damage response [154, 224]. Because of the well known role of KAP1 in chromatin structure and transcriptional regulation, KAP1 is an intriguing protein that may couple transcription repression to DNA damage repair.

Interestingly, KAP1 and SETDB1 were recently shown to be essential for the repression of retroelements in embryonic stem cells [145, 164]. Retroelements have been studied for possible deleterious effects on normal cell physiology caused by their intrinsic mobility throughout the genome. They have been implicated in the formation of deletions or amplifications through recombination and with the transcriptional misregulation of tumor suppressors or oncogenes through their "indiscriminate" re-insertion in the genome [175]. The majority of mobile elements are not active in somatic cells but a growing body of evidence identified some subfamilies of retroelements that remained active in the human genome. More specifically Alu, LINE-1, SVA and HERV-K retroelements are mobile within the genome thereby increasing genetic diversity of the human population [171]. In prostate in particular, LINE-1 and HERV-K elements have been suggested to be active and to promote prostate cancer formation and progression. Specifically the LINE-1 ORF2 encoded endonuclease was proposed to be important for the formation of the TMPRSS2:ETS translocation found in more than 40% of prostate cancers [13]. Also, a LINE-1 enriched domain within the AR gene was proposed to promote an intragenic rearrangement that causes the formation of androgen independent and constitutively active short splice variant of AR [55]. In this work we show that changes in URI expression can affect KAP1 repression function and therefore the regulation

of potentially dangerous retroelements. In line with this observation, deletion of the yeast homologue of URI, Bud27, was found to induce an increase in Ty1 mobility [119]. It is intriguing to suggest that alteration of URI levels can trigger misregulation of DNA structure through misregulation of KAP1 function, therefore inducing aberrant regulation of retroelements which are usually kept dormant in the heterochromatin region of the genome. These observations can potentially lead to new approaches and views in the understanding of prostate cancer initiation and progression as well as the role of retroelements and transposable elements in prostate and other cancers.

CHAPTER 4:

URI/Art-27 COMPLEX IS INVOLVED IN DNA DAMAGE RESPONSE

4.1 URI OR ART-27 DEPLETION INDUCES INCREASED CHK1 AND CHK2 PHOSPHORYLATION

In C. elegans and Drosophila, URI depletion induces DNA instability as measured by increased TUNEL staining [113, 114]. Both in Drosophila and C. elegans, URI mutants have reduced cell viability and differentiation in the germline and these phenotypes cause sterility. Depletion of URI induces cell cycle arrest and DNA breaks in somatic and germline cells, suggesting that URI may have a role in the induction or repair of DNA damage in mitotic and meiotic cells. To investigate a possible role of URI and its partner Art-27 in the DNA damage response of human prostate cells, we treated control LNCaP cells or cells depleted of Art-27 or URI by siRNA, with known DNA damage inducers such as camptothecin (cpt) or hydroxy-urea (HU). Cpt is an inhibitor of DNA topoisomerase I (topoI) that stalls this enzyme after DNA cleavage. The single strand break induced by topoI is converted into a double strand break after collision of the cpt-DNA-topoI ternary complex with the DNA replication fork [225]. HU reduces cellular deoxyribonucleotides (dNTPs) through the inhibition of the ribonucleotide reductase enzyme. This reduction induces DNA replication stall and consequently double strand breaks [226, 227]. As expected, LNCaP cells treated with either cpt or HU show a great increase of chk1 phophorylation on serine 317 and chk2 phosphorylation on threonine 68 (fig. 39). Depletion of Art-27 by siRNA did not induce appreciable differences in chk1 and chk2 post-transcriptional modification in cells treated with HU, but cells treated with cpt and depleted of Art-27 showed a higher phosphorylation of chk1 (fig.39a and b) and chk2 (fig. 39a). This result is consistent with previous data published by our group showing increased transcription of a subset of genes involved in DNA damage response upon Art-27 depletion [78]. The increase in phosphorylation of chk1 and chk2 also correlates with a small but reproducible increase in total chk1 and chk2 proteins, in line with our transcriptional data (figure 39c and [78]).
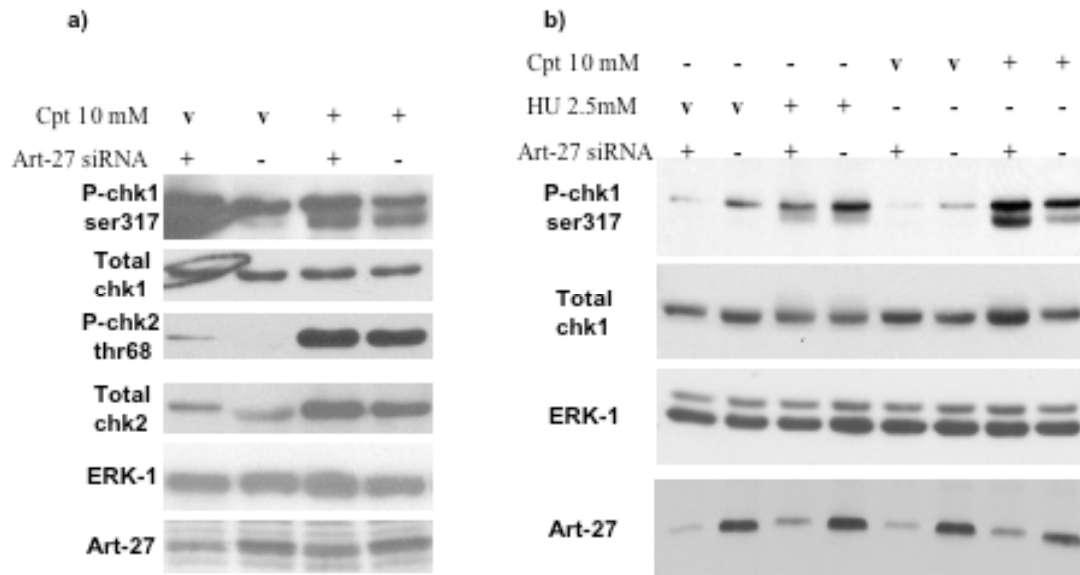
Figure 39. URI depletion induces increased cpt-dependent phosphorylation of chk1 and chk2. LNCaP cells were depleted of Art-27 by two sequential treatments with Art-27 siRNA (+) or scrambled siRNA(-) for 4 hours in OPTIMEM. Cells were left to recover for 24 hours in RPMI supplemented with 10% FBS. After recovery cells were treated with 2.5mM hydroxyurea, 10 μM camptothencin or with the corresponding vehicles (v) for 2 hours in complete media. Cells were then harvested and lysed in Triton buffer supplemented with proteases inhibitors. The expression of the indicated proteins was analyzed by Western blotting.

We also performed experiments using LNCaP-shNS and LNCaP-shURI stable cell lines. Cells were treated with cpt or etoposide (eto), an inhibitor of DNA topoisomerase II. Upon URI depletion we observed increased chk1 phosphorylation but no changes in chk2 phosphorylation (fig. 40). We also observed increased total chk1 protein as for Art-27 depletion. These differences were not as strong and reproducible compared to the changes observed upon Art-27 knock down and therefore we conclude that URI may have an indirect

effect on chk1 and chk2 phosphorylation through regulation of Art-27 protein stability. Indeed, as shown in fig. 40 and fig 6 (chapter 1), URI depletion induces destabilization and degradation of Art-27 protein. This conclusion is also in line with the observation reported in figure 8c (chapter 1) according to which URI depletion has a different transcriptional effect compared to Art-27 depletion, on the set of DNA damage and cell cycle genes shown to be repressed by Art-27.
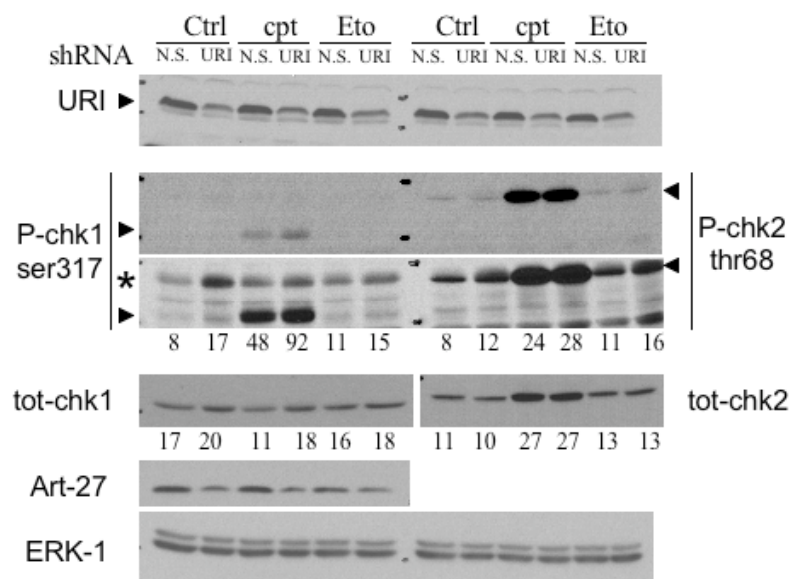
Figure 40. URI depletion increases chk1 phosphorylation. LNCaP-shNS and LNCaP-shURI were treated with cpt 50μM and eto 100μM for 5 hours and then lysed in Triton buffer. The expression of the indicated proteins was analyzed by Western blotting. The numbers indicate densitometry analysis of the corresponding bands and the asterisk indicates a non-aspecific band.

The difference in the amplitude of increased chk1 or chk2 phosphorylation between the URI or Art-27 depletion experiments does not seem to be due to the use of stably integrated shRNA, in the case of URI depletion, or transiently transfected siRNA, in the case of Art-27 depletion.

Indeed, experiments conducted using siRNA to deplete cellular URI did not show any difference in chk1 or chk2 phosphorylation between control or siRNA treated cells (data not shown).

Overall, these data suggest that the Art-27/URI complex depletion induces increased DNA damage response measured by increased phosphorylation of chk1 and chk2 proteins. Because URI and Art-27 expression is tightly inter-dependent, it is difficult to dissect specific roles for the two proteins. The smaller reported effect upon URI depletion compared to the stronger changes observed upon Art-27 depletion may suggest a more direct role of Art-27 in the DNA damage response pathway compared to URI.

4.2 URI DEPLETION INDUCES INCREASED FORMATION OF γH2AX FOCI IN RESPONSE TO CAMPTOTHECIN TREATMENT

To further explore the role of URI in the response to DNA damage we measured the formation of γH2AX foci upon cpt treatment in control LNCaP-shNS cells and in LNCaP-shURI cells depleted of URI. Phosphorylation of histone H2AX on serine 139 (γH2AX) is a well established marker of DNA damage. Upon DNA damage or replication stress ATM or ATR kinases respectively phosphorylate H2AX to trigger the recruitment of the DNA damage response machinery and repair the damage [228]. DNA damage induces the formation of nuclear γH2AX foci easily visualized by immunofluorence. Treatment of LNCaP-shNS and LNCaP-shURI cells with cpt 1μM induces accumulation of γH2AX foci that can be quantified by ImageJ. This analysis revealed that cells depleted of URI have a higher γH2AX fluorescence even in the absence of cpt (fig. 41).
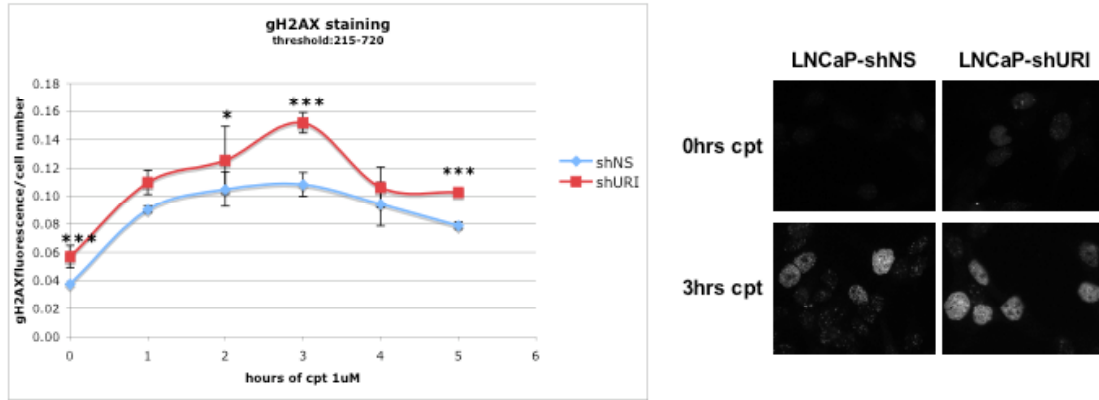
Figure 41. URI depletion induces increased γH2AX. LNCaP-shNS and LNCaP-shURI cells were treated with 1μM cpt for the indicated times. Cells were than fixed and stained for γH2AX with a specific antibody. Pictures were taken using a fluorescence microscope (20X magnitude) and the fluorescence signal was quantified using ImageJ (threshold 215-720). An upper threshold was also applied to avoid the quantification of cells with a uniform nuclear staining not resembling the characteristic "foci staining" of γH2AX. The error bar is the standard deviation of two duplicates. $p \leq 0.05$ (*), $p \leq 0.0005$ (***).

Because we and other laboratories showed interaction of URI with several phosphatases (namely PP1α, Pp1γ and PP2A) we asked if depletion of URI could also affect the de-phosphorylation of γH2AX. We therefore treated LNCaP-shNS and LNCaP-shURI with cpt 25μM or cpt 1μM for 5 hours to induce formation of the γH2AX foci. Cells were then extensively washed and incubated for 12 hours in complete media without cpt. At specific times cells were fixed and stained for γH2AX. We then measured γH2AX fluorescence using the same method used in the previous experiment and visualized the decrease of fluorescence with time (fig. 42).
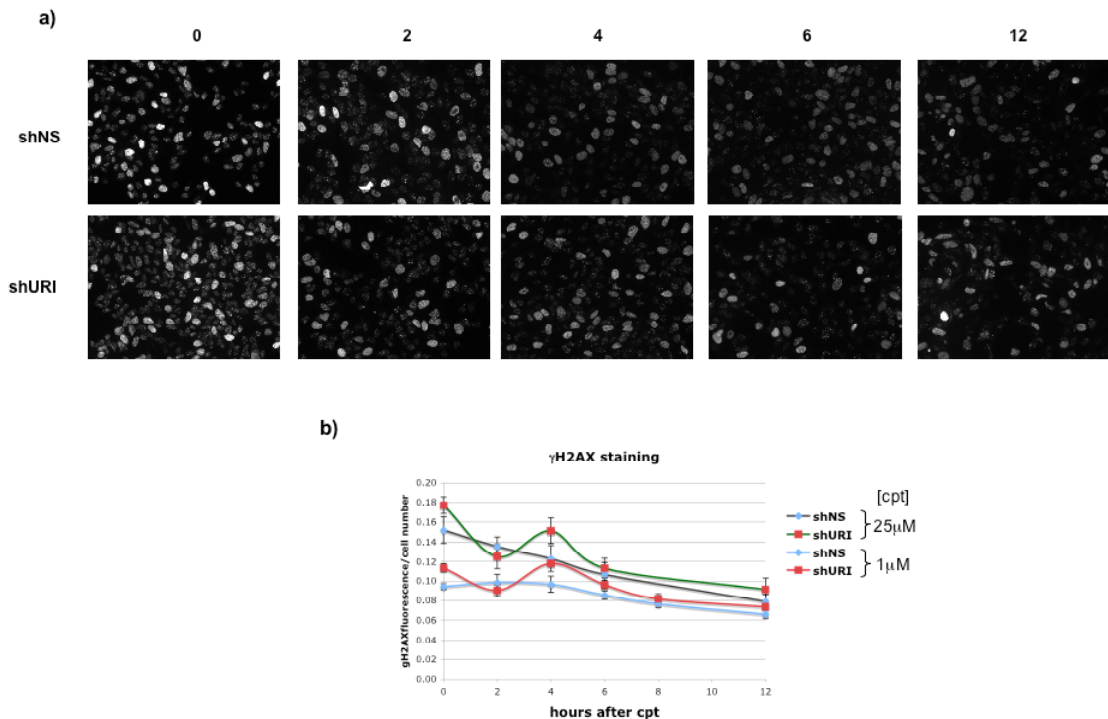
Figure 42. URI depletion induces non-linear dephosphorylation of γH2AX. LNCaP-shNS or LNCaP-shURI were treated for 5 hrs with 1 or 25 μM cpt. After DNA damage induction cells were washed and recovered for the indicated times (b) in complete media. Picture were taken (a) and analyzed by ImageJ as described for picture 39.

As expected, in control LNCaP-shNS cells γH2AX fluorescence decreases linearly after cpt treatment (R^2=0.98 for 25μM cpt treatment and R^2=0.87 for 1μM cpt treatment) (fig. 42b). In cells depleted of URI, γH2AX dephosphorylation is much more variable with a striking similarity between the two experiments performed using 25μM or 1μM cpt. This result is in line with the idea that URI controls phosphatases involved in the dephosphorylation of DNA damage related proteins. If that is the case, cells lacking URI lose the "buffer" that enables cell recovery from DNA damage in a linear and controlled fashion.

4.3   URI IS PHOSPHORYLATED IN RESPONSE TO UV TREATMENT DOWNSTREAM OF P38/MAPK14 KINASE

URI was shown to be phosphorylated downstream of the mToR pathway in response to different stimuli such as serum and IGF treatment [84]. In particular, in the mitochondria URI was demonstrated to be phosphorylated by the p70S6 kinase on serine 371 [104]. Phosphorylation of this particular site induces release of PP1γ from the binding to URI and dephosphorylation of BAD that in its dephosphorylated form, is able to induce apoptosis. Our experiments showed that, in prostate cells, URI can be phosphorylated upon androgen treatment downstream of the mToR pathway [82]. Phosphorylated URI can be easily visualized on a Western blot as a band with slower electrophoretic migration compared to the unphosphorylated URI (fig. 4 chapter 1 and [84]). Because we observed changes in DNA damage response in cells depleted of URI compared to control cells we investigated whether URI protein is post-transcriptionally modified upon DNA damage in a similar fashion to the URI phosphorylation triggered by hormone treatment. We used UV irradiation to induce DNA damage. Treatment of LNCaP cells with UV at increasing dosage showed that URI is phosphorylated when cells were treated with irradiation higher than 6 J/m^2 (fig. 43). Interestingly several pathways were activated upon UV treatment: the ATM/ATR pathway that induces phosphorylation of chk1 and chk2, the p38/MAPK14 stress pathway and the mToR pathway monitored by p70S6K phosphorylation. Phosphorylation of chk2 can be observed after 6 J/m^2 UV treatment when URI phosphorylation status is still comparable to control, suggesting that URI is not directly phosphorylated by ATM or ATR and that the pathway that triggers URI phosphorylation is likely downstream of the ATM/ATR pathway.
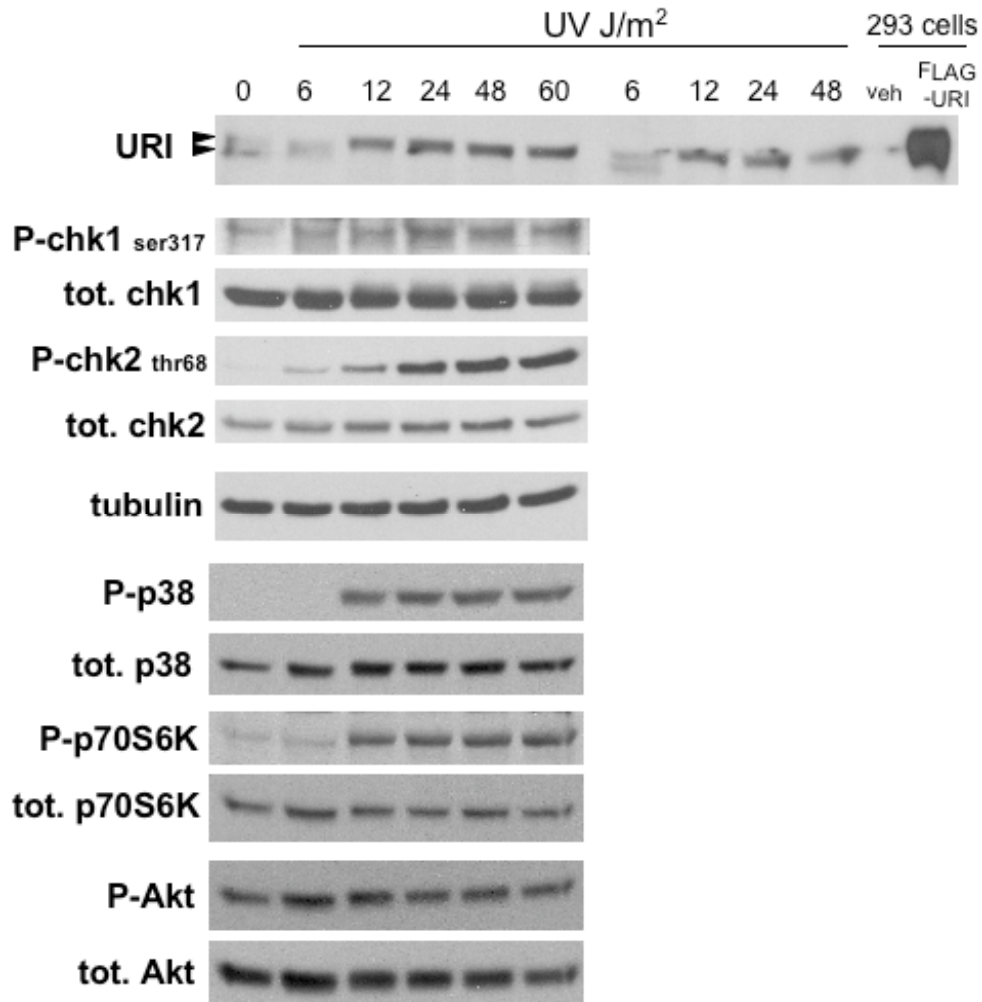
Figure 43. URI is phosphorylated upon UV treatment. LNCaP cells were UV irradiated in 2 ml of PBS and left to recover for 30' in complete media. Cells were then lysed and the expression of the indicated protein analyzed by Western blotting. The two arrowheads indicate the two forms of URI (dephosphorylated=lower band; phosphorylated=upper band). Lysates from 293 cells overexpressing an empty vector (veh) or a FLAG-tagged URI (FLAG-URI) were used as positive control for the specificity of the URI antibody.

Unlike Chk2, p38 and p70S6K were activated by UV treatment at doses higher than 6 J/m^2, mimicking URI response. This data suggests that these kinases may be directly involved in URI phosphorylation. To explore the involvement of the mToR pathway and the p38 kinase pathway on URI phosphorylation we irradiated LNCaP cells with UV 25 J/m^2 in the presence or absence of rapamycin, a specific inhibitor of mToR (fig. 44), or SB203580, a specific inhibitor of p38 kinase (fig. 45). After irradiation cells were left to recover in complete media for increasing time points.
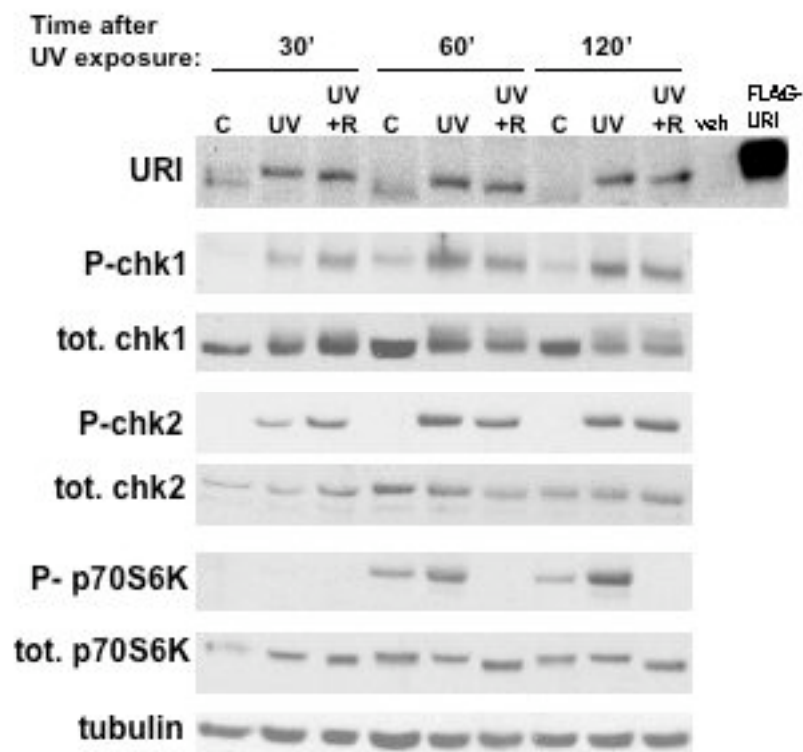
Figure 44. UV-induced URI phosphorylation is only partially inhibited by rapamycin. LNCaP cells were treated with UV 25J/m^2 in 2 ml of PBS and left to recover for the indicated times in complete media supplemented with or without 100nM rapamycin (UV+R) or DMSO (C or UV). Cells were then

lysed and the expression of the indicated proteins was analyzed by Western blotting. Lysates from 293 cells overexpressing an empty vector (veh) or a FLAG-tagged URI (FLAG-URI) were used as controls.

Treatment of LNCaP cells with UV induced phosphorylation of URI visualized as an increase of the URI upper band. Treatment of the irradiated cells with rapamycin just slightly shifted the URI phospho-band toward the unphosphorylated URI lower band suggesting that mToR is contributing but is not essential for the UV dependent phosphorylation of URI (fig. 44). We performed the same experiment using p38 inhibitor SB 203580 instead of rapamycin (fig.45).
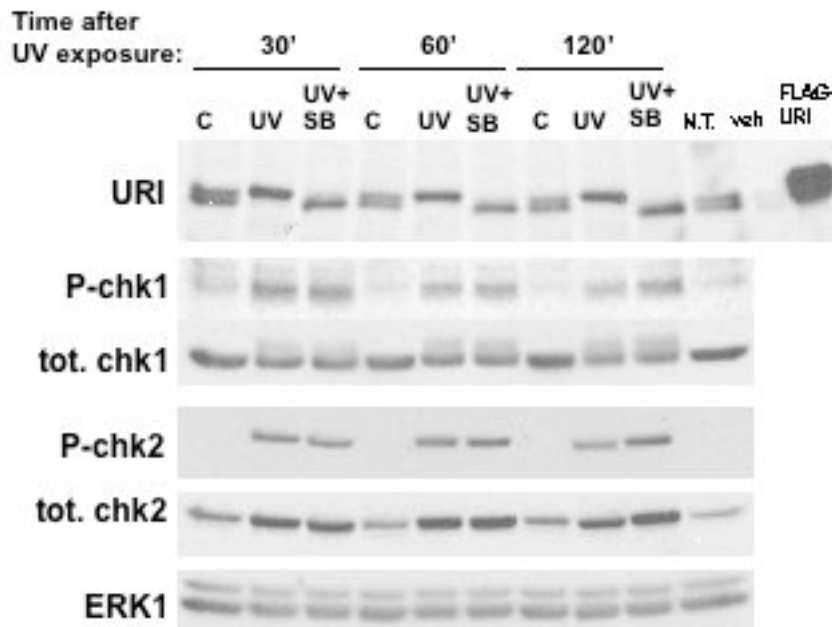
Figure 45. UV-induced URI phosphorylation is inhibited by p38 inhibitor SB203580. LNCaP cells were treated with UV 25J/m^2 in 2 ml of PBS and left to recover for the indicated times in complete media supplemented with or without p38 inhibitor SB203580 25µM (UV+SB) or DMSO (C or UV). Cells were then lysed and the expression of the indicated proteins was analyzed by Western blotting.

Lysates from 293 cells overexpressing an empty vector (veh) or a FLAG-tagged URI (FLAG-URI) and lysates from untreated cells were used as controls.

Treatment of LNCaP cells with UV induces a strong increase in the upper band of URI as expected, but treating the cells with p38 inhibitor SB203580 after exposure induced complete inhibition of URI phosphorylation, suggesting that URI is either phosphorylated by or downstream of the p38 kinase (fig. 45). Similar experiments were conducted using a DNA-PK inhibitor instead of rapamycin or SB 203580. Treatment of UV irradiated LNCaP cells with DNA-PK inhibitor did not affect phosphorylation of URI, suggesting that DNA-PK is not involved in UV-dependent URI post-transcriptional modification (data not shown).

Finally we tested wether the shift of the URI band induced by UV was due to actual URI phosphorylation vesus other post-transcriptional modifications. We performed λ-phosphatase assays incubating λ-phosphatase with UV treated LNCaP lysates or with URI immunoprecipiated from UV treated LNCaP cells (fig. 46).
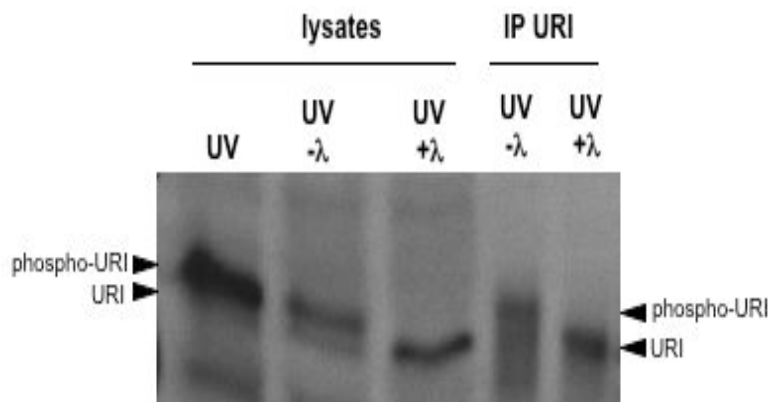
Figure 46. λ-phosphatase assay of UV treated URI. LNCaP cells were treated with UV 25J/m^2 in PBS and then left to recover for 30 minutes in complete media. After recovery cells were lysed and an aliquot was

137

used to IP URI. Lysates and IPed URI were either not treated (UV) or incubated at 30ºC for 30' in the presence (UV+λ) or absence (UV-λ) of λ-phosphatase. Lysates and IPed URI were then analysed by Western blotting using an anti-URI antibody.

Lambda phosphatase assay (fig. 45) clearly shows that the upper URI band induced by UV treatment is due to phosphorylation because treatment with λ-phosphatase induces complete disappearance of the URI upper band either using total lysates or IPed URI. We also observed a similar phosphorylation of URI upon cpt treatment of LNCaP cells but not upon doxorubicin treatment (data not shown).

Overall, these results show that URI is phosphorylated upon UV treatment, suggesting that URI function may be modulated by DNA damage and by components of the DNA damage response. In line with this observation are the effects observed on chk1, chk2 and H2AX phosphorylation upon URI loss that suggest a possible role of URI in DNA damage sensing or repair.

4.4   DISCUSSION

In C. elegans and Drosophila, URI deletion was shown to induce chromatin instability [113, 114]. Interestingly, the deleterious effect of URI deletion seemed more pronounced in the germline cells. In Drosophila, URI is expressed throughout development but it is most abundant during embryogenesis, pupariation and in adult gonads [113]. These observations led us to investigate the effect of URI and its partner Art-27 on the DNA damage response. As in C. elegans and Drosophila we found that depletion of Art-27 and URI induces increased phosphorylaton of chk1 and chk2, markers of an increased DNA damage response. As mentioned in chapter one, Art-27 and URI are tightly dependent on each other, and depletion of one protein induces decrease of the other. Therefore it is difficult to identify specific

functions for Art-27 or URI. The fact that the increase of chk1 and chk2 phosphorylation is more evident in Art-27 depleted cells compared to URI depleted cells, as well as the observation that Art-27 knock down increases transcription of a subset of genes involved in DNA damage response (chk1, ATR and HUS1), may suggest that URI effects on DNA damage response are mediated by a decrease in Art-27 protein. We also observed increased H2AX phosphorylation as well as a less linear and controlled dephosphorylation of H2AX in URI depleted cells. Interestingly, PP4 and PP2A phosphatases have been shown to mediate γH2AX dephosphorylation [229, 230]. We showed that URI interacts with PP2A phosphatase and mediates the phosphatase recruitment on the KAP1 complex (chapter 3). It is intriguing to hypothesize that the increase of γH2AX observed in URI depleted cells is due to loss of PP2A dephosphorylation. KAP1 protein has also been recently demonstrated to play a role in DNA damage response. KAP1 is rapidly recruited to sites of DNA damage and phosphorylated by ATM and chk1 [159, 224]. We showed that URI depletion induces hyperphosphorylation of KAP1 on serine 824, a site demonstrated to be important in allowing heterochromatin relaxation and repair of double-strand breaks [160].

We also show that URI can be robustly phosphorylated upon DNA damage induced by UV irradiation, further supporting the role of URI in the DNA damage response pathway. UV-dependent URI phosphorylation is dependent on p38 kinase because inhibition of p38 completely obliterates URI phosphorylation upon UV treatment.

Overall, the data presented in this chapter demonstrate a role for URI in chromatin stability and DNA damage response in mammalian cells. This data is in line with the studies of URI deletion in C. elegans and Drosophila. Further investigation will be necessary to clarify if URI depletion induces DNA damage through an unknown mechanism or if URI itself is directly involved in DNA damage response and repair. URI regulation of KAP1 protein and PP2A

phosphatase seem to suggest a direct role of URI in facilitating DNA damage repair through chromatin remodeling and control of DNA damage recovery.

CHAPTER 5:

THE URI/Art-27 COMPLEX IS INVOLVED IN PROSTATE CELL

DIFFERENTIATION

5.1 ART-27 IS EXPRESSED IN LUMINAL DIFFERENTIATED PROSTATE CELLS AND NOT IN BASAL CELLS WHILE URI IS EXPRESSED IN BOTH CELL TYPES.

Art-27 was shown to be expressed in differentiated epithelial cells of the prostate glands. On the contrary, Art-27 is not expressed in prostate buds originating from the urogenital sinus during human prostate development [79]. This observation suggests that Art-27 is a marker of prostate epithelial differentiation during development. Immunohistochemistry staining of Art-27, the Art-27 "partner" URI, and AR in adult human prostate (fig. 47) show that Art-27 is expressed specifically in prostate luminal epithelial cells and is not expressed in basal and stromal cells, which is in line with the previous observations correlating Art-27 specifically with prostate epithelial cell differentiation.
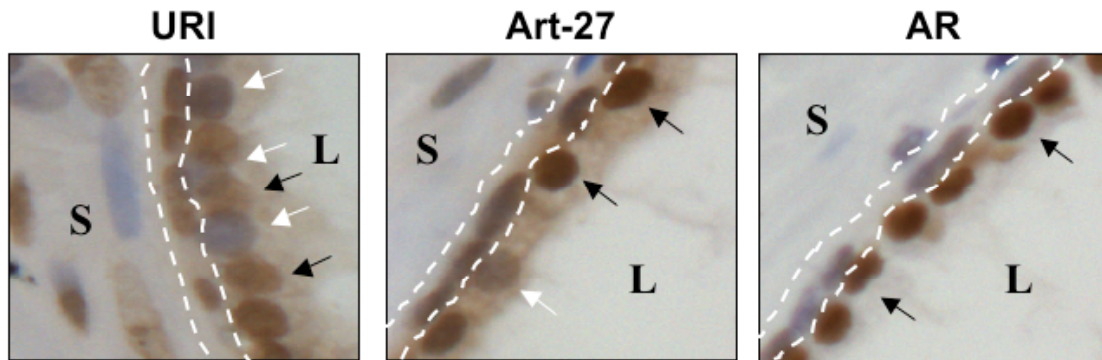
Figure 47. URI, Art-27 and AR expression in basal and luminal prostate epithelial cells. Consecutive sections of normal human prostate were stained for URI, Art-27 and AR using specific antibodies and a HRP-DAB (horseradish peroxidase/ 3,3'-Diaminobenzidine) system to visualize the proteins (brown staining). Haematoxylin was used to counter-stain the sections. The epithelial layer of a specific prostate gland is presented and the basal cells are outlined by two dashed lines. Positively (black arrows) and negatively (white arrows) stained luminal cells are indicated. L=gland lumen, S=gland stroma.

The androgen receptor expression has a pattern similar to Art-27 while URI is expressed in both basal and luminal epithelial cells. Interestingly, in luminal cells, Art-27 and URI staining is not present in all cells while AR is uniformly expressed. It is possible that the luminal cells that do not express Art-27 and URI are less differentiated cells. Indeed, several reports aimed at identifying a cancer stem cell population showed that pluripotent cells are not only part of the basal [231, 232] but also luminal [233] layer. Also, Liu and colleagues [234] showed, using lineage tracing techniques, that prostate luminal cells are derived from pre-existing luminal cells, suggesting that luminal cells can exist in different states of differentiation. Finally it has also been shown that in adult murine prostate both basal and luminal cells are self-sustained lineages that can both serve as targets for prostate cancer initiation [235].

To further explore the specific expression of Art-27 in luminal and basal cells we used NRP-152 rat prostate basal cells, which are able to differentiate in vitro into luminal cells [236, 237]. After 10 days of differentiation NRP-152 cells acquire a luminal phenotype demonstrated by expression of the luminal marker cytokeratin 18 (CK18). Luminal cells also express high levels of Art-27, but Art-27 is not expressed in basal NRP-152 cells (fig. 48). This observation clearly demonstrates luminal specific expression of Art-27.

Figure 48 (next page). Art-27 is specifically expressed in luminal but not basal prostate epithelial cells. NRP-152 were differentiated in vitro as described in [236]. After 10 days, control basal cells (left column, 0 days of differentiation) and luminal cells (right column, 10 days of differentiation) were fixed and stained for CK18 and Art-27 proteins. Pictures of the FITC-fluorescence (Art-27 and CK18 shown in green), DAPI fluorescence (blue) and of the corresponding bright fields (B.F.) were taken with a fluorescence microscope (20X magnification).
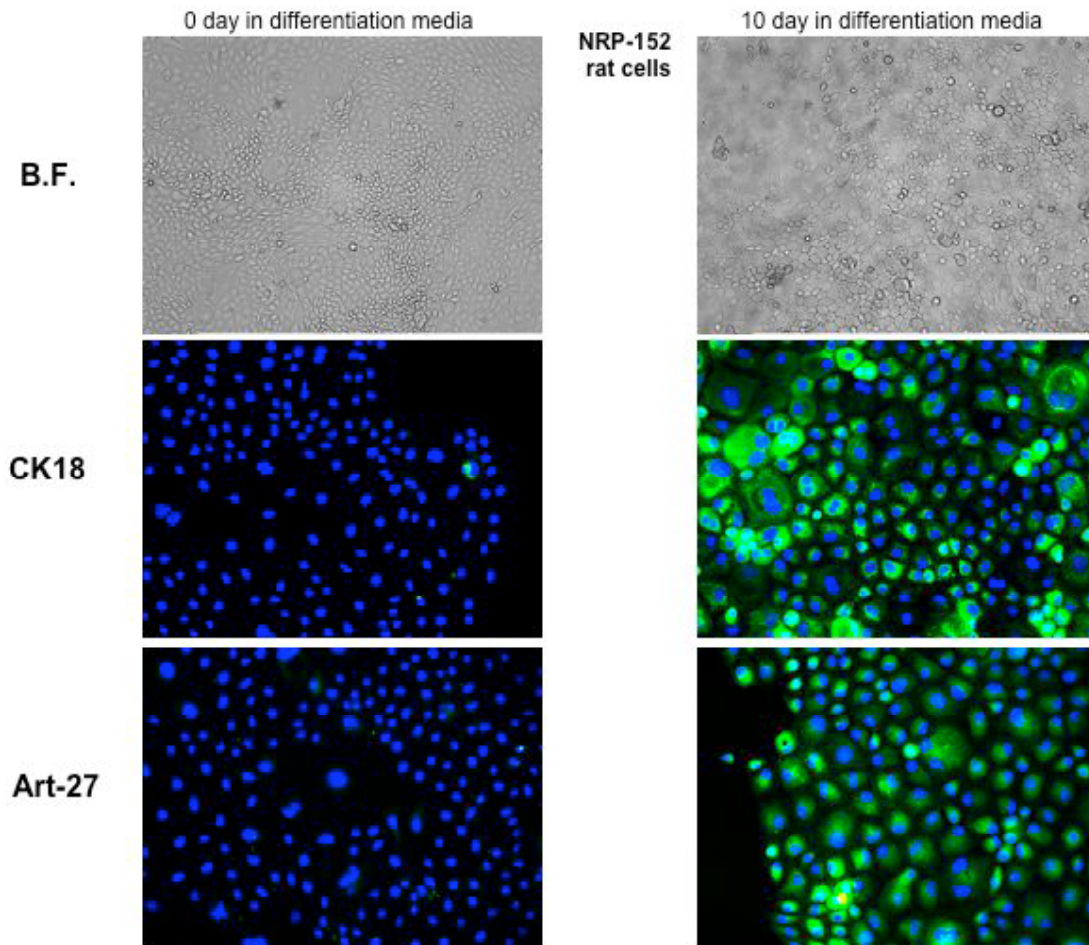
We also co-stained basal and luminal NRP152 cells for URI and CK18 (fig. 49). Unlike Art-27 URI is already expressed in basal prostate cells (fig. 49, upper row) but after 10 days of luminal differentiation the expression of URI is greatly increased (fig. 49, lower row). CK18, as expected, has a low expression in basal cells but it is highly expressed in luminal NRP-152. This observation suggests that URI protein correlates with Art-27 protein expression during basal to luminal differentiation of prostate epithelial cells.
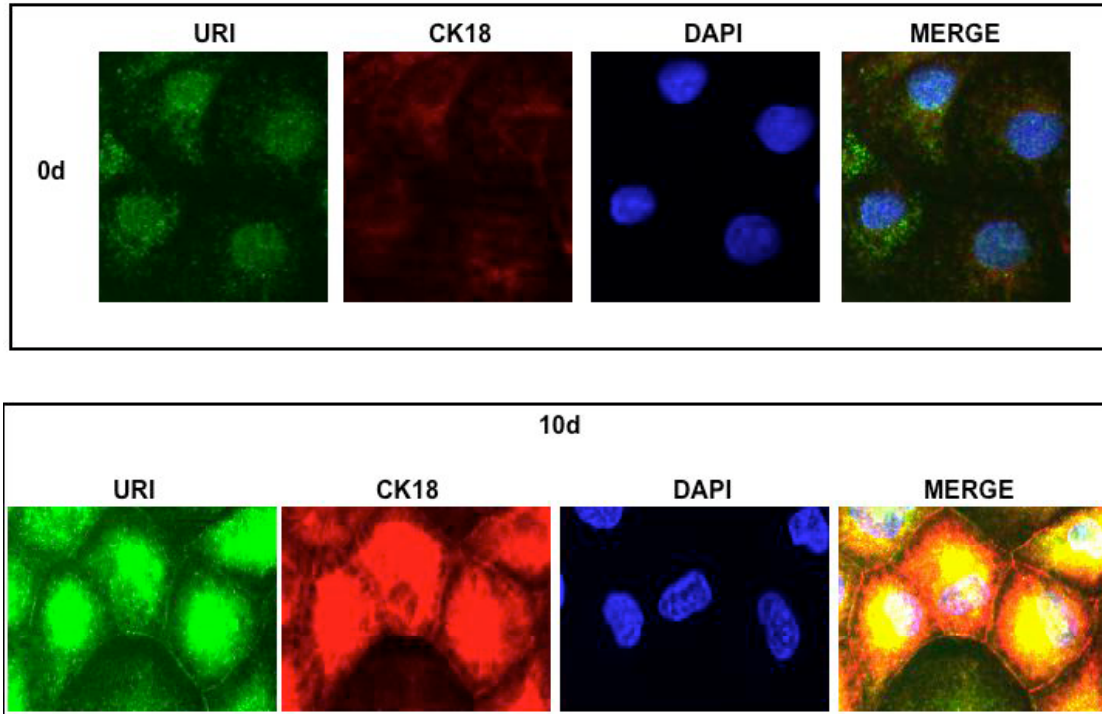
Figure 49. URI protein is increased during basal to luminal differentiation. NRP-152 rat prostate basal cells were differentiated for 10 days in vitro as in figure 48. Once differentiated cells were fixed and stained for URI (green) and CK18 (red). DAPI staining was used to label the nuclei in blue.

To further explore the role of URI in NRP-152 basal to luminal differentiation, we over-expressed a control vector or a construct encoding human URI in undifferentiated basal NRP152 cells and then co-stained for URI (green) and CK18 (red) (fig. 50). Cells overexpressing URI appear to have higher expression of CK18 marker suggesting that URI plays an active role in luminal differentiation. Most likely overexpression of URI induces Art-27 protein stabilization and therefore the increased CK18 expression is probably due to the increased amount of URI/Art-27 complex in cells overexpressing URI.
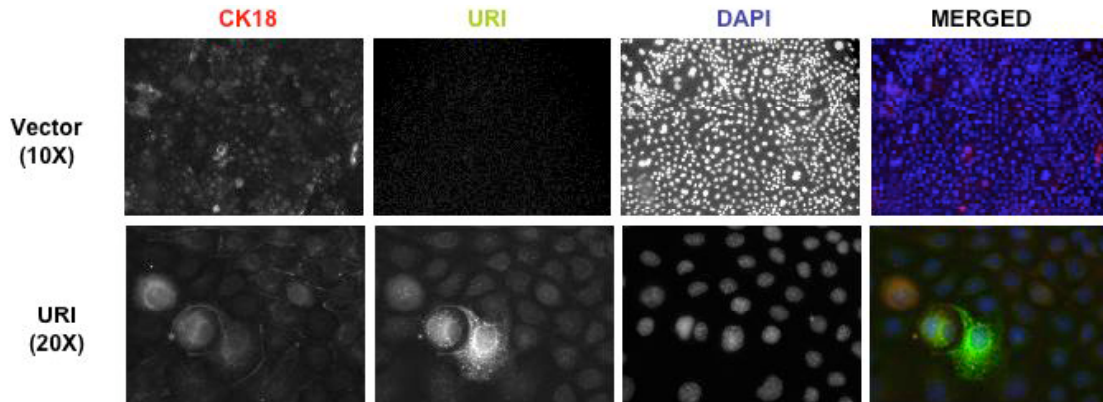
Figure 50. Human URI overexpression induces increased CK18 staining in NRP152. NRP152 were transfected with an empty vector or with a construct encoding human URI. After 48 hrs from transfection cells were fixed and stained with anti-URI (mouse) or anti-CK8 (rabbit) antibodies. FITC-conjugated anti-mouse IgG or TRITC-conjugated anti-rabbit IgG secondary antibodies were used to co-stain URI in green and CK18 in red. DAPI staining was also used to mark the nuclei (blue).

5.2   ART-27 BUT NOT URI EXPRESSION IS DECREASED IN A PROSTATE STEM CELL ENRICHED POPULATION

Prostate stem cells reside in the proximal region of prostatic ducts {Tsujimura, 2002 #288[238]. This Sca-1 highly expressing population of cells, [232] spatially distinguished from the distal region, posseses three features characteristic of stem cells: they are slow cycling, possess a high in vitro proliferative potential, and can reconstitute highly branched glandular ductal structures in collagen gels. We obtained the two populations of proximal and distal prostate epithelial cells from the Wilson laboratory and measured the expression of Art-27 and URI by Q-PCR (fig. 51). Art-27 expression was decreased in the mRNA isolated from proximal region cells that are enriched in stem cells compared to cells from the distal and intermediate region (fig. 51d). URI mRNA (fig.51c), on the other hand, has a negligible change between the

proximal and distal populations suggesting a marginal role in stem cell maintenance or perhaps involving a post-transcriptional modulation of URI protein that can not be measured by Q-PCR. The mRNA of the androgen receptor (fig. 51a) is also increased in distal compared to proximal cells, consistent with the idea that prostate stem cells do not depend on androgen for their survival [238] .
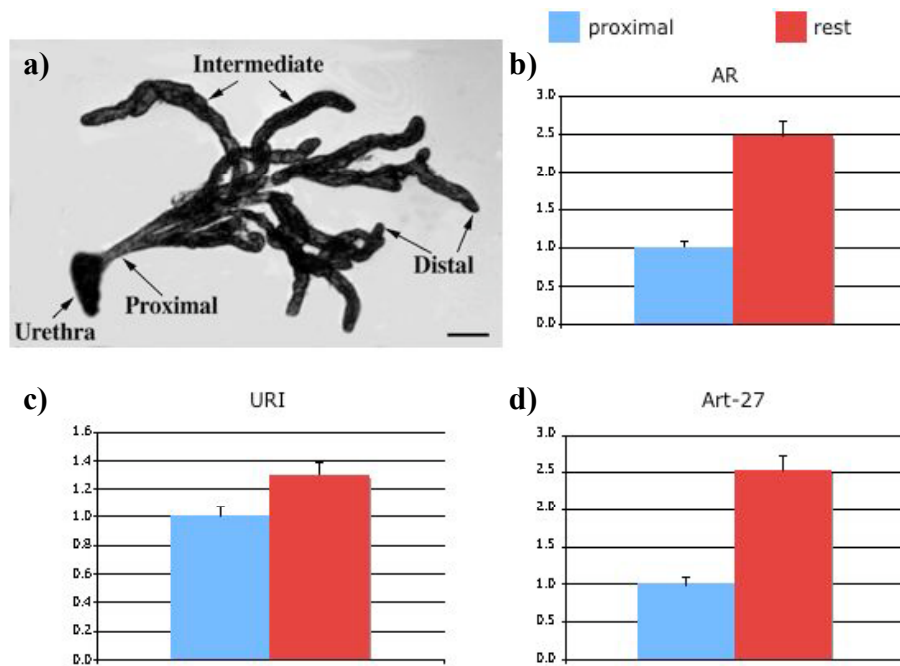
Figure 51. Art-27 mRNA is lower in cells from the proximal region of prostatic ducts with higher pluripotent capability. (a) A segment from a microdissected mouse ventral prostate illustrating the distal, intermediate, and proximal regions of prostatic ducts [238]. b-d) Q-PCR measurements of AR (b), URI (c) and Art-27 (d) mRNA in cells isolated from the proximal region versus the rest of the cells (intermediate and distal region).

Overall these data suggest that Art-27 expression can distinguish between two populations of prostate cells: a stem cell enriched population versus a population of more differentiated cells supporting a critical role for Art-27 in prostate cell differentiation.

5.3   URI DEPLETION DECREASES HORMONE DEPENDENT LIPOGENESIS

The LNCaP prostate cell line has a well established biphasic growth pattern dependent on androgen concentration. LNCaP cells grown at low concentrations of androgen (0.1 nM) exhibit a faster growth compared to cells grown in the presence of high concentrations of androgen (10nM). Higher concentrations of androgen promote cell differentiation and therefore interfere with proliferation [239, 240]. To assay cell differentiation we measured hormone dependent lipogenesis in LNCaP cells treated with low or high concentrations of hormone (R1881 0.1nM versus 10nM). To assess the importance of URI in this process we also depleted URI by siRNA treatment. In prostate cells lipogenesis is under the control of the androgen receptor [241] and it was shown to be correlated to differentiation rather than to proliferation [242] . We used oil red-O staining to measure the lipid content of LNCaP control cells (shNS) and LNCaP cells depleted of URI by shRNA (shURI) treated with or without 0.1 or 10nM R1881 (fig. 52). In line with the idea that URI and Art-27 expression leads to prostate cell differentiation, depletion of URI from LNCaP cells induces a decrease in lipogenesis, a process that has been associated with androgen dependent differentiation [242]. Interestingly, the URI dependent decrease in lipid production was only observed after treatment with a high concentration of androgens that is thought to have a pro-differentiation over a pro-proliferation effect (fig. 52, right panel). Treatment of LNCaP cells with the low, pro-proliferative concentration of hormone (0.1 nM) did not induce differences in lipogenesis between control cells and cells depleted of URI (fig. 52, left panel).
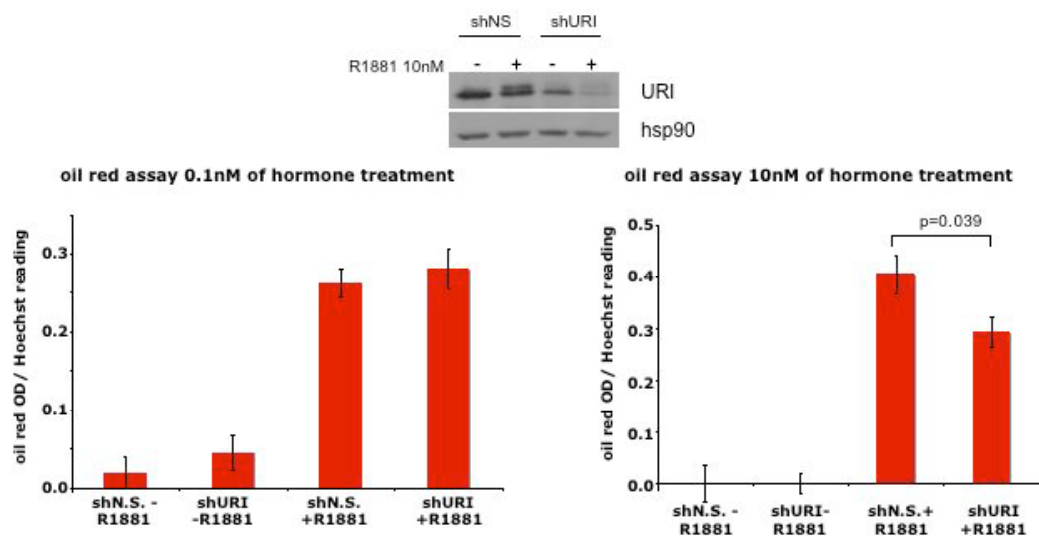
Figure 52. URI depletion decreases androgen dependent lipogenesis under pro-differentiaton conditions. LNCaP-shNS or LNCaP-shURI cells were hormone starved and then treated for 5 days with (+R1881) or without (-R1881) 0.1 or 10nM R1881. Cells were then fixed and stained with oil-red. Oil red was then extracted with isopropanol and quantified by absorbance measurement (λ=500nm). The absorbance was then normalized by the amount of cells measured by Hoechst staining. URI depletion in shURI cells was verified by Western blot using hsp90 as loading control (top panels). The values reported are the average of three independent experiments.

5.4 URI/ART-27 EXPRESSION NEGATIVELY CORRELATES WITH THE EXPRESSION OF HOMEOBOX TRANSCRIPTION FACTORS IN THE cBIO DATABASE

To explore the role of Art-27 and URI in prostate differentiation and the relevance of this process in cancer, we interrogated the cBio cancer genomic portal created and maintained by the Sloan Kettering Cancer Genomics and Computational Biology Center [208]. This database reports the gene expression profile of 216 prostate cancers compared to adjacent normal

prostate tissue. In collaboration with the Ostrer laboratory, we asked which genes positively or negatively correlate with URI expression. Analysis of the genes negatively correlated with URI (correlation index $\geq$-1 and $\leq$-0.8) showed a striking anti-correlation of URI with homeobox genes. Indeed, gene functional classification (DAVID bioinformatics resources 6.7) of URI anti-correlated genes shows that the most enriched class (enrichment score= 1.74) is the "homeobox transcription factors" class. Also the three most enriched protein domains in the group of genes with expression inversely correlated with URI were "homeobox, conserved site" (p= $1.3e^{-2}$), "homeobox" (p= $1.4e^{-2}$) and "homeodomain-related" (p= $1.4e^{-2}$). GO clustering revealed enrichment in "multicellular organismal process" (p= $1.3e^{-3}$), "developmental process" (p= $1.8e^{-2}$), and "biological regulation" (p= $3.6e^{-3}$). Moreover, visualization of the expression of the homeobox transcription factors with URI (C19orf2), Art-27, RPAP3 (subunit of the R2TP prefoldin like complex) and PTGES3/p23 (a chaperone protein that is part of the R2TP complex and involved in ER transcriptional regulation) clearly shows that prostate tumors with high expression of the URI/Art-27 complex have lower homeobox gene expression compared to normal prostate. In prostate samples with low expression of the URI/Art-27 complex, the homeobox gene expression is higher (fig. 53 top). RPAP3 and PTGSE3/p23 were included in the analysis because they are proteins highly correlated with URI and Art-27 expression and are part of the R2TP/prefoldin like complex. We included tumors with altered RPAP3 and PTGSE3/p23 to increase the "dissection" and subclassification of the different classes of tumors with altered URI or Art-27.
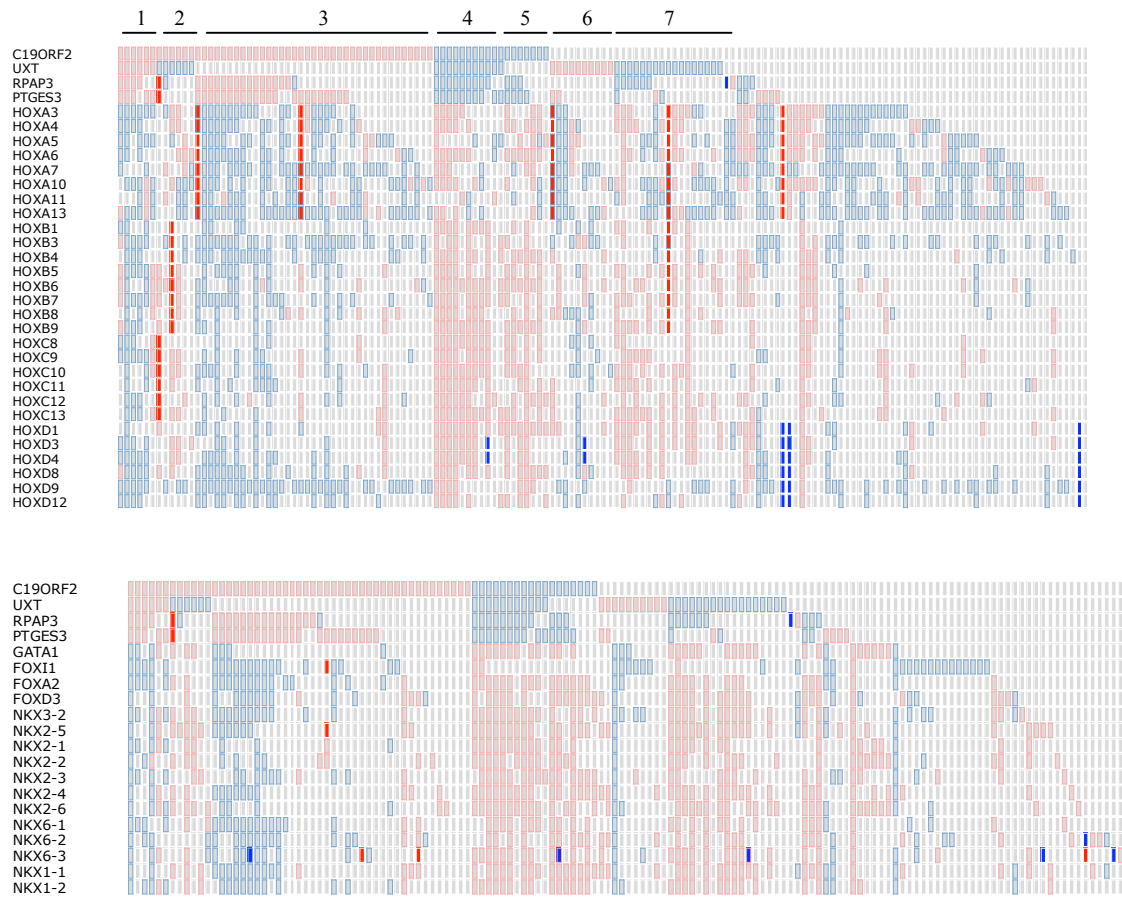
Figure 53. URI/Art-27 complex expression negatively correlates with the expression of homeobox and NKX genes. Oncoprints from the cBio Sloan Kettering cancer genomics database (http://www.cbioportal.org/public-portal/) correlating the expression of URI, Art27, RPAP3 and PTGES3/p23 to homeobox genes (top) or NKX genes (bottom). Each column corresponds to a prostate tumor sample and each row represents the expression of the corresponding gene in each tumor. Red box= increased expression compared to normal prostate, blue box= decreased expression compared to normal tissue, dark red box= gene amplification, dark blue box= gene deletion. The lines on top of the oncoprints indicate the tumor classes identified by different URI or Art-27 expression.

The oncoprints clearly show that the different classes of HOX genes (A, B, C and D) cluster together. Indeed, tumors with deletions (dark blue boxes) or amplifications (dark red boxes) of these genes present alteration of the entire class. Interestingly the expression of several NKX genes also negatively correlates with URI and Art-27 expression (fig. 53, bottom). More importantly survival of patients with altered (all tumors with 2≤ Z-score threshold ≤-2) URI, Art27, RPAP3 and PTGES3 is greatly decreased compared with the survival of patients with unaltered expression of these genes (log rank test P-value= 0.000131; log rank test P-value= 0.007381 for tumors with decreased expression and log rank test P-value= 0.000975 for tumors with increased expression) (fig. 54).
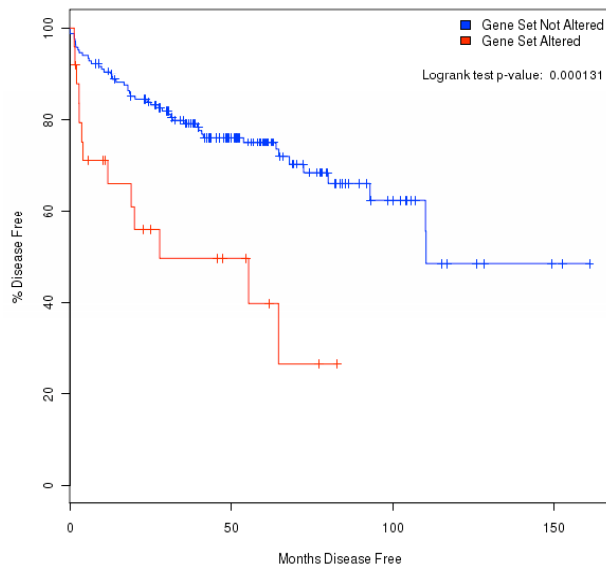
Figure 54. Disease free survival curves of patients with unaltered (blue line) or altered (red line) expression of URI, Art-27, RPAP3 and PTGES3.

The differences in survival are still statistically significant considering tumors with altered expression of only URI and Art27 (logrank test P-value= 0.007381 for tumors with decreased expression and logrank test P-value= 0.005 for tumors with increased expression).

152

All together these observations indicate that Art-27 and URI play a role, yet to be elucidated, in prostate cell differentiation. The presented data indicate that the Art-27-URI complex expression increases during prostate cell differentiation and is low in undifferentiated stages of prostate epithelial development. These observations are relevant in prostate cancer etiology as demonstrated by the reduction in survival for prostate cancer patients with altered expression of the Art-27/URI complex.

5.5   DISCUSSION

Art-27 was shown to be expressed in differentiating prostate epithelial cells during human embryogenesis [79]. The data presented in this chapter confirmed the role of Art-27 in the differentiation of prostate epithelial cells and more specifically we found that Art-27 is expressed in luminal and not basal prostate epithelial cells (fig. 47). We also explored the role of URI (which regulates Art-27 protein stability [82]) in differentiation. Interestingly, URI is not exclusively expressed in prostate luminal cells like Art-27, but we observed an increase of URI protein expression upon basal to luminal differentiation. It is also important to note that, unlike AR, URI and Art-27 are not expressed uniformly in all luminal cells suggesting that not all luminal cells are terminally differentiated. We propose that the luminal cells expressing low levels of Art-27 and URI are in a less differentiated stage and may play a role in tumors arising from the luminal compartment. Indeed, it has been shown that both the basal and luminal cells are self-sustained populations that include pluripotent cells able to regenerate an entire prostate in regeneration assays [232, 233, 235]. We also showed that Art-27 mRNA, but not URI, is less expressed in the proximal region of prostate ducts, a region enriched in prostate stem cells [238]. Finally, the exploration of the Sloan Kettering cBio portal containing the expression patterns of 216 prostate cancers compared to their normal counterparts, clearly identified the homeobox genes (HOX and NKX genes) negatively correlated with URI

expression. Indeed the expression of HOX and NKX genes is decreased in cancers with increased URI and Art-27 expression and increased in cancers with decreased expression of URI and Art-27 (fig. 52). This observation suggests that loss of the Art-27/URI complex could favor a more undifferentiated state of prostate tumors therefore inducing the development of more tumorigenic and aggressive cancers. It is interesting to note however, that either decreased or increased expression of URI and Art-27 leads to a statistically significant decrease in survival. This observation suggests that the URI/Art-27 complex is probably involved in multiple pathways, likely including feed-back regulatory mechanisms. A possible involvement of the complex in the regulation of phosphatases like PP2A and PP1γ may explain the fact that any changes in Art-27 or URI expression lead to decreased survival.

Overall the data presented in this chapter demonstrate a role for Art-27 and URI in prostate development and more specifically, in epithelial cell differentiation. Genes and proteins involved in organ embryogenesis have already been linked to prostate and breast cancer suggesting a strong correlation between embryonic development and cancer progression. For prostate, NKX3.1 [243] and FOXA1 [244] transcription factors are examples of genes essential for prostate development and they are also clearly involved in prostate cancer formation and progression. In this chapter we suggest that Art-27 and URI are part of a class of genes that play a role in both development and cancer.

CONCLUSION

AND

FUTURE DIRECTIONS

In 1998 URI was identified as a transcriptional repressor that binds the RNA polymerase II subunit RPB5 [94]. Since then several new interactors of URI were identified and a mitochondrial function as PP1γ regulator was unveiled for URI [104]. URI was found to play a role in translation initiation [120], nutrient sensing [84], apoptosis [105], DNA damage [113, 114] and RNA polymerase II cytoplasmic assembly [87]. Despite the increasing amount of data supporting a key role of URI in cellular regulation, the nuclear role of URI remains still unknown. Among the interactors of URI, Gstaiger and colleagues [84] identified Art-27, a known androgen receptor (AR) co-repressor. We found that Art-27 and URI are part of a novel repressor complex able to interfere with androgen receptor mediated transcription. Several lines of evidence suggest that the Art-27/URI complex does not behave as a classic co-repressor complex because it is not recruited on the DNA by the androgen receptor and it also affects AR binding to the DNA. We hypothesized that the URI/Art-27 complex affects chromatin structure and therefore regulates the androgen receptor transcriptional landscape. ChIP-seq analysis of AR recruitment in the presence or absence of URI showed a very limited effect of URI depletion on the hormone dependent recruitment of AR on the DNA (data not shown). This result may indicate a more indirect role of URI on AR mediated transcription. URI may affect the transcription or activity of other proteins involved in transcription regulation and that, in turn, affects AR mediated transcription. In line with the idea that the URI/Art-27 complex could affect chromatin structure and epigenetic gene regulation, we found that URI binds and regulates the phosphorylation of the KAP1 protein. KAP1 is a scaffolding protein that represses transcription and induces heterochromatinization through the binding and recruitment of the HP1 protein, SETDB1 histone methyl transferase and HDAC1 and 2 histone deacetylases [126]. We showed that, in the presence of doxorubicin-induced DNA damage, URI recruits PP2A phosphatase on the KAP1 complex controlling KAP1 phosphorylation downstream of the ATM kinase. Phosphorylation of KAP1 interferes with the recruitment of the

156

repression complex [153] and therefore, depletion of URI resulting in increased KAP1 phosphorylation causes increased transcription of known KAP1 regulated genes such as p21, BAX, NOXA and IGFBP3. Interestingly, this function of URI resembles the URI function in the mitochondria. In this cellular organelle URI binds and represses PP1γ. Upon URI phosphorylation PP1γ is released from URI binding, whereby it becomes active and dephosphorylates BAD, triggering apoptosis. In a similar manner we show that, in the nucleus, URI binds PP2A phosphatase and targets it to the KAP1 complex. Regulation of KAP1 phosphorylation controls the expression of genes involved in apoptosis and cell cycle arrest. Therefore, depletion of URI triggers apoptosis through two different mechanisms: BAD dephosphorylation in the mitochondria and KAP1 phosphorylation in the nucleus (fig. 55). The effect of URI depletion on expression of KAP1 regulated genes is evident only in cells with a compromised p53 pathway because the genes repressed by KAP1 are also potently activated by the p53 protein.
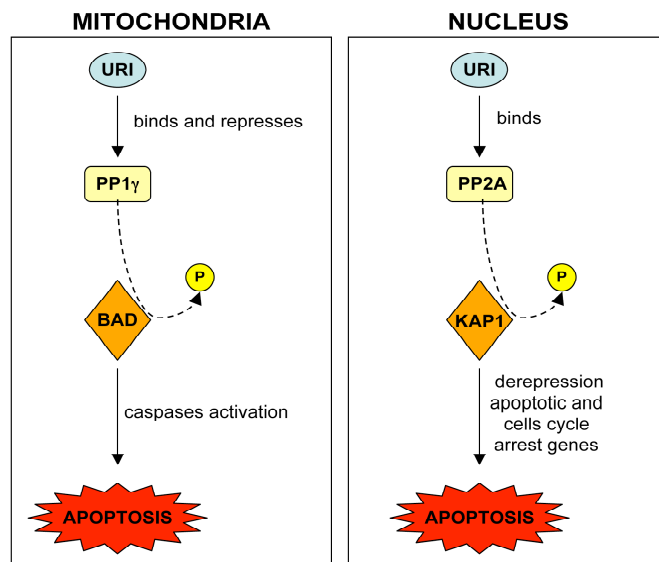
Figure 55. Scheme depicting the parallels between the mitochondrial and nuclear function of URI.

We also showed that URI can be phosphorylated downstream of several pathways such as the mToR and the p38 kinase pathways. Interestingly URI is heavily modified upon DNA damage induced by UV. It is possible that, as in the mitochondria, the nuclear function of URI can be modulated by its post-transciptional modification. Our mass spectrometry analysis revealed several novel sites of phosphorylation and acetylation of URI protein and these modifications correlate with polymerase II assembly and elongation. Additional experiments are required to elucidate the impact of URI post-transcriptional modification on transcriptional repression.

Interestingly KAP1 was shown to be essential for the repression of retroelements in embryonic stem cells [164]. Depletion of URI induced partial reactivation of some LINE1, Alu and endogenous retroelements in a cell specific manner, suggesting that URI regulates the KAP1 mediated repression of retroelements. This result is particularly interesting in prostate cells because of the reported [13] role of LINE1 ORF2 in the formation of the TMPRSS2:ERG translocation found in the majority of prostate cancers. This observation suggests that misregulation of URI during prostate cancer progression could favor the formation of the TMPRSS2:ERG translocation. Further analysis of cells over-expressing or depleted of URI will shed light on the relevance of URI misregulation in the formation of the TMPRSS2:ETS translocation, a common feature of prostate tumors. Also, similar analysis using cells with depleted or over-expressed KAP1 will confirm a role of this protein in the formatin of the TMPRSS2:ETS translocation. KAP1 is, indeed, likely part of the DNA damage induced complex comprising LINE1 ORF2, GADD45α and AID proteins, that was hypothesized to cause the TMPRSS2:ETS translocation [13]. In B lymphocytes KAP1 binds AID protein and it is involved in class switch recombination [245], a process that involves a mechanism similar to

158

the one proposed to be responsible for the formation of the TMPRSS2:ERG translocation in prostate cancer cells.

KAP1, also called TIF1β or TRIM28, is known to be a crucial protein in cell differentiation and development. Transgenic mice lacking KAP1 develop until blastocyst implantation but do not undergo gastrulation arresting their development after embryonic day E5.5. Analysis of the embryos showed lack of mesoderm differentiation, implicating TIF1β in egg-cylinder organization and mesoderm induction [134]. It is intriguing to speculate that the role of URI and Art-27 in prostate epithelial cell differentiation is dependent on KAP1 activity but further experiments are needed to evaluate the role of KAP1 and KAP1 phosphorylation in prostate and prostate cancer development. Intriguingly, we showed that the phosphatase PP2A (more specifically PP2A beta), binds URI and regulates KAP1 phosphorylation. PP2A is a known tumor suppressor lost in a subset of prostate cancers. The analysis of PP2A protein expression in normal prostate glands reported in the Human Protein Atlas (www.proteinatlas.org) showed an interesting basal restricted expression suggesting a possible role for this phosphatase in prostate epithelial basal to luminal differentiation.

Given the direct binding of URI and Art-27 to the RNA polymerase II complex, it is also likely that URI and Art-27 affect transcription through a direct effect on pol II. This idea is supported by the clear interaction of URI with several proteins directly involved in polII transcription initiation and elongation such as RPB5, TFIIF, the Paf-I complex and the R2TP-prefoldin like complex responsible for the RNA polymerase II complex assembly. We also observed these interactions in our mass spectrometry analysis of nuclear URI interactors. This hypothesis implies that URI has a more general role in transcription regulation not restricted to androgen receptor mediated transcription. URI was previously shown to repress the

159

transcription mediated by the VP16 activator, and we also showed that URI fused to the GAL4 DNA binding domain is able to repress transcription controlled by a TK promoter downstream of a GAL4 binding domain. We also showed that Art-27 is part of the URI repression complex. These data suggest that URI and Art-27 are part of a novel repressor complex that may act through the RNA polymerase II complex. Our whole genome microarray analysis of LNCaP cells depleted of URI protein identified genes affected by URI depletion in a hormone dependent or independent manner. Surprisingly, only 5% of the genes were affected by URI depletion suggesting gene-specific control and rejecting the idea of a general and non-specific effect of URI on RNA polymerase transcription. Moreover, in our cell model of URI-GAL4 overexpressing cells, the URI-GAL4/Art-27 complex is tethered to the promoter region of a luciferase gene supporting the idea that the URI/Art-27 complex has a role in transcription initiation. Our mass spectrometry analysis, on the other hand, clearly shows binding of URI to elongating polymerase, characterized by phosphorylated CTD, suggesting that the URI/Art-27 complex "travels" with polII in the body of the gene, probably also affecting and controlling transcription elongation. Therefore the 293T-REX-URI-GAL4 system is not suitable to study the role of the URI/Art-27 complex in RNA polymerase elongation. On the other hand, is an ideal model for dissecting the involvement of URI and Art-27 in the first steps of polII-mediated transcription. It may be possible that the URI/Art-27 complex controls the phosphorylation of the RNA polymerase II complex and/or the phosphorylation of other proteins involved in transcription including histones. This effect would imply a role for the URI/Art-27 complex in polymerase II stalling, a process previously demonstrated to be controlled by polII CTD phosphorylation on serine 2 and serine 5 [246]. Polymerase stalling was shown to affect specific genes and to be important for transcriptional regulation of particular classes of genes. Interestingly, polymerase II stalling was shown to be a regulatory step particularly important in the transcription of developmental genes [247]. It is also important to mention that ChIP-

sequence analysis performed to identify KAP1 binding sites on chromatin revealed that KAP1 can bind at the transcription start site of numerous genes in a KRAB-ZFP independent manner [148]. The mechanism and function of this KAP1 recruitment is still unknown, but it may be indicative of KAP1 binding to the URI/Art-27 complex recruited at the transcription start site to regulate polymerase II function.

Overall, these data demonstrate that URI is a crucial node downstream of several cellular pathways in the cytoplasm as well as in the nucleus. In particular, URI is part of a novel transcription repression complex involved in the transcription of genes controlling apoptosis, cell cycle, DNA damage and development. The exact mechanism by which URI, probably in complex with its partner Art-27, controls transcription still remains elusive and further studies will be necessary to gain insight into the molecular function of URI. Moreover, we identified a novel interaction between URI and KAP1 protein that links URI to the regulation of retroelements and the formation of the TMPRSS2:ETS translocation, a common chromosomal aberration found in the majority of prostate cancers. In conclusion, the study of URI and URI cellular function is a complex scientific challenge because of the involvement of this protein in several basic mechanisms and pathways. Once these puzzles are solved they will certainly help us understand basic and important cellular processes involved in cancer and in normal cellular physiology.

APPENDIX

I. SUPPLEMENTAL RESULTS

Table S1. genes up-regulated by R1881 only in the presence of URI (URI=activator)

Probesets			2XUP BY R1881 just in siCTRL(foldCTRL/foldURI.1.2)	siCTRL+/siCTRL-	siURI+/siURI-	foldCTRL/foldURI
210095_s_at	IGFBP3	insulin-like growth factor binding protein 3		4.505986527	1.09709085	4.107213662
212143_s_at	IGFBP3	insulin-like growth factor binding protein 3		4.057283181	1.170498431	3.466286733
209540_at	IGF1	insulin-like growth factor 1 (somatomedin C)		2.319755251	1.504799839	1.54157064
209541_at	IGF1	insulin-like growth factor 1 (somatomedin C)		2.824893934	1.877637812	1.504493527
214036_at	EFNA5	Ephrin-A5		2.8325315	1.890075677	1.498633909
211494_s_at	SLC4A4	solute carrier family 4, sodium bicarbonate cotransporter, member 4		2.792433066	1.939166929	1.440016857
220382_s_at	ARHGAP28	Rho GTPase activating protein 28		2.432267661	1.736251571	1.400872835
210739_x_at	SLC4A4	solute carrier family 4, sodium bicarbonate cotransporter, member 4		2.490150606	1.783594925	1.396141338
217967_s_at	FAM129A	family with sequence similarity 129, member A		2.666036441	1.966856904	1.355480633
207574_s_at	GADD45B	growth arrest and DNA-damage-inducible, beta		2.288038931	1.760350854	1.299763014
221897_at	TRIM52	tripartite motif-containing 52		2.381725255	1.83708961	1.296466565
209125_at	KRT6A	keratin 6A		2.131358088	1.64785774	1.293411462
207087_x_at	ANK1	ankyrin 1, erythrocytic		2.00044297	1.609611369	1.242811159
217966_s_at	FAM129A	family with sequence similarity 129, member A		2.049270457	1.651370456	1.240951387
204069_at	MEIS1	Meis homeobox 1		2.205193723	1.779194212	1.239433957
207121_s_at	MAPK6	mitogen-activated protein kinase 6		2.295800849	1.874944641	1.224463271
205830_at	CLGN	calmegin		2.378340045	1.949301161	1.220098819
206177_s_at	ARG1	arginase, liver		2.012957203	1.657811183	1.214225856
208353_x_at	ANK1	ankyrin 1, erythrocytic		2.417568051	1.9932097	1.21290201

Table S2. genes up-regulated by R1881 only in the absence of URI (URI=repressor)

Probesets			2XUP BY R1881 just in siURI(foldURI/foldCTRL>1.2)	siCTRL+/siCTRL-	siURI+/siURI-	foldURI/foldCTRL
211864_s_at	FER1L3	fer-1-like 3, myoferlin (C. elegans)		1.470679113	2.590560901	1.761472559
211919_s_at	CXCR4	chemokine (C-X-C motif) receptor 4		1.861033467	3.108514697	1.670316387
201798_s_at	FER1L3	fer-1-like 3, myoferlin (C. elegans)		1.629631418	2.633719131	1.616144057
201289_at	CYR61	cysteine-rich, angiogenic inducer, 61		1.269280564	2.041049258	1.608036328
211020_at	GCNT2	glucosaminyl (N-acetyl) transferase 2, I-branching enzyme (I blood group)		1.292219006	2.050133702	1.58652186
209201_x_at	CXCR4	chemokine (C-X-C motif) receptor 4		1.82353438	2.82617147	1.549831745
218885_s_at	GALNT12	UDP-N-acetyl-alpha-D-galactosamine:polypeptide N-acetylgalactosaminyltransferase 12 (GalNAc-T12)		1.367138969	2.058595531	1.505769038
209830_s_at	SLC9A3R2	solute carrier family 9 (sodium/hydrogen exchanger), member 3 regulator 2		1.378913253	2.063872574	1.496738515

204241_at	ACOX3	acyl-Coenzyme A oxidase 3, pristanoyl	1.931329874	2.834840372	1.467817802
209631_s_at	GPR37	G protein-coupled receptor 37 (endothelin receptor type B-like)	1.567082029	2.298832738	1.46695112
204911_s_at	TRIM3	tripartite motif-containing 3	1.710908967	2.506384929	1.464943476
221994_at	PDLIM5	PDZ and LIM domain 5	1.640009305	2.402474803	1.464915349
203973_s_at	CEBPD	CCAAT/enhancer binding protein (C/EBP), delta	1.850833991	2.677064687	1.446409943
218245_at	TSKU	tsukushin	1.679806435	2.380256419	1.416982558
204309_at	CYP11A1	cytochrome P450, family 11, subfamily A, polypeptide 1	1.469479772	2.023604426	1.377088998
213884_s_at	TRIM3	tripartite motif-containing 3	1.696373205	2.310310405	1.361911635
219302_s_at	CNTNAP2	contactin associated protein-like 2	1.765369527	2.403099526	1.361244481
217981_s_at	FXC1	fracture callus 1 homolog (rat)	1.559099498	2.113712266	1.355726347
206923_at	PRKCA	protein kinase C, alpha	1.777966079	2.405194892	1.352778841
204017_at	KDELR3	KDEL (Lys-Asp-Glu-Leu) endoplasmic reticulum protein retention receptor 3	1.545621856	2.078849332	1.344992194
203293_s_at	LMAN1	lectin, mannose-binding, 1	1.732414317	2.305243262	1.330653551
201950_x_at	CAPZB	capping protein (actin filament) muscle Z-line, beta	1.621042595	2.156975067	1.330609741
37012_at	CAPZB	capping protein (actin filament) muscle Z-line, beta	1.541163582	2.047567482	1.328585432
47553_at	DFNB31	deafness, autosomal recessive 31	1.851351714	2.456482566	1.326858936
202934_at	HK2	hexokinase 2	1.733152977	2.299161805	1.326577535
201374_x_at	PPP2CB	protein phosphatase 2 (formerly 2A), catalytic subunit, beta isoform	1.615779464	2.120111294	1.312129124
212915_at	PDZRN3	PDZ domain containing ring finger 3	1.538444075	2.003657196	1.302391961
213325_at	PVRL3	poliovirus receptor-related 3	1.772085238	2.300721887	1.29831333
219118_at	FKBP11	FK506 binding protein 11, 19 kDa	1.784433329	2.306891258	1.292786466
219592_at	MCPH1	microcephalin 1	1.560520165	2.001340164	1.282482731
217013_at	AZGP1P1	alpha-2-glycoprotein 1, zinc-binding pseudogene 1	1.927024481	2.446173273	1.269404357
217790_s_at	SSR3	signal sequence receptor, gamma (translocon-associated protein gamma)	1.838315003	2.333307583	1.269264288
201387_s_at	UCHL1	ubiquitin carboxyl-terminal esterase L1 (ubiquitin thiolesterase)	1.629172424	2.061221577	1.265195474
218193_s_at	GOLT1B	golgi transport 1 homolog B (S. cerevisiae)	1.769397267	2.23544802	1.263395203
204242_s_at	ACOX3	acyl-Coenzyme A oxidase 3, pristanoyl	1.7423579	2.201142428	1.263312451
204435_at	NUPL1	nucleoporin like 1	1.968061085	2.439381666	1.239484732
203294_s_at	LMAN1	lectin, mannose-binding, 1	1.847824832	2.285441673	1.236828098
202558_s_at	HSPA13	heat shock protein 70kDa family, member 13	1.914004206	2.366124521	1.236216992
203921_at	CHST2	carbohydrate (N-acetylglucosamine-6-O) sulfotransferase 2	1.696263268	2.094339025	1.234678051
217943_s_at	MAP7D1	MAP7 domain containing 1	1.817809477	2.233549147	1.228703654
213618_at	CENTD1	centaurin, delta 1	1.837394226	2.255932967	1.227789298
203463_s_at	EPN2	epsin 2	1.757934114	2.158097432	1.227632717
220153_at	ENTPD7	ectonucleoside triphosphate diphosphohydrolase 7	1.677239835	2.05311153	1.22410134
209287_s_at	CDC42EP3	CDC42 effector protein (Rho GTPase binding) 3	1.987107607	2.429665994	1.222714857
203279_at	EDEM1	ER degradation enhancer, mannosidase alpha-like 1	1.831383589	2.229376838	1.217318344
213763_at	HIPK2	homeodomain interacting protein kinase 2	1.795633603	2.182582216	1.215494192
218189_s_at	NANS	N-acetylneuraminic acid synthase	1.846394715	2.239218017	1.21275153
201325_s_at	EMP1	epithelial membrane protein 1	1.905024696	2.304684714	1.209792565
213684_s_at	PDLIM5	PDZ and LIM domain 5	1.834526825	2.217195985	1.20859284

220200_s_at	SETD8	SET domain containing (lysine methyltransferase) 8	1.770473193	2.137468264	1.207286432
211467_s_at	NFIB	nuclear factor I/B	1.73409147	2.092430929	1.20664392
205294_at	BAIAP2	BAI1-associated protein 2	1.818217766	2.191599227	1.205355743
201689_s_at	TPD52	tumor protein D52	1.860643292	2.237433804	1.202505506

Table S3. genes down-regulated by R1881 only in the presence of URI (URI=repressor)

Probesets		2XDOWN BY R1881 just in siCTRL(foldCtrl/foldURI>1.2)	siCTRL-/siCTRL+	siURI-/siURI+	foldCTRL/foldURI
210305_at	PDE4DIP	phosphodiesterase 4D interacting protein	3.286847224	1.296260792	2.535637307
214130_s_at	PDE4DIP	phosphodiesterase 4D interacting protein	2.022214311	1.094981959	1.846801488
221236_s_at	STMN4	stathmin-like 4	2.588677062	1.473063375	1.757342628
218087_s_at	SORBS1	sorbin and SH3 domain containing 1	2.600745988	1.575445448	1.650800408
204653_at	TFAP2A	transcription factor AP-2 alpha (activating enhancer binding protein 2 alpha)	2.000992833	1.235236253	1.619927223
205872_x_at	PDE4DIP	phosphodiesterase 4D interacting protein	2.539130949	1.608188368	1.578876579
210117_at	SPAG1	sperm associated antigen 1	2.118295415	1.419381099	1.492407794
213388_at	PDE4DIP	phosphodiesterase 4D interacting protein	2.767630989	1.865088126	1.483914326
205191_at	RP2	retinitis pigmentosa 2 (X-linked recessive)	2.220994161	1.497512453	1.483122332
41329_at	SCYL3	SCY1-like 3 (S. cerevisiae)	2.073870055	1.413043618	1.467661739
213230_at	CDR2L	cerebellar degeneration-related protein 2-like	2.165911808	1.522446994	1.422651702
205891_at	ADORA2B	adenosine A2b receptor	2.470442539	1.765717448	1.399115437
219777_at	GIMAP6	GTPase, IMAP family member 6	2.18072447	1.57691074	1.382909263
203002_at	AMOTL2	angiomotin like 2	2.209337772	1.615049071	1.367969439
209307_at	SWAP70	SWAP-70 protein	2.346379546	1.730993971	1.355509947
209846_s_at	BTN3A2	butyrophilin, subfamily 3, member A2	2.205272596	1.636594036	1.347476862
201929_s_at	PKP4	plakophilin 4	2.370140527	1.764227976	1.343443455
201810_s_at	SH3BP5	SH3-domain binding protein 5 (BTK-associated)	2.025045747	1.519297081	1.332883326
208092_s_at	FAM49A	family with sequence similarity 49, member A	2.001537575	1.502189272	1.332413706
201340_s_at	ENC1	ectodermal-neural cortex (with BTB-like domain)	2.140667907	1.611353468	1.328490582
205017_s_at	MBNL2	muscleblind-like 2 (Drosophila)	2.21738195	1.670430663	1.327431302
209683_at	FAM49A	family with sequence similarity 49, member A	2.194653379	1.661100659	1.321204327
212992_at	AHNAK2	AHNAK nucleoprotein 2	2.3024881	1.750313564	1.31547178
213478_at	RP1-21O18.1	kazrin	2.083979376	1.592448151	1.30866388
202254_at	SIPA1L1	Signal-induced proliferation-associated 1 like 1	2.195553972	1.697178491	1.293649421
218611_at	IER5	immediate early response 5	2.510055041	1.940438084	1.293550699
201927_s_at	PKP4	plakophilin 4	2.028781507	1.587002609	1.278373139
219338_s_at	LRRC49	leucine rich repeat containing 49	2.452637467	1.931587858	1.269751959
217483_at	FOLH1	folate hydrolase (prostate-specific membrane antigen) 1	2.154186265	1.708179991	1.26110028
210654_at	TNFRSF10D	tumor necrosis factor receptor superfamily, member 10d, decoy with truncated death domain	2.233352537	1.772784902	1.259798938
209781_s_at	KHDRBS3	KH domain containing, RNA binding, signal transduction associated 3	2.044405673	1.624653997	1.258363736
211300_s_at	TP53	tumor protein p53	2.325082649	1.867825916	1.244806932
210731_s_at	LGALS8	lectin, galactoside-binding, soluble, 8	2.010257065	1.618144785	1.242322123
204404_at	SLC12A2	solute carrier family 12	2.368551432	1.933910461	1.224747206

		(sodium/potassium/chloride transporters), member 2			
211962_s_at	ZFP36L1	zinc finger protein 36, C3H type-like 1	2.071525098	1.712831223	1.209415773
220937_s_at	ST6GALNAC4	ST6 (alpha-N-acetyl-neuraminyl-2,3-beta-galactosyl-1,3)-N-acetylgalactosaminide alpha-2,6-sialyltransferase 4	2.323015049	1.926571728	1.205776569
209615_s_at	PAK1	p21 protein (Cdc42/Rac)-activated kinase 1	2.066165903	1.720062515	1.201215587

Table S4. genes down-regulated by R1881 only in the absence of URI (URI=activator)

Probesets		2XDOWN BY R1881 just in siURI(foldURI/foldCTRL>1.2)	siCTRL-/siCTRL+	siURI-/siURI+	foldURI/foldCTRL
216244_at	IL1RN	interleukin 1 receptor antagonist	1.831510028	3.548564427	1.937507507
201185_at	HTRA1	HtrA serine peptidase 1	1.448772834	2.503696	1.728149466
222376_at	---	---	1.446270391	2.353244952	1.627112721
203397_s_at	GALNT3	UDP-N-acetyl-alpha-D-galactosamine:polypeptide N-acetylgalactosaminyltransferase 3 (GalNAc-T3)	1.813183578	2.886227457	1.591801014
220979_s_at	ST6GALNAC5	ST6 (alpha-N-acetyl-neuraminyl-2,3-beta-galactosyl-1,3)-N-acetylgalactosaminide alpha-2,6-sialyltransferase 5	1.352308585	2.091982815	1.546971481
213737_x_at	GOLGA9P	golgi autoantigen, golgin subfamily a, 9 pseudogene	1.587735946	2.388235988	1.50417706
219923_at	TRIM45	tripartite motif-containing 45	1.585645757	2.350687891	1.482479854
204622_x_at	NR4A2	nuclear receptor subfamily 4, group A, member 2	1.520324619	2.216456425	1.457883664
209598_at	PNMA2	paraneoplastic antigen MA2	1.415367208	2.054905857	1.451853515
210306_at	L3MBTL	l(3)mbt-like (Drosophila)	1.463588515	2.118433439	1.447424202
205259_at	NR3C2	nuclear receptor subfamily 3, group C, member 2	1.467163446	2.107355924	1.436347075
206417_at	CNGA1	cyclic nucleotide gated channel alpha 1	1.70138342	2.434033459	1.430620183
216675_at	---	---	1.507027141	2.096277922	1.391002102
218854_at	DSE	dermatan sulfate epimerase	1.674864403	2.262854307	1.351067168
220322_at	IL1F9	interleukin 1 family, member 9	1.555694739	2.096524951	1.347645459
201829_at	NET1	neuroepithelial cell transforming gene 1	1.712667391	2.295233611	1.340151405
204179_at	MB	myoglobin	1.560255178	2.087036743	1.337625263
209522_s_at	CRAT	carnitine acetyltransferase	1.601560169	2.127362666	1.328306427
215599_at	SMA4	glucuronidase, beta pseudogene	1.741227246	2.262741221	1.299509427
207524_at	ST7	suppression of tumorigenicity 7	1.656546384	2.152221406	1.299221939
204440_at	CD83	CD83 molecule	1.611599206	2.087208899	1.295116609
201830_s_at	NET1	neuroepithelial cell transforming gene 1	1.77960493	2.292740381	1.288342341
207117_at	ZNF117	zinc finger protein 117	1.710385586	2.201639105	1.287217995
205794_s_at	NOVA1	neuro-oncological ventral antigen 1	1.831133023	2.334518304	1.27490372
203256_at	CDH3	cadherin 3, type 1, P-cadherin (placental)	1.647307516	2.084275087	1.265261687
205525_at	CALD1	caldesmon 1	1.850246901	2.327034016	1.257688374
220999_s_at	CYFIP2	cytoplasmic FMR1 interacting protein 2	1.820547017	2.285170166	1.255210739
213367_at	LOC791120	hypothetical LOC791120	1.765722956	2.213427317	1.253553005
219033_at	PARP8	poly (ADP-ribose) polymerase family, member 8	1.841833437	2.293038535	1.24497606
215470_at	GTF2H2B	general transcription factor IIH, polypeptide 2B	1.763388065	2.183552169	1.238270924
204099_at	SMARCD3	SWI/SNF related, matrix associated, actin dependent regulator of chromatin, subfamily d, member 3	1.949021493	2.406135685	1.234535224
209281_s_at	ATP2B1	ATPase, Ca++ transporting, plasma	1.896378576	2.332843457	1.23015704

166

		membrane 1			
206556_at	CLUL1	clusterin-like 1 (retinal)	1.858592511	2.274379026	1.223710422
217049_x_at	PCDH11Y	protocadherin 11 Y-linked	1.857303263	2.271245097	1.222872506
213622_at	COL9A2	collagen, type IX, alpha 2	1.686816455	2.062699413	1.22283572
215785_s_at	CYFIP2	cytoplasmic FMR1 interacting protein 2	1.729752948	2.115133904	1.222795374
212415_at	6-Sep	septin 6	1.809872415	2.207738042	1.219830759
214823_at	ZNF204	zinc finger protein 204 pseudogene	1.664924666	2.028549068	1.218402916
221874_at	KIAA1324	KIAA1324	1.886623313	2.281900681	1.209515787
212692_s_at	LRBA	LPS-responsive vesicle trafficking, beach and anchor containing	1.676855067	2.021283942	1.205401696
214877_at	CDKAL1	CDK5 regulatory subunit associated protein 1-like 1	1.912517568	2.302430008	1.203873913

Table S5. genes with R1881 dependent increase in control cells higher than R1881 dependent fold in URI depleted cells

probe ID		up siCTRL>siURI	foldC	foldU	foldCTRL/foldURI
207103_at	KCND2	potassium voltage-gated channel, Shal-related subfamily, member 2	4.2	2.03	**2.0690**
220302_at	MAK	male germ cell-associated kinase	18.75	9.33	**2.0096**
202133_at	WWTR1	WW domain containing transcription regulator 1	5.42	3.42	**1.5848**
204582_s_at	KLK3	kallikrein-related peptidase 3	25.14	16.01	**1.5703**
206143_at	SLC26A3	solute carrier family 26, member 3	6.72	4.3	**1.5628**
206262_at	ADH1C	alcohol dehydrogenase 1C (class I), gamma polypeptide	5.66	3.67	**1.5422**
201739_at	SGK1	serum/glucocorticoid regulated kinase 1	13.23	9	**1.4700**
202363_at	SPOCK1	sparc/osteonectin, cwcv and kazal-like domains proteoglycan (testican) 1	10.91	7.5	**1.4547**
212546_s_at	FRYL	FRY-like	3.75	2.58	**1.4535**
218782_s_at	ATAD2	ATPase family, AAA domain containing 2	5.66	3.9	**1.4513**
203908_at	SLC4A4	solute carrier family 4, sodium bicarbonate cotransporter, member 4	2.93	2.07	**1.4155**
215806_x_at	TRGC2	T cell receptor gamma constant 2	22.87	16.51	**1.3852**
202643_s_at	TNFAIP3	tumor necrosis factor, alpha-induced protein 3	4.58	3.4	**1.3471**
218376_s_at	MICAL1	microtubule associated monoxygenase, calponin and LIM domain containing 1	7.51	5.65	**1.3292**
209813_x_at	TARP	TCR gamma alternate reading frame protein	20.71	16.11	**1.2855**
220116_at	KCNN2	potassium intermediate/small conductance calcium-activated channel, subfamily N, member 2	2.57	2.03	**1.2660**
221581_s_at	LAT2	linker for activation of T cells family, member 2	4.58	3.63	**1.2617**
204394_at	SLC43A1	solute carrier family 43, member 1	3.98	3.19	**1.2476**
202783_at	NNT	nicotinamide nucleotide transhydrogenase	2.62	2.11	**1.2417**

218224_at	PNMA1	paraneoplastic antigen MA1	3.87	3.13	1.2364
208195_at	TTN	titin	3.44	2.8	1.2286
207147_at	DLX2	distal-less homeobox 2	2.58	2.11	1.2227
210951_x_at	RAB27A	RAB27A, member RAS oncogene family	4.25	3.48	1.2213
210017_at	MALT1	mucosa associated lymphoid tissue lymphoma translocation gene 1	5.37	4.41	1.2177
212789_at	NCAPD3	non-SMC condensin II complex, subunit D3	10.93	9.01	1.2131
205498_at	GHR	growth hormone receptor	2.77	2.29	1.2096
219049_at	CSGALNACT1	chondroitin sulfate N-acetylgalactosaminyltransferase 1	25.6	21.2	1.2075

Table S6. genes with R1881 dependent increase in control cells lower than R1881 dependent

fold in URI depleted cells

probe ID		up siURI>siCTRL	foldC	foldU	foldURI/foldCTRL
217028_at	CXCR4	chemokine (C-X-C motif) receptor 4	2.13	5.34	2.507
220187_at	STEAP4	STEAP family member 4	6.01	14.29	2.378
210328_at	GNMT	glycine N-methyltransferase	7.29	13.78	1.890
205876_at	LIFR	leukemia inhibitory factor receptor alpha	9.75	17.54	1.799
209173_at	AGR2	anterior gradient homolog 2 (Xenopus laevis)	2.94	5.28	1.796
214087_s_at	MYBPC1	myosin binding protein C, slow type	6.18	10.58	1.712
202786_at	STK39	serine threonine kinase 39 (STE20/SPS1 homolog, yeast)	4.59	7.65	1.667
218886_at	PAK1IP1	PAK1 interacting protein 1	5.1	8.29	1.625
207030_s_at	CSRP2	cysteine and glycine-rich protein 2	2.05	3.33	1.624
211913_s_at	MERTK	c-mer proto-oncogene tyrosine kinase	3.44	5.58	1.622
37005_at	NBL1	neuroblastoma, suppression of tumorigenicity 1	2.47	3.95	1.599
205572_at	ANGPT2	angiopoietin 2	3.26	5.19	1.592
201324_at	EMP1	epithelial membrane protein 1	3.68	5.84	1.587
201650_at	JUP /// KRT19	junction plakoglobin /// keratin 19	2.93	4.52	1.543
205214_at	STK17B	serine/threonine kinase 17b	5.69	8.63	1.517
200632_s_at	NDRG1	N-myc downstream regulated gene 1	8.66	13.03	1.505
212665_at	TIPARP	TCDD-inducible poly(ADP-ribose) polymerase	2.99	4.37	1.462
205566_at	ABHD2	abhydrolase domain containing 2	3.75	5.4	1.440
217894_at	KCTD3	potassium channel tetramerisation domain containing 3	2.03	2.9	1.429
213139_at	SNAI2	snail homolog 2 (Drosophila)	25.45	36.25	1.424

217080_s_at	HOMER2	homer homolog 2 (Drosophila)	4.11	5.73	**1.394**
210260_s_at	TNFAIP8	tumor necrosis factor, alpha-induced protein 8	3.29	4.57	**1.389**
205040_at	ORM1	orosomucoid 1	20.51	28.42	**1.386**
213506_at	F2RL1	coagulation factor II (thrombin) receptor-like 1	2.6	3.6	**1.385**
205994_at	ELK4	ELK4, ETS-domain protein (SRF accessory protein 1)	2.35	3.24	**1.379**
217503_at	---	---	4.29	5.85	**1.364**
216568_x_at	---	---	2.17	2.93	**1.350**
204541_at	SEC14L2	SEC14-like 2 (S. cerevisiae)	3.01	4.06	**1.349**
220076_at	ANKH	ankylosis, progressive homolog (mouse)	2.81	3.79	**1.349**
221781_s_at	DNAJC10	DnaJ (Hsp40) homolog, subfamily C, member 10	2.18	2.94	**1.349**
201662_s_at	ACSL3	acyl-CoA synthetase long-chain family member 3	4.93	6.57	**1.333**
203030_s_at	PTPRN2	protein tyrosine phosphatase, receptor type, N polypeptide 2	2.02	2.67	**1.322**
214079_at	DHRS2	dehydrogenase/reductase (SDR family) member 2	2.28	3	**1.316**
218823_s_at	KCTD9	potassium channel tetramerisation domain containing 9	2.38	3.11	**1.307**
220018_at	CBLL1	Cas-Br-M (murine) ecotropic retroviral transforming sequence-like 1	4.27	5.54	**1.297**
208499_s_at	DNAJC3	DnaJ (Hsp40) homolog, subfamily C, member 3	2.33	3.02	**1.296**
216044_x_at	FAM69A	family with sequence similarity 69, member A	2.41	3.12	**1.295**
220816_at	LPAR3	lysophosphatidic acid receptor 3	3.37	4.36	**1.294**
220283_at	HHIPL2	HHIP-like 2	2.18	2.8	**1.284**
220342_x_at	EDEM3	ER degradation enhancer, mannosidase alpha-like 3	2.72	3.49	**1.283**
203196_at	ABCC4	ATP-binding cassette, sub-family C (CFTR/MRP), member 4	3.69	4.7	**1.274**
209309_at	AZGP1	alpha-2-glycoprotein 1, zinc-binding	4.21	5.36	**1.273**
205084_at	BCAP29	B-cell receptor-associated protein 29	2.16	2.75	**1.273**
206363_at	MAF	v-maf musculoaponeurotic fibrosarcoma oncogene homolog (avian)	7.46	9.48	**1.271**
221841_s_at	KLF4	Kruppel-like factor 4 (gut)	4.12	5.23	**1.269**
202805_s_at	ABCC1	ATP-binding cassette, sub-family C (CFTR/MRP), member 1	2.68	3.39	**1.265**
201170_s_at	BHLHB2	basic helix-loop-helix domain containing, class B, 2	2.46	3.11	**1.264**
221584_s_at	KCNMA1	potassium large conductance calcium-activated channel, subfamily M, alpha member 1	3.99	5.04	**1.263**

209286_at	CDC42EP3	CDC42 effector protein (Rho GTPase binding) 3	2.88	3.63	1.260
206351_s_at	PEX10	peroxisomal biogenesis factor 10	3.04	3.82	1.257
203827_at	WIPI1	WD repeat domain, phosphoinositide interacting 1	4.58	5.75	1.255
205261_at	PGC	progastricsin (pepsinogen C)	3.26	4.09	1.255
211549_s_at	HPGD	hydroxyprostaglandin dehydrogenase 15-(NAD)	12.26	15.34	1.251
202843_at	DNAJB9	DnaJ (Hsp40) homolog, subfamily B, member 9	3.27	4.09	1.251
217824_at	UBE2J1	ubiquitin-conjugating enzyme E2, J1 (UBC6 homolog, yeast)	2.2	2.75	1.250
214947_at	---	---	3.21	4.01	1.249
213562_s_at	SQLE	squalene epoxidase	2.14	2.67	1.248
218817_at	SPCS3	signal peptidase complex subunit 3 homolog (S. cerevisiae)	2.68	3.33	1.243
206136_at	FZD5	frizzled homolog 5 (Drosophila)	4.1	5.09	1.241
209008_x_at	KRT8	keratin 8	2.48	3.07	1.238
204298_s_at	LOX	lysyl oxidase	3	3.7	1.233
204818_at	HSD17B2	hydroxysteroid (17-beta) dehydrogenase 2	2.56	3.15	1.230
208963_x_at	FADS1 /// FADS3	fatty acid desaturase 1 /// fatty acid desaturase 3	2.01	2.46	1.224
217173_s_at	LDLR	low density lipoprotein receptor	3.12	3.81	1.221
205576_at	SERPIND1	serpin peptidase inhibitor, clade D (heparin cofactor), member 1	2	2.44	1.220
1320_at	PTPN21	protein tyrosine phosphatase, non-receptor type 21	3.55	4.33	1.220
219760_at	LIN7B	lin-7 homolog B (C. elegans)	2.61	3.18	1.218
213988_s_at	SAT1	spermidine/spermine N1-acetyltransferase 1	3.35	4.08	1.218
221693_s_at	MRPS18A	mitochondrial ribosomal protein S18A	2.51	3.05	1.215
202499_s_at	SLC2A3	solute carrier family 2 (facilitated glucose transporter), member 3	8.68	10.52	1.212
216627_s_at	B4GALT1	UDP-Gal:betaGlcNAc beta 1,4- galactosyltransferase, polypeptide 1	2.35	2.84	1.209
206857_s_at	FKBP1B	FK506 binding protein 1B, 12.6 kDa	2.71	3.26	1.203
209822_s_at	VLDLR	very low density lipoprotein receptor	3.76	4.52	1.202
205924_at	RAB3B	RAB3B, member RAS oncogene family	3.95	4.74	1.200
201625_s_at	INSIG1	insulin induced gene 1	3.2	3.84	1.200

Table S7. genes with R1881 dependent decrease in control cells higher than R1881 dependent fold in URI depleted cells

probe		DOWN siCTRL>siURI	foldC	foldU	foldCTRL/foldURI
203559_s_at	ABP1	amiloride binding protein 1 (amine oxidase (copper-containing))	0.49	0.18	2.722
215028_at	SEMA6A	sema domain, transmembrane domain (TM), and cytoplasmic domain, (semaphorin) 6A	0.38	0.23	1.652
207655_s_at	BLNK	B-cell linker	0.5	0.33	1.515
212657_s_at	IL1RN	interleukin 1 receptor antagonist	0.09	0.06	1.500
207245_at	UGT2B17	UDP glucuronosyltransferase 2 family, polypeptide B17	0.16	0.11	1.455
205433_at	BCHE	butyrylcholinesterase	0.16	0.11	1.455
209925_at	OCLN	occludin	0.37	0.26	1.423
203504_s_at	ABCA1	ATP-binding cassette, sub-family A (ABC1), member 1	0.27	0.19	1.421
203636_at	MID1	midline 1 (Opitz/BBB syndrome)	0.24	0.17	1.412
218421_at	CERK	ceramide kinase	0.31	0.22	1.409
205345_at	BARD1	BRCA1 associated RING domain 1	0.28	0.2	1.400
219389_at	SUSD4	sushi domain containing 4	0.44	0.32	1.375
222184_at	---	---	0.42	0.31	1.355
204199_at	RALGPS1	Ral GEF with PH domain and SH3 binding motif 1	0.5	0.37	1.351
221729_at	COL5A2	collagen, type V, alpha 2	0.16	0.12	1.333
207012_at	MMP16	matrix metallopeptidase 16 (membrane-inserted)	0.29	0.22	1.318
218346_s_at	SESN1	sestrin 1	0.42	0.32	1.313
207553_at	OPRK1	opioid receptor, kappa 1	0.13	0.1	1.300
210495_x_at	FN1	fibronectin 1	0.44	0.34	1.294
214156_at	MYRIP	myosin VIIA and Rab interacting protein	0.31	0.24	1.292
215596_s_at	ZNF294	zinc finger protein 294	0.23	0.18	1.278
205027_s_at	MAP3K8	mitogen-activated protein kinase kinase kinase 8	0.38	0.3	1.267
219872_at	C4orf18	chromosome 4 open reading frame 18	0.19	0.15	1.267
206464_at	BMX	BMX non-receptor tyrosine kinase	0.34	0.27	1.259
207242_s_at	GRIK1	glutamate receptor, ionotropic, kainate 1	0.39	0.31	1.258
207705_s_at	RP4-691N24.1	ninein-like	0.44	0.35	1.257
213331_s_at	NEK1	NIMA (never in mitosis gene a)-related kinase 1	0.4	0.32	1.250
222108_at	AMIGO2	adhesion molecule with Ig-like domain 2	0.1	0.08	1.250
215465_at	ABCA12	ATP-binding cassette, sub-family A (ABC1), member 12	0.2	0.16	1.250
209031_at	CADM1	cell adhesion molecule 1	0.47	0.38	1.237
205352_at	SERPINI1	serpin peptidase inhibitor, clade I (neuroserpin), member 1	0.21	0.17	1.235
203649_s_at	PLA2G2A	phospholipase A2, group IIA (platelets, synovial fluid)	0.32	0.26	1.231
210829_s_at	SSBP2	single-stranded DNA binding protein 2	0.43	0.35	1.229
207871_s_at	ST7	suppression of tumorigenicity 7	0.27	0.22	1.227

204364_s_at	REEP1	receptor accessory protein 1	0.27	0.22	**1.227**
204180_s_at	ZBTB43	zinc finger and BTB domain containing 43	0.45	0.37	**1.216**
205311_at	DDC	dopa decarboxylase (aromatic L-amino acid decarboxylase)	0.23	0.19	**1.211**
204798_at	MYB	v-myb myeloblastosis viral oncogene homolog (avian)	0.29	0.24	**1.208**
201008_s_at	TXNIP	thioredoxin interacting protein	0.35	0.29	**1.207**
219832_s_at	HOXC13	homeobox C13	0.41	0.34	**1.206**
218510_x_at	FAM134B	family with sequence similarity 134, member B	0.41	0.34	**1.206**
209409_at	GRB10	growth factor receptor-bound protein 10	0.24	0.2	**1.200**

Table S8. genes with R1881 dependent decrease in control cells lower than R1881 dependent fold in URI depleted cells

probe		down siURI>siCTRL	foldC	foldU	foldURI/foldCTRL
208116_s_at	MAN1A1	mannosidase, alpha, class 1A, member 1	0.09	0.19	**2.111**
218926_at	MYNN	myoneurin	0.11	0.18	**1.636**
219313_at	GRAMD1C	GRAM domain containing 1C	0.13	0.21	**1.615**
209735_at	ABCG2	ATP-binding cassette, sub-family G (WHITE), member 2	0.16	0.25	**1.563**
220622_at	LRRC31	leucine rich repeat containing 31	0.09	0.14	**1.556**
210002_at	GATA6	GATA binding protein 6	0.32	0.49	**1.531**
221884_at	EVI1	ecotropic viral integration site 1	0.26	0.36	**1.385**
208933_s_at	LGALS8	lectin, galactoside-binding, soluble, 8	0.24	0.33	**1.375**
220122_at	MCTP1	multiple C2 domains, transmembrane 1	0.35	0.48	**1.371**
215723_s_at	PLD1	phospholipase D1, phosphatidylcholine-specific	0.19	0.26	**1.368**
209160_at	AKR1C3	aldo-keto reductase family 1, member C3 (3-alpha hydroxysteroid dehydrogenase, type II)	0.25	0.34	**1.360**
222139_at	KIAA1466	KIAA1466 gene	0.28	0.38	**1.357**
214581_x_at	TNFRSF21	tumor necrosis factor receptor superfamily, member 21	0.31	0.42	**1.355**
218999_at	TMEM140	transmembrane protein 140	0.2	0.27	**1.350**
203518_at	LYST	lysosomal trafficking regulator	0.35	0.47	**1.343**
204790_at	SMAD7	SMAD family member 7	0.36	0.48	**1.333**
203989_x_at	F2R	coagulation factor II (thrombin) receptor	0.37	0.49	**1.324**
206204_at	GRB14	growth factor receptor-bound protein 14	0.28	0.37	**1.321**
211829_s_at	GPER	G protein-coupled estrogen receptor 1	0.28	0.37	**1.321**
219232_s_at	EGLN3	egl nine homolog 3 (C. elegans)	0.37	0.48	**1.297**
208502_s_at	PITX1	paired-like homeodomain 1	0.31	0.4	**1.290**
200618_at	LASP1	LIM and SH3 protein 1	0.38	0.49	**1.289**
203640_at	MBNL2	muscleblind-like 2 (Drosophila)	0.21	0.27	**1.286**
210993_s_at	SMAD1	SMAD family member 1	0.32	0.41	**1.281**
213489_at	MAPRE2	Microtubule-associated protein, RP/EB family, member	0.25	0.32	**1.280**

		2			
214774_x_at	TOX3	TOX high mobility group box family member 3	0.18	0.23	**1.278**
218980_at	FHOD3	formin homology 2 domain containing 3	0.3	0.38	**1.267**
204861_s_at	LOC652755 /// NAIP	similar to Baculoviral IAP repeat-containing protein 1 (Neuronal apoptosis inhibitory protein) /// NLR family, apoptosis inhibitory protein	0.31	0.39	**1.258**
211580_s_at	PIK3R3	phosphoinositide-3-kinase, regulatory subunit 3 (gamma)	0.32	0.4	**1.250**
213552_at	GLCE	glucuronic acid epimerase	0.4	0.5	**1.250**
202458_at	PRSS23	protease, serine, 23	0.28	0.35	**1.250**
218943_s_at	DDX58	DEAD (Asp-Glu-Ala-Asp) box polypeptide 58	0.37	0.46	**1.243**
203595_s_at	IFIT5	interferon-induced protein with tetratricopeptide repeats 5	0.33	0.41	**1.242**
218236_s_at	PRKD3	protein kinase D3	0.38	0.47	**1.237**
201341_at	ENC1	ectodermal-neural cortex (with BTB-like domain)	0.34	0.42	**1.235**
201811_x_at	SH3BP5	SH3-domain binding protein 5 (BTK-associated)	0.35	0.43	**1.229**
218724_s_at	TGIF2	TGFB-induced factor homeobox 2	0.41	0.5	**1.220**
205190_at	PLS1	plastin 1 (I isoform)	0.41	0.5	**1.220**
213424_at	KIAA0895	KIAA0895 protein	0.41	0.5	**1.220**
212148_at	PBX1	Pre-B-cell leukemia homeobox 1	0.14	0.17	**1.214**
202609_at	EPS8	epidermal growth factor receptor pathway substrate 8	0.25	0.3	**1.200**
203392_s_at	CTBP1	C-terminal binding protein 1	0.2	0.24	**1.200**
204493_at	BID	BH3 interacting domain death agonist	0.35	0.42	**1.200**

II. MATERIALS AND METHODS

Cell culture and stable cell lines

LNCaP cells were cultured in complete media: RPMI 1640 (Cellgro) supplemented with 10% fetal bovine serum (FBS; Hyclone) and 1% penicillin-streptomycin (Cellgro). HEK293, and PC3 cells were cultured in Dulbecco's Modification of Eagle's Medium (Cellgro), and F-12 (Ham) (Invitrogen), respectively, supplemented with 10% FBS and 1% penicillin-streptomycin. Rapamycin was purchased from Sigma-Aldrich and AKT inhibitor VIII from EMD Biosciences.

LNCaP cells or HEK293 cells stably over-expressing the FLAG-URI alpha construct (7) or an empty vector were generated by transfecting cells with pcDNA3-FLAG-URI or empty vector

pcDNA3 using Lipofectamine 2000 (Invitrogen). 48 hours post-transfection, cells stably over-expressing the construct were selected with Geneticin (500µg/ml; Invitrogen) for 15 days.

LNCaP and PC3 cells that are doxycycline-inducible for reduced expression of URI were generated with lentiviral pTRIPZ shRNA against URI (Open Biosystems, RHS4696-99683127) or a control shRNA (Open Biosystems, RHS4743). After infection, cells were selected for 10 days with 1 µg/ml puromycin (Sigma-Aldrich). In addition, stable cell line pools were screened for inducible knockdown of URI using 1µg/ml doxycycline (Sigma-Aldrich).

Immunohistochemistry, immunoblot, and immunoprecipitation

Human prostate samples were obtained from J. Melamed, NYU School of Medicine. Tissue sections were stained as previously described [82] using antibodies against Art-27 (1:250) (previously described in [82], URI (rabbit polyclonal antibody from Dr. N. Djouder, 1:1000), and AR (N-20, Santa Cruz Biotechnology, 1:500).

For immunoblot analysis, cells were lysed in Triton buffer (50mM Hepes pH7.5, 150 mM NaCl, 1mM EDTA, 1mM EGTA, 10% glycerol, 1% triton X-100, 10mM NaF, 25µM $ZnCl_2$) and supplemented with 1mM PMSF, 1mM $NaVO_4$, 10mg/ml of leupeptin and 10mg/ml of aprotinin. Protein lysates were quantified using BioRad Protein Assay Dye and normalized for total protein concentration. Total protein was subjected to SDS-PAGE and immunoblotted with the following antibodies against: Art-27 previously described in (22); AR #441 and ERK-1 (Santa Cruz Biotechnology); tubulin (Covance); hsp90 (BD Biosciences); p70S6 kinase (total), phosphorylated p70S6 kinase threonine 389, AKT (total), and phosphorylated AKT serine 473 (Cell Signaling); Brg1 (H-88, Santa Cruz); histone H3 antibody (96C100, Cell Signaling); POLR2E (RPB5, AbCam); and URI (A301-164A-1; Bethyl). Protein bands were visualized using ECL Western Blotting detection reagents (GE Healthcare). Protein expression levels were quantified using ImageJ 1.42q software (National Institutes of Health).

In immunoprecipitation experiments cells were lysed as described above. Primary antibodies were added to 1.5mg of total protein and incubated overnight at 4ºC followed by the addition of Protein A/G agarose beads (Santa Cruz Biotechnology) for 2 hours. For immunoprecipitation of URI, an antibody purchased from Abnova (H00008725-A01) was used. Immune complexes were extensively washed with Triton buffer and solubilized using Laemmli sample buffer (BioRad). Normal mouse IgG (Santa Cruz Biotechnology) or normal rabbit sera (Sigma-Aldrich) were used as controls.

Subcloning of the URI deletions

All the URI deletions and truncations were generated using a pcDNA3-flag-URI construct previously used in (82). Deletions were generated by PCR using specific primers with flanking XhoI restriction sequences. Therefore URI deletions have a unique XhoI restriction site in the point of deletion. Truncations were also generated by PCR using specific primers with XbaI restriction sequence. XbaI was chosen because it was a unique restriction site present just downstream of the URI STOP codon. The flag tag was maintained in all the deletions and truncations. The generated truncations of wild type URI are the following: URIΔ150 is a URI deleted of aa 151-535 and maintaining just the prefoldin-like domain, URIΔ270 is a URI deleted of aa 271-535 that maintains the prefoldin-like and the RPB5 binding domain, URIΔ340 is a URI deleted of aa 341-535 that maintains the prefoldin-like domain, the RPB5 binding domain and the asparagin rich domain. The generated deletions are the following: URIΔprefoldin is a URI deleted of aa 11-153 encompassing the entire prefoldin-like domain, URIΔhook is a URI deleted of aa 85-100 encoding 2 of the 4 beta strands of the prefoldin-like domain, URIΔRPB5 is a URI deleted of aa 177-224 encompassing the essential domain for the binding of RPB5. All constructs were confirmed by sequencing.

Nuclear-cytoplasmic fractionation

For the isolation of cytoplasmic and nuclear fractions cells were scraped in PBS and resuspended in one packed cell volume of hypotonic 1X Buffer A (10X Buffer A: 100 mM Hepes, 15 mM MgCl2, 100 mM KCl; solution pH 7.9). Cells were left swelling in buffer A for 15 minues on ice and then passed through a 23-26 gauge syringe needle. The solution was then centrifuged at 17,000xg for 6 minutes at 4°C. The supernatant (cytoplasmic fraction) was spun again at 17,000xg for 15 minutes while the pellet was resuspended in one pellet volume of Buffer B (10 mM Hepes, 25% glycerol, 420 mM NaCl, 1.5 mM MgCl2, 0.2 mM EDTA; solution pH 7.9). Nuclei solution was incubated for 30 minutes on ice while stirring and then spun at 17,000xg for 6 minutes. The supernatant (nuclear extract) was collected and the salt concentration adjusted to 300mM using HEMG0 buffer (25mM Hepes, 12.5 mM MgCl2, 10% glycerol, 1 mM EDTA). Triton X-100 was added to a final concentration of 1% and, after 30 minutes incubation on ice, the solution was centrifuged at 17,000xg for 15 minutes. The supernatant was then used for immunoprecipitation experiments.

Immunoprecipitation and mass spectrometry analysis

15X108 LNCaP-vector and LNCaP-flagURI cells were used to isolate nuclear extracts as described above. Flag-URI was immuno-precipitated from the nuclear extracts using FLAG-conjugated agarose beads (SIGMA A2220). After 4 hours incubation with the samples, the beads were washed 3 times in HEMG300 (HEMG buffer with 300mM KCl), 3 times in HEMG150 (HEMG buffer with 150mM KCl) and twice in TBS. After the last wash beads were resuspended in 35 µl of TBS and 3µl of 3XFLAG peptide 5mg/ml (SIGMA F4799) were added. The solutions were incubated for 1 hour at 4°C tapping the tubes every 10 minutes to resuspend the beads. The supernatant containing the URI interacting proteins was collected and proteins precipitated with Trichloroacetic acid (TCA).

Phosphatase assay

PP2A phosphatase assay was performed using a kit (Millipore cat. number 17-313) and following the protocol provided by the company. Briefly, PP2A, PP1α, PP1β and URI were immunoprecipitated from total lysate or nuclear extract using specific antibodies. Protein A/G beads were added to the solutions and after one hour beads were washed 5 times in Triton buffer (50mMHEPES [pH 7.5], 150 mM NaCl, 1 mM EDTA, 1 mM EGTA, 10% glycerol, 1% Triton X-100, 10 mM NaF, 25 M ZnCl2) and twice in phosphatase buffer (50mM Tris-HCl, pH 7.0, 100µM CaCl2). Beads were then resuspended in 60µl of phosphopeptide (K-R-pT-I-R-R) solution 1mM. The beads/peptide solutions were then incubated at 30ºC for 10 minutes and 25 µl of supernatant was mixed with 100 µl of malachite green detection solution. After 10 minutes incubation at room temperature the absorbance of the solution at $\lambda=650nm$ was read.

Luciferase assay

HEK293 cells were seeded in a 24-well plate at a density of $1x10^5$ cells per well. Cells were transfected with 0.2 µg ARR3 luciferase reporter, 0.05µg of AR and increasing concentration of pcDNA3-URI (0.05 µg, 0.1 µg or 0.2µg), and pCDNA3 (vector only) up to a total of 0.5 µg of DNA. Transfection was achieved using Lipofectamine reagent (Invitrogen). After transfection, the cells were allowed to recover in phenol red-free DMEM media supplemented with 10% charcoal stripped FBS (CFBS). 24 hours post-transfection, cells were treated with or without 10nM R1881 (Perkin Elmer) for an additional 24 hours. Following treatment, cells were lysed in 1X Reporter Lysis buffer (Promega). Luciferase activity was quantified in a reaction mixture containing 25mM glycine pH 7.8, 10mM MgSO4, 1mM ATP, 0.1mg/ml BSA, 1mM

dithiothreitol, and 1mM D-luciferin (BD Biosciences) using a Lumat LB luminometer. Luciferase activity was normalized for protein content as calculated by BioRad Protein Assay.

Chromatin immunoprecipitation (ChIP) assay

ChIP was performed as previously described [82] with minor differences. Briefly, LNCaP cells stably expressing a non-silencing shRNA (LNCaP-shNS) or an shRNA against URI (LNCaP-shURI) were grown in complete media for 2 days in the presence of 1µg/ml doxycycline to induce the expression of the shRNA. Proteins were double cross-linked with DSP (Pierce) for 20 minutes and 1% formalin for 10 minutes. Cells were lysed, nuclei collected and lysed in sonication buffer (1% SDS, 10mM EDTA, 50mM Tris-HCl pH8.0), and sonicationed for 12 minutes (30 sec. on, 30 sec. off) in a Bioruptor sonicator (Diagenode, model XL). Sonicated lysates were pre-cleared for 2 hours with Protein A/G agarose beads blocked with salmon sperm DNA (Millipore). Supernatants were then incubated overnight with a mixture of 2µg AR (441) and 2µg AR (N20), 5µg of Art-27(22), or 4µg of polymerase II (4H8, CTD repeat antibody-ChIP grade from Abcam). Control ChIP was performed with normal mouse IgG and normal rabbit IgG sera. Immunocomplexes were then washed and cross-linking reversed. DNA was isolated with the Qiagen PCR purification kit and quantitative-PCR (Q-PCR) was performed using 1-5µl of DNA. Relative enrichment was calculated as a percentage of 4% input normalized to IgG. ChIP primers used for NKX3.1 transcription start site (TSS) and UPS have been previously described [82]. ChIP primers used for the NKX3.1 3' UTR AREs have been previously described [82]. The primers used in figure 10 are reported: P1F-TGCACTTCTAGGGCACATTG, P1R-GGATGCATGACTGTTTTTGG, P2F-GCTGTGCAAACATCATAGAGC, P2R-AGGAGCAATAGGGCATACCA, P2.5F-CTGATCAAACGTCACGATGC, P2.5R-GAGGAACAGCTGCTCTCATACA, P3F-GGCAGGACATCAAAATCACA, P3R-GCTTGTGTTTCCATCCCTCTA, P4F-

GTCTCAGCACTTTGGGTGGT, P4R-AGTGCAGTGGAGAGATCATGG, P4.5F-TGTCTTTGGAGGACACTGGA, P4.5R-TTGGCAAAGCTGGTTTTCTT, P5F-AGCCGTCTTAGACCAGGACA, P5R-TAGATCCCACGCCATAAAGC, P6F-CAGTCACAGTACCGGTTGGA, P6R-TTTTAGGCCAGGACAAATGC, P7F-CCCCTGTAATTGGCTCTGAC, P7R-TGGGACGATCAAGACAAACA, P8F-ATCCCCAGGAGCTTCTCTCT, P8R-TAGGGGATTCCTTCCCCAGT, G1(TSS)F-GTCCTTCCTCATCCAGGACA, G1(TSS)R-CTGTCTCTGGCTGCTCGTG, I1F-GTGACAAAGCAGGGGTTGAC, I1R-CTTTACTGCCCACGGGATT, I2F-TCCGGAGAGCTCCTTAGTCA, I2R-GAACAAACAGCCCACTGTCA, G2F-CCGCAGAAGCGCTCCCGAGCT, G2R-CGAGGAGAGCTGCTTTCGCTT, U1F-AGGGGAGAGAGGGAAAATCA, U1R-ACACAGGAGGATGGAGTTGC, U2(AREI UTR)F-GATGGGTGGGAGGAGATGA, U2(AREI UTR)R-TGTCTTGGACAAGCGGAG, U3F-AGCCCGAGATCTGGTCTTTT, U3R-CAGAATCTGCCCCCAAACT, U4(AREII UTR)F-GGTTCTGCTGTTACGTTTG, U4(AREII UTR)R-CTTGCTTGCTCAGTGGAC, U5F-AACCATTTCACCCAGACAGC, U5R-CAGATTGGAGCAGGGTTTGT, UPSF-GGAGACCATTGCATGAACCT, UPSR-AGAGCTGAGGGCTCTGAGTG.

Consecutive siRNA transient transfection

siGENOME SMARTpool siRNAs against URI or Art-27 and control siRNA were purchased from Dharmacon. 1.2×10^6 cells were plated in 6 cm plates and transfected for 4 hours with siRNAs and Lipofectamine 2000 on 2 consecutive days with an overnight recovery in media supplemented with 10% CFBS in between the 1st and 2nd transfection and after the 2nd transfection. Recovery in media supplemented with 10% FBS was done for the experiment shown in figure 6a. 48 hours after the first transfection, cells were treated according to the specific conditions described in the text.

179

For LAPC4 a reverse transfection was used. A total of 3×10^6 trypsinized cells were mixed with 12µl of HiPerFect reagent (QIAGEN) and 5.4µl of 50µM siRNA. The cells/RNA mixtures were plated in 3.5 diameter dishes in 1ml of media. The next day 1ml of fresh media containing a 2X concentration of doxorubicin (2µM) was added to the plates.

Q-PCR

Total RNA was isolated using the RNeasy kit (Qiagen, Inc.). Total RNA was reverse transcribed at 55ºC for 1 h using Superscript III reverse transcriptase and oligo- (dT) 20 primers (Invitrogen). Real-time PCR was performed using gene-specific primers (previously described in [80]) and 2X SYBR green Taq-ready mix (Sigma-Aldrich). Data were analyzed by the ΔΔCT method using RPL19 as a control gene and normalized to control samples, which were arbitrarily set to 1.

Microarray analysis

URI was depleted in LNCaP cells using consecutive transient transfection of a control siRNA or URI directed siRNA, as described above. 48 hours after the first transfection, cells were treated with or without 10nM R1881 for 24 hours. Total RNA was then isolated using the RNeasy kit (Qiagen, Inc.). Hybridization and analysis was performed at the Memorial Sloan-Kettering genomics core facility using the Affymetrix one-cycle protocol and HG_U133A 2.0 gene chips (Affymetrix). Androgen-regulated genes were determined using the RMAExpress software and the MeV multiexperiment viewer v4.2 for statistical analysis. A two-fold change threshold was used and the NetAffx online tool was used to compare regulated genes in the Art-27 and URI knock down experiments. Principle component analysis (PCA) was performed using Agilent Genespring GX10 software. PCA was performed for all experimental conditions with unfiltered gene contents. The three principal components representing the greatest

variance in expression were plotted in a three-dimensional gene expression space to visualize the general relationship among the different samples.

Soft agar assay and neutral red growth assay

8.5X103 cells were resuspended in 1ml of 0.35% agar and layered on top of a previously prepared, solid layer of 0.7 % agarose (3ml) in a 6 cm plate. Complete media with or without 1μg/ml doxycycline or with or without bicalutamide (Sigma-Aldrich) was added on top of the upper layer. Media was changed every 2 days and after 14-15 days images of the colonies were taken using an inverted broad field fluorescence microscope (Nikon Eclipse TE2000-E). Colonies in 10 random fields were counted and colony area was measured using ImageJ software. Statistical significance was calculated using the Wilcoxon signed-rank test. The neutral red growth assay was performed by plating $5x10^5$ cells in 24 well plates. Neutral red dye was added directly to the media to obtain a 2% final concentration. After 1 hour cells were washed in PBS and the dye extracted with lysis buffer (Tris 50mM pH 7.4, NaCl 150mM, DTT 5mM, 1% Triton X-100, acetic acid 1%). The absorbance of the solution at λ=540nm was then measured.

Biochemical fractionation

Biochemical fractionation for the isolation of the chromatin-insoluble fraction P3 was performed as described in [82]. Briefly, nuclei were lysed in a hypotonic buffer and centrifuged to separate the nuclear soluble (S3), insoluble and chromatin enriched (P3) fractions. The P3 fraction was treated with 5U of MNase and incubated at 37°C for the indicated time. The reaction was stopped with the addition of EGTA, centrifuged at 1,700 x g for 5 minutes, and Laemmli buffer added to the supernatant.

181

Oil-red-O staining

0.5×10^5 LNCaP-shRNA cells per well were plated in 24 well plates. After 5 days of culture in doxycycline $1\mu g/ml$ complete media cells were prefixed adding $100\mu l$ of 11X formalin solution (50mM Hepes pH 8.0, 1mM EDTA, 100mM NaCl, 11% formalin) directly to the media (1ml). After 10 minutes of pre-fixation a 10% formalin solution in PBS was added to the cells for an additional hour. After 1 hour the formalin was removed, cells were washed with $300\mu l$ of distilled H_2O and wells were then dried at room temperature to ensure that all the water was completely removed. $300\mu l$ of 60% isopropanol was then added to each well for 5 minutes. Isopropanol was removed and wells were again left to dry at room temperature. Cells were then stained for 15' with oil-red solution (3 parts of 0.3% oil red in isopropanol and 2 parts of distilled water. The solution was left unmoved for 20 minutes and then filtered with Wattman paper). Cells were thoroughly washed with tap water and the plates were then dried at room temperature. Oil-red dye was then extracted for 15' with $200\mu l$ of isopropanol and the absorbance of this solution was then measured at $\lambda=500nm$. The absorbance is normalized for the DNA content of each well proportional to the number of cells. The number of cells was quantified in a replicate plate as described. The media was removed and cells were frozen at -80ºC for 30'. Cells were then thawed at room temperature and $400\mu l$ of H_2O were added to each well. Plates were incubated at 37ºC for 1 hour and then cells were frozen again at -80ºC and thawed at room temperature. $100\mu l$ of Hoechst 33258 0.1mg/ml in TNE (100mM Tris, 2M NaCl, 10mM EDTA; final solution pHed at 7.4) were added to each well and the fluorescence measured (excitation=360nm, emission=460nm).

λ-phosphatase assay

The lambda phosphatase assay was carried out as previously described [82]. Briefly cells were lysed in PL buffer (50mM Tris-HCl pH7.5, 0.1mM EDTA, 5mM DTT, 250mM NaCl, 0.5% NP40) supplemented with protease inhibitors, and 200µg of protein was used for the λ-phosphatase assay. The reaction was carried out in λ-phosphatase buffer in the presence of MnCl2 and 400U of λ-phosphatase enzyme (BioLabs). The reaction mix (50µl total volume) was incubated for 5 minutes at 30ºC and then terminated by adding 6X Laemmli buffer and boiled for 10 minutes at 95ºC.

REFERENCES

1. Tronnersjo, S., et al., *The jmjN and jmjC domains of the yeast zinc finger protein Gis1 interact with 19 proteins involved in transcription, sumoylation and DNA repair.* Molecular genetics and genomics : MGG, 2007. **277**(1): p. 57-70.

2. Siegel, R., D. Naishadham, and A. Jemal, *Cancer Statistics, 2012.* Ca-a Cancer Journal for Clinicians, 2012. **62**(1): p. 10-29.

3. Shen, M.M. and C. Abate-Shen, *Molecular genetics of prostate cancer: new prospects for old challenges.* Genes & Development, 2010. **24**(18): p. 1967-2000.

4. O'Rourke, M.E., *The Prostate-Specific Antigen Screening Conundrum: Examining the Evidence.* Seminars in Oncology Nursing, 2011. **27**(4): p. 9.

5. Epstein, J.I., *An Update of the Gleason Grading System.* Journal of Urology, 2010. **183**(2): p. 433-440.

6. Mahon, K.L., et al., *Pathways of chemotherapy resistance in castration-resistant prostate cancer.* Endocrine-Related Cancer, 2011. **18**(4): p. R103-R123.

7. Bostwick, D.G., *Prostatic Intraepithelial Neoplasia (Pin).* Urology, 1989. **34**(6): p. 16-22.

184

8.   Tomlins, S.A., et al., *Recurrent fusion of TMPRSS2 and ETS transcription factor genes in prostate cancer.* Science, 2005. **310**(5748): p. 644-8.

9.   Shaffer, D.R. and P.P. Pandolfi, *Breaking the rules of cancer.* Nature Medicine, 2006. **12**(1): p. 14-15.

10.   Gasi, D. and J. Trapman, *Androgen regulation of ETS gene fusion transcripts in prostate cancer.* Methods in molecular biology, 2011. **776**: p. 335-48.

11.   Bastus, N.C., et al., *Androgen-induced TMPRSS2:ERG fusion in nonmalignant prostate epithelial cells.* Cancer Research, 2010. **70**(23): p. 9544-8.

12.   Mani, R.S., et al., *Induced chromosomal proximity and gene fusions in prostate cancer.* Science, 2009. **326**(5957): p. 1230.

13.   Lin, C., et al., *Nuclear receptor-induced chromosomal proximity and DNA breaks underlie specific translocations in cancer.* Cell, 2009. **139**(6): p. 1069-83.

14.   Boeke, K.A.O.D.a.J.D., *Mighty Piwis Defend the Germline against Genome Intruders.* Cell, 2007. **129**(1): p. 8.

15.   Malone, C.D., et al., *Specialized piRNA pathways act in germline and somatic tissues of the Drosophila ovary.* Cell, 2009. **137**(3): p. 522-35.

16.   Tomlins, S.A., et al., *Role of the TMPRSS2-ERG gene fusion in prostate cancer.* Neoplasia, 2008. **10**(2): p. 177-88.

17.   Clark, J.P. and C.S. Cooper, *ETS gene fusions in prostate cancer.* Nature reviews. Urology, 2009. **6**(8): p. 429-39.

18.   Mertz, K.D., et al., *Molecular characterization of TMPRSS2-ERG gene fusion in the NCI-H660 prostate cancer cell line: a new perspective for an old model.* Neoplasia, 2007. **9**(3): p. 200-6.

19.   Massie, C.E., et al., *New androgen receptor genomic targets show an interaction with the ETS1 transcription factor.* EMBO reports, 2007. **8**(9): p. 871-8.

20.   Grignon, D.J., *Unusual subtypes of prostate cancer.* Modern Pathology, 2004. **17**(3): p. 316-327.

21.   Schalken, J.A. and G. Van Leenders, *Cellular and molecular biology of the prostate: Stem cell biology.* Urology, 2003. **62**(5A): p. 11-20.

22.   Komiya, A., et al., *Neuroendocrine differentiation in the progression of prostate cancer.* International Journal of Urology, 2009. **16**(1): p. 37-44.

23.   Yuan, T.C., S. Veeramani, and M.F. Lin, *Neuroendocrine-like prostate cancer cells: neuroendocrine transdifferentiation of prostate adenocarcinoma cells.* Endocrine-Related Cancer, 2007. **14**(3): p. 531-47.

24.   Aihara, M., et al., *Heterogeneity of prostate cancer in radical prostatectomy specimens.* Urology, 1994. **43**(1): p. 60-6; discussion 66-7.

25.   Liu, W., et al., *Copy number analysis indicates monoclonal origin of lethal metastatic prostate cancer.* Nature Medicine, 2009. **15**(5): p. 559-65.

26.   Bonkhoff, H. and R. Berges, *From Pathogenesis to Prevention of Castration Resistant Prostate Cancer.* Prostate, 2010. **70**(1): p. 100-112.

27.   Centenera, M.M., et al., *The Contribution of Different Androgen Receptor Domains to Receptor Dimerization and Signaling.* Molecular Endocrinology, 2008. **22**(11): p. 2373-2382.

28.   Nahleh, Z., *Functional and structural analysis of androgen receptors for anti-cancer drug discovery.* Cancer Therapy, 2008. **6**: p. 6.

29.   Heery, D.M., et al., *A signature motif in transcriptional co-activators mediates binding to nuclear receptor.* Nature, 1997. **387**(6634): p. 733-736.

30.   Heinlein, C.A. and C.S. Chang, *Androgen receptor (AR) coregulators: An overview.* Endocrine Reviews, 2002. **23**(2): p. 175-200.

31.   Wang, L., C.L. Hsu, and C.S. Chang, *Androgen receptor corepressors: An overview.* Prostate, 2005. **63**(2): p. 117-130.

32.   Hsu, C.L., et al., *Androgen receptor (AR) NH2- and COOH-terminal interactions result in the differential influences on the AR-mediated transactivation and cell growth.* Molecular Endocrinology, 2005. **19**(2): p. 350-361.

33.   Trepel, J., et al., *Targeting the dynamic HSP90 complex in cancer.* Nature Reviews Cancer, 2010. **10**(8): p. 537-549.

34.   Jenster, G., J. Trapman, and A.O. Brinkmann, *Nuclear Import of the Human Androgen Receptor.* Biochemical Journal, 1993. **293**: p. 761-768.

35.   van de Wijngaart, D.J., et al., *Androgen receptor coregulators: Recruitment via the coactivator binding groove.* Molecular and cellular endocrinology, 2012. **352**(1-2): p. 57-69.

36.   Zaret, K.S. and J.S. Carroll, *Pioneer transcription factors: establishing competence for gene expression.* Genes & Development, 2011. **25**(21): p. 2227-2241.

37.   Wang, Q.B., et al., *Androgen Receptor Regulates a Distinct Transcription Program in Androgen-Independent Prostate Cancer.* Cell, 2009. **138**(2): p. 245-256.

38.   Wang, D., et al., *Reprogramming transcription by distinct classes of enhancers functionally defined by eRNA.* Nature, 2011. **474**(7351): p. 390-+.

39.   Sahu, B., et al., *Dual role of FoxA1 in androgen receptor binding to chromatin, androgen signalling and prostate cancer.* Embo Journal, 2011. **30**(19): p. 3962-3976.

40.   Wu, C.T., et al., *Increased prostate cell proliferation and loss of cell differentiation in mice lacking prostate epithelial androgen receptor (vol 104, pg 12679, 2007).* Proceedings of the National Academy of Sciences of the United States of America, 2007. **104**(43): p. 17240-17240.

41.   Niu, Y.J., et al., *Androgen receptor is a tumor suppressor and proliferator in prostate cancer.* Proceedings of the National Academy of Sciences of the United States of America, 2008. **105**(34): p. 12182-12187.

42.   Bai, V.U., et al., *Androgen receptor regulates Cdc6 in synchronized LNCaP cells progressing from G(1) to S phase.* Journal of Cellular Physiology, 2005. **204**(2): p. 381-387.

43.   Litvinov, I.V., et al., *Androgen receptor as a licensing factor for DNA replication in androgen-sensitive prostate cancer cells.* Proceedings of the National Academy of Sciences of the United States of America, 2006. **103**(41): p. 15085-15090.

44.   Vander Griend, D.J., I.V. Litvinov, and J.T. Isaacs, *Stabilizing androgen receptor in mitosis inhibits prostate cancer proliferation.* Cell Cycle, 2007. **6**(6): p. 647-651.

45.   Watson, P.A., et al., *Context-dependent hormone-refractory progression revealed through characterization of a novel murine prostate cancer cell line.* Cancer Research, 2005. **65**(24): p. 11565-11571.

46.   Gao, J., J.T. Arnold, and J.T. Isaacs, *Conversion from a paracrine to an autocrine mechanism of androgen-stimulated growth during malignant transformation of prostatic epithelial cells.* Cancer Research, 2001. **61**(13): p. 5038-5044.

47.   Pritchard, C.C. and P.S. Nelson, *Gene expression profiling in the developing prostate.* Differentiation, 2008. **76**(6): p. 624-640.

48.   Zhang, Y.Y., et al., *Role of epithelial cell fibroblast growth factor receptor substrate 2 alpha in prostate development, regeneration and tumorigenesis.* Development, 2008. **135**(4): p. 775-784.

49.   Prins, G.S. and O. Putz, *Molecular signaling pathways that regulate prostate gland development.* Differentiation, 2008. **76**(6): p. 641-659.

50.   Feldman, B.J. and D. Feldman, *The development of androgen-independent prostate cancer.* Nature reviews. Cancer, 2001. **1**(1): p. 34-45.

51.   Locke, J.A., et al., *Androgen levels increase by intratumoral de novo steroidogenesis during progression of castration-resistant prostate cancer.* Cancer Research, 2008. **68**(15): p. 6407-15.

52. Linja, M.J., et al., *Amplification and overexpression of androgen receptor gene in hormone-refractory prostate cancer.* Cancer Research, 2001. **61**(9): p. 3550-5.

53. Zhao, X.Y., et al., *Glucocorticoids can promote androgen-independent growth of prostate cancer cells through a mutated androgen receptor.* Nature Medicine, 2000. **6**(6): p. 703-6.

54. Taplin, M.E. and S.P. Balk, *Androgen receptor: a key molecule in the progression of prostate cancer to hormone independence.* Journal of cellular biochemistry, 2004. **91**(3): p. 483-90.

55. Li, Y., et al., *Intragenic rearrangement and altered RNA splicing of the androgen receptor in a cell-based model of prostate cancer progression.* Cancer Research, 2011. **71**(6): p. 2108-17.

56. Li, Y., et al., *AR intragenic deletions linked to androgen receptor splice variant expression and activity in models of prostate cancer progression.* Oncogene, 2012.

57. Hu, R., et al., *Ligand-independent androgen receptor variants derived from splicing of cryptic exons signify hormone-refractory prostate cancer.* Cancer Research, 2009. **69**(1): p. 16-22.

58. Gao, H., et al., *Combinatorial activities of Akt and B-Raf/Erk signaling in a mouse model of androgen-independent prostate cancer.* Proceedings of the National Academy of Sciences of the United States of America, 2006. **103**(39): p. 14477-82.

59.   Zhu, P., et al., *Macrophage/cancer cell interactions mediate hormone resistance by a nuclear receptor derepression pathway.* Cell, 2006. **124**(3): p. 615-29.

60.   Chang, C.Y. and D.P. McDonnell, *Androgen receptor-cofactor interactions as targets for new drug discovery.* Trends in pharmacological sciences, 2005. **26**(5): p. 225-8.

61.   Heery, D.M., et al., *A signature motif in transcriptional co-activators mediates binding to nuclear receptors.* Nature, 1997. **387**(6634): p. 733-6.

62.   Wolf, I.M., et al., *Coactivators and nuclear receptor transactivation.* Journal of cellular biochemistry, 2008. **104**(5): p. 1580-6.

63.   He, B., J.A. Kemppainen, and E.M. Wilson, *FXXLF and WXXLF sequences mediate the NH2-terminal interaction with the ligand binding domain of the androgen receptor.* The Journal of biological chemistry, 2000. **275**(30): p. 22986-94.

64.   Buchanan, G., et al., *Corepressor effect on androgen receptor activity varies with the length of the CAG encoded polyglutamine repeat and is dependent on receptor/corepressor ratio in prostate cancer cells.* Molecular and cellular endocrinology, 2011. **342**(1-2): p. 20-31.

65.   Belakavadi, M., et al., *MED1 phosphorylation promotes its association with mediator: implications for nuclear receptor signaling.* Molecular and cellular biology, 2008. **28**(12): p. 3932-42.

66.   Jin, F., F. Claessens, and J.D. Fondell, *Regulation of androgen receptor-dependent transcription by coactivator MED1 is mediated through a newly discovered noncanonical binding motif.* The Journal of biological chemistry, 2012. **287**(2): p. 858-70.

67.   Pandey, P.K., et al., *Activation of TRAP/mediator subunit TRAP220/Med1 is regulated by mitogen-activated protein kinase-dependent phosphorylation.* Molecular and cellular biology, 2005. **25**(24): p. 10695-710.

68.   Chen, Z., et al., *Phospho-MED1-enhanced UBE2C locus looping drives castration-resistant prostate cancer growth.* The EMBO journal, 2011. **30**(12): p. 2405-19.

69.   Wu, D., et al., *Androgen receptor-driven chromatin looping in prostate cancer.* Trends in endocrinology and metabolism: TEM, 2011. **22**(12): p. 474-80.

70.   Wang, Q., J.S. Carroll, and M. Brown, *Spatial and temporal recruitment of androgen receptor and its coactivators involves chromosomal looping and polymerase tracking.* Molecular cell, 2005. **19**(5): p. 631-42.

71.   Lee, D.K., H.O. Duan, and C. Chang, *Androgen receptor interacts with the positive elongation factor P-TEFb and enhances the efficiency of transcriptional elongation.* The Journal of biological chemistry, 2001. **276**(13): p. 9978-84.

72.   Pascual-Le Tallec, L. and M. Lombes, *The mineralocorticoid receptor: a journey exploring its diversity and specificity of action.* Molecular Endocrinology, 2005. **19**(9): p. 2211-21.

73. Aiyar, S.E., et al., *Attenuation of estrogen receptor alpha-mediated transcription through estrogen-stimulated recruitment of a negative elongation factor.* Genes & Development, 2004. **18**(17): p. 2134-46.

74. Perissi, V., et al., *Deconstructing repression: evolving models of co-repressor action.* Nature reviews. Genetics, 2010. **11**(2): p. 109-23.

75. Wang, Z., et al., *Genome-wide mapping of HATs and HDACs reveals distinct functions in active and inactive genes.* Cell, 2009. **138**(5): p. 1019-31.

76. Perissi, V., et al., *A corepressor/coactivator exchange complex required for transcriptional activation by nuclear receptors and other regulated transcription factors.* Cell, 2004. **116**(4): p. 511-26.

77. Markus, S.M., et al., *Identification and characterization of ART-27, a novel coactivator for the androgen receptor N terminus.* Molecular biology of the cell, 2002. **13**(2): p. 670-82.

78. Nwachukwu, J.C., et al., *Genome-wide impact of androgen receptor trapped clone-27 loss on androgen-regulated transcription in prostate cancer cells.* Cancer Research, 2009. **69**(7): p. 3140-7.

79. Taneja, S.S., et al., *ART-27, an androgen receptor coactivator regulated in prostate development and cancer.* The Journal of biological chemistry, 2004. **279**(14): p. 13944-52.

80. Nwachukwu, J.C., et al., *Transcriptional regulation of the androgen receptor cofactor androgen receptor trapped clone-27.* Molecular Endocrinology, 2007. **21**(12): p. 2864-76.

81. Weinmann, A.S., et al., *Isolating human transcription factor targets by coupling chromatin immunoprecipitation and CpG island microarray analysis.* Genes & Development, 2002. **16**(2): p. 235-44.

82. Mita, P., et al., *Regulation of androgen receptor-mediated transcription by RPB5 binding protein URI/RMP.* Molecular and cellular biology, 2011. **31**(17): p. 3639-52.

83. Li, W., et al., *Androgen receptor mutations identified in prostate cancer and androgen insensitivity syndrome display aberrant ART-27 coactivator function.* Molecular Endocrinology, 2005. **19**(9): p. 2273-82.

84. Gstaiger, M., et al., *Control of nutrient-sensitive transcription programs by the unconventional prefoldin URI.* Science, 2003. **302**(5648): p. 1208-12.

85. Cloutier, P., et al., *High-resolution mapping of the protein interaction network for the human transcription machinery and affinity purification of RNA polymerase II-associated complexes.* Methods, 2009. **48**(4): p. 381-6.

86. Jeronimo, C., et al., *Systematic analysis of the protein interaction network for the human transcription machinery reveals the identity of the 7SK capping enzyme.* Molecular cell, 2007. **27**(2): p. 262-74.

87. Boulon, S., et al., *HSP90 and its R2TP/Prefoldin-like cochaperone are involved in the cytoplasmic assembly of RNA polymerase II.* Molecular cell, 2010. **39**(6): p. 912-24.

88. Sun, S., et al., *UXT is a novel and essential cofactor in the NF-kappaB transcriptional enhanceosome.* The Journal of cell biology, 2007. **178**(2): p. 231-44.

89. Huang, Y., et al., *UXT-V1 facilitates the formation of MAVS antiviral signalosome on mitochondria.* Journal of immunology, 2012. **188**(1): p. 358-66.

90. McGilvray, R., M. Walker, and C. Bartholomew, *UXT interacts with the transcriptional repressor protein EVI1 and suppresses cell transformation.* The FEBS journal, 2007. **274**(15): p. 3960-71.

91. Enunlu, I., M. Ozansoy, and A.N. Basak, *Alfa-class prefoldin protein UXT is a novel interacting partner of Amyotrophic Lateral Sclerosis 2 (Als2) protein.* Biochemical and biophysical research communications, 2011. **413**(3): p. 471-5.

92. Zhao, H., et al., *UXT is a novel centrosomal protein essential for cell viability.* Molecular biology of the cell, 2005. **16**(12): p. 5857-65.

93. Van Leuven, F., et al., *Molecular cloning of a gene on chromosome 19q12 coding for a novel intracellular protein: analysis of expression in human and mouse tissues and in human tumor cells, particularly Reed-Sternberg cells in Hodgkin disease.* Genomics, 1998. **54**(3): p. 511-20.

94.   Dorjsuren, D., et al., *RMP, a novel RNA polymerase II subunit 5-interacting protein, counteracts transactivation by hepatitis B virus X protein.* Molecular and cellular biology, 1998. **18**(12): p. 7546-55.

95.   Miyao, T. and N.A. Woychik, *RNA polymerase subunit RPB5 plays a role in transcriptional activation.* Proceedings of the National Academy of Sciences of the United States of America, 1998. **95**(26): p. 15281-6.

96.   Todone, F., et al., *Crystal structure of RPB5, a universal eukaryotic RNA polymerase subunit and transcription factor interaction target.* Proceedings of the National Academy of Sciences of the United States of America, 2000. **97**(12): p. 6306-10.

97.   Wei, W., et al., *Interaction with general transcription factor IIF (TFIIF) is required for the suppression of activated transcription by RPB5-mediating protein (RMP).* Cell research, 2003. **13**(2): p. 111-20.

98.   Le, T.T., et al., *Mutational analysis of human RNA polymerase II subunit 5 (RPB5): the residues critical for interactions with TFIIF subunit RAP30 and hepatitis B virus X protein.* Journal of biochemistry, 2005. **138**(3): p. 215-24.

99.   Yart, A., et al., *The HRPT2 tumor suppressor gene product parafibromin associates with human PAF1 and RNA polymerase II.* Molecular and cellular biology, 2005. **25**(12): p. 5052-60.

100.   Cloutier, P. and B. Coulombe, *New insights into the biogenesis of nuclear RNA polymerases?* Biochemistry and cell biology = Biochimie et biologie cellulaire, 2010. **88**(2): p. 211-21.

101. Bennett-Lovsey, R.M., et al., *Exploring the extremes of sequence/structure space with ensemble fold recognition in the program Phyre.* Proteins, 2008. **70**(3): p. 611-25.

102. Dephoure, N., et al., *A quantitative atlas of mitotic phosphorylation.* Proceedings of the National Academy of Sciences of the United States of America, 2008. **105**(31): p. 10762-7.

103. Rosner, M. and M. Hengstschlager, *Cytoplasmic and nuclear distribution of the protein complexes mTORC1 and mTORC2: rapamycin triggers dephosphorylation and delocalization of the mTORC2 components rictor and sin1.* Human molecular genetics, 2008. **17**(19): p. 2934-48.

104. Djouder, N., et al., *S6K1-mediated disassembly of mitochondrial URI/PP1gamma complexes activates a negative feedback program that counters S6K1 survival signaling.* Molecular cell, 2007. **28**(1): p. 28-40.

105. Guicciardi, M.E. and G.J. Gores, *Cell stress gives a red light to the mitochondrial cell death pathway.* Science signaling, 2008. **1**(7): p. pe9.

106. Ceulemans, H. and M. Bollen, *Functional diversity of protein phosphatase-1, a cellular economizer and reset button.* Physiological reviews, 2004. **84**(1): p. 1-39.

107. Wakula, P., et al., *Degeneracy and function of the ubiquitous RVXF motif that mediates binding to protein phosphatase-1.* The Journal of biological chemistry, 2003. **278**(21): p. 18817-23.

108.   Hurley, T.D., et al., *Structural basis for regulation of protein phosphatase 1 by inhibitor-2.* The Journal of biological chemistry, 2007. **282**(39): p. 28874-83.

109.   Theurillat, J.P., et al., *URI is an oncogene amplified in ovarian cancer cells and is required for their survival.* Cancer cell, 2011. **19**(3): p. 317-32.

110.   Wrzeszczynski, K.O., et al., *Identification of tumor suppressors and oncogenes from genomic and epigenetic features in ovarian cancer.* PloS one, 2011. **6**(12): p. e28503.

111.   Yang, H., et al., *RPB5-mediating protein is required for the proliferation of hepatocellular carcinoma cells.* The Journal of biological chemistry, 2011. **286**(13): p. 11865-74.

112.   Negoro, E., et al., *Characterization of cytarabine-resistant leukemic cell lines established from five different blood cell lineages using gene expression and proteomic analyses.* International journal of oncology, 2011. **38**(4): p. 911-9.

113.   Parusel, C.T., et al., *URI-1 is required for DNA stability in C. elegans.* Development, 2006. **133**(4): p. 621-9.

114.   Kirchner, J., et al., *Drosophila Uri, a PP1alpha binding protein, is essential for viability, maintenance of DNA integrity and normal transcriptional activity.* BMC molecular biology, 2008. **9**: p. 36.

115.   Ni, L. and M. Snyder, *A genomic study of the bipolar bud site selection pattern in Saccharomyces cerevisiae.* Molecular biology of the cell, 2001. **12**(7): p. 2147-70.

116.   Wissmann, M., et al., *Cooperative demethylation by JMJD2C and LSD1 promotes androgen receptor-dependent gene expression.* Nature cell biology, 2007. **9**(3): p. 347-53.

117.   Wolf, S.S., V.K. Patchev, and M. Obendorf, *A novel variant of the putative demethylase gene, s-JMJD1C, is a coactivator of the AR.* Archives of biochemistry and biophysics, 2007. **460**(1): p. 56-66.

118.   Yamane, K., et al., *JHDM2A, a JmjC-containing H3K9 demethylase, facilitates transcription activation by androgen receptor.* Cell, 2006. **125**(3): p. 483-95.

119.   Nyswaner, K.M., et al., *Chromatin-associated genes protect the yeast genome from Ty1 insertional mutagenesis.* Genetics, 2008. **178**(1): p. 197-214.

120.   Deplazes, A., et al., *Yeast Uri1p promotes translation initiation and may provide a link to cotranslational quality control.* The EMBO journal, 2009. **28**(10): p. 1429-41.

121.   Friedman, J.R., et al., *KAP-1, a novel corepressor for the highly conserved KRAB repression domain.* Genes & Development, 1996. **10**(16): p. 2067-78.

122. Moosmann, P., et al., *Transcriptional repression by RING finger protein TIF1 beta that interacts with the KRAB repressor domain of KOX1.* Nucleic acids research, 1996. **24**(24): p. 4859-67.

123. Kim, S.S., et al., *A novel member of the RING finger family, KRIP-1, associates with the KRAB-A transcriptional repressor domain of zinc finger proteins.* Proceedings of the National Academy of Sciences of the United States of America, 1996. **93**(26): p. 15299-304.

124. Urrutia, R., *KRAB-containing zinc-finger repressor proteins.* Genome biology, 2003. **4**(10): p. 231.

125. Abrink, M., et al., *Conserved interaction between distinct Kruppel-associated box domains and the transcriptional intermediary factor 1 beta.* Proceedings of the National Academy of Sciences of the United States of America, 2001. **98**(4): p. 1422-6.

126. Iyengar, S. and P.J. Farnham, *KAP1 protein: an enigmatic master regulator of the genome.* The Journal of biological chemistry, 2011. **286**(30): p. 26267-76.

127. Peng, H., I. Feldman, and F.J. Rauscher, 3rd, *Hetero-oligomerization among the TIF family of RBCC/TRIM domain-containing nuclear cofactors: a potential mechanism for regulating the switch between coactivation and corepression.* Journal of molecular biology, 2002. **320**(3): p. 629-44.

128. Le Douarin, B., et al., *The N-terminal part of TIF1, a putative mediator of the ligand-dependent activation function (AF-2) of nuclear receptors, is fused to*

B-raf in the oncogenic protein T18. The EMBO journal, 1995. **14**(9): p. 2020-33.

129.   vom Baur, E., et al., *Differential ligand-dependent interactions between the AF-2 activating domain of nuclear receptors and the putative transcriptional intermediary factors mSUG1 and TIF1.* The EMBO journal, 1996. **15**(1): p. 110-24.

130.   He, W., et al., *Hematopoiesis controlled by distinct TIF1gamma and Smad4 branches of the TGFbeta pathway.* Cell, 2006. **125**(5): p. 929-41.

131.   Peng, H., et al., *Reconstitution of the KRAB-KAP-1 repressor complex: a model system for defining the molecular anatomy of RING-B box-coiled-coil domain-mediated protein-protein interactions.* Journal of molecular biology, 2000. **295**(5): p. 1139-62.

132.   Cammas, F., et al., *Association of the transcriptional corepressor TIF1beta with heterochromatin protein 1 (HP1): an essential role for progression through differentiation.* Genes & Development, 2004. **18**(17): p. 2147-60.

133.   Schultz, D.C., J.R. Friedman, and F.J. Rauscher, 3rd, *Targeting histone deacetylase complexes via KRAB-zinc finger proteins: the PHD and bromodomains of KAP-1 form a cooperative unit that recruits a novel isoform of the Mi-2alpha subunit of NuRD.* Genes & Development, 2001. **15**(4): p. 428-43.

134. Cammas, F., et al., *Mice lacking the transcriptional corepressor TIF1beta are defective in early postimplantation development.* Development, 2000. **127**(13): p. 2955-63.

135. Weber, P., et al., *Germ cell expression of the transcriptional co-repressor TIF1beta is required for the maintenance of spermatogenesis in the mouse.* Development, 2002. **129**(10): p. 2329-37.

136. Herzog, M., et al., *TIF1beta association with HP1 is essential for post-gastrulation development, but not for Sertoli cell functions during spermatogenesis.* Developmental biology, 2011. **350**(2): p. 548-58.

137. Quenneville, S., et al., *In embryonic stem cells, ZFP57/KAP1 recognize a methylated hexanucleotide to affect chromatin and DNA methylation of imprinting control regions.* Molecular cell, 2011. **44**(3): p. 361-72.

138. Shibata, M., et al., *TRIM28 is required by the mouse KRAB domain protein ZFP568 to control convergent extension and morphogenesis of extra-embryonic tissues.* Development, 2011. **138**(24): p. 5333-43.

139. Xiao, T.Z., et al., *MAGE I transcription factors regulate KAP1 and KRAB domain zinc finger transcription factor mediated gene repression.* PloS one, 2011. **6**(8): p. e23747.

140. Peng, H., et al., *Epigenetic gene silencing by the SRY protein is mediated by a KRAB-O protein that recruits the KAP1 co-repressor machinery.* The Journal of biological chemistry, 2009. **284**(51): p. 35670-80.

141. Tevosian, S.G., et al., *Gonadal differentiation, sex determination and normal Sry expression in mice require direct interaction between transcription partners GATA4 and FOG2.* Development, 2002. **129**(19): p. 4627-34.

142. Koopman, P., *Sry and Sox9: mammalian testis-determining genes.* Cellular and molecular life sciences : CMLS, 1999. **55**(6-7): p. 839-56.

143. Seki, Y., et al., *TIF1beta regulates the pluripotency of embryonic stem cells in a phosphorylation-dependent manner.* Proceedings of the National Academy of Sciences of the United States of America, 2010. **107**(24): p. 10926-31.

144. Zuo, X., et al., *Zinc finger protein ZFP57 requires its co-factor to recruit DNA methyltransferases and maintains DNA methylation imprint in embryonic stem cells via its transcriptional repression domain.* The Journal of biological chemistry, 2012. **287**(3): p. 2107-18.

145. Karimi, M.M., et al., *DNA methylation and SETDB1/H3K9me3 regulate predominantly distinct sets of genes, retroelements, and chimeric transcripts in mESCs.* Cell stem cell, 2011. **8**(6): p. 676-87.

146. Underhill, C., et al., *A novel nuclear receptor corepressor complex, N-CoR, contains components of the mammalian SWI/SNF complex and the corepressor KAP-1.* The Journal of biological chemistry, 2000. **275**(51): p. 40463-70.

147. O'Geen, H., et al., *Genome-wide analysis of KAP1 binding suggests autoregulation of KRAB-ZNFs.* PLoS genetics, 2007. **3**(6): p. e89.

148. Iyengar, S., et al., *Functional analysis of KAP1 genomic recruitment.* Molecular and cellular biology, 2011. **31**(9): p. 1833-47.

149. Groner, A.C., et al., *KRAB-zinc finger proteins and KAP1 can mediate long-range transcriptional repression through heterochromatin spreading.* PLoS genetics, 2010. **6**(3): p. e1000869.

150. Zeng, L., et al., *Structural insights into human KAP1 PHD finger-bromodomain and its role in gene silencing.* Nature structural & molecular biology, 2008. **15**(6): p. 626-33.

151. Lee, Y.K., et al., *Doxorubicin down-regulates Kruppel-associated box domain-associated protein 1 sumoylation that relieves its transcription repression on p21WAF1/CIP1 in breast cancer MCF-7 cells.* The Journal of biological chemistry, 2007. **282**(3): p. 1595-606.

152. Ivanov, A.V., et al., *PHD domain-mediated E3 ligase activity directs intramolecular sumoylation of an adjacent bromodomain required for gene silencing.* Molecular cell, 2007. **28**(5): p. 823-37.

153. Li, X., et al., *Role for KAP1 serine 824 phosphorylation and sumoylation/desumoylation switch in regulating KAP1-mediated transcriptional repression.* The Journal of biological chemistry, 2007. **282**(50): p. 36177-89.

154. White, D.E., et al., *KAP1, a novel substrate for PIKK family members, colocalizes with numerous damage response factors at DNA lesions.* Cancer Research, 2006. **66**(24): p. 11594-9.

155.   Ziv, Y., et al., *Chromatin relaxation in response to DNA double-strand breaks is modulated by a novel ATM- and KAP-1 dependent pathway.* Nature cell biology, 2006. **8**(8): p. 870-6.

156.   Blasius, M., et al., *A phospho-proteomic screen identifies substrates of the checkpoint kinase Chk1.* Genome biology, 2011. **12**(8): p. R78.

157.   Chang, C.W., et al., *Phosphorylation at Ser473 regulates heterochromatin protein 1 binding and corepressor function of TIF1beta/KAP1.* BMC molecular biology, 2008. **9**: p. 61.

158.   Li, X., et al., *SUMOylation of the transcriptional co-repressor KAP1 is regulated by the serine and threonine phosphatase PP1.* Science signaling, 2010. **3**(119): p. ra32.

159.   Noon, A.T., et al., *53BP1-dependent robust localized KAP-1 phosphorylation is essential for heterochromatic DNA double-strand break repair.* Nature cell biology, 2010. **12**(2): p. 177-84.

160.   Goodarzi, A.A., T. Kurka, and P.A. Jeggo, *KAP-1 phosphorylation regulates CHD3 nucleosome remodeling during the DNA double-strand break response.* Nature structural & molecular biology, 2011. **18**(7): p. 831-9.

161.   Wang, C., et al., *MDM2 interaction with nuclear corepressor KAP1 contributes to p53 inactivation.* The EMBO journal, 2005. **24**(18): p. 3279-90.

162. Okamoto, K., I. Kitabayashi, and Y. Taya, *KAP1 dictates p53 response induced by chemotherapeutic agents via Mdm2 interaction.* Biochemical and biophysical research communications, 2006. **351**(1): p. 216-22.

163. Yang, B., et al., *MAGE-A, mMage-b, and MAGE-C proteins form complexes with KAP1 and suppress p53-dependent apoptosis in MAGE-positive cell lines.* Cancer Research, 2007. **67**(20): p. 9954-62.

164. Rowe, H.M., et al., *KAP1 controls endogenous retroviruses in embryonic stem cells.* Nature, 2010. **463**(7278): p. 237-40.

165. Matsui, T., et al., *Proviral silencing in embryonic stem cells requires the histone methyltransferase ESET.* Nature, 2010. **464**(7290): p. 927-31.

166. Allouch, A., et al., *The TRIM family protein KAP1 inhibits HIV-1 integration.* Cell host & microbe, 2011. **9**(6): p. 484-95.

167. Wolf, D., K. Hug, and S.P. Goff, *TRIM28 mediates primer binding site-targeted silencing of Lys1,2 tRNA-utilizing retroviruses in embryonic cells.* Proceedings of the National Academy of Sciences of the United States of America, 2008. **105**(34): p. 12521-6.

168. Wolf, D. and S.P. Goff, *TRIM28 mediates primer binding site-targeted silencing of murine leukemia virus in embryonic cells.* Cell, 2007. **131**(1): p. 46-57.

169.   Blahnik, K.R., et al., *Characterization of the contradictory chromatin signatures at the 3' exons of zinc finger genes.* PloS one, 2011. **6**(2): p. e17121.

170.   Romanish, M.T., C.J. Cohen, and D.L. Mager, *Potential mechanisms of endogenous retroviral-mediated genomic instability in human cancer.* Seminars in cancer biology, 2010. **20**(4): p. 246-53.

171.   Mills, R.E., et al., *Which transposable elements are active in the human genome?* Trends in genetics : TIG, 2007. **23**(4): p. 183-91.

172.   Cordaux, R. and M.A. Batzer, *The impact of retrotransposons on human genome evolution.* Nature reviews. Genetics, 2009. **10**(10): p. 691-703.

173.   Goering, W., T. Ribarska, and W.A. Schulz, *Selective changes of retroelement expression in human prostate cancer.* Carcinogenesis, 2011. **32**(10): p. 1484-92.

174.   Maksakova, I.A., et al., *Retroviral elements and their hosts: insertional mutagenesis in the mouse germ line.* PLoS genetics, 2006. **2**(1): p. e2.

175.   Belancio, V.P., A.M. Roy-Engel, and P.L. Deininger, *All y'all need to know 'bout retroelements in cancer.* Seminars in cancer biology, 2010. **20**(4): p. 200-10.

176.   Rowe, H.M. and D. Trono, *Dynamic control of endogenous retroviruses during development.* Virology, 2011. **411**(2): p. 273-87.

177. Okano, M., et al., *DNA methyltransferases Dnmt3a and Dnmt3b are essential for de novo methylation and mammalian development.* Cell, 1999. **99**(3): p. 247-57.

178. Chu, C.Y. and T.M. Rana, *Small RNAs: regulators and guardians of the genome.* Journal of Cellular Physiology, 2007. **213**(2): p. 412-9.

179. Senti, K.A. and J. Brennecke, *The piRNA pathway: a fly's perspective on the guardian of the genome.* Trends in genetics : TIG, 2010. **26**(12): p. 499-509.

180. Kuramochi-Miyagawa, S., et al., *Two mouse piwi-related genes: miwi and mili.* Mechanisms of development, 2001. **108**(1-2): p. 121-33.

181. Carmell, M.A., et al., *MIWI2 is essential for spermatogenesis and repression of transposons in the mouse male germline.* Developmental cell, 2007. **12**(4): p. 503-14.

182. Muotri, A.R., et al., *The necessary junk: new functions for transposable elements.* Human molecular genetics, 2007. **16 Spec No. 2**: p. R159-67.

183. Rangwala, S.H., L. Zhang, and H.H. Kazazian, Jr., *Many LINE1 elements contribute to the transcriptome of human somatic cells.* Genome biology, 2009. **10**(9): p. R100.

184. Kazazian, H.H., Jr., *Mobile DNA transposition in somatic cells.* BMC biology, 2011. **9**: p. 62.

209

185. Baillie, J.K., et al., *Somatic retrotransposition alters the genetic landscape of the human brain.* Nature, 2011. **479**(7374): p. 534-7.

186. Faulkner, G.J., *Retrotransposons: mobile and mutagenic from conception to death.* FEBS letters, 2011. **585**(11): p. 1589-94.

187. Kubo, S., et al., *L1 retrotransposition in nondividing and primary human somatic cells.* Proceedings of the National Academy of Sciences of the United States of America, 2006. **103**(21): p. 8036-41.

188. Kozeretska, I.A., S.V. Demydov, and L.I. Ostapchenko, *Mobile genetic elements and cancer. From mutations to gene therapy.* Experimental oncology, 2011. **33**(4): p. 198-205.

189. Belancio, V.P., D.J. Hedges, and P. Deininger, *Mammalian non-LTR retrotransposons: for better or worse, in sickness and in health.* Genome research, 2008. **18**(3): p. 343-58.

190. Kurth, R. and N. Bannert, *Beneficial and detrimental effects of human endogenous retroviruses.* International journal of cancer. Journal international du cancer, 2010. **126**(2): p. 306-14.

191. Morse, B., et al., *Insertional mutagenesis of the myc locus by a LINE-1 sequence in a human breast carcinoma.* Nature, 1988. **333**(6168): p. 87-90.

192.   Machado, P.M., et al., *Screening for a BRCA2 rearrangement in high-risk breast/ovarian cancer families: evidence for a founder effect and analysis of the associated phenotypes.* Journal of clinical oncology : official journal of the American Society of Clinical Oncology, 2007. **25**(15): p. 2027-34.

193.   Miki, Y., et al., *Disruption of the APC gene by a retrotransposal insertion of L1 sequence in a colon cancer.* Cancer Research, 1992. **52**(3): p. 643-5.

194.   Mazoyer, S., *Genomic rearrangements in the BRCA1 and BRCA2 genes.* Human mutation, 2005. **25**(5): p. 415-22.

195.   Gebow, D., N. Miselis, and H.L. Liber, *Homologous and nonhomologous recombination resulting in deletion: effects of p53 status, microhomology, and repetitive DNA length and orientation.* Molecular and cellular biology, 2000. **20**(11): p. 4028-35.

196.   Harris, C.R., et al., *p53 responsive elements in human retrotransposons.* Oncogene, 2009. **28**(44): p. 3857-65.

197.   Carlini, F., et al., *The reverse transcription inhibitor abacavir shows anticancer activity in prostate cancer cell lines.* PloS one, 2010. **5**(12): p. e14221.

198.   Tomlins, S.A., et al., *Integrative molecular concept modeling of prostate cancer progression.* Nature genetics, 2007. **39**(1): p. 41-51.

199. Xu, Y., et al., *Androgens induce prostate cancer cell proliferation through mammalian target of rapamycin activation and post-transcriptional increases in cyclin D proteins.* Cancer Research, 2006. **66**(15): p. 7783-92.

200. Mellinghoff, I.K. and C.L. Sawyers, *TORward AKTually useful mouse models.* Nature Medicine, 2004. **10**(6): p. 579-80.

201. Rai, J.S., M.J. Henley, and H.L. Ratan, *Mammalian target of rapamycin: a new target in prostate cancer.* Urologic oncology, 2010. **28**(2): p. 134-8.

202. Thomas, M.A., D.M. Preece, and J.M. Bentel, *Androgen regulation of the prostatic tumour suppressor NKX3.1 is mediated by its 3' untranslated region.* The Biochemical journal, 2010. **425**(3): p. 575-83.

203. Wysocka, J., P.T. Reilly, and W. Herr, *Loss of HCF-1-chromatin association precedes temperature-induced growth arrest of tsBN67 cells.* Molecular and cellular biology, 2001. **21**(11): p. 3820-9.

204. Vaquero, A., et al., *Human SirT1 interacts with histone H1 and promotes formation of facultative heterochromatin.* Molecular cell, 2004. **16**(1): p. 93-105.

205. Li, G., et al., *Jarid2 and PRC2, partners in regulating gene expression.* Genes & Development, 2010. **24**(4): p. 368-80.

206.   Vainberg, I.E., et al., *Prefoldin, a chaperone that delivers unfolded proteins to cytosolic chaperonin.* Cell, 1998. **93**(5): p. 863-73.

207.   Freeman, B.C., et al., *The p23 molecular chaperones act at a late step in intracellular receptor action to differentially affect ligand efficacies.* Genes & Development, 2000. **14**(4): p. 422-34.

208.   Taylor, B.S., et al., *Integrative genomic profiling of human prostate cancer.* Cancer cell, 2010. **18**(1): p. 11-22.

209.   Delgermaa, L., et al., *Subcellular localization of RPB5-mediating protein and its putative functional partner.* Molecular and cellular biology, 2004. **24**(19): p. 8556-66.

210.   Luo, X., Y. Huang, and M.S. Sheikh, *Cloning and characterization of a novel gene PDRG that is differentially regulated by p53 and ultraviolet radiation.* Oncogene, 2003. **22**(46): p. 7247-57.

211.   Jiang, L., et al., *PDRG1, a novel tumor marker for multiple malignancies that is selectively regulated by genotoxic stress.* Cancer biology & therapy, 2011. **11**(6): p. 567-73.

212.   Dundr, M., et al., *A kinetic framework for a mammalian RNA polymerase in vivo.* Science, 2002. **298**(5598): p. 1623-6.

213. Gorski, S.A., et al., *Modulation of RNA polymerase assembly dynamics in transcriptional regulation.* Molecular cell, 2008. **30**(4): p. 486-97.

214. Zhao, R., et al., *Navigating the chaperone network: an integrative map of physical and genetic interactions mediated by the hsp90 chaperone.* Cell, 2005. **120**(5): p. 715-27.

215. Nguyen, V.T., et al., *In vivo degradation of RNA polymerase II largest subunit triggered by alpha-amanitin.* Nucleic acids research, 1996. **24**(15): p. 2924-9.

216. Fornerod, M., et al., *CRM1 is an export receptor for leucine-rich nuclear export signals.* Cell, 1997. **90**(6): p. 1051-60.

217. Olsen, J.V., et al., *Global, in vivo, and site-specific phosphorylation dynamics in signaling networks.* Cell, 2006. **127**(3): p. 635-48.

218. Belakavadi, M. and J.D. Fondell, *Role of the mediator complex in nuclear hormone receptor signaling.* Reviews of physiology, biochemistry and pharmacology, 2006. **156**: p. 23-43.

219. Malik, S. and R.G. Roeder, *The metazoan Mediator co-activator complex as an integrative hub for transcriptional regulation.* Nature reviews. Genetics, 2010. **11**(11): p. 761-72.

220. Bakkenist, C.J. and M.B. Kastan, *DNA damage activates ATM through intermolecular autophosphorylation and dimer dissociation.* Nature, 2003. **421**(6922): p. 499-506.

221. Goodarzi, A.A., et al., *Autophosphorylation of ataxia-telangiectasia mutated is regulated by protein phosphatase 2A.* Embo Journal, 2004. **23**(22): p. 4451-4461.

222. Meylan, S., et al., *A gene-rich, transcriptionally active environment and the pre-deposition of repressive marks are predictive of susceptibility to KRAB/KAP1-mediated silencing.* BMC genomics, 2011. **12**: p. 378.

223. Li, B., M. Carey, and J.L. Workman, *The role of chromatin during transcription.* Cell, 2007. **128**(4): p. 707-19.

224. White, D., et al., *The ATM Substrate KAP1 Controls DNA Repair in Heterochromatin: Regulation by HP1 Proteins and Serine 473/824 Phosphorylation.* Molecular cancer research : MCR, 2012. **10**(3): p. 401-14.

225. Wan, S., H. Capasso, and N.C. Walworth, *The topoisomerase I poison camptothecin generates a Chk1-dependent DNA damage checkpoint signal in fission yeast.* Yeast, 1999. **15**(10A): p. 821-8.

226. Koc, A., et al., *Hydroxyurea arrests DNA replication by a mechanism that preserves basal dNTP pools.* The Journal of biological chemistry, 2004. **279**(1): p. 223-30.

227.   Petermann, E., et al., *Hydroxyurea-stalled replication forks become progressively inactivated and require two different RAD51-mediated pathways for restart and repair.* Molecular cell, 2010. **37**(4): p. 492-502.

228.   Lukas, J., C. Lukas, and J. Bartek, *More than just a focus: The chromatin response to DNA damage and its role in genome integrity maintenance.* Nature cell biology, 2011. **13**(10): p. 1161-9.

229.   Chowdhury, D., et al., *gamma-H2AX dephosphorylation by protein phosphatase 2A facilitates DNA double-strand break repair.* Molecular cell, 2005. **20**(5): p. 801-9.

230.   Nakada, S., et al., *PP4 is a gamma H2AX phosphatase required for recovery from the DNA damage checkpoint.* EMBO reports, 2008. **9**(10): p. 1019-26.

231.   Goldstein, A.S., et al., *Identification of a cell of origin for human prostate cancer.* Science, 2010. **329**(5991): p. 568-71.

232.   Burger, P.E., et al., *Sca-1 expression identifies stem cells in the proximal region of prostatic ducts with high capacity to reconstitute prostatic tissue.* Proceedings of the National Academy of Sciences of the United States of America, 2005. **102**(20): p. 7180-5.

233.   Wang, X., et al., *A luminal epithelial stem cell that is a cell of origin for prostate cancer.* Nature, 2009. **461**(7263): p. 495-500.

234.   Liu, J., et al., *Regenerated luminal epithelial cells are derived from preexisting luminal epithelial cells in adult mouse prostate.* Molecular Endocrinology, 2011. **25**(11): p. 1849-57.

235.   Choi, N., et al., *Adult murine prostate basal and luminal cells are self-sustained lineages that can both serve as targets for prostate cancer initiation.* Cancer cell, 2012. **21**(2): p. 253-65.

236.   Danielpour, D., *Transdifferentiation of NRP-152 rat prostatic basal epithelial cells toward a luminal phenotype: regulation by glucocorticoid, insulin-like growth factor-I and transforming growth factor-beta.* Journal of cell science, 1999. **112 (Pt 2)**: p. 169-79.

237.   Shim, J.H., et al., *Proteome profile changes during transdifferentiation of NRP-152 rat prostatic basal epithelial cells.* Molecules and cells, 2004. **17**(1): p. 108-16.

238.   Tsujimura, A., et al., *Proximal location of mouse prostate epithelial stem cells: a model of prostatic homeostasis.* The Journal of cell biology, 2002. **157**(7): p. 1257-65.

239.   Hofman, K., et al., *E2F activity is biphasically regulated by androgens in LNCaP cells.* Biochemical and biophysical research communications, 2001. **283**(1): p. 97-101.

240.   Sherwood, E.R., et al., *Epidermal growth factor receptor activation in androgen-independent but not androgen-stimulated growth of human prostatic carcinoma cells.* British journal of cancer, 1998. **77**(6): p. 855-61.

241. Sikkeland, J., T. Lindstad, and F. Saatcioglu, *Analysis of androgen-induced increase in lipid accumulation in prostate cancer cells.* Methods in molecular biology, 2011. **776**: p. 371-82.

242. Esquenet, M., et al., *Retinoids stimulate lipid synthesis and accumulation in LNCaP prostatic adenocarcinoma cells.* Molecular and cellular endocrinology, 1997. **136**(1): p. 37-46.

243. Bhatia-Gaur, R., et al., *Roles for Nkx3.1 in prostate development and cancer.* Genes & Development, 1999. **13**(8): p. 966-77.

244. Bernardo, G.M. and R.A. Keri, *FOXA1: a transcription factor with parallel functions in development and cancer.* Bioscience reports, 2012. **32**(2): p. 113-30.

245. Jeevan-Raj, B.P., et al., *Epigenetic tethering of AID to the donor switch region during immunoglobulin class switch recombination.* The Journal of experimental medicine, 2011. **208**(8): p. 1649-60.

246. Wu, J.Q. and M. Snyder, *RNA polymerase II stalling: loading at the start prepares genes for a sprint.* Genome biology, 2008. **9**(5): p. 220.

247. Zeitlinger, J., et al., *RNA polymerase stalling at developmental control genes in the Drosophila melanogaster embryo.* Nature genetics, 2007. **39**(12): p. 1512-6.